# ROTORDYNAMIC STUDY OF PUMPS IN THE NUCLEAR INDUSTRY

RAPPORT 2015:117





# Rotordynamic study of pumps in the nuclear industry

STAFFAN LUNDHOLM, MATTIAS LARSSON, MATTIAS LINDBLAD

# Preface

This project has been commenced within the research program Vibrations, which is part of the Energiforsk Nuclear Energy Research program. Lloyd's Register Consulting AB have analyzed the rotordynamical behaviour of pumps, evaluated rotrodynamical requirements and discussed current standards on pump vibrations. The stakeholders of Vibrations are Vattenfall, E.ON, Fortum, TVO, Skellefteå Kraft och Karlstads Energi.

# Sammanfattning

På uppdrag av Elforsk AB har Lloyd's Register Consulting (LR Consulting) genomfört en studie avseende pumpars rotordynamik inom kärnkraftsindustrin. Den av kärnkraftsverken framtagna TBM (Tekniska Bestämmelser för Mekaniska anordningar) har granskats med hänsyn till rotordynamik och jämförts med andra tillgängliga internationella standarder för pumpar.

Utöver detta har två rotordynamiska lateralanalyser genomförts på två pumpar inom kärnkraftsindustrin: en vertikal- och en horisontell pump. Valet av pumpar gjordes av en styrgrupp på Elforsk som bestod av representanter från de svenska verken OKG, RAB och FKA samt de finska verken TVO och Loviisa.

Resultaten visar att TBM innehåller begränsat med information gällande rotordynamiska problemställningar. Framförallt saknas någon form av klassificering av pumpar vilka kan skilja väldigt mycket i egenskaper och potentiella problem. En jämförelse visar att TBM ligger något konservativt i sina vibrationsgränser, lägre än både ISO 10816, del 7 och API 610, Ed. 11. En klassificering av pumpar kan leda till att resurser för vibrationsdämpning på vissa icke-kritiska pumpar kan omfördelas till mer kritiska pumpar med högre krav på driftsäkerhet.

Rutiner gällande rotordynamisk analys är mycket begränsat i TBM, och den enda egentliga kravspecifikationen omfattar den kritiska hastigheten som skall vara 25% över det högsta varvtalet. Detta förutsätter att alla pumpar inom kärnkraftsindustrin opererar subkritiskt, dvs under den första kritiska hastigheten. Krav gällande torsionsproblem och torsionsanalys finns ej omnämnt i TBM trots att detta är en relativt vanligt rotordynamiskt problem.

LR Consulting föreslår i denna studie ett antal förändringar i TBM som skulle förbättra krav och rutiner inom rotordynamisk analys på verken. En ökad frekvens av rotordynamisk tredjepartsanalys leder till att man undviker problem vid driftsättning och vid normal drift. Rotordynamik är ett komplext och användare av kritiska pumpar måste redan i specialistämne gällande ställa рå tillverkare inköpsstadium krav rotordynamisk dokumentation. Tredjepartsanalys och granskning av nydesignade och ombyggda pumpar är normalt en god investering och en jämförelsevis liten kostnad i en inköpsbudget.

# Summary

At the request of Elforsk AB, Lloyd's Register Consulting (LR Consulting) has performed a study regarding the rotordynamics of pumps in the nuclear industry. The Swedish nuclear industry has developed a standard, Tekniska Bestämmelser för Mekaniska anordningar (TBM). The TBM has been reviewed and compared with other available pump standards.

Aside from this, the study has comprised two lateral analyses of pumps; one horizontal- and one vertical pump which were selected by a steering group at Elforsk consisting of representatives from the Swedish plants OKG, FKA, RAB as well as the Finnish plants TVO and Loviisa.

The results show that the TBM is a limited source of information with regards to rotordynamic analysis and design requirements. Primarily, the standard lacks classification of the pumps and thus does not consider the major differences which exist between different pump designs. The TBM vibration limits are conservative compared to ISO 10816 part 7 and API 610, 11<sup>th</sup> Ed. A classification of pumps may have the advantage of routing resources for vibration damping on less critical pumps to critical pumps with higher demands on operational up-time.

Further, the design requirements with regards to rotordynamics are poor; the main requirement in TBM states that the pumps shall be designed to have the first critical speed 25% above the maximum operating speed. This implicitly excludes all supercritical pumps in the nuclear industry from the standard. Requirements regarding torsional problems- and analysis are non-existing although this is a relatively common rotordynamic problem.

To improve the rotordynamic aspects of machinery dynamics, modifications and additions to the TBM have been suggested by LR Consulting. An increased focus on rotordynamic analyses already at the procurement stage will minimize problems at commissioning and operation. The field of rotordynamic is complex and the end user must push the OEMs to provide sufficient documentation on the rotordynamic properties of the pump. 3rd party analysis and review of new designs and major revamps is normally a sound investment and a comparatively small cost in a procurement budget.

# Innehåll

1	Intr	roduction	1
2	Back	kground	2
3	Roto	ordynamic definitions	3
	3.1	Natural frequency	3
		3.1.1 Undamped natural frequency	3
		3.1.2 Damped natural frequency	
		3.1.3 Torsional natural frequency	
	3.2	Critical speed	
	3.3	Separation margin	
	3.4	Unbalance response analysis	
		3.4.1 Stability analysis	5
4	Com	nmon rotordynamic problems on water pumps	$\epsilon$
	4.1	Potential problem sources	<i>6</i>
		4.1.1 Seal forces	
		4.1.2 Impeller forces	
		4.1.3 Bearings	
		4.1.4 Fluid forces	
		4.1.5 Stall	
		4.1.6 Gear box torsional excitation	
		4.1.7 Electric motor torsional excitation	
		4.1.8 Rigid couplings	8
	4.2	Rotordynamic problems in the nuclear industry	
5	Dovi	iou of applicable standards	,
5	5.1	iew of applicable standards  TBM	7
	3.1	5.1.1 Pump specifics in TBM	
		5.1.2 Documentation	
	5.2	API 610	
	5.2	5.2.1 Classification	
		5.2.2 Lateral analysis	
		5.2.3 Torsional analysis	
		5.2.4 Vibration levels	
		5.2.5 Balancing	
	5.3	ISO	
	0.0	5.3.1 ISO 1940	
		5.3.2 ISO 11342	
		5.3.3 ISO 10816 – part 7	
		5.3.4 ISO 10816 – part 3	
		5.3.5 ISO 7919	
		5.3.6 ISO 13373	
	5.4	NORSOK	
	5.5	DIN	23
4	Dica	cussion	3.4
6	6.1	Vibration levels	24
	6.2	Motivation for rotordynamic analysis	
	0.2	6.2.1 API 610 requirements	
	6.3	Third-party analysis	
	0.3	mina-party analysis	25
7	Sug	gested modifications to TBM	27

	7.1		n levels (Section 4.4.4.3)	
	7.2		namic analysis (New Section)	
	7.3		n measurements (New Section)	
			Measurement positions	
		7.3.2	Commissioning of new pumps and revamps	28
8	Rotor	dynam	ic analysis	29
	8.1	Horizon	tal pump	29
	8.2	Vertical	pump	30
9		usions		32
	9.1 9.2		tal pumppump	
10	Refer	ences		34
App	endix	A.	Minutes of meeting	
Арр	endix	В.	Horizontal pump	
Арр	endix	C.	Vertical pump	

# 1 Introduction

At the request of Elforsk, Lloyd's Register Consulting (LR Consulting) has performed a study on the rotordynamics of pumps in the nuclear industry. The project has been a collaboration between LR Consulting, Elforsk and a steering group with representatives from the following Scandinavian plants:

- Oskarshamn (OKG), Sweden
- Forsmark (FKA), Sweden
- Ringhals (RAB), Sweden
- Olkiluoto (TVO), Finland
- Loviisa, Finland

The steering group has made decisions on the framing of the project and decided which pumps to be selected for lateral analysis.

# 2 Background

In 2013, Elforsk organized a workshop with representatives from plant owners and vendors in the nuclear industry. The workshop identified a need for third party rotordynamic analyses of pumps on the plants. The objective of such analyses is to increase knowledge, identify possible design issues and possibly rectify these before commissioning of new- or modified pump strings.

Several plants also expressed experience with dynamic problems on coolingand feed water pumps, and the project was framed around the outcome of this workshop.

LR Consulting was chosen to perform the study after an invitation to tender in May 2013. A kick-off meeting was held at Elforsk premises in September 2013.

# 3 Rotordynamic definitions

This section summarizes the definitions and terminology used in the rotordynamic literature. The definitions will be frequently referred to in the present report.

## 3.1 Natural frequency

The natural frequency of a rotor is the frequency at which the rotor oscillates if it is impacted by an external force. Compared to static systems such as skids and supporting structures, the rotors natural frequency may vary with rotor speed due to dynamic reaction forces from e.g. bearings, seals and from gyroscopic effects Also the properties of the surrounding fluid might influence the dynamic characteristics of the system. This is due to the interaction between impeller and the surrounding fluid as well as fluid bearing interactions etc.

#### 3.1.1 Undamped natural frequency

Is the natural frequency of a rotor-support system without any presence of damping or liquid effects. The location of natural frequency thus depends on the rotor- and support stiffness.

#### 3.1.2 Damped natural frequency

Is the natural frequency of the rotor-support system when all sources of damping are included. Damping is in this perspective energy absorbing effects. The relationship between damped natural frequencies and rotational speed is normally presented in rotordynamic analyses as a "Campbell diagram", see Figure 1.

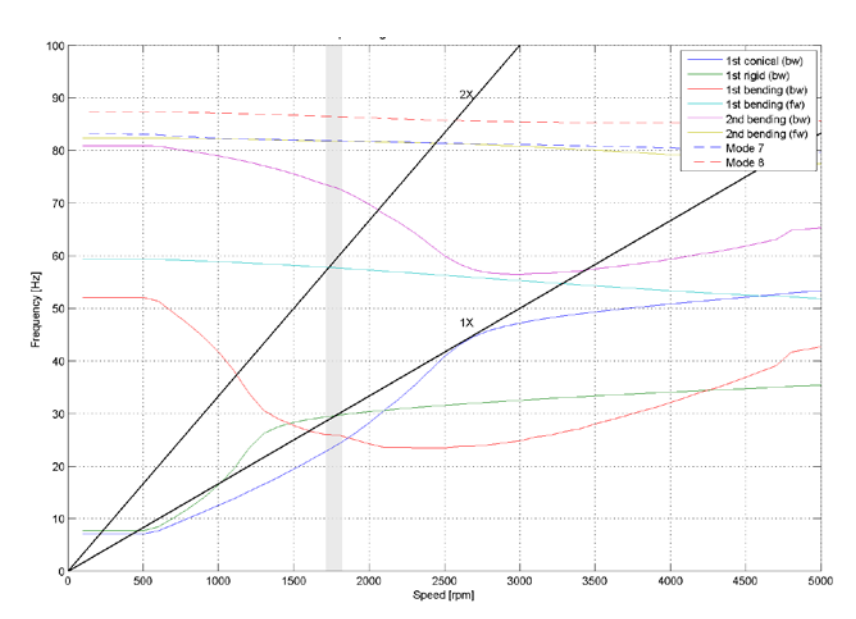


Figure 1. Example of a "campbell diagram" for a rotor which relates the damped natural frequencies (y-axis) with rotor speed (x-axis).

As a complement, the Campbell diagram with damping instead of the natural frequency on the vertical axis is sometimes presented. This is a helpful addition to evaluate the damping and thus the stability properties of the system.

#### 3.1.3 Torsional natural frequency

Is the natural frequency in the torsional domain. The torsional natural frequencies consider a complete system, i.e. pump + driver rather than single shafts.

## 3.2 Critical speed

A critical speed is the shaft rotational speed at which the rotor system is in a state of resonance [7], i.e. when the rotational frequency coincides with a natural frequency. Note that resonance can be with rotor modes, support structure modes or a combination.

## 3.3 Separation margin

Is the margin between critical speeds (or natural frequencies) to the operational speed range.

# 3.4 Unbalance response analysis

An unbalance response analysis is a rotordynamic analysis where a rotating mass is added at positions along the rotor suspected to excite the natural frequency mode shapes. A speed sweep is thereafter performed which

produces Bode plots, see Figure 2. These plots are used to determine the location (speed), separation margin and amplification factor (damping) of critical speeds.

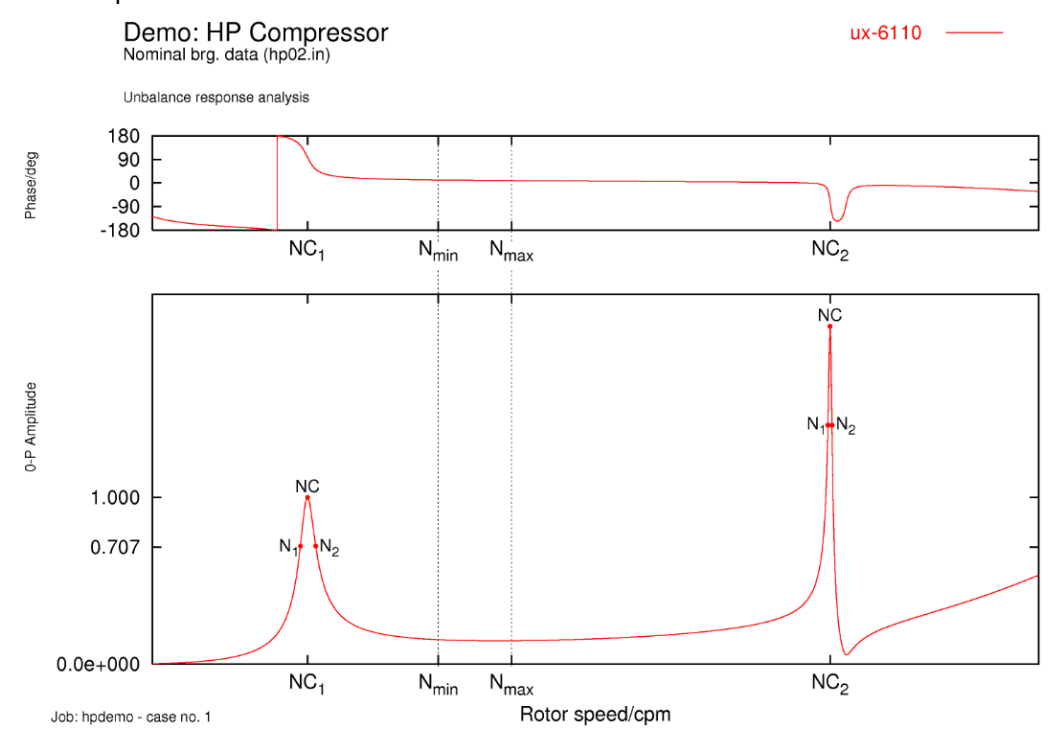


Figure 2. Typical bode plot for a supercritical rotor showing the rotor response and phase versus speed. NC: critical speed.  $N_{min}$  and  $N_{max}$  are the minimum- and maximum operational speed.

#### 3.4.1 Stability analysis

A stability analysis investigates the rotors susceptibility to become in an instable condition, where the internal forces drive the rotor to steadily increasing vibration. The key parameter for the evaluation is the total resulting damping of the rotors natural frequencies, which is extracted from the analysis. The dynamic reaction forces from bearings, seals, impellers etc. at conservative, worst-case configurations are usually included.

By studying the amount of damping present, judgement can be made on the stability. This phenomenon is primarily an issue for flexible and supercritical rotors, i.e. rotors operating above its 1<sup>st</sup> critical speed. Typically, subsynchronous vibrations from flow related excitations can trigger the rotors natural frequency.

# 4 Common rotordynamic problems on water pumps

LR Consulting has provided consulting services on rotating equipment for more than 25 years. This section strives to make use of this experience and list common problems seen on pumps in the industry.

The main failures in pumps occur from fatigue or rubbing between rotor and stator. Up to 90 % [1] of all pump failures are in some way related to:

- Rotor unbalance
- Driver/pump misalignment
- Hydraulic forces
  - × Recirculation stall
  - × Vane pass pressure pulsations
- Natural frequency excitation (both lateral and torsional)

It should be noted that all of the above problems can have several causes, but it is proven that many of them can be avoided with proper analyses performed already at the design stage. If a failure does occur, a mechanical failure analysis of the pump and rotor parts will provide good insight to what has gone wrong.

#### 4.1 Potential problem sources

Several machine elements in a rotordynamic system may affect the dynamics. Below follows a compilation machine elements or design features that, if poorly designed can cause problems during operation.

#### 4.1.1 Seal forces

The annular seals on pumps affect the rotors dynamics by adding stiffness to the rotor which affects the rotor natural frequencies. This is commonly called "the Lomakin Effect", and for multistage pumps these effects can be strong and must be accounted for in rotordynamic analyses. The seals also contribute with damping, and sometimes inertia. The damping, inertia and the Lomakin effect sometimes causes cross-coupled terms in the stiffness- and damping matrices. These cross-coupled terms are what causes rotor instability. As the seals wear, the dynamic properties of the rotor system change which is a common source of problems for pumps.

#### 4.1.2 Impeller forces

The Impeller can cause direct and cross-coupled reaction forces on the rotor due to the static pressure distribution around the impeller. For high-speed pumps with low damping, these forces may cause instability of the rotor system. Also, dynamic pressure variations due to vane passes are well known and may trigger structural resonances of the skid and support system at the vane pass frequency and its harmonics (integer multiples).

#### 4.1.3 Bearings

The effects of bearing dynamics shall be differentiated between oil film journal bearings and rolling element bearings. Many designs of journal bearings exist, where plain journal bearings may cause instability due to high cross-coupled forces. These forces are eliminated in the tilt-pad design and commonly used in high-speed applications.

Rolling element bearings are common for small- and medium sized pumps. They may fail due to overload or fatigue, but use of condition monitoring may reveal problems by means of envelope detection and spectral analysis.

#### 4.1.4 Fluid forces

The added mass from the pumped liquid will increase the rotating inertia of the system in several ways. The liquid inside the impeller adds mass, and so do the fluid surrounding the impeller which is "squeezed" and displaced by the axial and radial forces. For rotordynamic analyses, these effects are normally included, and calculations are performed in "wet" and "dry" conditions to assess the influence on the dynamics.

#### 4.1.5 Stall

When the pump is operating at flow rates below the BEP (Best Efficiency Point), the flow incidence angles on the impeller vanes are different from optimum design. This loads up the vanes and can in extreme cases cause stall, which is characterised by formation of vortices in the impeller or diffuser. This creates sub-synchronous vibrations, i.e. with frequency contents below the rotational frequency, which can be very strong in nature.

#### 4.1.6 Gear box torsional excitation

A gear box will inevitable create torsional excitation forces in a rotating string. This excitation (and its harmonics) can match the torsional natural frequencies and subject the shafts and coupling to very high torques. In gear box systems coupling of bending and torsion is also possible.

#### 4.1.7 Electric motor torsional excitation

For electric induction motors, torsional excitations occur at 1X and 2X the line frequency which may trigger torsional natural frequencies. For variable frequency drives (VFD), additional inter-harmonic frequencies can excite torsional natural frequencies. The specific harmonics depend on the design of

the VFD. Further, energization or short-circuiting of the motor may cause transient events that can force the pump string into a torsional resonance and cause heavy loads on the couplings.

#### 4.1.8 Rigid couplings

For small, and medium-sized pumps, it is common that pump and driver are delivered with a non-flexible (rigid) coupling. These packages can be dynamically problematic since the rotor natural frequencies are a combination of both driver- and pump shafts rather than individual rotor modes. This has to be considered already in the design phase. Also skid stiffness may influence the dynamics and should ideally be considered in the analysis. It is however common that the package provider (for instance the pump manufacturer) provides calculations of only the pump, which can lead to unforeseen vibration problems during commissioning.

## 4.2 Rotordynamic problems in the nuclear industry

On 23 September 2013, representatives from the nuclear industry and LR Consulting met at Elforsk premises in Stockholm, with the purpose of outlining common rotordynamic problems specific for the nuclear industry, see Appendix A. Employees from FKA, Fortum, Elforsk, TVO, RAB and OKG were present.

FKA mentioned possible problems with the critical speed located to close to the operating speed range on one pump. OKG had recently changed the impeller on one major pump which led to vibration problems. RAB shared problems with system resonances and vibration problems due to electrical motor replacements. TVO also mention some minor vibration issues on some pumps.

In general, the nuclear industry contains a vast amount of pumps in a variety of sizes and ratings. Both vertical-, horizontal-, single stage-, multistage-pumps are represented and it is evident that a broad spectra of vibration related problems can be expected. No statistics of rotordynamic-related failures has been presented to LR Consulting.

# 5 Review of applicable standards

Both for balancing and vibration measurement criteria, the ISO standards are the most commonly used in the industry. In addition to ISO, various trade organizations such as National Electrical Manufacturers Association (NEMA) and American Petroleum Institute (API) have developed and published vibration standards, which are widely accepted and applied (and therefore relevant). In most cases, these standards have been developed by consensus of consumers and manufacturers, and their use is therefore considered voluntary. The present section summarizes a selection of standards with focus on pump rotordynamics.

#### 5.1 TBM

The TBM – Tekniska Bestämmelser för Mekaniska Anordningar [2] is a document authored by the Swedish nuclear companies to serve as a guideline and standard for equipment in the nuclear industry.

The TBM is a governing document for reparations, retrofits and rebuilds for mechanical equipment in the primary system, safety system and production. It does however not cover certain parts, such as:

- Moving parts within turbines, motors and generators
- Lifting equipment
- Mechanical devices used for transportation of nuclear waste
- Etc.

As the field of rotordynamics deals with the rotating parts of the units, it is tempting to assume that the TBM may have limitations with regards to advice on design, testing and purchasing rotating equipment. However, it claims that it can be used "as a guide for repairs, exchanges and the remodelling and construction of mechanical devices, such as mobile and internal machine parts in pumps, valves, turbines and generators".

### 5.1.1 Pump specifics in TBM

Chapter 4.4 in [2] lists the specific requirements with regards to vibration and balancing. The most important bullets are:

- The installed pump (including its skid) shall have no resonances which can disturb the operation:
  - o  $\pm 20\%$  from 1X-, 2X and 1X blade pass frequency and 2X grid frequency
  - The first critical speed shall be at least 25% above the highest operating speed

- Rotors and rotor parts shall be dynamically balanced according to SS ISO 1940-1. The complete rotor shall be balanced according to grade G2.5 and rotor parts according to G1.
- Flexible rotors shall be balanced according to SS-ISO 11342. The surfaces shall be checked for misalignment which normally should not exceed 0.03 mm TIR (Total Indicator Reading)
- For a fully installed pump, the maximum allowed bearing vibration level in the operating range shall follow the guidelines outlined in SS-ISO 10816 for zone A (newly installed pump). The pump shall however not exceed 2.8 mm/s RMS in all horizontal, vertical or axial directions.
- For low speed rotors such as the main cooling water pumps, the maximum allowable vibration level is 1 mm/s RMS

Section 4.4.3.1. of TBM contains some additional requirements on the rotating parts:

- Impellers larger than Ø250 mm or with a diameter/length ratio larger than 10 shall be dynamically balanced according to SS-ISO-1940-1.
   The specific balancing grade is not mentioned here.
- Rolling element- or plain bearings shall be designed with a fatigue life
   50 000 hours

#### 5.1.2 Documentation

Section 4.4.7 in TBM specifies the required documentation in the proposal-, manufacturing- and delivery stage of pump procurement. The listed documentation holds little requirements on documentation of vendor rotordynamic reports, such as lateral or torsional analysis of pump and the train. Only the "critical speeds" are listed as required documentation before the manufacturing.

#### 5.2 API 610

The API (American Petroleum Institute) standards are a collection of the American oil & gas experience in a set of standards which are machinery specific. This means that unique standards have been developed for pumps, compressors, motors etc. The standards contain for example guidelines and requirements with regards to balancing, testing and calculation.

API610 [7] is the standard which is specific for centrifugal pumps. Other API standards are:

API546 Brushless Synchronous Machines – 500 kVA and larger

API617 Axial- and centrifugal compressors
 API613 Special purpose Gear Units
 API618 Reciprocating compressors
 API611 General-purpose Steam Turbines
 API684 Standard paragraphs rotordynamic tutorial

#### 5.2.1 Classification

API 610 classifies the pumps in three main categories with subcategories: 'Vertically suspended' (6 types), 'Between-bearing' (5 types) and 'Overhung' (7 types). Some of the pump designs have individual requirements regarding design specifics.

The standard denotes pumps with heads greater than 200 m or more than 225 kW/stage as 'high-energy' pumps and specifies that provisions shall be made to ensure vibration issues from vane passing and low-flow situations see section 6.1.15 in [7].

Single or two-stage pump rotors shall be designed so the first dry critical speed<sup>1</sup> is located at least 20% above maximum continuous speed, see 6.9.1.2 in [7].

At worst case conditions, the total deformation under the primary seal faces shall not exceed 50  $\mu$ m. For single or two-stage pumps, no stiffening effect of impeller wear rings from the liquid shall be considered whereas it shall be considered for multistage pumps.

#### 5.2.2 Lateral analysis

Section 9.2.4.1 of [7], a screening criterion for 'Between bearing' pump designers are presented. It essentially states that a lateral analysis is necessary if the conditions in Table 1 are fulfilled.

#### A lateral analysis shall be performed if:

The pump and operation conditions in service are unique (i.e. no existing similar pump)

The rotor has its first dry critical speed

- Located less than 20% above the MCOS and designed for wet running only
- located less than 30% above the MCOS for rotors designed to be able to run dry

Table 1. API 610 criteria for performing lateral analysis on pumps

\_

<sup>&</sup>lt;sup>1</sup> Dry critical speed is the predicted critical speeds with no fluid effects and on infinitely stiff bearings.

The lateral report shall contain the following information (API610, Annex I):

- a) Result of initial assessment (does the analyses predict any critical interactions with running speed?)
- b) Fundamental rotor data
- c) Campbell diagram, see Figure 3.
- d) Plot of damping ratio vs. frequency ratio<sup>2</sup>, see Figure 4.
- e) Mode shape at the critical speeds where damped response is evaluated
- f) Bode plots from shop verification tests
- g) Summary of analysis corrections to reach agreement with shop verification

Items e)-g) are only necessary if the screening analysis requires it, or if the purchaser specifies this.

The model shall include stiffness and damping effects of seals and bearings. Added mass from the liquid shall be included for multistage pumps. For one-or two stage pumps, it is however not necessary to account for stiffening effects of impeller wear rings, see section 6.9.1.3. in reference [7].

<sup>&</sup>lt;sup>2</sup> Frequency ratio is the natural frequency divided by the running speed.

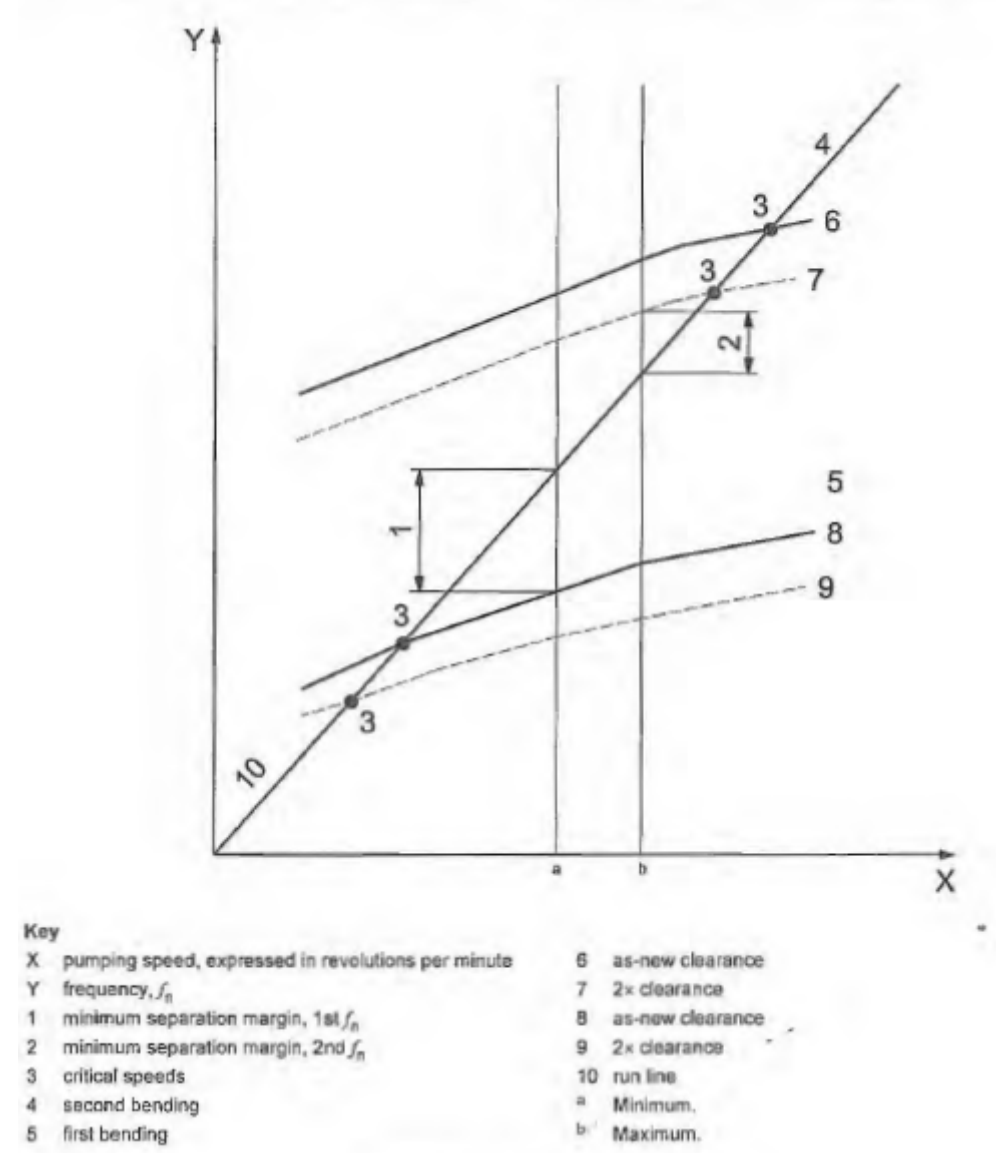


Figure 3. Example of Campbell plot which reveals the change in damped lateral natural frequency versus the running speed. Points 1 and 2 represent the minimum separation margins to the running speed. A short explanation of the numbers in the diagram is listed in the bottom of the figure. More information is found in [7]. Cited from [7].

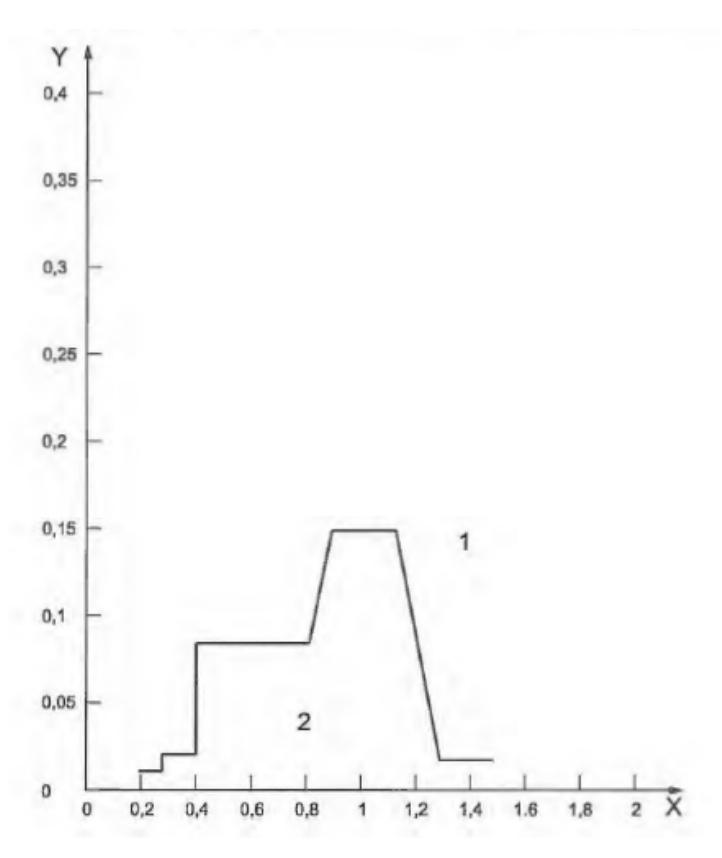


Figure 4. Damping factor (Y) vs. frequency ratio (X). If the analysis falls within zone 2, a lateral response analysis shall be performed. Cited from [7].

#### 5.2.3 Torsional analysis

Section 6.9.2 of API 610 covers torsional analysis on pump trains. The standard presents a screening flow chart which can be used to determine whether or not a train torsional analysis shall be provided with the pump train. In general, trains with electrical drives are more susceptible to torsional excitations, but vane pass frequencies, gear mesh frequencies etc. are also potential sources for torsional vibration in pump trains. The standard suggests three main analyses to be performed:

#### 1. Undamped natural frequency analysis

The purpose of this analysis is to predict the systems torsional natural frequencies and check for potential interferences in a Campbell diagram, see Figure 5. All torsional natural frequencies shall be separated from any possible excitation frequency in the operating range with  $\pm 10$  %.

#### 2. Damped harmonic response analysis

This analysis evaluates whether a potential torsional conflict can cause damaging torsional response in the system, mainly in the couplings. The train is subjected to a known dynamic torque excitation and the response amplitude and damping are extracted from different axial positions along the train.

#### 3. Transient response analysis

For trains with electrical drives, a transient event (e.g. short circuit) can cause heavy loads on the couplings. These analyses evaluate such events.

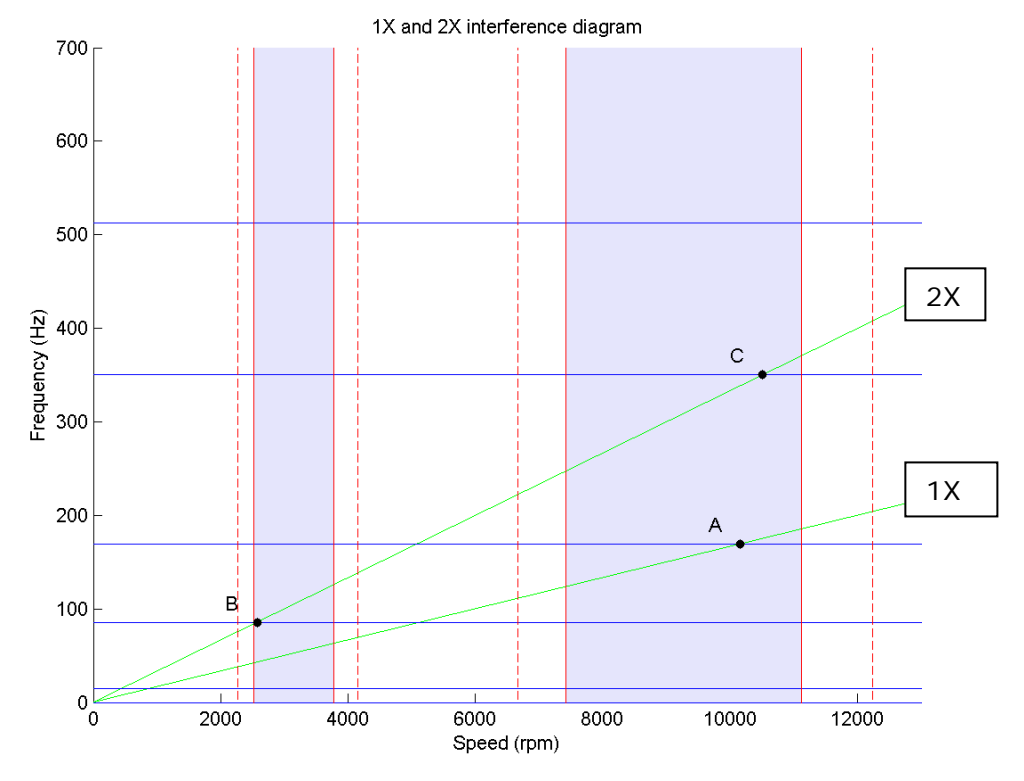


Figure 5. Example of Campbell diagram used for undamped natural frequency analysis. The interferences (A,B,C) are examples where the natural frequencies (blue horizontal lines) conflict with the 1X- and 2X frequencies (green lines). The dashed lines are  $\pm 10\%$  lines from the operating ranges.

#### 5.2.4 Vibration levels

API 610 reasons that the vibration level of a pump can be divided in two regions: the "preferred operating region" and the "allowable operating region". The "preferred" region is located around the 'best efficiency point'. Figure 6 depicts this. API suggests that the "allowable" operating region shall be explicitly stated in the vendors tender.

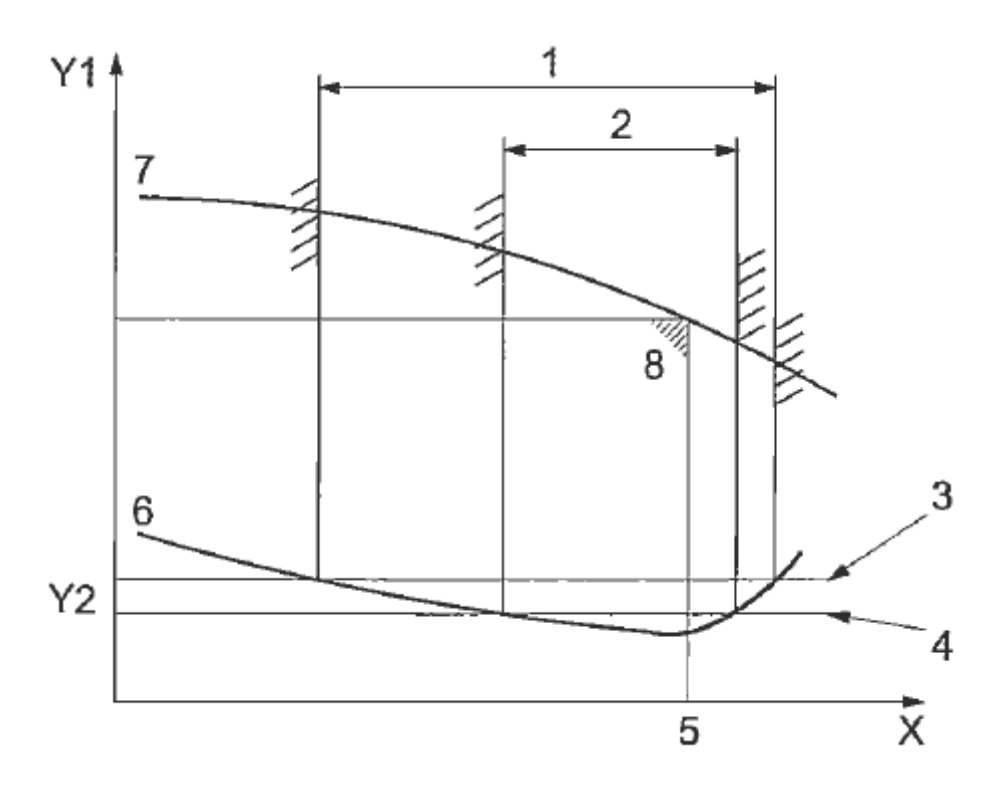


Figure 6. Head (Y1) vs. Flow (X) and associated vibration response (curve 6). (1) is the "allowable" region and (2) is the "preferred" region. Lines (3) and (4) are the vibration limits corresponding to these regions. (5) is the 'best efficiency point'. Cited from [7].

The API 610 also presents figures of the different pump types with recommended measurement positions during performance testing of the pumps. If the unit is equipped with hydrodynamic bearings and radial proximity probes, measurement data shall also be recorded at these positions. If the rotor is equipped with radial proximity probes, these shall be guaranteed to have less combined runout than 25% of the allowable peak-to-peak vibration amplitude or 6  $\mu$ m, whichever is smaller. For axial probes, the limit is 13  $\mu$ m. The combined (mechanical and electrical) runout shall be properly documented and can be vectorial subtracted from vibration levels during the test.

From each measurement position, a FFT spectrum from 5-1000 Hz shall be provided at each test point except shutoff. Optionally, the upper spectrum frequency range can be increased to  $2\cdot Z$ , where Z is the number of vanes on the impeller. If it is a multistage pump, Z is the highest number of vanes in any stage. The bearing housing measurements shall be presented in [mm/s] RMS and the shaft displacement shall be presented in [ $\mu$ m] Peak-Peak.

The vibration limits are differentiated based on the pump classifications as explained in Section 5.2.1. Table 2 summarize these limits for the overhead, between bearing-, and vertical type pumps operating within the "preferred" operating region, as stated in Figure 6 above. API 610 allows for additional 30% vibration limit increase outside the 'preferred' region, but inside the

'allowable' region. For 'high energy' pumps, the limits shown in Figure 7 are governing.

Apart from the limits presented in Table 2 and Figure 7, the vibration levels above the maximum continuous speed up to trip speed shall not exceed 150% of the vibration reading at MCOS.

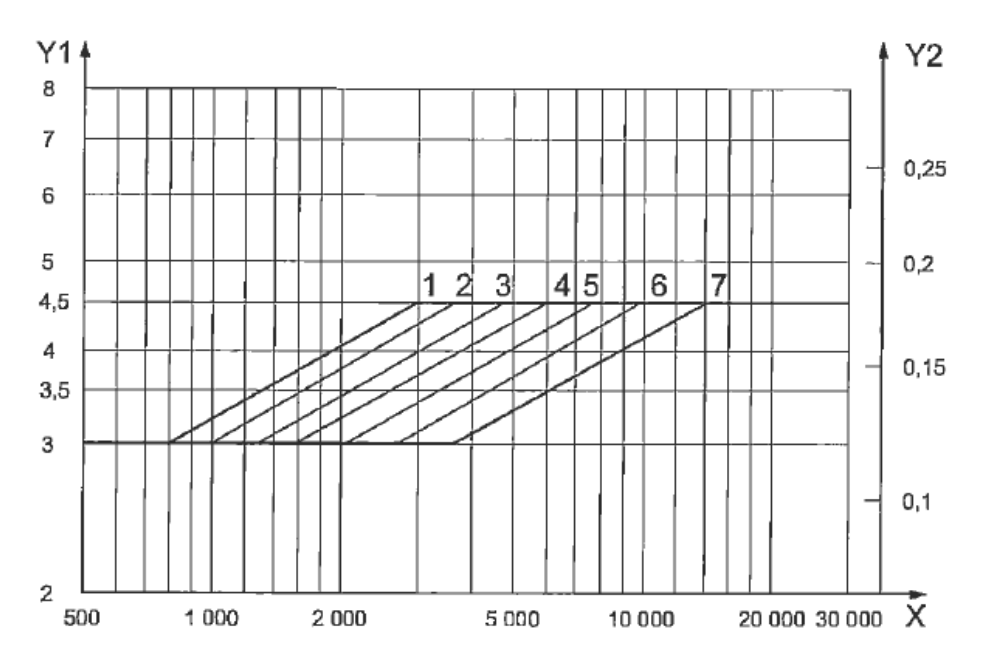
	Bearing housing measurements			
Classification	Overhung	Between bearing	Vertical	
Overall Velocity				
[mm/s] RMS	3 (3.9)	3 (3.9)	5 (6.5)	
At discrete frequencies				
[mm/s] RMS	2 (2.6)	2 (2.6)	3.4 (4.4)	
	Pump shaft measurements			
Classification	Overhung	Between bearing	Vertical	
Overall Displacement				
[µm] PP	50 <sup>3</sup> (65)	50 <sup>1</sup> (65)	100 <sup>4</sup> (130)	
At discrete frequencies				
below running speed				
[µm] PP	16.5 (21.5)	16.5 (21.5)	33 (42.9)	

Table 2 API 610 vibration limits at any flow within the pumps 'preferred' operating region. Please note that outside the 'preferred' region, but inside the 'allowable' region, the vibration levels can be increased with 30% for all cases which is indicated by the levels in brackets ().

-

<sup>&</sup>lt;sup>3</sup> The criteria applies for speeds below 2080 rpm, above 2080 rpm the vibration level shall be  $< (5200000/n)^{0.5}$  where n is the operating speed

<sup>&</sup>lt;sup>4</sup> The criteria applies for speeds below 620 rpm, above 620 rpm the vibration level shall be  $< (6200000/n)^{0.5}$  where n is the operating speed



#### Kev

- X rotational speed, expressed in revolutions per minute
- Y1 vibrational velocity, expressed in millimetres per second, RMS
- Y2 vibrational velocity, expressed in inches per second, RMS
- 1 P ≥ 3 000 kW/stage
- 2 P = 2 000 kW/stage
- 3 P = 1 500 kW/stage
- 4 P = 1 000 kW/stage
- 5 P = 700 kW/stage
- 6 P = 500 kW/stage
- 7 P ≤ 300 kW/stage

Figure 7. Vibration limits for 'high energy pumps', i.e. pumps running above 3600 rpm or absorbing more than 300 kW per stage. Cited from [7].

#### 5.2.5 Balancing

API610 recommends that the main rotating bodies, such as impellers, thrust collars and balance drums are balanced according to ISO grade G2.5. Although it may be possible to realize balancing at grades below G2.5, the mass eccentricity, *e*, associated with such balance grade are so small, the balanced part may not show repeated results when dismounted and reassembled in a balancing machine.

#### 5.3 ISO

The ISO standards are commonly used in a wide range of industries, both for products, services and good practice. For pump applications, the ISO 1940 [3] covers the balancing requirements of rigid rotors. ISO 10816-3 [4] covers guidelines on measuring non-rotating parts for >15kW Industrial machines and was historically used for pumps. ISO 10816-7 [4] is currently used for pumps and the latest version was issued 2009.

#### 5.3.1 ISO 1940

The ISO 1940 contains an overview of the balancing of rigid rotors. A rigid rotor is for many applications such as pumps a good assumption as the critical speed of the rotor is located above the operating speed range. The API 1940 states that after balancing (in one or two planes) the rotor shall not exceed the balancing tolerances at any speed up to maximum service speed.

The ISO standard use "quality grades" in order to distinguish between different applications. The grading is based on the idea that the allowable displacement in the mass centre of the rotor times the rotating speed should be constant:

$$G = e_{per} \times \omega$$

 $G = e_{per} \times \omega I.e.$  as the speed  $\omega$  [rad/s] increase, the rotor displacement  $e_{per}$  [mm] must decrease to keep G constant.

#### 5.3.2 ISO 11342

For balancing of flexible rotors, such as large multi-stage pumps with between bearing designs, the rigid approach may be inadequate since the bending of the rotor can increase the vibration level of the rotor at speeds below the operating speed range. In such cases, the ISO 11342 [5] which is applicable for flexible rotors may be used as an amendment to ISO 1940.

#### 5.3.3 ISO 10816 - part 7

For testing, operational and troubleshooting purposes, the ISO 10816 may be used. It covers techniques on evaluating vibration by measurements on non-rotating parts. The standard consist of seven parts where part 7 [4] is applicable for most pump machinery found in nuclear plants. Note that torsional vibrations are not covered in the standard.

The standard applies to pumps with rating "... above 1 kW ". Guidelines for measurements both on site and at manufacturers test shops are presented. For other machinery such as compressors, drivers etc., part 3 of ISO 10816 are applicable. Also, reciprocating pumps are not included in this standard.

The standard specifies that the measurement quantity to use shall be [mm/s] RMS, but for speeds below 600 rpm, displacement measurements [ $\mu$ m] PP shall be provided at 0.5X, 1X and 2X, see Table 5. Details on the measurement equipment, sensor mounting techniques and data logger settings are given.

Measurements shall be taken at nominal steady state conditions (flow, temperature etc.) and within the 'Preferred operating range', see Figure 6. The 'preferred' and 'allowable' operating range shall be specified by the pump manufacturer and in line with the user's specifications.

The vibration level evaluation is classified in two parts:

- 1. Vibration magnitude
- 2. Change in vibration magnitude

It should be underlined that the vibration criteria does not apply at transient conditions, such as resonance, start-up and shut-down. Thus it may be necessary to allow intermittent increase of vibration levels during these events. It should however still be assured that running clearances are not exceeded, i.e. rubbing should be prevented. It is therefore recommended that for bearing vibration, the maximum vibration velocity during transient operations shall be below the upper boundary of zone C, see Table 3. For measurements on rotating parts, ISO 7919 [6] shall be used, see Section 5.3.5 below.

#### Vibration magnitude

Four zones (A,B,C,D) divides the machinery in decreasing severity grade where zone A represent "newly commissioned machines" and zone D are "levels of sufficient severity to cause damage to the machine".

The machinery itself is divided in two main categories:

- Category I: Rotordynamic pumps with high reliability, availability or security requirements
- Category II: Rotordynamic pumps for general or less critical applications

The vibration evaluation chart is shown in Table 3. For acceptance tests, the standard also presents vibration acceptance levels, see Table 4. As seen in the charts, higher demands on vibration levels are expected from the category I type pumps. Further, pumps with higher rating are allowed slightly higher vibration levels.

	Category I [	mm/s] RMS			Category II	[mm/s] RMS
	< 200 kW	> 200 kW			< 200 kW	> 200 kW
	D				D	
7.6 <sup>1</sup>				9.5 <sup>↑</sup>		
6.5 <sup>†</sup>	С			8.5 <sup>†</sup>	С	
5 <sup>†</sup>				6.1 <sup>↑</sup>		
4 <b>^</b>	В			5.1 <sup>1</sup>	В	
3.5 <sup>†</sup>				4.2 <sup>1</sup>		
2.5 <sup>†</sup>				3.2 <sup>†</sup>		
	Α				Α	
	Newly comm	nissioned mad	hines			
Unrestricted long term opera			eration			
Restricted long term opera			ation			
Vibration causing damage						

Table 3. ISO 10816 – part 7 over-all vibration criteria in mm/s RMS, for pumps in category I and II.

		Cateo	gory I	Category II	
		< 200 kW	> 200 kW	< 200 kW	> 200 kW
In situ	POR	2.5	3.5	3.2	4.2
acceptance test	AOR	3.4	4.4	4.2	5.2
Factory	POR	3.3	4.3	4.2	5.2
acceptance test	AOR	4	5	5.1	6.1

Table 4. ISO 10816 – part 7 over-all vibration criteria in mm/s RMS, for acceptance testing of pumps. POR: preferred operating region; AOR: acceptable operating region

Zone	Decription	Displacement [µm] PP
Α	Newly commissioned machines	≤ 50
В	Unrestricted long term operation	≤ 80
С	Limited operation	≤ 130
D	Hazard of damage	≤ 130

Table 5. ISO 10816-part 7 additional criteria for slow speed pumps (<600 rpm). Displacement values shall be filtered at 0.5X, 1X and 2X running speed.

#### Change in vibration magnitude

If a reference value for vibration has been established, continuous or repeated spot measurements at the same machine position may reveal intermittent increase in the vibration levels. If the vibration level at any position exceeds 25% of the zone B boundary in Table 4, action shall be taken to troubleshoot the excitation source and propose possible actions.

#### 5.3.4 ISO 10816 - part 3

For machinery not covered in the part 7 of ISO 10816, part 3 shall be used.

Instead of pointing out specific machine positions, the standard contains general information about measurement techniques and recommended practice on how to perform successful diagnostics on machinery.

Machinery is classified according to:

- 1 machine type, rated power or shaft height
- 2 support system flexibility

For point 1 the machinery are subdivided in four groups.

Point 2 represents a differentiation between flexible and rigid machinery support. If the systems (support + rotor) lowest natural frequency in one direction is 25% higher than its main excitation frequency, then the support can be considered rigid in that direction. If not, the support is denoted flexible.

For large and slow units, the rigid support assumption is normally the valid approximation. It should however be noted that a system may be rigid in one direction and flexible in the other. The classification of machinery can

normally be performed with rotordynamic calculations or through measurements.

The vibration level evaluation is classified in two parts:

- 3 Vibration magnitude
- 4 Change in vibration magnitude

#### Vibration magnitude

For part 1, four zones (A,B,C,D) divides the machinery in decreasing severity grade where zone A represent "newly commissioned machines" and zone D is "levels of sufficient severity to cause damage to the machine". Table 6 summarize the criteria for the two groups applicable to pumps. The levels listed in the table shall be read at rated flow. As vibration levels can increase at flow rates higher or lower than rated, increased vibration levels may be accepted for short term operation.

ISO 10816-3	Zone boundary		ocity s] RMS	Displacement [µm] RMS	
		Group 3	Group 4	Group 3	Group 4
Rigid	A/B	2.3	1.4	18	11
	B/C	4.5	2.8	36	22
	C/D	7.1	4.5	56	36
Flexible	A/B	3.5	2.3	28	18
	B/C	7.1	4.5	56	36
	C/D	11	7.1	90	56

Table 6. Vibration criteria from ISO 10813, part 3. Group 3 covers pumps with separate drivers whereas group 4 covers pumps with integrated drivers. The levels are measured at the positions of radial and axial bearings at the rated flow rate of the pump.

#### Change in vibration magnitude

If a reference value for vibration has been established, continuous or repeated spot measurements at the same machine position may reveal intermittent increase in the vibration levels. If the vibration level at any position exceeds 25% of the zone B boundary in Table 6, action shall be taken to troubleshoot the excitation source and propose possible actions.

#### 5.3.5 ISO 7919

ISO 7919 [6] contains shaft vibration criteria of non-reciprocating machines. The machinery classification covers machinery with higher speed rating (1000-30 000 rpm) than what is covered in ISO 10816 (Section 5.3.3), i.e. the standard is applicable to turbopumps equipped with proximity probes. The evaluation zones are however similar to ISO 10816 (A,B,C,D) and corresponding limits are presented in Table 7.

Zone boundary	Displacement [µm] PP
A/B	4800/( <i>n</i> ) <sup>0.5</sup>
B/C	9000/( <i>n</i> ) <sup>0.5</sup>
C/D	13200/( <i>n</i> ) <sup>0.5</sup>

Table 7. ISO 7919 shaft vibration evaluation criteria for pumps rotating above 1000 rpm up to 30 000 rpm. *n* is the rotational speed in [rpm]

#### 5.3.6 ISO 13373

ISO 13373 [8] provides general guidelines for the measurement of machinery vibration for condition monitoring. Recommendations are provided for the following:

- measurement methods and parameters
- transducer selection, location, and attachment
- data collection
- machine operating conditions
- vibration monitoring systems
- signal conditioning systems
- · interfaces with data processing systems
- continuous and periodic monitoring

#### 5.4 NORSOK

The NORSOK standards are widely used in the Norwegian Oil & Gas Industry. The standard "Mechanical Equipment" [9] describes the technical requirements for design, installation, testing etc. of mechanical equipment. For pumps, the standard reference is API 610 for centrifugal pumps and NFPA 20 for centrifugal fire pumps.

#### 5.5 DIN

The DIN (Deutches Institut für Normung) is a German non-profit association which organize, steer and moderate procedures and standards for the German federal government.

For vibration on pumps, the DIN use ISO 10816, Part 7, [4] which is thoroughly described in Section 5.3.3 above.

# 6 Discussion

#### 6.1 Vibration levels

The vibration level limits vary depending on which standard is used. TBM specifies that the vibration criteria shall be based on SS ISO 10816, but with 2.8 mm/s RMS as a maximum level. It does however not clearly state which edition or part of the ISO 10816 is to be used. If the latest version for pumps are used (part 7, 2009), this means that all pumps except Category I pumps < 200 kW shall be limited to 2.8 mm/s RMS. This means that the TBM contains small amount of pump categorization, and that less critical pumps may have too conservative limits on vibration levels.

In API 610, the vibration levels are more categorized with differentiated vibration levels based on the operating region as well as the type of pump (Overhung, Between bearing or Vertical). Further, a separate criterion is outlined for high energy-pumps with ratings above 300 kW/stage or running above 3600 rpm. For all cases, allowed velocity is at least 3 mm/s, hence higher than what is stated in TBM.

The TBM does further not state any settings on measurement equipment, or whether the vibration levels are overall or discrete frequency. The latter is of high importance as many flow related or misalignment issues may be discovered by looking at non-synchronous vibration components.

It should also be mentioned that vibration limits are not exact science. There exist pumps which are equipped with non-standard impellers and/or support with operational conditions where the acceptable vibration level may not be suited to evaluate against a specific standard. For these situations, the limits must be agreed upon between vendor and buyer.

# 6.2 Motivation for rotordynamic analysis

During procurement of pumps, it is important to differentiate between critical and non-critical units as well as "custom made" and "standard" pumps.

From a vendor's perspective, a driving factor when producing and selling pumps is to make a profit while maintaining competitive selling rates. This can have effect on the engineering efforts in custom projects. Systematic rotordynamic analyses may be omitted due to the extra cost, with the motivation being that the vendor has 'sufficient experience' to predict successful commissioning and operation of pumps without proper analysis.

For custom-made pumps, the end user must be aware of the possible pitfalls involved with new designs. Seemingly small modifications, such as replacement of couplings, bearings, seals etc. may have a large effect on the rotordynamics of the system. Larger rebuilds, such as impeller-, driver- or rotor replacement shall be thoroughly evaluated with rotordynamic analysis. If such analyses has already been performed during the original installation, the original rotor numerical model exist whereby small modifications (e.g.

coupling exchange, change of oil type, added mass, new rotor diameter, etc.) can easily be made and new analysis done with little effort.

For 'standard' or 'off the shelf' pump packages with small ratings, the motivation for full rotordynamic analysis may not always be needed as the packages likely have been tested and optimised with years of vendor experience. Care should however be taken when purchasing new packages not tested *in situ*. If the pump is located in the vicinity of other large machinery, or in groups of several identical pump packages, structural resonances and foundation flexibility can influence the pumps. Other rotating equipment may have forcing frequencies which conflicts with rotor natural frequencies.

#### 6.2.1 API 610 requirements

The API 610 is the only standard which thoroughly describes lateral- and torsional calculations of pumps. The user may refer to a screening criterion (see Table 1) to decide whether or not to perform lateral analysis. For torsional analysis, a screening chart is presented to aid the user in a decision.

As a rule of thumb, the main motivators for performing rotordynamic analyses are:

- Pump operational criticality a high demand on uptime motivates rotordynamic calculations
- Pump rating higher rating often means higher risk of stability problems
- New designs for newly designed and custom made pumps, it is essential that proper rotordynamic analyses is performed to assure that the pump and supporting structure are well designed
- Revamps when modifications are performed on the pump rotor or the main supporting structure a rotordynamic analysis will show the effect such modification have on the operation. If this is combined with measurements prior to rebuild, the original rotor model may be finetuned to comply with actual vibration levels, damping etc.
- Troubleshooting if repeated operational difficulties or failures occur on a pump, the user is forced to initiate some form of troubleshooting or MFA (Mechanical Failure Analysis) to understand and solve the issue. A rotordynamic model can aid in such situations to extract mode shapes, bearing loads etc.

## 6.3 Third-party analysis

If the end user decides that rotordynamic analysis shall be performed on a new or existing pump, a couple of options exist for the provision:

#### Vendor analysis

The rotordynamic analysis is delivered by the vendor as part of the pump package. The vender use both lateral and torsional calculations as part of their internal design process and is readily available. However, vendor reports may not always comply with API 610,

especially in how information is presented. Often, assumptions on forces from seals, bearings, liquid etc. are based on experience and inhouse knowledge and omitted in the report to maintain company proprietary. Thus, the report may not be readily interpreted by the user. It is customary and often beneficial that the engage a third-party to review the vendor report and highlight any potential problems.

#### Third-party analysis

Third-party analysis shall be presented in transparent reports which clearly present results, boundary conditions, assumptions and theory used for the calculations. Any potential problems shall be highlighted as well as recommendations on how to mitigate the risks in the design. Further, the cost of third-party analysis is normally comparably small in a procurement or revamp budget. The third-party analyst will be unbiased and present results for worst case and conservative situations which may not always be performed by the vendor.

The use of a third-party analysis does however place demands on the user by providing the correct data (drawings, reports etc.) for a proper analysis. A meaningful rotordynamic analysis depends on a correct model with proper boundary conditions. Assumptions made in the analysis must be minimized. The rotordynamic modelling may be a controversial part of the analysis as the user may not have all required information for the pump available in-house while the vendor is reluctant to release drawings and information to third parties. This can be simplified by deciding on third-party analysis already at the first phase of procurement. By specifying data to be supplied by the vendors already in the call for tender, the manufacturers are 'forced' to provide all data together with delivery of the pump.

# 7 Suggested modifications to TBM

This section proposes modifications to the TBM with a clear focus on preventing rotordynamic problems during design-, commissioning- and operation of pumps.

## 7.1 Vibration levels (Section 4.4.4.3)

- Specify more pump classifications in order to differentiate vibration classes. As a minimum, differentiate between critical and non-critical pumps.
- Prior to any presentation of vibration limits, clearly present whether
  the limit reflects overall, synchronous or non-synchronous vibration. If
  the vibration level is overall velocity [mm/s] RMS, state settings on the
  measurement equipment, for instance limited to 10-1000 Hz with
  Hanning filter applied.
- For slow machines (<600 rpm), the vibration criteria shall be in displacement [µm] PP, filtered at 0.5X, 1X and 2X and compared against criteria and limits in ISO 10816-7.

# 7.2 Rotordynamic analysis (New Section)

- Propose OEM-independent lateral- and torsional analysis for new and unique pumps, i.e. pumps which have never been installed on site.
   Prepare the OEM/Vendor for this already at the invitation to tender in order to assure the proper documentation (drawings, data sheets, etc.) are delivered as part of the package
- For major revamps on critical pumps (e.g. skid modifications, bearing, impeller or rotor replacements etc.), suggest 3<sup>rd</sup> party lateral- and torsional analysis to assess the impact such a modification would have on the rotordynamic system
- For revamps on less critical pumps, request the OEM to present calculations which assures that no operational interactions are expected, both lateral and torsional.

## 7.3 Vibration measurements (New Section)

#### 7.3.1 Measurement positions

- The measurement positions on the pump shall conform to positions outlined in Section 6.9.3 in API610 [7].
- If the pump is equipped with a gear box, measurements shall be performed on the gear box. The frequency range setting shall be at

- least 10% above the gear mesh frequency<sup>5</sup>. The spectral content of the gear measurements shall be compared against torsional frequencies.
- If a torsional resonance within the operational range is suspected, torque/stress measurements shall be performed with e.g. strain gauge equipment shall be mounted on the coupling (s), if applicable. This will provide the correct input for fatigue calculations and troubleshooting.

#### 7.3.2 Commissioning of new pumps and revamps

- During commissioning of newly installed pumps and during recommissioning of revamped pumps, it is recommended to perform continuous vibration monitoring on bearing pedestals and shaft proximity probes (if installed).
- The measurements shall be performed at a minimum during start-up, shut-down, at the Best Efficiency point, at low- and high flow conditions.
- Vibration readings shall be evaluated against the limits in Section 4.4.4.3 (TBM) as well as predicted natural frequencies and torsional natural frequencies.

\_

<sup>&</sup>lt;sup>5</sup> Gear mesh frequency: (Number of teeth [-] on pinion or bull rotor) x (Rotating frequency [Hz] of corresponding rotor)

# 8 Rotordynamic analysis

The project scope has included the lateral analysis of two pumps selected by the steering group at Elforsk AB. The features of the two pumps are described below. The actual analyses are stand-alone reports which are found in Appendix B and Appendix C.

# 8.1 Horizontal pump

The main features of this pump are (see also Figure 9)

- Single-stage overhung (API610 type code is OH1)
- Rigid coupling between pump and driver (electric motor)
- Nominal power is 64 kW
- · Pumped fluid is water
- Four bearings (two on pump, two on motor)
- Running speed is 1494 rpm

The complete lateral report of the horizontal pump is found in Appendix B. A summary of the results is found in Section 9 below.

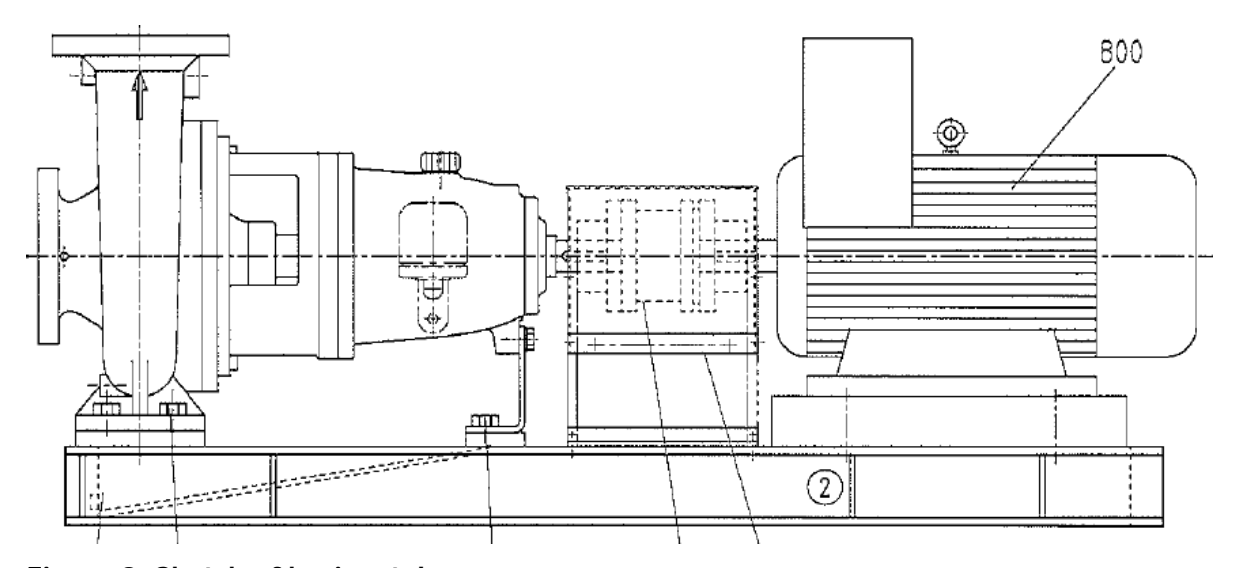


Figure 8. Sketch of horizontal pump.

# 8.2 Vertical pump

The main features of this pump are (see also Figure 9).

- Single-stage axial flow vertically suspended (API610 type code is VS3)
- Nominal power is 406 kW
- Pumped fluid is water
- Three bearings
- Running speed is 371 rpm

The complete lateral report of the vertical pump is found in Appendix C. A summary of the results is found in Section 9 below.

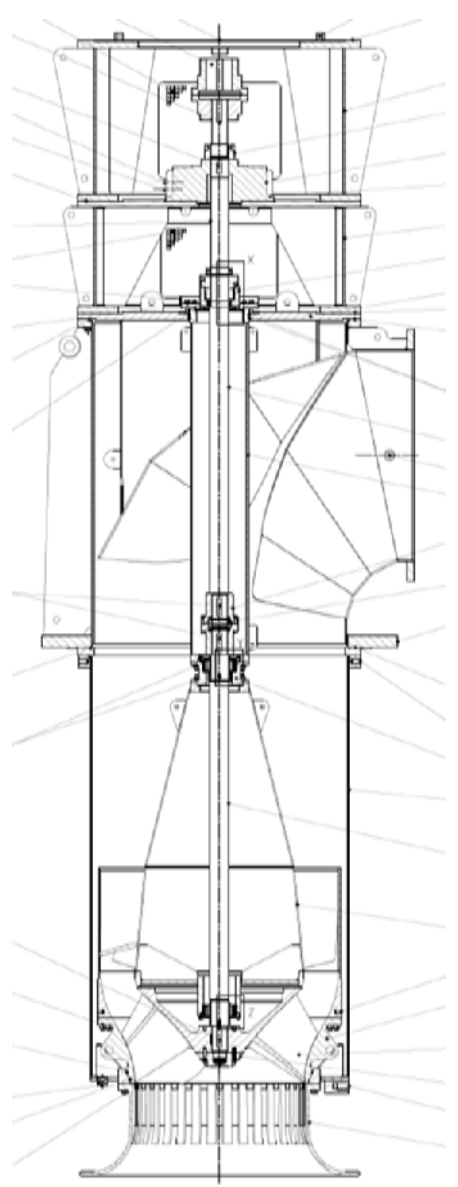


Figure 9. Sketch of vertical pump.

# 9 Conclusions

At the request of Elforsk AB, Lloyd's Register Consulting has performed a rotordynamic evaluation of pumps in the nuclear industry. The TBM standard has been reviewed and compared with other available pump standards. To improve the rotordynamic aspects of machinery dynamics, modifications and additions to the TBM are suggested.

Aside from this, the study has comprised two lateral analyses of pumps; one horizontal- and one vertical pump which were selected by a steering group at Elforsk consisting of representatives from the Swedish plants OKG, FKA, RAB as well as the Finnish plants TVO and Lovisa.

## 9.1 Horizontal pump

The horizontal pump is connected to its driver via a rigid coupling. It is therefore essential to consider the coupled rotordynamic system with both driver and pump included.

The 1st critical speed of the horizontal pump is located at 6228 rpm with a separation margin of 317% compared with the line frequency. The stability calculations show that the pump/motor is within the API criteria of being critically damped. With 4 times the G2.5 unbalance weight, the worst response in the string appears at the motor NDE bearing with response at 0.12 mm/s RMS which is very low compared to the TBM limit of 2.5 mm/s RMS. A clearance check could not be performed as these data were not provided to LR Consulting.

The data provided to LR Consulting was limited, and assumptions based on experience have been made. The supporting skid was assumed rigid, however skid stiffness calculations can be performed in an FE environment to provide improved analysis input.

#### 9.2 Vertical pump

The vertical pumps 1st critical speed is located at 1520 rpm with a separation margin of 310%. The stability analysis and Campbell diagram concluded that the unit is stable at nominal conditions.

With 4 times the G2.5 unbalance weight, the worst response occurs at the mid bearing with levels up to 0.81 mm/s RMS compared to the TBM limit of 1 mm/s RMS for slow running pumps.

The nature of a vertical pump is however intricate since the bearings may be unloaded- or heavily loaded depending on the operational circumstances. This will have large effects on the natural frequencies. Bearing information was not provided to LR Consulting; therefore assumed values of stiffness and damping were used as nominal. Moreover, a parameter variation of the two bottom bearings was performed to identify the influence this had on the natural frequencies of the pump.

The results show that in the event of a sudden stiffness reduction in the two water-lubricated bearing, the systems natural frequencies may be altered such that it conflicts with the operating speed. However, when considering factors such as misalignment, water forces and residual unbalance it is likely that the rotor will load the bearing sufficiently to maintain the support valid for the present calculations.

# 10 References

- [1] "An End User's Guide to Centrifugal Pump Rotordynamics", W.D. Marcher, p69-84, Proceedings of the 23<sup>rd</sup> International Pump Users Symposium, 2007.
- [2] "TBM Tekniska Bestämmelser för Mekaniska Anordningar" Utgåva 6, 2013-06-32, Svenska Kärnkraftsföretagen
- [3] "International standard ISO 1940/1", 1986
- [4] " ISO 10 816-7: Mechanical vibration Evaluation of Machine vibration by measurements on non-rotating parts Part 7: Rotodynamic pumps for industrial application " 2003
- [5] " ISO 11342: Mechanical vibration Methods and criteria for the mechanical balancing of flexible rotors", 1998
- [6] "ISO 7919: Mechanical vibration of non-reciprocating machines Measurements on rotating shafts and evaluation criteria part 3", 1st Edition, 1996
- [7] "Centrifugal Pumps for Petroleum, Petrochemical and Natural Gas Industries", API 610 11<sup>th</sup> Edition, 2010, American Petroleum Institute
- [8] "Condition monitoring and diagnostics of machines Vibration condition monitoring part 1 General procedures", ISO13373, 2001
- [9] "Mechanical Equipment" NORSOK R-001, rev. 3 November 1997.

# Appendix A. Minutes of meeting

# Minutes of meeting

	accs of meeting		
Elforsk	rotordynamic workshop September 23		
Date a 10:00-1	nd time of meeting: 2013-09-23, 14:00	Location:	Olof Palmes gata 31
Date n	ninutes issued: 25 September 2013	Prepared by:	Mattias Lindblad
Minute	es ref: Mattias Lindblad, Revision: 00	Project no.:	13.320179
Particip	ants:	Distribution:	
Carl Mö	ller, OKG		
Farid Ala	avyoon, Forsmark		
Heikki H	aapaniemi, Fortum		
Monika	Adsten, Elforsk		
Niklas Se	ehlstedt, Lloyd's Register Consulting		
Mattias	Lindblad, Lloyd's Register Consulting		
Paul Sm	eekes, TVO		
Petri Len	nettinen, TVO		
Stefan N	Леlby, Ringhals		
Tobias T	örnström, OKG		
Descrip	otion: Description		
No.:	Item		Action
1	Presentation of Lloyd's Register Consultin	9	
2	Round the table, short description of the vibration problems on the different sites.		
	OKG mentioned that they have upgraded water pumps with higher power and cha With slight vibration problems (the pump	nged the impeller	'S.
	3 .	peed is closer tha d questions abou	
	calculated to the running speed. Have had questions about torsional resonances on the upgraded main sea water		

Minutes ref: Mattias Lindblad, Revision: 00

pumps.

RAB Have had issues with -System resonances

-Electrical motor replacements

TVO Vibration related problems with the main circulation pumps and sea water pumps with small vibration issues

Lovisa have Russian pumps without problems

Date: 25 September 2013

Page 1 of 2 ©Lloyd's Register 2013. All rights reserved. 3 The plants were requesting a data list of the input data for rotordynamic calculations. And a short description of the outcome of the analysis. LRC will issue the document before 30/9

Telephone meeting were a decision on which pumps to evaluate will be revealed for LRC.

Nov 5 9:00-11:00

# Lateral rotordynamic analysis

Horizontal pump

Appendix B

Mattias Larsson 4 March 2014

# Summary

At the request of Elforsk AB, a lateral analysis has been carried out on a horizontal overhung cooling water circulation pump. The pump rotor shaft with its bearings and impeller, the coupling and the motor unit has been modelled and analysed with the Lloyd's Register Consulting (LRC) in-house software RP. The investigation has been carried out according to API 610 [1], and includes the items below:

- Undamped critical speed map (UCSM). The undamped natural frequencies are determined against rotor speed and bearing stiffness.
- Stability analysis, *i.e.* a damped eigenvalue analysis. In this analysis the systems tendency towards unstable vibrations is investigated. A Campbell diagram is produced and the ratio between the line frequency and the natural frequencies are investigated against the damping factor.
- Unbalance response analysis. The systems response due to an assumed unbalance is determined. The most severe unbalance cases have been investigated.

#### Results

- The UCSM shows that the pump operates well below the first critical speed. This applies for both minimum and maximum bearing stiffness. The two first dry natural frequencies are 161.4 Hz and 187.8 Hz.
- The Campbell diagram show no resonances throughout the operating speed range set by API (25%-125% of rated speed). The first frequency with minimum bearing stiffness, 103.8 Hz, has a separation margin of 317% compared to the line frequency. This is far above the API recommended value of a 20% separation margin.
- The damping factor vs. frequency ratio analysis show that, between 25% to 125% of operational speed, the first three modes (found at 261 Hz, 153 HZ and 122 Hz respectively for 0.25x- 1x- and 1.25xMCOS) fulfils the criteria of being critically damped according to API.
- The radial velocities at the bearing locations retrieved from the unbalance analysis have been compared against the TBM limit value of 2.5 mm/s RMS [2]. It can be seen that the greatest velocity, with a value of 0.12 mm/s RMS, appears at the motor NDE bearing for unbalance at the motor windings. This is assumed safe since it measures to approximately 4.8% of the allowed TBM value.

The calculated radial displacement values have not been compared against the diametral clearance of the pump unit due to lack of data.

### Model assumptions

No estimation of the stiffness and damping contribution from the foundation plate has been done. The fact that both the pump and the motor are mounted onto the same foundation could cause discrepancies between the results from this analysis and measured vibrations. Due to large margins against the allowed limits, it is however likely that the string will comply with API610 regardless of foundation effects.

#### Recommendations

The analysis shows no risk of interference between the running speed and resonance speeds. It has also been concluded that the system is sufficiently damped for the three first modes, as required by API610. The velocities at the bearing housings are sufficiently low to comply with TBM. No comparison has been carried out regarding the radial displacements of the impeller compared to the diametral clearance as this information has been unavailable. LRC recommends that it is ensured that the calculated displacements at the impeller, as presented in Table 17, does not exceed 35% of the diametral clearance.

# Table of contents

1	Intr	oduction	1
2	Mac	chinery data	2
	2.1	Pump	2
	2.2	Motor	
	2.3	Bearings	
	2.4	Coupling	
	2.5	Mechanical seal	
3	Calc	culation model	7
	3.1	Shafts	
	3.2	Impeller	
	3.3	Bearings	
		3.3.1 Stiffness	
		3.3.2 Damping	
4	Resi	ults	17
	4.1	UCSM	
	4.2	Stability analysis	
		4.2.1 Campbell diagram	
		4.2.2 Frequency ratio vs damping	
	4.3	Unbalance response	
5	Con	clusion	31
	Resu	ılts	
		elling assumptions	
		ommendations	
	11000		
6	Refe	erences	33

# 1 Introduction

At the request of Elforsk AB a lateral analysis of a horizontal cooling water circulation pump has been carried out. The pump is a single stage overhung pump, driven by an induction motor. The coupling is a torsional rigid steel coupling.

Both the pump and motor are mounted onto a steel foundation. On the DE side of the pump the bearing is supported by a thin plate. Neither the dynamic properties of the foundation or the plate are considered during the calculations. A figure of the string and its mounting can be seen in Figure 1.

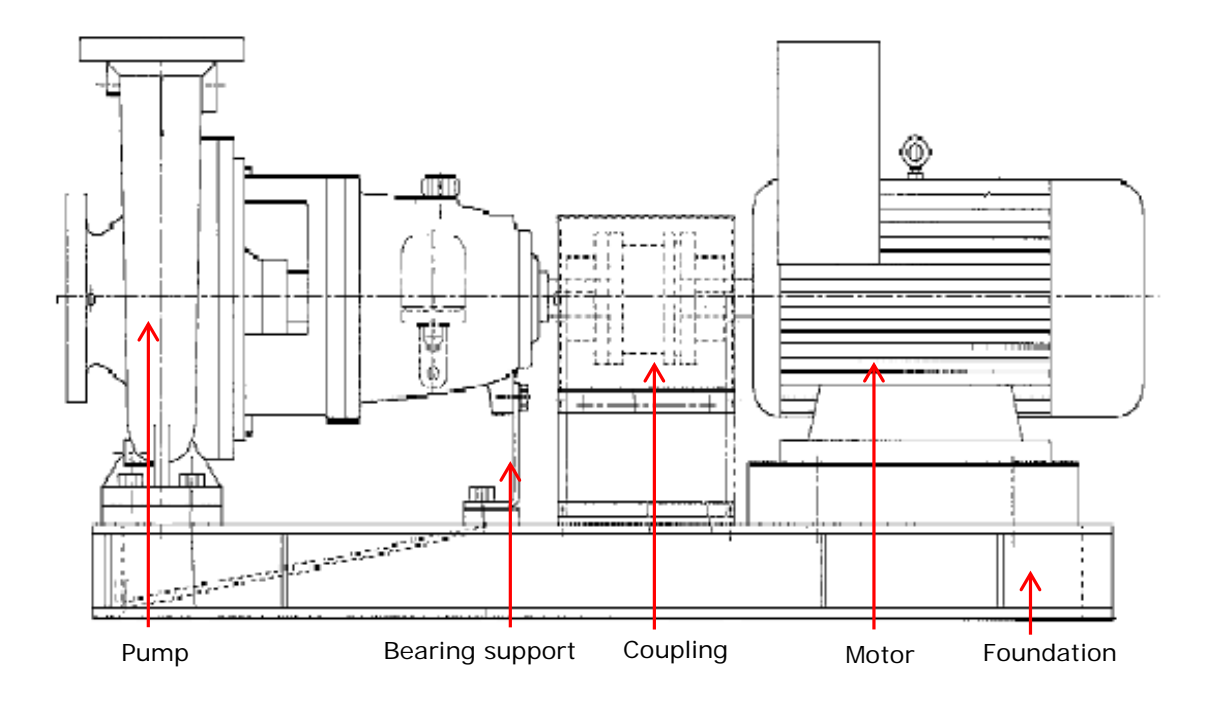


Figure 1. Sketch of the pump string and its foundation taken from [3].

The rigid coupling imposes a need to perform a lateral analysis of the entire string in order to fully evaluate the lateral dynamics. For the rotordynamic calculations the LR Consulting in-house FE software RP has been used. It is assumed throughout the entire analysis that the pumped fluid is water at 95°C, as in the operational state (page 6 in [4]).

The analyses are carried out for minimum and maximum bearing clearance in order to evaluate the extreme cases. The report presents the following calculations:

- Undamped critical speed map (UCSM). The undamped natural frequencies are determined against rotor speed and bearing stiffness.
- Stability analysis, *i.e.* a damped eigenvalue analysis. In this analysis the systems tendency towards unstable vibrations is investigated. A Campbell diagram is produced and the ratio between the line frequency and the natural frequency is investigated vs the damping factor.
- Unbalance response analysis. The systems response due to an assumed unbalance is determined. The most severe unbalance cases are investigated.

# 2 Machinery data

# 2.1 Pump

The pump is a single stage overhung horizontal pump. The pump rated speed and power are taken from pg. 6 in the OEM report [4], and the impeller mass and moments of inertia are taken from pg. 92 in the same report. The impeller geometry is provided from correspondence with Elforsk AB. The pump data can be seen in Table 1.

Table 1. Machinery specifics of the investigated pump.

Property	Value	Unit
Rated speed	1494	rpm
Rated power	63.72	kW
Density of pumped liquid	962	kg/m³
Temperature of pumped liquid	95	°C
Impeller diameter	389	mm
Diffuser width	33	mm
Impeller mass	21	kg
Impeller polar Mol	0.34	kgm²
Impeller transverse MoI	0.19	kgm²

### 2.2 Motor

The driving unit is an induction motor. It is modelled in RP from data provided by an OEM drawing [5].

# 2.3 Bearings

The pump unit is supported by three bearings. Two angular contact ball bearings back to back at the DE side of the pump, and one radial cylindrical roller at the NDE side. The properties of the bearings used in the calculations can be seen in Table 2 and Table 3. It is assumed that the clearance in the DE bearings is negligible, while the NDE bearing is assumed to be of clearance class C3. The data is taken from the OEM catalogue [6].

Table 2. Properties of the angular contact back to back ball bearings.

Property	Value	Unit
Inner diameter	80	mm
Outer diameter	140	mm
Mass	1.49	kg
Static radial load	-268.7	N
Radial clearance	0	μm
Ball diameter	20	mm
Pitch diameter	110	mm
Outer race curvature	0.54	-
Inner race curvature	0.54	-
Young's modulus	208	GPa
Poisson's ratio	0.3	-
Contact angle	40	Deg
Ball density	7850	kg/m³

Table 3. Properties of the cylindrical roller bearing.

Property	Value	Unit
Inner diameter	80	mm
Outer diameter	140	mm
Mass	1.7	kg
Static radial load	658.5	N
Radial clearance	65- 100	μm
Cylinder diameter	20.5	mm

Pitch diameter	110.5	mm
Outer race curvature	0.54	-
Inner race curvature	0.54	-
Young's modulus	208	GPa
Poisson's ratio	0.3	-
Contact angle	0	Deg
Cylinder density	7850	kg/m³

The motor unit is supported by two radial deep grove ball bearings. Both bearings are of clearance class C3. The properties of the motor bearings are taken from the OEM catalogue [6] and can be seen in Table 4 and Table 5.

Table 4. Properties used in the bearing stiffness calculations of the deep grove ball bearing.

Property	Value	Unit
Inner diameter	80	mm
Outer diameter	170	mm
Mass	3.67	kg
Static radial load	823.3	N
Radial clearance	25-51	μm
Ball diameter	34	mm
Pitch diameter	125	mm
Outer race curvature	0.54	-
Inner race curvature	0.54	-
Young's modulus	208	GPa
Poisson's ratio	0.3	-
Contact angle	0	Deg
Ball density	7850	kg/m³

Table 5. Properties used in the bearing stiffness calculations of the deep grove ball bearing.

Property	Value	Unit
Inner diameter	95	mm
Outer diameter	200	mm
Mass	5.76	kg
Static radial load	1380.8	N
Radial clearance	30-58	μm
Ball diameter	39.5	mm
Pitch diameter	147.5	mm
Outer race curvature	0.54	-
Inner race curvature	0.54	-
Young's modulus	208	GPa
Poisson's ratio	0.3	-
Contact angle	0	Deg
Ball density	7850	kg/m³

# 2.4 Coupling

The coupling is a torsional rigid coupling. The rigidity of the coupling impose that lateral vibrations might be transmitted between the motor and the pump, so the coupling has been included in the analysis. No exact dimensions of the coupling have been provided, but the lumped mass used in the pump OEM calculations is known from pg. 93 in [4]. Together with the information provided in the drawings in the coupling OEM catalogue [7] and a drawing from the pump OEM [8], enough data is provided to create a rough model in RP of the coupling. The mass and the Moment of Inertias (MoI) are seen in Table 6.

Table 6. Properties of the coupling taken from provided drawings and OEM catalogue.

Property	Value	Unit	
Mass	19.15	kg	
Polar Mol	0.0722	kgm²	
Transverse Mol	0.303	kgm²	

## 2.5 Mechanical seal

A mechanical seal made of steel is placed in front of the impeller. The mass, the MoI and the CoG of the seal are calculated from the pump OEM drawing [9]. It is thereafter modelled in RP as a disk element with discrete mass and MoIs, placed at the CoG of the seal. The properties of the seal can be seen in Table 7.

Table 7. Properties of the mechanical seal.

Property	Value	Unit	
Mass	1.44	kg	
Polar Mol	0.00154	kgm²	
Transverse Mol	0.00368	kgm²	

# 3 Calculation model

#### 3.1 Shafts

The rotor shafts are modelled in RP with Timoshenko theory beam elements and disk elements representing discrete masses and MoIs. Nodes are placed where there are changes in the cross-section, in the axial CoG of rotor elements such as the impeller, and where possible forces or unbalances might be applied.

The pump rotor shaft is modelled in RP based on the dimensions provided by the pump OEM on pg. 92 in [4]. It is modelled with 30 beam elements. The mass and inertias of the impeller and the mechanical seal are modelled with discrete disks. Massless disk elements are also used for visualising the bearings. The total mass of the pump rotor is 44.28 kg. The pump rotor shaft can be seen in Figure 2.

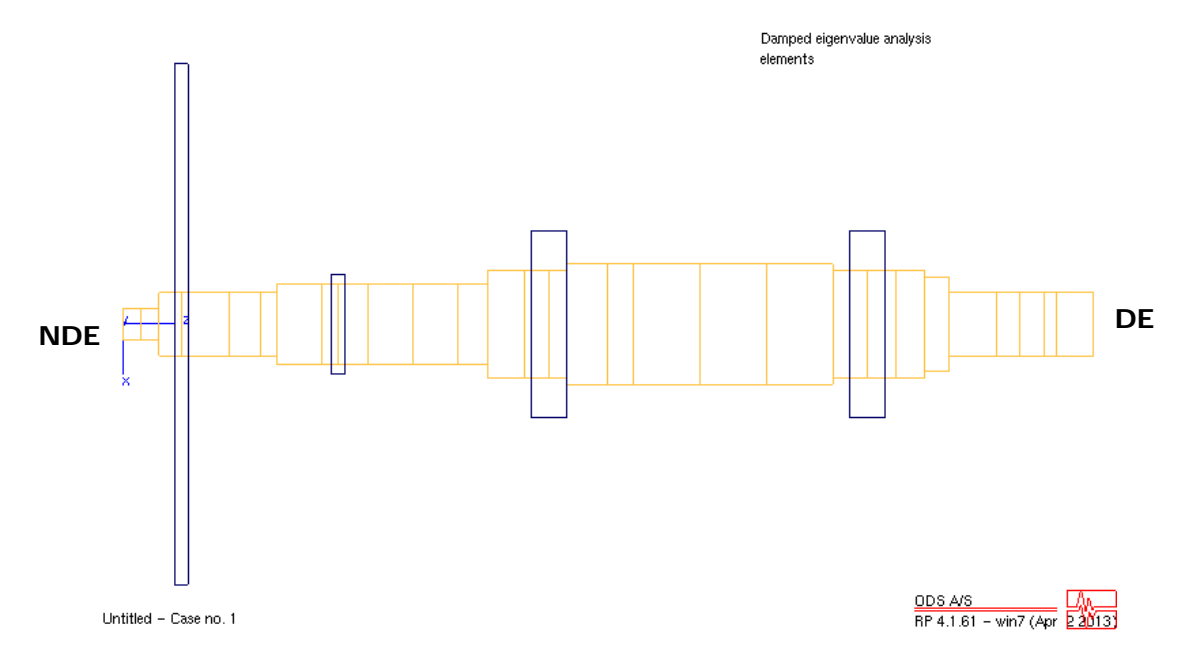


Figure 2. RP model of the pump shaft. The model consists of 30 beam elements (yellow) and 4 disk elements (blue). Please note that the disks representing the bearings are massless and does not contribute to the modal mass of the system.

The part of the pump shaft after the mechanical seal will be surrounded by water. This has to be accounted for by adding the mass of the water that is set in movement during the lateral vibrations. Because of the symmetry of the cross-section, no cross-coupled masses or MoIs has to be accounted for. According to [10], the added mass per unit length for a cylindrical cross-section in water is calculated as

$$m_a = \pi \rho_w R^2, \tag{1}$$

where the added mass per unit length is denoted  $m_{a}$ , the density of the water is denoted  $\rho_{w}$  and the radius of the cross-section of the shaft is denoted R.

The coupling shaft is modelled based on information in the coupling OEM catalogue [7] and from a rough pump OEM drawing [8]. It is modelled using 16 beam elements, of which 9 are hollow. The total mass of the coupling is 19.14 kg and can be seen in Figure 3.

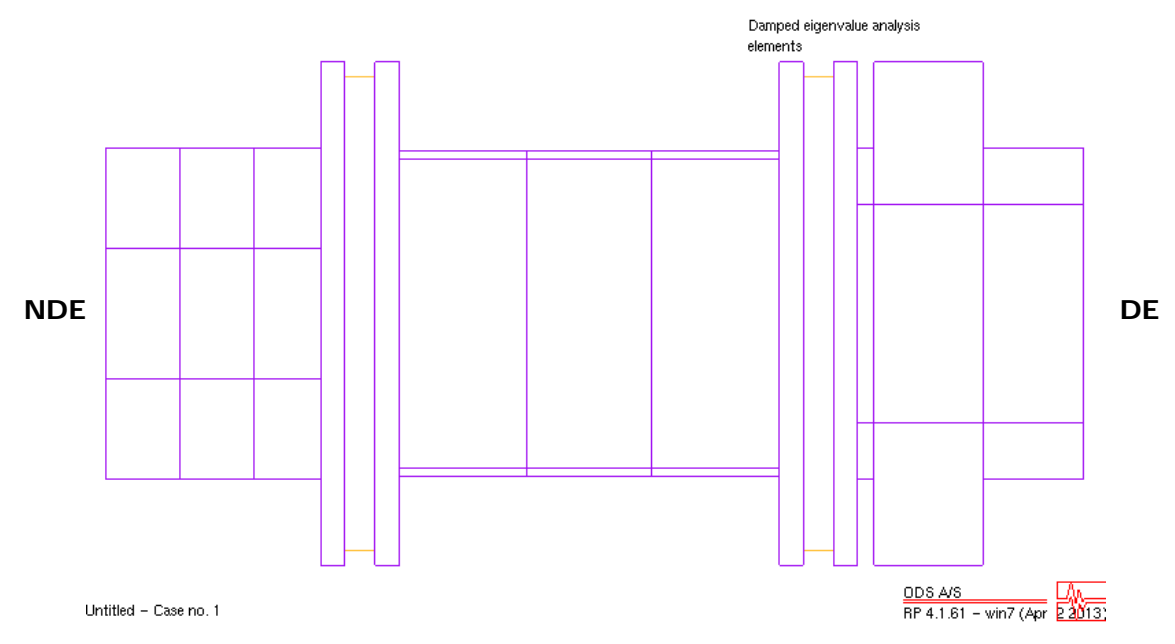


Figure 3. RP model of the coupling shaft. The model consists of 16 beam elements.

The motor shaft is modelled according to a motor OEM drawing [5]. It consists of 47 elements, of which 33 are beam elements and 14 are disk elements. Two of the disks represent the bearings, and are massless, while the 12 disk elements in between the bearings represents the motor windings and its mass and MoIs. The total mass of the motor rotor model is 199.9 kg. The model can be seen in Figure 4.

Damped eigenvalue analysis elements

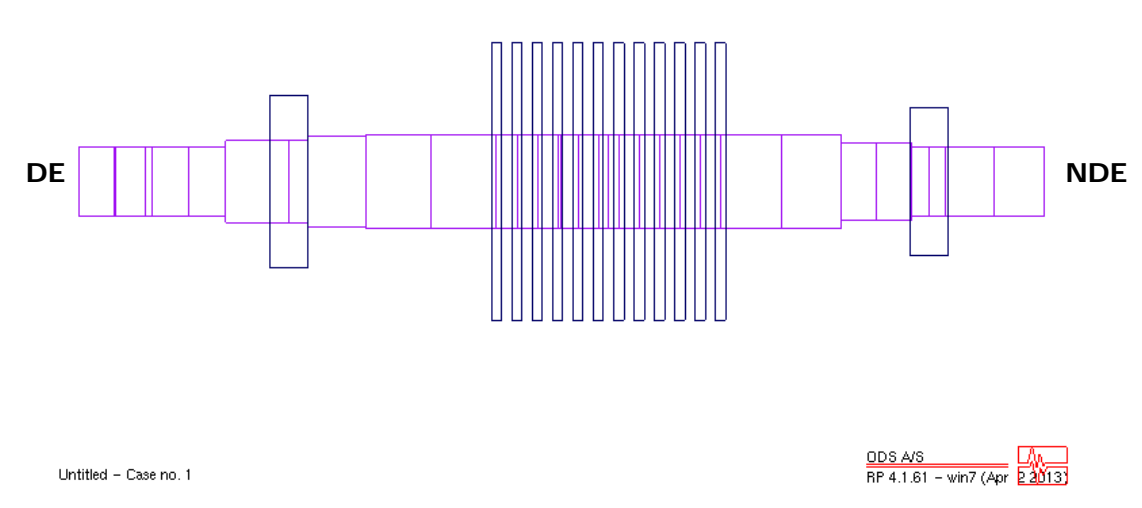


Figure 4. RP model of the motor shaft. The model consists of 33 beam elements (purple) and 14 disk elements (blue).

In total the RP model weighs 263.4 kg. It consists of 97 elements, of which 79 are beam elements and 18 are disk elements. The model of the entire string is seen in Figure 5.

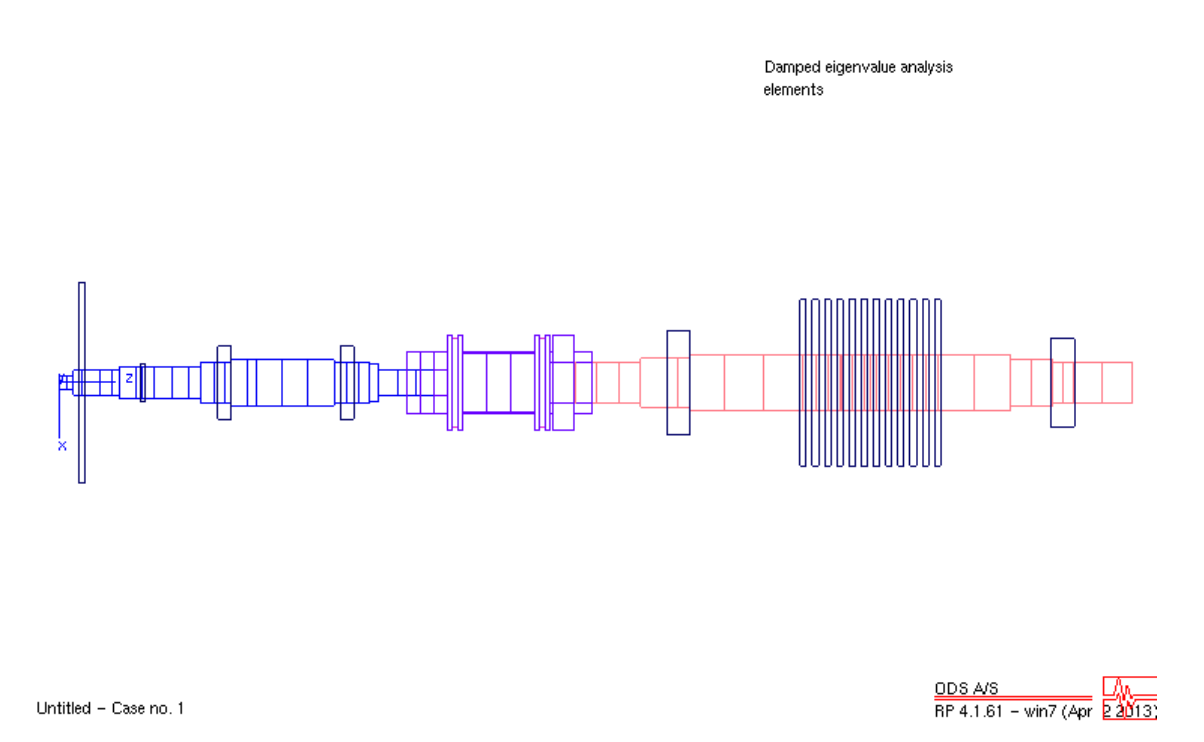


Figure 5. RP model of the full string. The model consists of 79 beam elements and 18 disk elements.

#### 3.2 **Impeller**

The dynamic stiffness and damping coefficients arising from the interaction between the impeller and the pumped water are modelled in RP as a bearing element. Mainly two phenomena from the impeller/water interaction are causing the dynamic radial effects on the rotor. These are:

- Forces between the impeller shroud and the fluid.
- Interaction effects between the impeller and the diffuser.

No state of the art analytical methods for taking both these effects fully into account currently exist, which is why the coefficients are calculated from a theory further described in [11]. The equations used in this theory, seen in Equations (2) to (5), are based on experimental data. This method has proven to produce reliable in earlier work by LR Consulting. The dynamic coefficients are seen in the matrices below. The entity Kis the stiffness matrix, B is the damping matrix and M is the added mass matrix.

$$\mathbf{K} = \begin{pmatrix} K_{xx} & K_{xy} \\ -K_{yx} & K_{yy} \end{pmatrix}, \quad \mathbf{B} = \begin{pmatrix} B_{xx} & B_{xy} \\ -B_{yx} & B_{yy} \end{pmatrix}, \quad \mathbf{M} = \begin{pmatrix} M_{xx} & M_{xy} \\ -M_{yx} & M_{yy} \end{pmatrix}$$

The stiffness coefficients are calculated according to Equation (2), the damping coefficients are calculated according to Equation (3) and the added mass coefficients are calculated according to Equation (4).

$$\mathbf{K} = \begin{pmatrix} -4.2C\omega^2 & 5.1C\omega^2 \\ -5.1C\omega^2 & -4.2C\omega^2 \end{pmatrix} \tag{2}$$

$$K = \begin{pmatrix} -4.2C\omega^2 & 5.1C\omega^2 \\ -5.1C\omega^2 & -4.2C\omega^2 \end{pmatrix}$$

$$B = \begin{pmatrix} 4.6C\omega & 13.5C\omega \\ -13.5C\omega & 4.6C\omega \end{pmatrix}$$

$$M = \begin{pmatrix} 11C & 4C \\ -4C & 11C \end{pmatrix}$$

$$(2)$$

$$\mathbf{M} = \begin{pmatrix} 11C & 4C \\ -4C & 11C \end{pmatrix} \tag{4}$$

In Equations (2) to (4),  $\omega$  is the shaft angular frequency and  $\mathcal{C}$  is the mass coefficient of the pumped fluid, calculated as:

$$C = \pi \rho b_2 r^2. \tag{5}$$

In Equation (5) the entities  $\rho$ ,  $b_2$  and r represents the mean density of the fluid, the impeller discharge width and the impeller tip radius, respectively.

The stiffness, damping and mass terms are determined for a number of shaft running speeds. Based on these values, RP then interpolates the coefficients corresponding to the speed to be analysed.

#### 3.3 Bearings

The bearings contribute to the dynamic stiffness and damping of the model. These coefficients are determined for the minimum and maximum clearance for the radial bearings. No clearance is assumed to exist in the pump DE angular contact bearings. In order to calculate the stiffness coefficients the static load on each bearing has to be

determined. This solution is retrieved by solving the problem for zero frequency and gravity load in RP. The load distribution among the bearings is seen in Table 8.

Table 8. Total mass and gravity load of the rotor and the load distribution among the bearings.

Entity	Value	Unit
Total rotor mass	263.4	kg
Rotor gravity load	2584.0	N
Rotor length	2073.6	mm
Rotor CoG	1276.9	mm
Motor NDE bearing load	823.3	N
Motor DE bearing load	1370.8	N
Pump DE bearing load	-268.7	N
Pump NDE bearing load	658.5	N

#### 3.3.1 Stiffness

The stiffness coefficients of the bearings are determined with the Texas A&M University (TAMU) program code XLTRC2. Only values of the direct stiffness are calculated for the roller bearings, since the code assumes that the cross-coupling stiffness effects are negligible. There is also no distinguishable difference in the direct stiffness in the x- and y-directions.

For the angular contact bearings, half the static load is used in the calculations since two bearings share the load. The calculated stiffness values are then multiplied with the factor 2 so that both bearing stiffness is accounted for.

The stiffness coefficients used in the model for the angular contact bearings can be seen versus shaft running speed in Table 9.

Table 9. Stiffness values in the radial direction of the back to back angular contact ball bearings placed at the DE side of the pump. No minimum and maximum values are determined for this bearing, but only the nominal ones.

Shaft speed [rpm]	Direct radial stiffness [N/m]
1	5.31·10 <sup>7</sup>
250	5.32·10 <sup>7</sup>
500	$5.34 \cdot 10^{7}$
750	5.36·10 <sup>7</sup>
1000	5.39·10 <sup>7</sup>
1250	5.42·10 <sup>7</sup>
1500	5.45·10 <sup>7</sup>
1750	5.48·10 <sup>7</sup>
2000	5.51·10 <sup>7</sup>
2250	5.55·10 <sup>7</sup>
2500	5.58·10 <sup>7</sup>
2750	5.62·10 <sup>7</sup>
3000	5.65·10 <sup>7</sup>
5000	5.94·10 <sup>7</sup>
10000	6.65·10 <sup>7</sup>

Cylindrical roller bearings usually have a higher stiffness than roller bearings. According to a presentation by the National Renewable Energy Laboratory (NREL), numerous investigations of the ball vs cylindrical bearing stiffness has been carried out [12]. All of the investigations mentioned in [12] shows that the cylindrical stiffness is approximately 3-6 times stiffer than ball bearings. Based on this, it is assumed that the cylindrical roller bearing has stiffness coefficients of a magnitude 5 greater than one roller bearing of similar dimensions. In Table 10 the minimum and maximum stiffness coefficients of the NDE side cylindrical roller bearing are presented.

Table 10. Minimum and maximum values of the direct stiffness of the cylindrical roller bearing placed at the NDE side of the pump.

Shaft speed [rpm]	Min stiffness [N/m]	Max stiffness [N/m]	
0	3.12·10 <sup>8</sup>	3.53·108	
250	3.13·10 <sup>8</sup>	3.54·108	
500	3.14·10 <sup>8</sup>	3.55·108	
750	3.15·10 <sup>8</sup>	3.56·108	
1000	3.16·10 <sup>8</sup>	3.58·10 <sup>8</sup>	
1250	3.16·10 <sup>8</sup>	3.59·10 <sup>8</sup>	
1500	3.16·10 <sup>8</sup>	3.61·10 <sup>8</sup> 3.63·10 <sup>8</sup> 3.65·10 <sup>8</sup>	
1750	3.16·10 <sup>8</sup>		
2000	3.16·10 <sup>8</sup>		
2250	3.14·10 <sup>8</sup>	3.67·108	
2500	3.12·10 <sup>8</sup>	3.69·108	
2750	3.10·10 <sup>8</sup>	3.70·10 <sup>8</sup>	
3000	3.06·10 <sup>8</sup>	3.72·108	
5000	2.34·10 <sup>8</sup>	3.85·10 <sup>8</sup> 3.85·10 <sup>8</sup>	
10000	2.53·10 <sup>8</sup>		

In Table 11 the minimum and maximum values of the motor NDE bearing are presented.

Table 11. Minimum and maximum values of the direct stiffness of the deep grove ball bearing placed at the NDE side of the motor.

Shaft speed [rpm]	Min stiffness [N/m]	Max stiffness [N/m	
0	9.44·10 <sup>7</sup>	9.68·10 <sup>7</sup>	
250	$9.51 \cdot 10^{7}$	9.74·10 <sup>7</sup>	
500	$9.60 \cdot 10^{7}$	$9.83 \cdot 10^{7}$	
750	$9.70 \cdot 10^{7}$	$9.94 \cdot 10^{7}$	
1000	$9.81 \cdot 10^{7}$	1.01·10 <sup>8</sup>	
1250	$9.93 \cdot 10^{7}$	1.02·10 <sup>8</sup>	
1500	1.00·10 <sup>8</sup>	1.03·10 <sup>8</sup>	
1750	1.02·10 <sup>8</sup>	1.04·10 <sup>8</sup>	
2000	1.03·10 <sup>8</sup>	1.06·10 <sup>8</sup>	
2250	1.04·10 <sup>8</sup>	1.07·10 <sup>8</sup>	
2500	1.05·10 <sup>8</sup>	1.08·10 <sup>8</sup>	
2750	1.06·10 <sup>8</sup>	1.10·10 <sup>8</sup>	
3000	1.06·10 <sup>8</sup>	·10 <sup>8</sup> 1.11·10 <sup>8</sup>	
5000	1.10·10 <sup>8</sup>	$1.10 \cdot 10^8$ $1.18 \cdot 10^8$ $7.50 \cdot 10^7$ $1.15 \cdot 10^8$	
10000	$7.50 \cdot 10^7$		

In Table 12 the minimum and maximum direct stiffness values used for the motor DE bearing are presented.

Table 12. Minimum and maximum values of the direct stiffness of the deep grove ball bearing placed at the DE side of the motor.

Shaft speed [rpm]	Min stiffness [N/m]	Max stiffness [N/m]	
0	1.19·10 <sup>8</sup>	1.21·108	
250	1.20·10 <sup>8</sup>	1.22·108	
500	1.21·10 <sup>8</sup>	1.23·108	
750	1.22·10 <sup>8</sup>	1.24·108	
1000	1.24·10 <sup>8</sup>	1.26·108	
1250	1.26·10 <sup>8</sup>	1.28·10 <sup>8</sup> 1.29·10 <sup>8</sup> 1.31·10 <sup>8</sup>	
1500	1.27·10 <sup>8</sup>		
1750	1.29·10 <sup>8</sup>		
2000	1.30·10 <sup>8</sup>	1.33·108	
2250	1.32·10 <sup>8</sup>	1.35·10 <sup>8</sup>	
2500	1.33·10 <sup>8</sup>	1.36·10 <sup>8</sup>	
2750	1.34·10 <sup>8</sup>	1.38·108	
3000	1.36·10 <sup>8</sup>	1.39·108	
5000	1.41·10 <sup>8</sup>	1.49·108	
10000	9.44·10 <sup>7</sup>	1.43·108	

#### 3.3.2 Damping

The TAMU code XLTRC2 does not calculate the damping in the roller bearings, and the damping of the bearings themselves is usually low in roller bearings. But damping of some extent will always be present because of lubrication and the material losses. Due to this, a value of  $1\cdot10^5$  has been assumed and used for each one of the bearings.

The pump DE bearing is supported by a steel plate, as seen in Figure 6. This plate is assumed to be at least as stiff as the pump DE bearing, and is therefore not taken into account since it will not weaken the structure or contribute significantly with any damping.

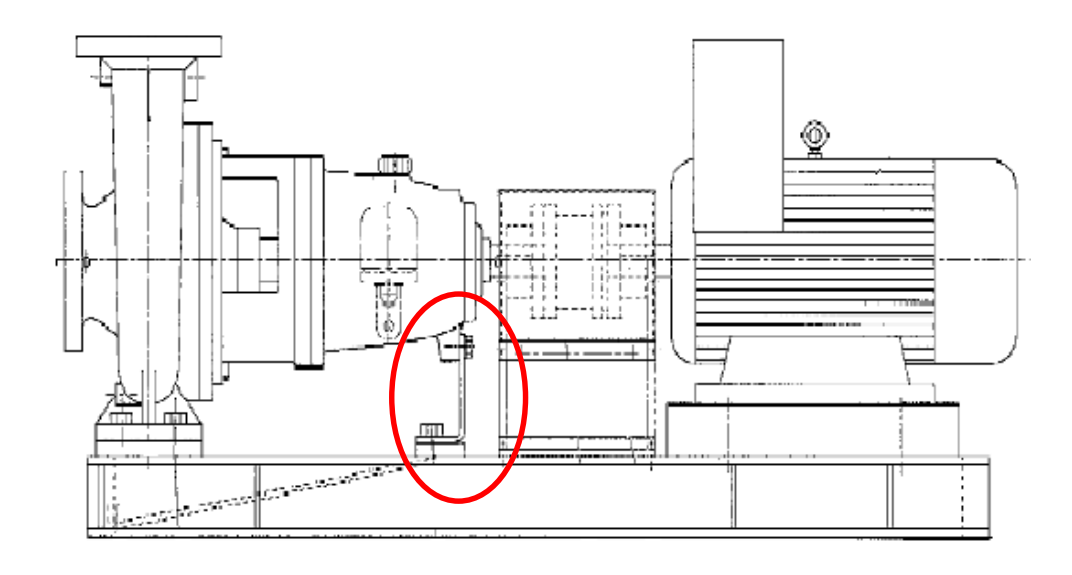


Figure 6. The steel plate supporting the pump DE bearing is marked with the red ellipse. The drawing is taken from [3].

# 4 Results

The results presented in this chapter are divided into three subchapters. First the UCSM, which presents the undamped critical speeds vs. bearing stiffness. It is followed by a stability analysis that introduces damping in the model. Finally the results from the unbalance analysis are presented, which assumes rotor unbalance at certain, critical points, and calculates the response due to these unbalances.

#### 4.1 UCSM

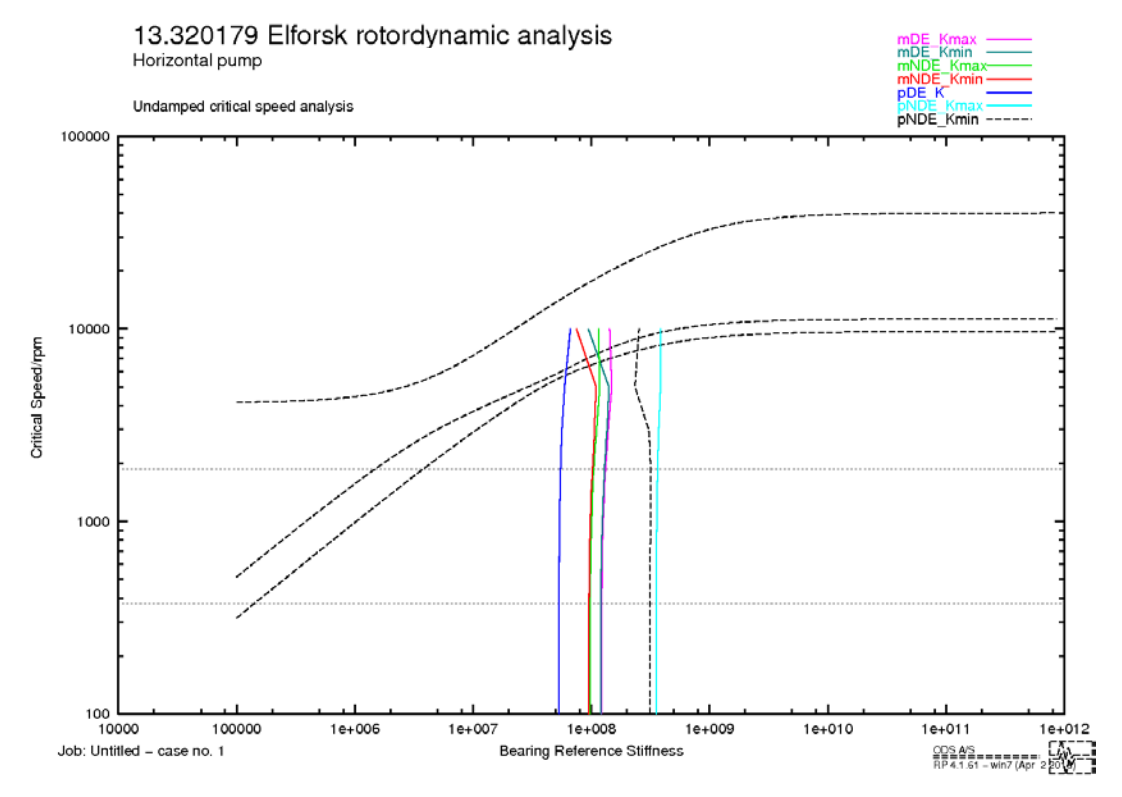


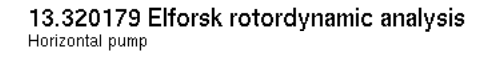
Figure 7. Unbalanced critical speed map for the pump. The black dashed lines going from left to right represents the natural frequencies of the system and the coloured lines going in the vertical direction represents the minimum and maximum bearing stiffness of the different bearings. The grey horizontal lines mark the by API determined speed region to be investigated (25% and 125% of the rated speed).

The UCSM in Figure 7 shows the three first dry forward modes versus bearing stiffness for an undamped rotor. No damping or stiffness from the bearings or the impeller is taken into account. The minimum and maximum values of the bearing stiffness calculated from XLTRC2 are overlaid. It is seen in the UCSM that the pump is operating well below the first critical speed. The critical speeds and natural frequencies of the first three dry forward modes, i.e. for infinitely stiff bearings, are presented in Table 13.

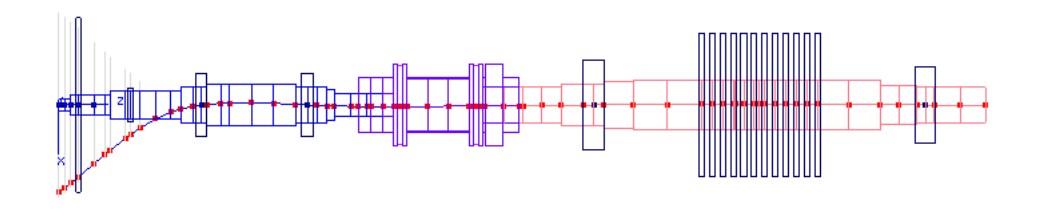
Table 13. The three first dry critical speeds and their corresponding natural frequencies.

Mode	Critical speed [rpm]	Natural frequency [Hz]
1	9685	161.4
2	11265	187.8
3	40044	667.4

The corresponding mode shapes of the modes presented in Table 13 are presented in Figure 8 to Figure 10. Overlaid on the plots is the initial rotor configuration for comparison.



Undamped critical speed analysis elements, critical speed no. 1: 9685.08 rpm K: 8.65964e+011 (112)



Untitled - Case no. 1

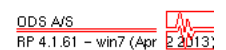
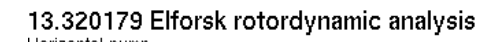
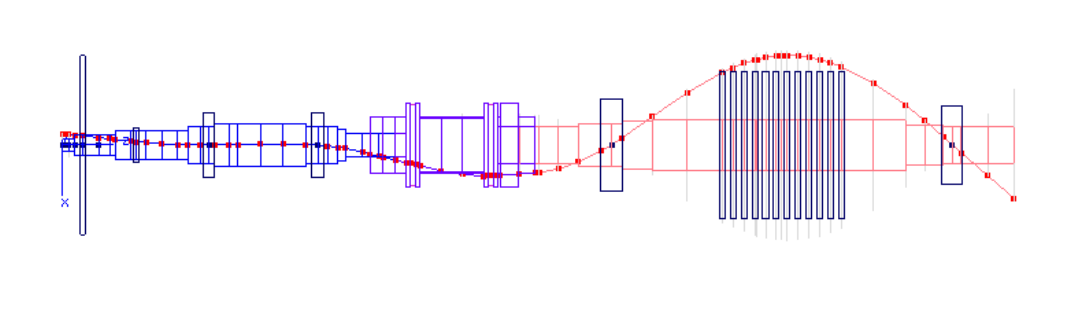


Figure 8. Deflection shape of the first dry forward whirl mode at 9685 rpm.



Undamped critical speed analysis elements, critical speed no. 2: 11264.9 rpm K: 8.65964e+011 (112)



Untitled - Case no. 1



Figure 9. Defection shape of the second dry forward whirl mode at 11265 rpm.

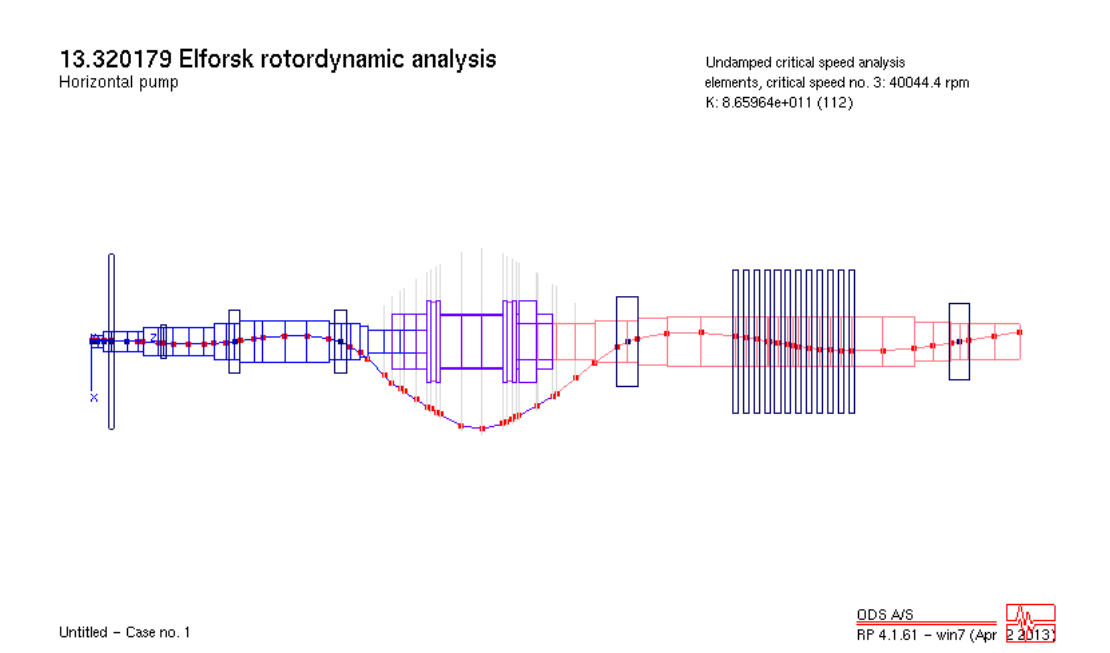


Figure 10. Deflection shape of the third dry forward whirl mode at 40044 rpm.

It should be noted that the mode shapes in Figure 8 to Figure 10 are governed by the flexibility of the rotor. This is in line with what to be expected for a system with high bearing stiffness. Figure 8 to Figure 10 implies that the unbalances are to be applied at the impeller, at the motor bearing mid-span and at the coupling respectively.

# 4.2 Stability analysis

The stability analysis is a damped eigenvalue analysis of the system. From the results a Campbell diagram is produced in order to investigate possible conflicts between the operating speed and resonance. Also, the damping is investigated against the ratio between the natural frequencies and the running frequency. The calculations are carried out for minimum and maximum bearing stiffness.

#### 4.2.1 Campbell diagram

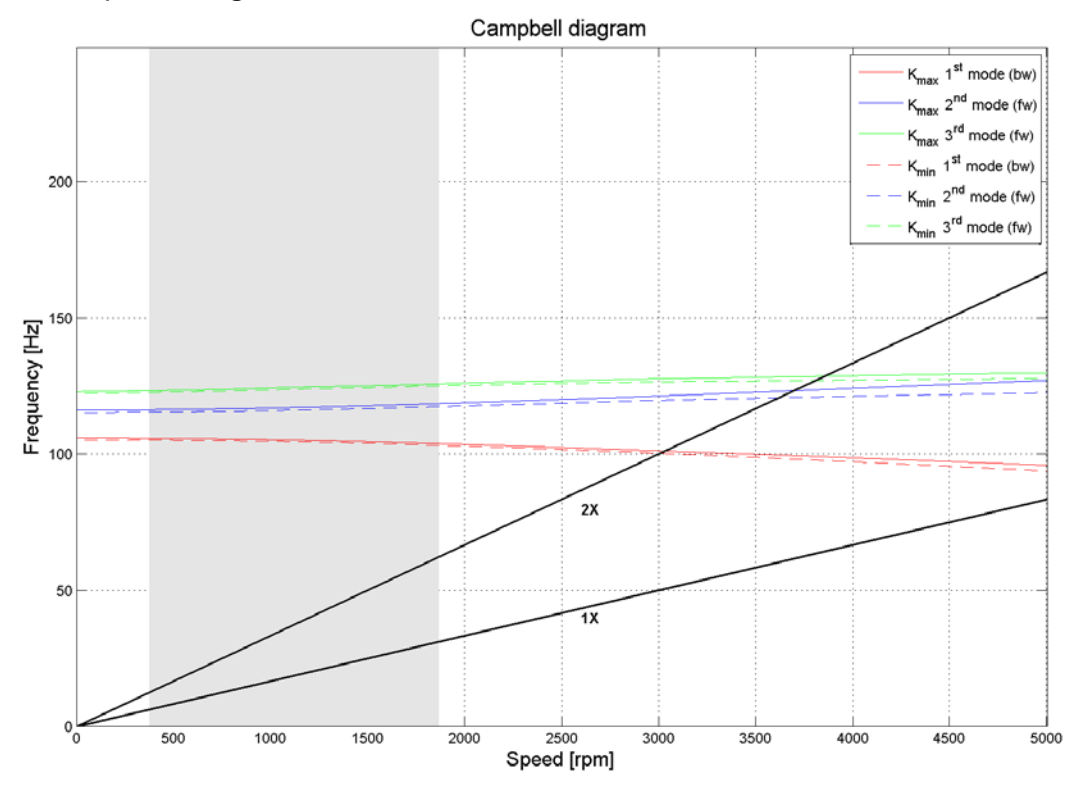


Figure 11. Campbell diagram showing the pumps first three damped natural frequencies for minimum and maximum bearing stiffness respectively. Mode 1 is backward whirling and mode 2 and 3 are forward whirling modes. The black lines are the 1X and 2X frequencies, the solid coloured lines represent the modes calculated with maximum bearing stiffness, and the dashed coloured lines represent the modes calculated with the minimum bearing stiffness. Finally, the grey area is the operational area according to [1], 25%-125% of the rated speed.

In Figure 11 the Campbell diagram over the lateral dynamics is seen. Since no damped modes are crossing the 1X or 2X frequency lines in the operating range, no possible conflicts are indicated. The mode frequencies at rated speed are presented in Table 14.

Table 14. Frequencies of the three first damped modes for minimum and maximum bearing stiffness at rated speed, *i.e.* 1494 rpm. Mode 1 is backward whirling and mode 2 and 3 are forward whirling modes.

Mode #	Min bearing stiffness frequency [Hz]	Max bearing stiffness frequency [Hz]	
1	103.8	104.5	
2	116.6	117.6	
3	124.2	124.9	

It can be seen in Table 14 that the lowest natural frequency is approximately 317% higher than the running frequency of 24.9 Hz.

#### 4.2.2 Frequency ratio vs damping

According to [1] the frequency ratio,  $F_{r_i}$  for centrifugal pumps is defined as

$$F_r = \frac{f_{nat,i}}{f_{run}},\tag{6}$$

where  $f_{nat,i}$  is the natural frequency number i and  $f_{run}$  is the running frequency. This is compared against the damping factor,  $\xi$ , which is defined through the logarithmic decrement  $\delta$  as

$$\delta = \frac{(2\pi\xi)}{(1-\xi^2)^{0.5}}. (7)$$

Equation (7) can, for damping factors lower than 0.4, be approximated as

$$\delta = 2\pi\xi \Rightarrow \xi = \frac{\delta}{2\pi}.\tag{8}$$

The approximation of the damping factor in Equation (8) is used in the comparisons of the damping factor vs the frequency ratio in the calculations in this report.

The damping ratio is compared against the frequency ratio for three different running speeds. These are 0.25xMCOS, MCOS and 1.25xMCOS, where the MCOS is the same as the rated speed, *i.e.* 1494 rpm.

The comparison is carried out for the first three damped modes, presented in Table 15 as defined in the Campbell diagram in Figure 11.

Table 15. Frequencies of the first three modes for the shaft speeds used in the frequency ratio investigation presented in Figure 12 to Figure 14. The frequencies are presented for both minimum and maximum bearing stiffness.

Mode #	Min bearing stiffness natural frequency [Hz]	Max bearing stiffness natural frequency [Hz]	
0.25xMCOS (374 rpm)			
1	105.0	105.7	
2	115.3	116.2	
3	122.5 123.2		
MCOS (1494 rpm)			
1	103.8	104.5	
2	116.6	117.6	
3	124.2 124.9		
1.25xMCOS (1868 rpm)			
1	103.1	103.8	
2	117.3	118.4	
3	124.9	125.7	

In Figure 12 to Figure 14 the damping ratios vs. the frequency ratios are presented in increasing operational speed order. The area inside the black lines, marked "UA", in the plot represents unacceptable damping ratios, while the area outside of the lines, marked "A", represents acceptable damping ratios. The circles represent the minimum stiffness case while the crosses represent the maximum stiffness case.

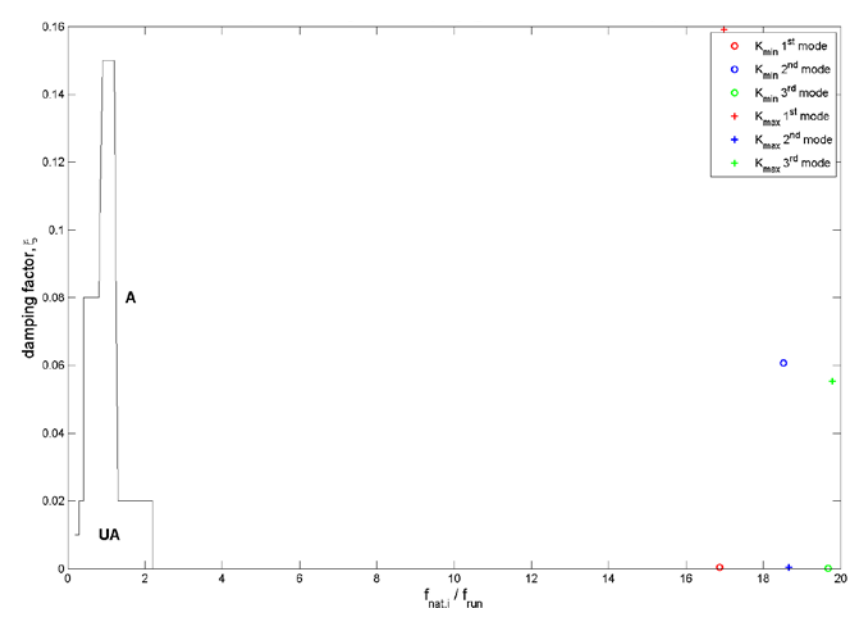


Figure 12. Damping vs frequency ratio plot for 0.25xMCOS. The circles represent the minimum bearing stiffness case and the crosses the maximum stiffness case. The region marked "A" is the acceptable region and the region marked "UA" is the unacceptable region.

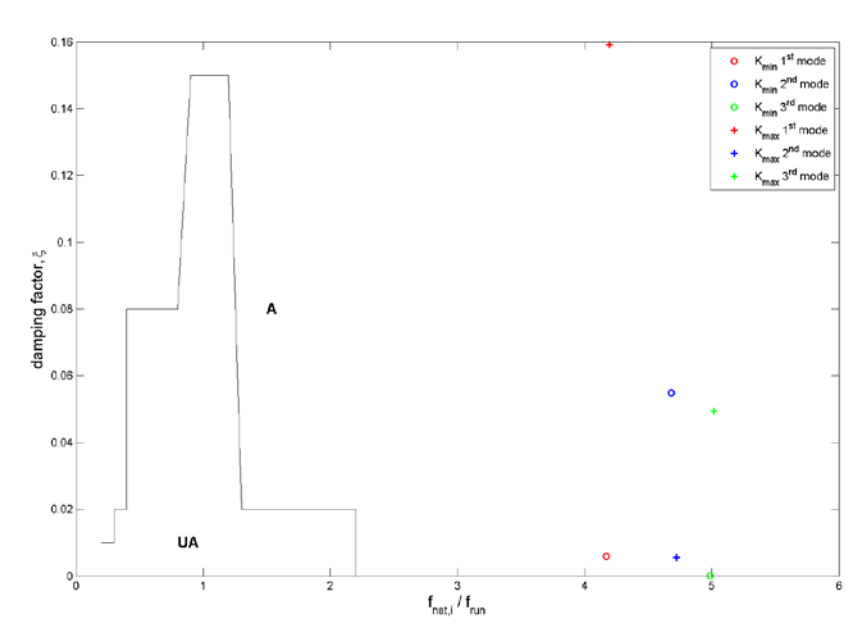


Figure 13. Damping vs frequency ratio plot for MCOS. The circles represent the minimum bearing stiffness case and the crosses the maximum stiffness case. The region marked "A" is the acceptable region and the region marked "UA" is the unacceptable region.

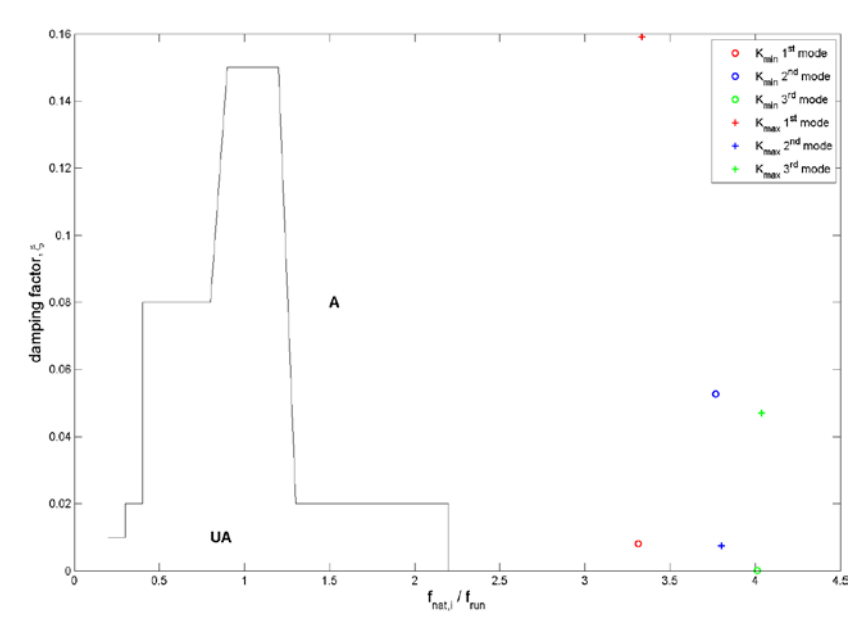


Figure 14. Damping vs frequency ratio plot for 1.25xMCOS. The circles represent the minimum bearing stiffness case and the crosses the maximum stiffness case. The region marked "A" is the acceptable region and the region marked "UA" is the unacceptable region.

If Figure 12 to Figure 14 are studied it is seen that for the OSR decided by API, (25% to 125% of the rated speed), all modes pass the damping vs frequency ratio criterion with a good margin. The API criterion for centrifugal pumps is that there should be no non-critically damped modes in the speed range 0.25xMCOS to 1.25xMCOS. These criteria are fulfilled according to Figure 12 to Figure 14.

## 4.3 Unbalance response

The unbalance response analysis is carried out for three different unbalance cases chosen to excite the three first modes according to the dry mode shapes presented in Figure 8 to Figure 10. The unbalance is calculated according to the ISO standard [13] as.

$$U = (e_{per}W), (9)$$

where U is the unbalance in  $g \cdot mm$ ,  $e_{per}$  is the permissible residual unbalance value per unit mass in  $g \cdot mm/kg$ , and W is the rotating mass in kg. For the rated speed of the investigated pump,  $e_{per}$  is set to 15  $g \cdot mm/kg$ . The unbalance determined by Equation (9) is multiplied with a safety factor 4 according to Equation (10) in order to comply with [1].

$$U = 4 \cdot (e_{per}W). \tag{10}$$

In order to be conservative a relatively large mass has been used when calculating the unbalance. For unbalances placed at the pump, the entire mass of the pump is used, for unbalances placed at the coupling the entire coupling mass is used and for unbalance at

the motor the entire motor weight is used. The analysis is carried out for minimum and maximum bearing stiffness. In Table 16 the unbalance cases and their corresponding unbalance can be seen.

Table 16. The three unbalance cases to be investigated and their corresponding application points.

Case	Unbalance position	W [kg]	e <sub>per</sub> [g·mm/kg]	<i>U</i> [g·mm]
Α	Impeller	44.28	15	2.6568·10 <sup>3</sup>
В	Motor bearing mid- span	199.9	15	11.994·10 <sup>3</sup>
С	Coupling midpoint	19.4	15	1.1484·10 <sup>3</sup>

A typical Bode plot for an unbalance analysis can be seen in Figure 15. The spatial entity (displacement, velocity or acceleration) is represented by the green line in the horizontal direction and the red line in the vertical direction. The upper plot displays the phase of the entity. Typical resonance behaviour is a phase shift of 90 degrees. The lower plot displays the spatial entity amplitude.

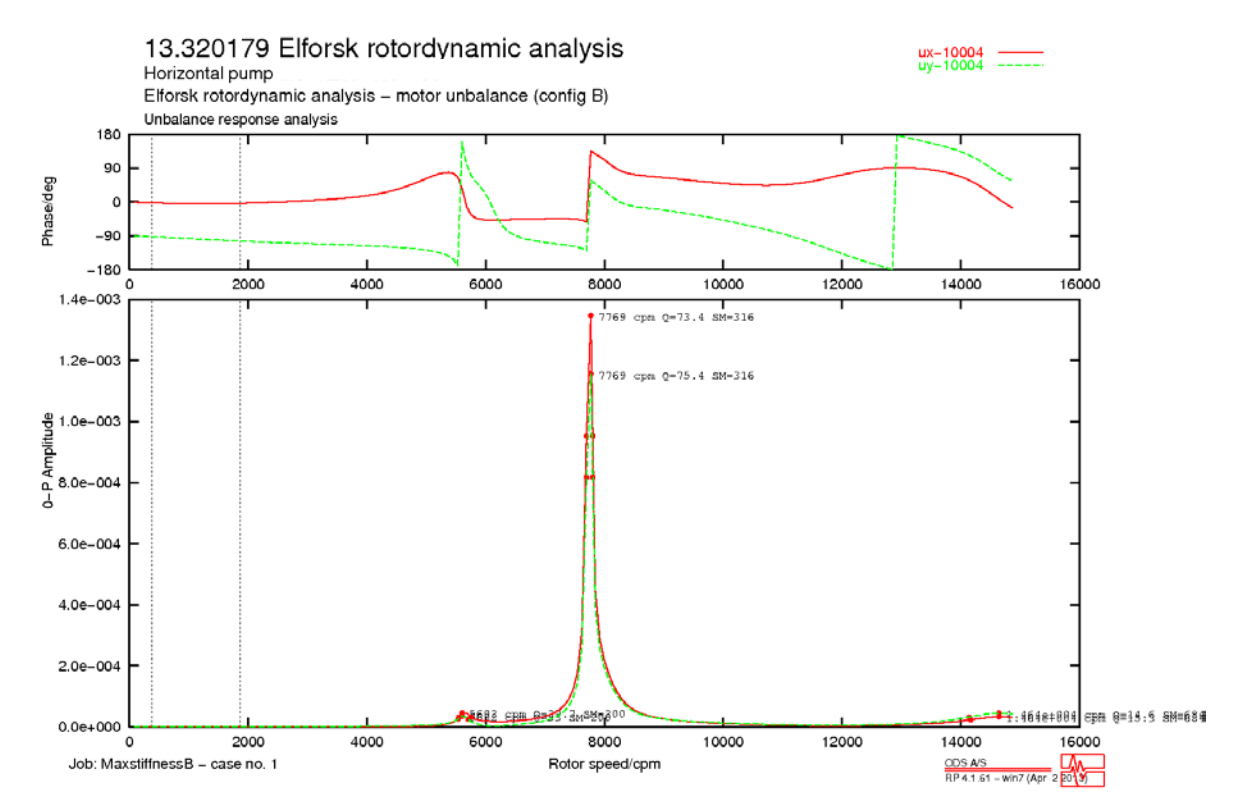


Figure 15. Bode plot of an unbalance response. This particular response is the displacement at the impeller when unbalance case B from Table 16 is exciting the system for running speeds of 0xMCOS to 10xMCOS. The maximum bearing stiffness is used. The red curve represents displacement in the vertical direction and the green curve represents displacement in the horizontal direction. The vertical grey lines represent the speed range to be investigated in order to comply with API. The displayed numbers at the resonance peaks are the shaft running speed, the amplification factor and the separation margin.

In Appendix A the Bode plots and the response shape at rated speed are presented for each unbalance case and for minimum and maximum bearing stiffness.

For centrifugal pumps the system is assumed critically damped if any of the three following conditions is fulfilled:

• 
$$\xi \ge 0.15$$
  
•  $\delta \ge 0.95$   
•  $Q \le 3.3$  (11)

In Equation (11) the entity  $\xi$  is the damping factor, the entity  $\delta$  is the log dec and the entity Q is the amplification factor. The amplification factor is connected to the damping factor and the log dec as in Equation (12)

$$Q = \frac{1}{2\xi} = \frac{\pi}{\delta}.\tag{12}$$

If any of the two conditions regarding the damping factor or the log dec is fulfilled, no unbalance response analysis is required (these criteria correspond to the accepted area in Figure 12 to Figure 14). The amplification factor is usually determined from the Bode plots. For the investigated speed region (374-1868 rpm), no peaks in the Bode plots exist, so no amplification factors can be determined. Hence there is no possibility of comparison against the criteria in Equation (11). Instead, API recommends a comparison of the maximum displacement against the diametral clearance of the rotor [1]. No information is available regarding the diametral clearance of the investigated pump, but the displacement values at the impeller and the motor bearing mid-span are presented in Table 17 and Table 18 in spite of this.

Table 17. Presentation of the radial displacement of the impeller for the three different unbalance cases. The running speed is 1494 rpm, *i.e.* 100% of rated speed.

Unbalance case	<i>u</i> <sub>x</sub> [μm p-p]	<i>u<sub>y</sub></i> [μm p-p]	
Minimum bearing stiffness			
Case A (Impeller unb.)	10.0	11.1	
Case B (Motor unb.)	0.21	0.28	
Case C (Coupling unb.)	0.35	0.66	
Maximum bearing stiffness			
Case A (Impeller unb.)	9.8	10.9	
Case B (motor unb.)	0.21	0.29	
Case C (Coupling unb.)	0.35	0.66	

Table 18. Presentation of the radial displacement of the motor bearing mid-span for the three different unbalance cases. The running speed is 1494 rpm, *i.e.* 100% of rated speed.

Unbalance case	<i>u</i> <sub>x</sub> [µm p-р]	<i>u<sub>y</sub></i> [µm p- p]	
Minimum bearing stiffness			
Case A (Impeller unb.)	0.071	0.094	
Case B (Motor unb.)	3.8	4.3	
Case C (Coupling unb.)	0.012	0.027	
Maximum bearing stiffness			
Case A (Impeller unb.)	0.071	0.097	
Case B (motor unb.)	3.8	4.3	
Case C (Coupling unb.)	0.011	0.025	

A comparison of the velocities at the bearing locations against a limit value of 2.5 mm/s RMS, taken from [2] is carried out. The velocities at the bearing positions can be seen in Table 19 to Table 22.

Table 19. Presentation of the radial velocities of the motor NDE bearing for the three different unbalance cases. The running speed is 1494 rpm, *i.e.* 100% of rated speed.

Unbalance case	v <sub>x</sub> [mm/s RMS]	v <sub>y</sub> [mm/s RMS]	
Minimum bearing stiffness			
Case A (Impeller unb.)	2.8·10 <sup>-3</sup>	6.8·10-3	
Case B (Motor unb.)	0.084	0.12	
Case C (Coupling unb.)	1.9·10 <sup>-3</sup>	3.2·10-3	
Maximum bearing stiffness			
Case A (Impeller unb.)	2.7·10 <sup>-3</sup>	6.7·10-3	
Case B (motor unb.)	0.082	0.11	
Case C (Coupling unb.)	1.8·10-3	3.1·10-3	

Table 20. Presentation of the radial velocities of the motor DE bearing for the three different unbalance cases. The running speed is 1494 rpm, *i.e.* 100% of rated speed.

Unbalance case	$v_x$ [mm/s RMS]	v <sub>y</sub> [mm/s RMS]	
Minimum bearing stiffness			
Case A (Impeller unb.)	8.8·10-3	0.020	
Case B (Motor unb.)	0.089	0.11	
Case C (Coupling unb.)	0.011	0.016	
Maximum bearing stiffness			
Case A (Impeller unb.)	8.4·10-3	0.019	
Case B (motor unb.)	0.088	0.11	
Case C (Coupling unb.)	0.011	0.016	

Table 21. Presentation of the radial velocities of the pump DE bearing for the three different unbalance cases. The running speed is 1494 rpm, *i.e.* 100% of rated speed.

Unbalance case	v <sub>x</sub> [mm/s RMS]	v <sub>y</sub> [mm/s RMS]	
Minimum bearing stiffness			
Case A (Impeller unb.)	0.054	0.10	
Case B (Motor unb.)	9.8·10-3	0.014	
Case C (Coupling unb.)	0.015	0.030	
Maximum bearing stiffness			
Case A (Impeller unb.)	0.055	0.10	
Case B (motor unb.)	9.9.10-3	0.014	
Case C (Coupling unb.)	0.015	0.030	

Table 22. Presentation of the radial velocities of the pump NDE bearing for the three different unbalance cases. The running speed is 1494 rpm, *i.e.* 100% of rated speed.

Unbalance case	v <sub>x</sub> [mm/s RMS]	v <sub>y</sub> [mm/s RMS]	
Minimum bearing stiffness			
Case A (Impeller unb.)	0.044	0.046	
Case B (Motor unb.)	0.27·10 <sup>-3</sup>	1.1.10-3	
Case C (Coupling unb.)	1.1.10-3	0.81·10-3	
Maximum bearing stiffness			
Case A (Impeller unb.)	0.039	0.040	
Case B (motor unb.)	0.24·10 <sup>-3</sup>	0.93·10 <sup>-3</sup>	
Case C (Coupling unb.)	1.0.10-3	0.71·10 <sup>-3</sup>	

In Table 19 to Table 22 it is seen that the vibration velocities are far below the limit of 2.5 mm/s RMS at all bearing locations, and hence the TBM criterion is fulfilled.

### 5 Conclusion

On behalf of Elforsk, a lateral analysis of a horizontal overhung centrifugal pump has been carried out. The pump is rigidly connected to the driving motor, so in order to create a realistic model the entire string has been analysed.

#### Results

Inspection of the results in section 4 yields the conclusions below:

- The results from the UCSM show that the pump operates well below the first critical speed. This applies for both minimum and maximum bearing stiffness. The two first dry natural frequencies are 161.4 Hz and 187.8 Hz.
- The Campbell diagram no resonance behaviour throughout the OSR set by API (25%-125% of rated speed). The first frequency with minimum bearing stiffness, 103.8 Hz, has a separation margin of 317% compared to the line frequency. This is far above the API recommended value of a 20% separation margin.
- The damping factor vs. separation margin analysis in section 4.2.2 show that, for 25% to 125% of operational speed, the first three modes fulfils the criteria of being critically damped according to API.
- The radial velocities at the bearing locations retrieved from the unbalance analysis (Table 19 to Table 22) have been compared against the limit value of 2.5 mm/s RMS [2]. It can be seen that the highest velocity has a value of 0.12 mm/s RMS and appears at the motor NDE bearing for unbalance at the motor windings. This is assumed safe since it measures to approximately 4.8% of the allowed TBS value.

The radial displacement values seen in Table 17 and Table 18 have not been compared against the diametral clearance of the pump unit due to lack of information.

#### Modelling assumptions

The rolling bearings have been modelled with aid of the TAMU code XLTRC2. While this code produce reliable direct stiffness coefficients, it does not take lubrication into account, and therefore it does not calculate the damping contributed by the bearings. In order to account for this, the ball bearings are given a direct damping coefficient of  $1\cdot10^5$  in both radial directions, which is assumed to be a fairly representative value based on experience. No cross-coupled damping or stiffness coefficients are assumed to exist in the bearings.

No detailed analysis regarding the stiffness coefficients of the cylindrical roller bearing has been carried out, but it is assumed to be 5 times stiffer than one ball bearing and to have the same damping coefficients. This is based on data that shows that a cylindrical bearing is approximately 3-6 times stiffer than a ball bearing [12]. Based on this data it is assumed that the stiffness coefficients of cylindrical bearing are accurate enough for the scope of this analysis.

No considerations have been made of the foundation plate or the pump DE bearing support plate. It is assumed that taking the support plate into account would not cause a significant change in the results. Further, the support plate is made out of steel so it is

assumed to contribute little to the damping properties of the system. Because of the fact that both the pump and the motor are mounted onto the same foundation, the properties of the foundation might contribute to the response of the system. Calculating the contribution in stiffness and damping from the foundation might increase the accuracy of the model and cause discrepancies with the current results. This could be considered a future extension of the analysis.

#### Recommendations

Based on the discussion above it is concluded that:

- The pump should be able to operate at its operational speed of 1494 rpm with no risk of damage to the machinery due to vibrations.
- It might be of interest to incorporate the skid and the pump DE bearing support plate in the model, especially calculation of the stiffness and damping from the skid might lower the natural frequencies, since it is now considered rigid. Since all criterions are fulfilled with a good margin however, this should not be considered crucial to the analysis.
- With the model of the full string used in this analysis all criteria according to API 610 and TBM are fulfilled, but with the exception of a comparison of the impeller radial displacement and the diametral clearance of the pump due to unbalance. LR Consulting recommends that the radial displacements presented in Table 17 and Table 18 is compared against, and that it is ensured that these do not exceed 35% of, the diametral clearance.

### 6 References

- [1] American Petroleum Institute, "Standard 610; Centrifugal Pumps for Petroleum, Petrochemical and Natural Gas Industries, 9th edition," 2003.
- [2] Svenska Kärnkraftsföretagen, *TBM Tekniska Bestämmelser för Mekaniska Anordningar, Utgåva 8,* 2013.
- [3] Pump OEM, Drawing UG1445598 Assembly Drawing rev 03, 2013.
- [4] Pump OEM, "Detailed design documentation Proof of strength for the pump rotor rev 00," 2013.
- [5] Motor OEM, *Drawing no: 3GZF500731-242 A 14 BP 315 R,* 2009.
- [6] Bearing OEM, Bearing OEM Online catalog (Bearings), 2014.
- [7] Coupling OEM, Flender Standard Couplings Catalog MD 10.1, 2011.
- [8] Pump OEM, Drawing UG1438651 Installation plan rev 06, 2013.
- [9] Pump OEM, Drawing UG1445594 Assembly drawing rev 02, 2013.
- [10] R. D. Blevins, Formulas for Natural Frequencies and Mode Shapes, Florida: Krieger Publishing Company, 1995.
- [11] D. W. Childs, Turbomachinery Rotordynamics, Phenomena, Modelling, and Analysis, John Wiley & Sons, 1993.
- [12] National Renewable Energy Laboratory, Rolling Element Bearing Stiffness Matrix Determination, 2012.
- [13] ISO, "ISO 1940/1 Mechanical vibration Balance quality requirements of rigid rotors Part 1: Determination of permissible residual unbalance," 1986.

13.320179 Elforsk rotordynamic analysis

# Bode plots and mode shapes from the unbalance response analysis

In Appendix A.1 to A.6 all Bode plots and mode shapes determined from the unbalance analysis are presented. The response in the Bode plots is taken at the impeller, at the motor bearing mid-span and at the bearing locations. For the impeller and the motor mid-span positions the displacement is presented, while the velocity is presented at the bearing locations. The mode shape for each case is presented for the rated speed. The mode shapes are plotted relative the reference model seen in Figure A 1.

Damped eigenvalue analysis

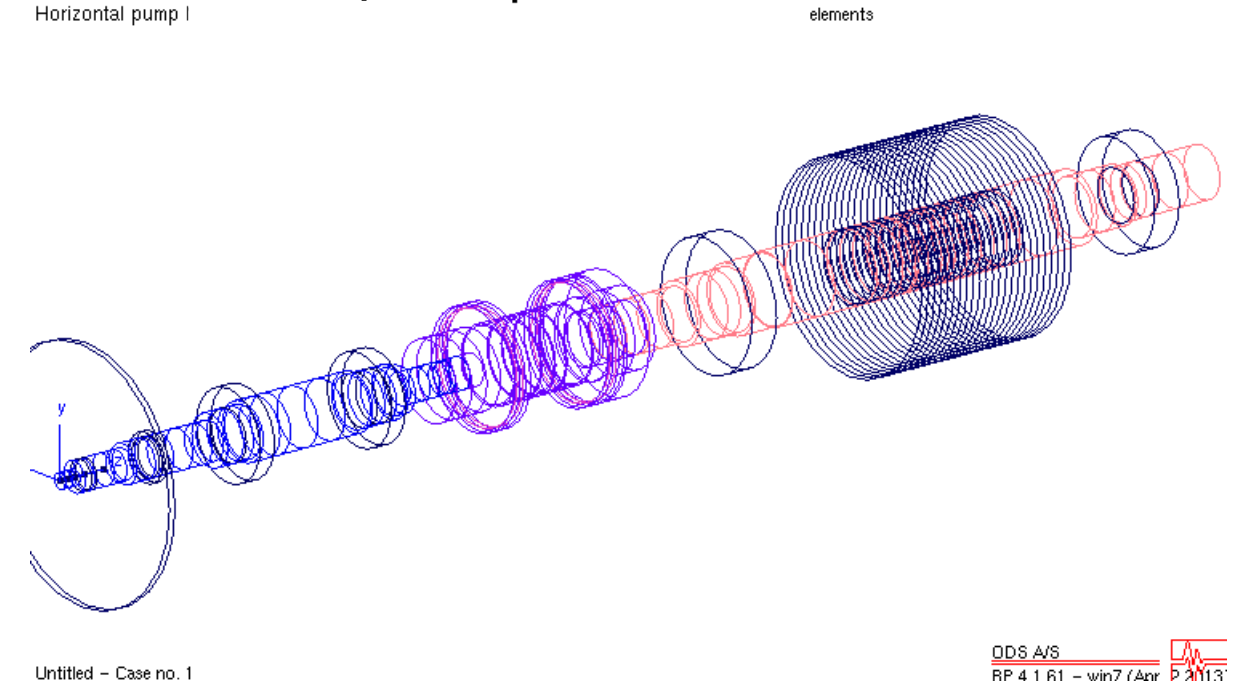


Figure A 1. Reference model for comparison with the mode shapes for each unbalance case.

Impeller unbalance (Configuration A) – Minimum bearing stiffness

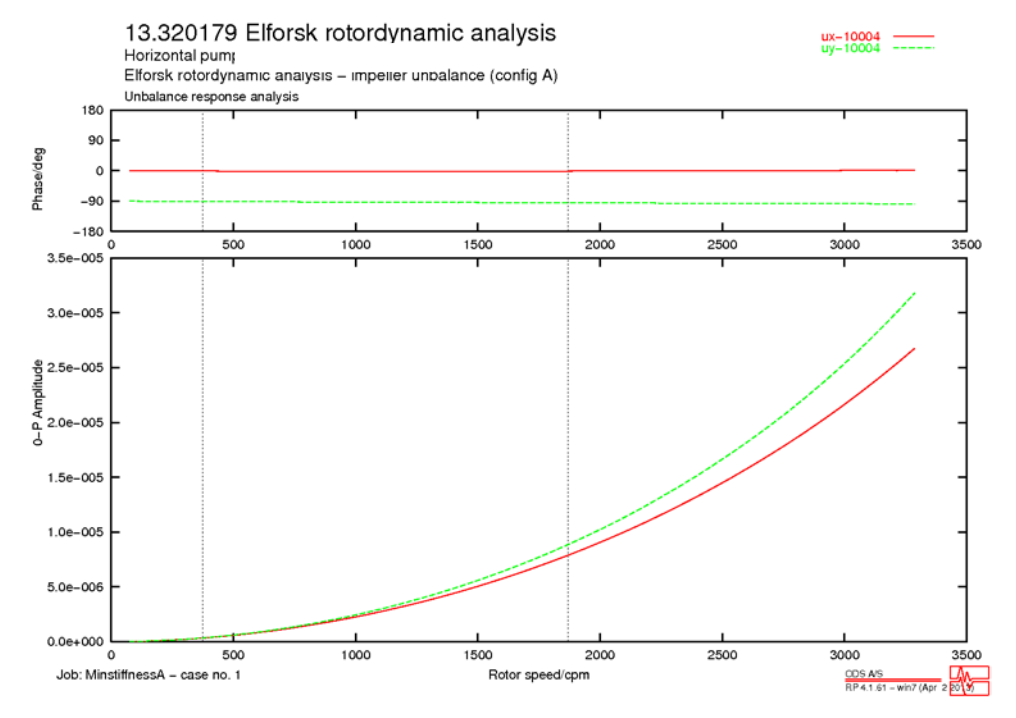


Figure A 2. Bode plot showing the displacement at impeller for unbalance Case A. Minimum bearing stiffness is used.

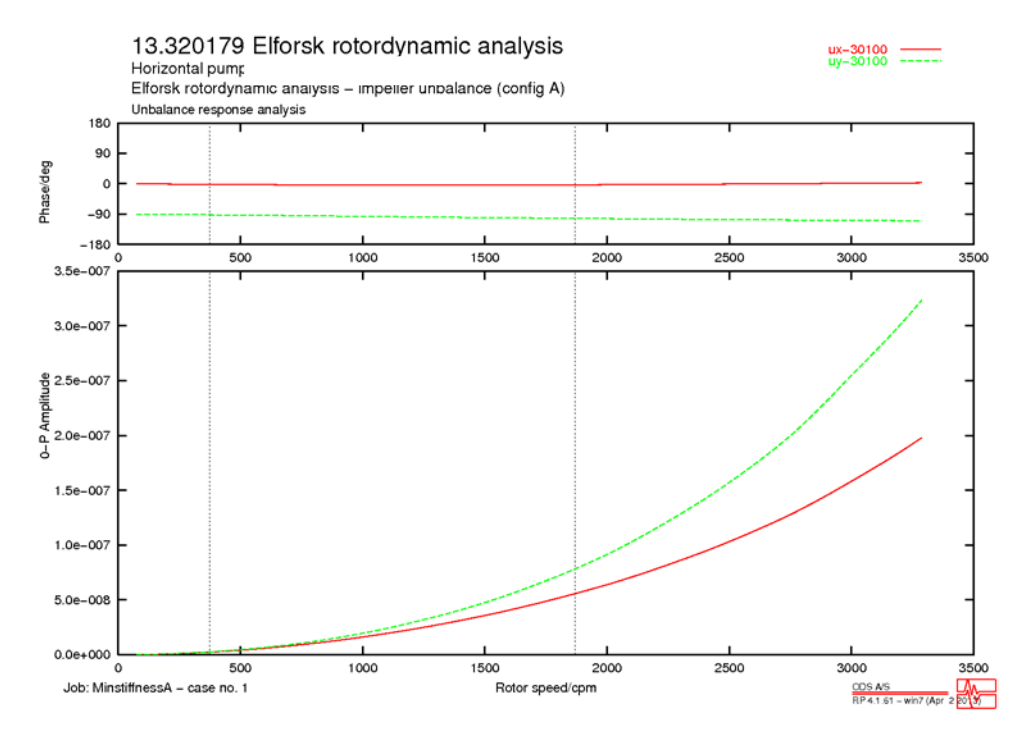


Figure A 3. Bode plot showing the displacement at the motor bearing mid-span for unbalance Case A. Minimum bearing stiffness is used.

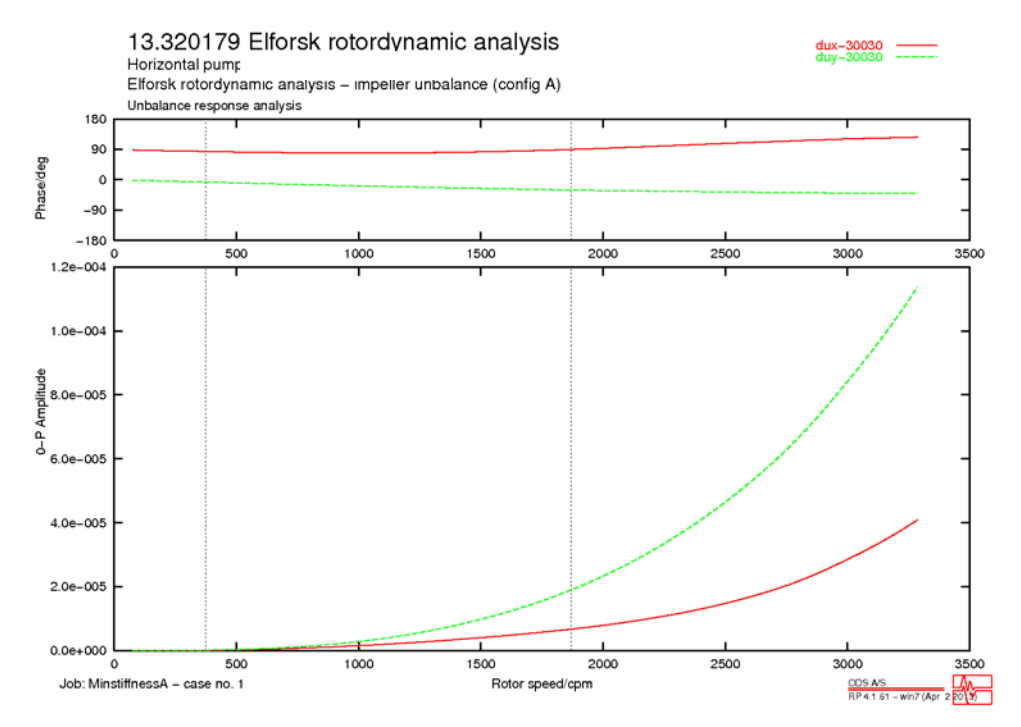


Figure A 4. Bode plot showing the velocity at the motor NDE bearing for unbalance Case A. Minimum bearing stiffness is used.

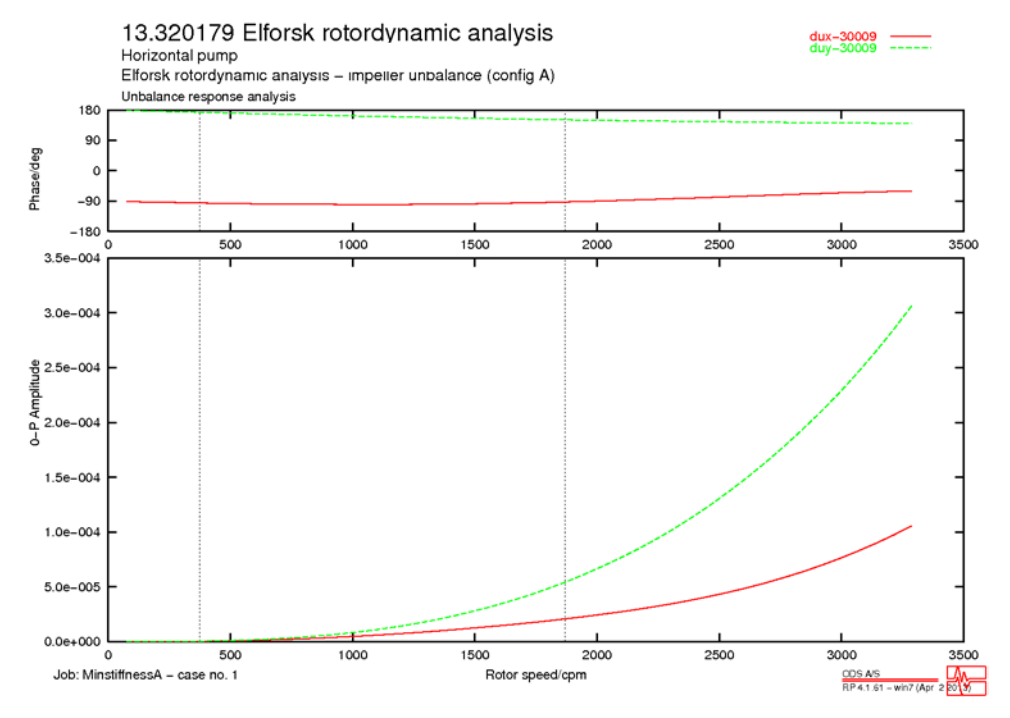


Figure A 5. Bode plot showing the velocity at the motor DE bearing for unbalance Case A. Minimum bearing stiffness is used.

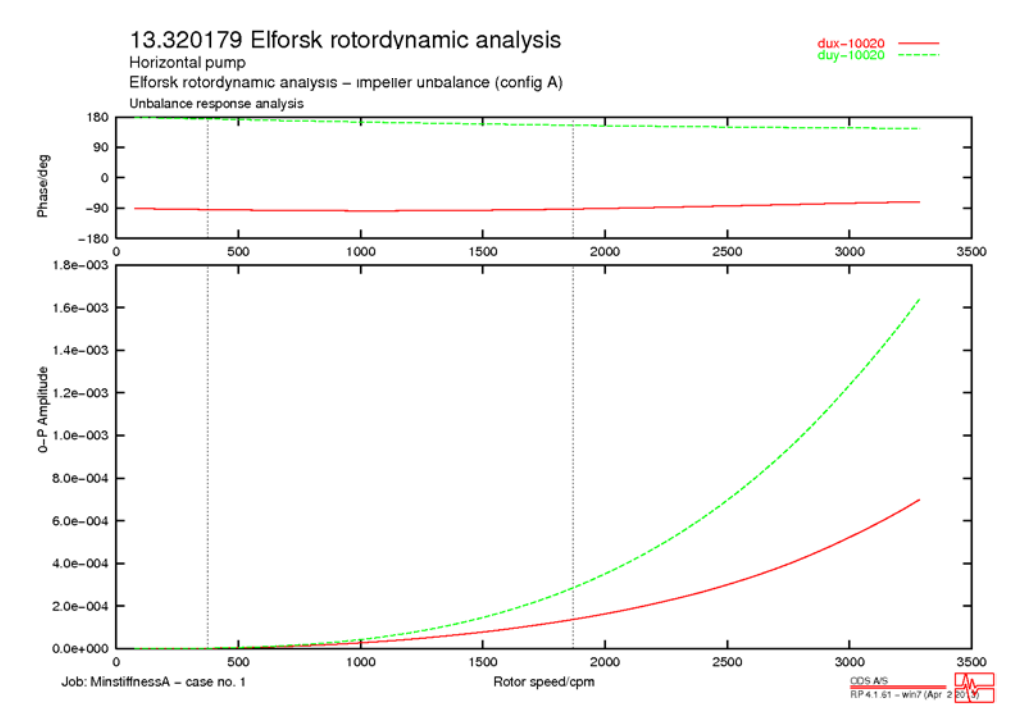


Figure A 6. Bode plot showing the velocity at the pump DE bearing for unbalance Case A. Minimum bearing stiffness is used.

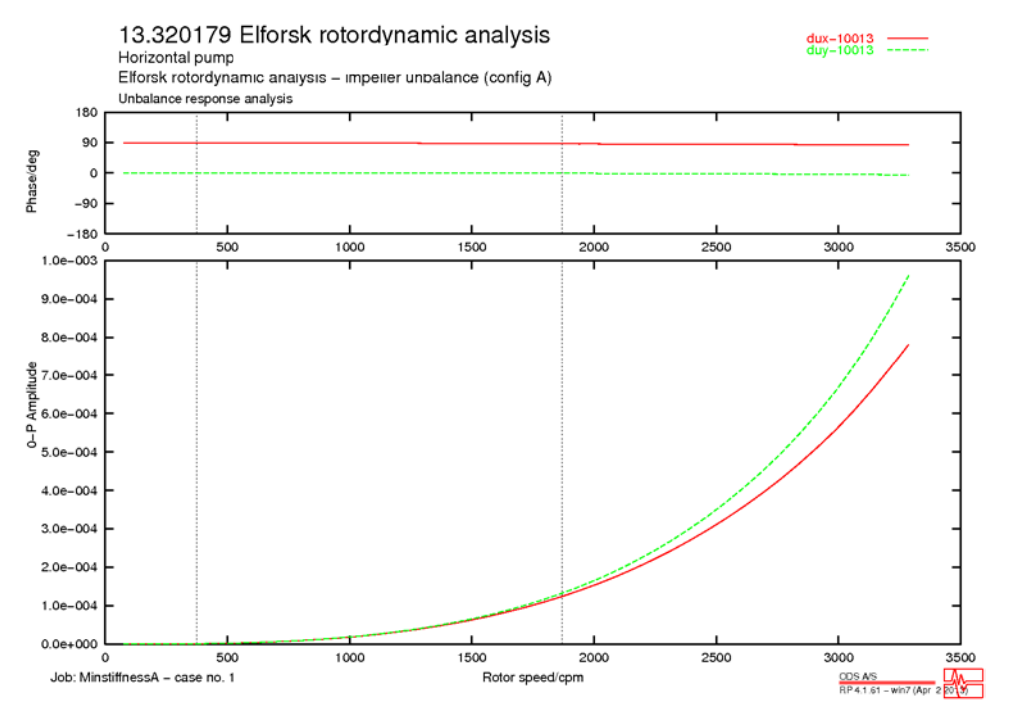


Figure A 7. Bode plot showing the velocity at the pump NDE bearing for unbalance Case A. Minimum bearing stiffness is used.

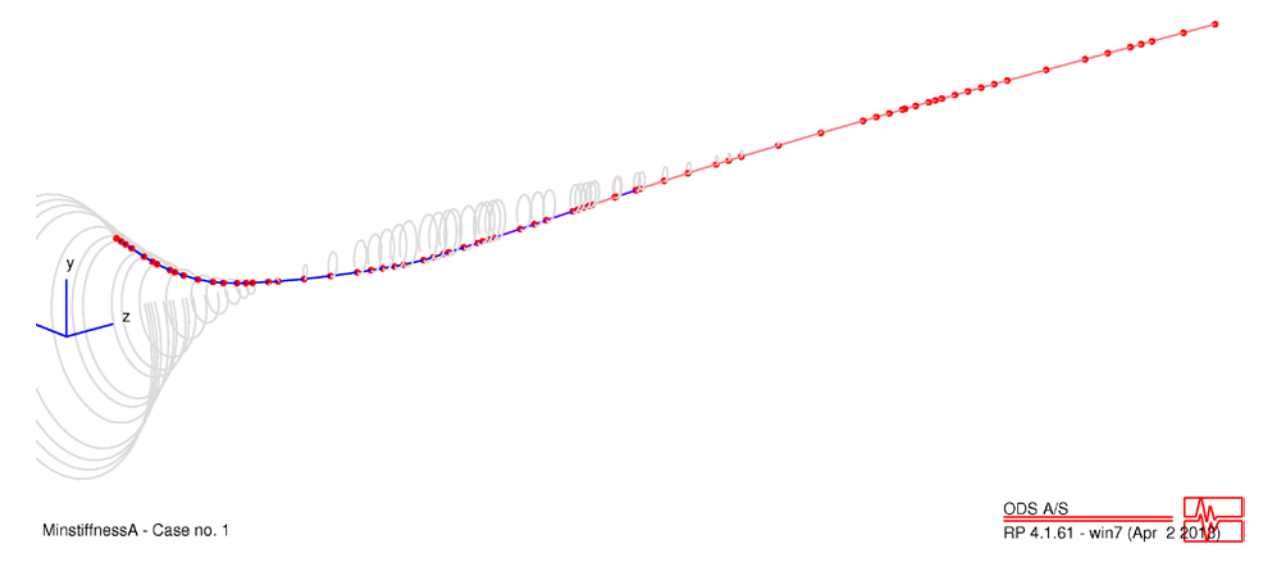


Figure A 8. Shape of the first mode at rated speed (1494 rpm). Unbalance case A and minimum bearing stiffness is used.

Impeller unbalance (Configuration A) – Maximum bearing stiffness

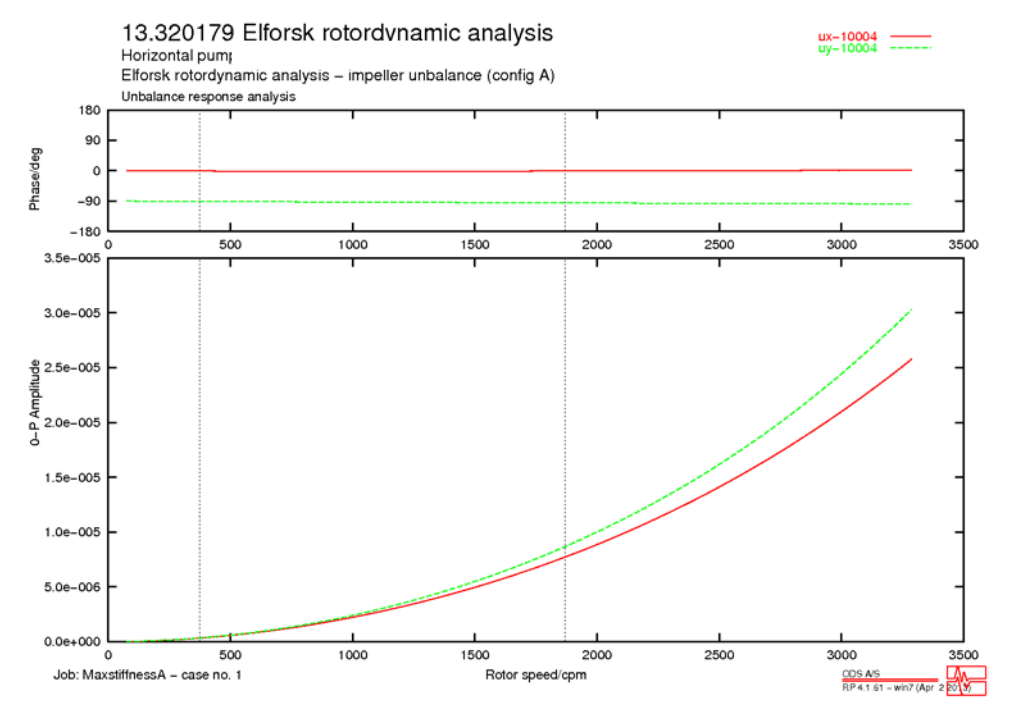


Figure A 9. Bode plot showing the displacement at the impeller for unbalance Case A. Maximum bearing stiffness is used.

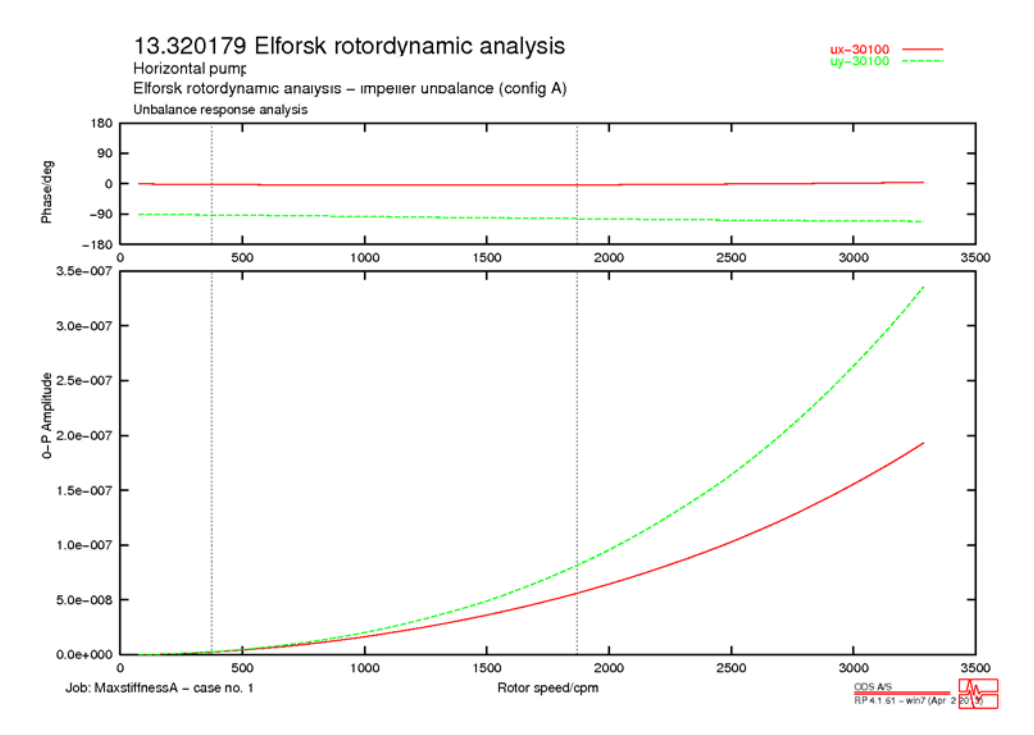


Figure A 10. Bode plot showing the displacement at the motor bearing mid-span for unbalance Case A. Maximum bearing stiffness is used.

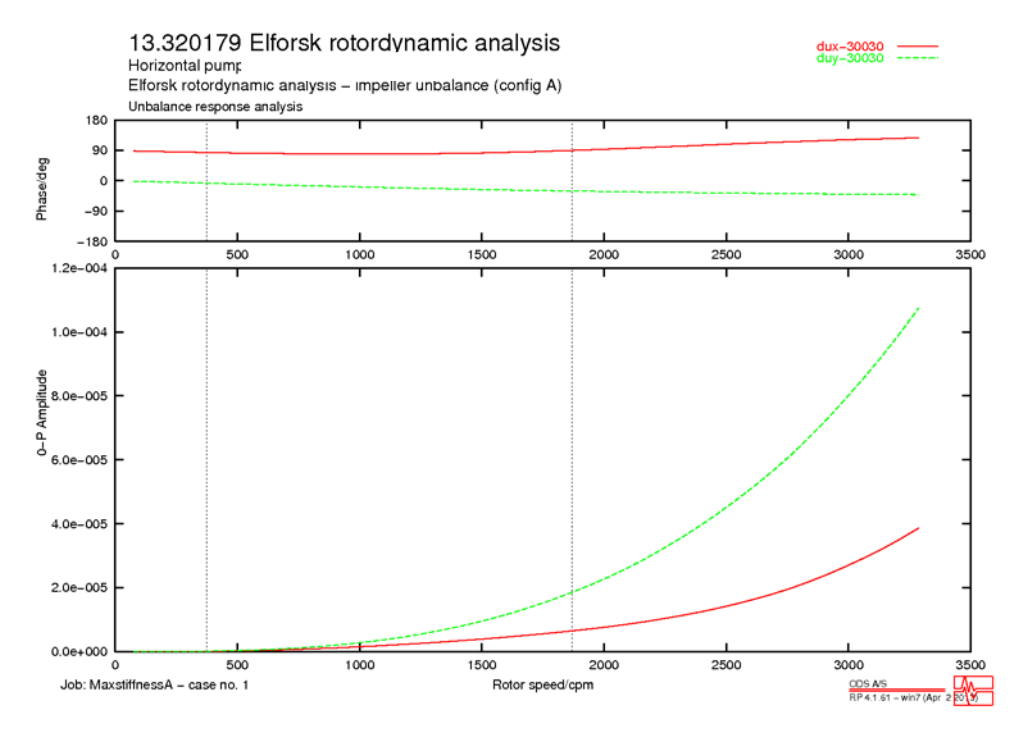


Figure A 11. Bode plot showing the velocity at the motor NDE bearing for unbalance Case A. Maximum bearing stiffness is used.

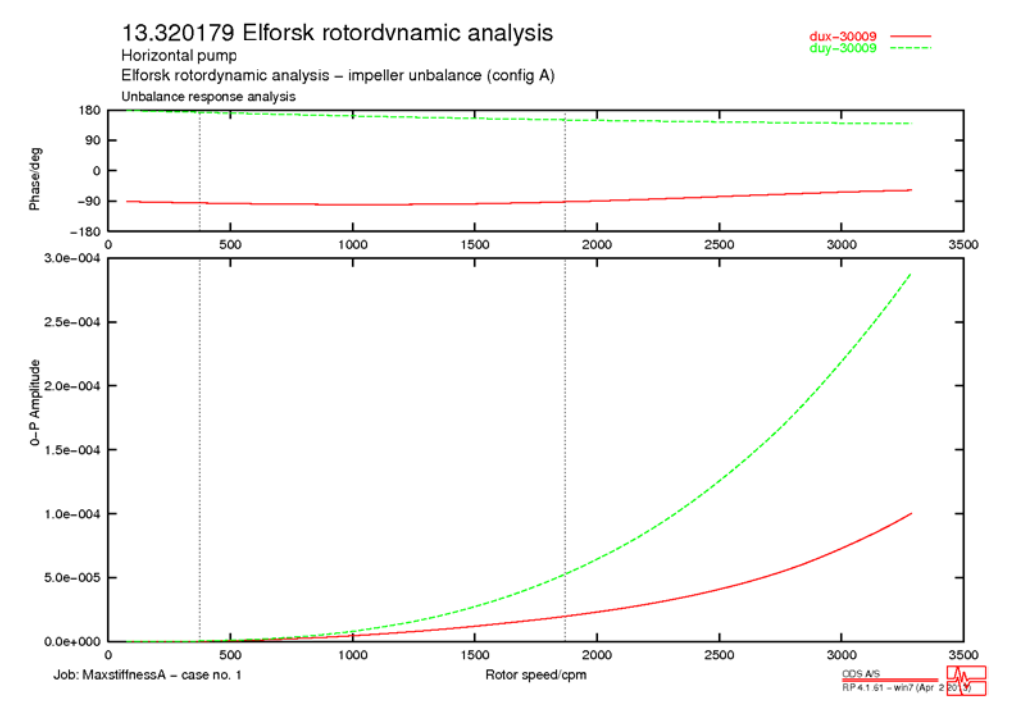


Figure A 12. Bode plot showing the velocity at the motor DE bearing for unbalance Case A. Maximum bearing stiffness is used.

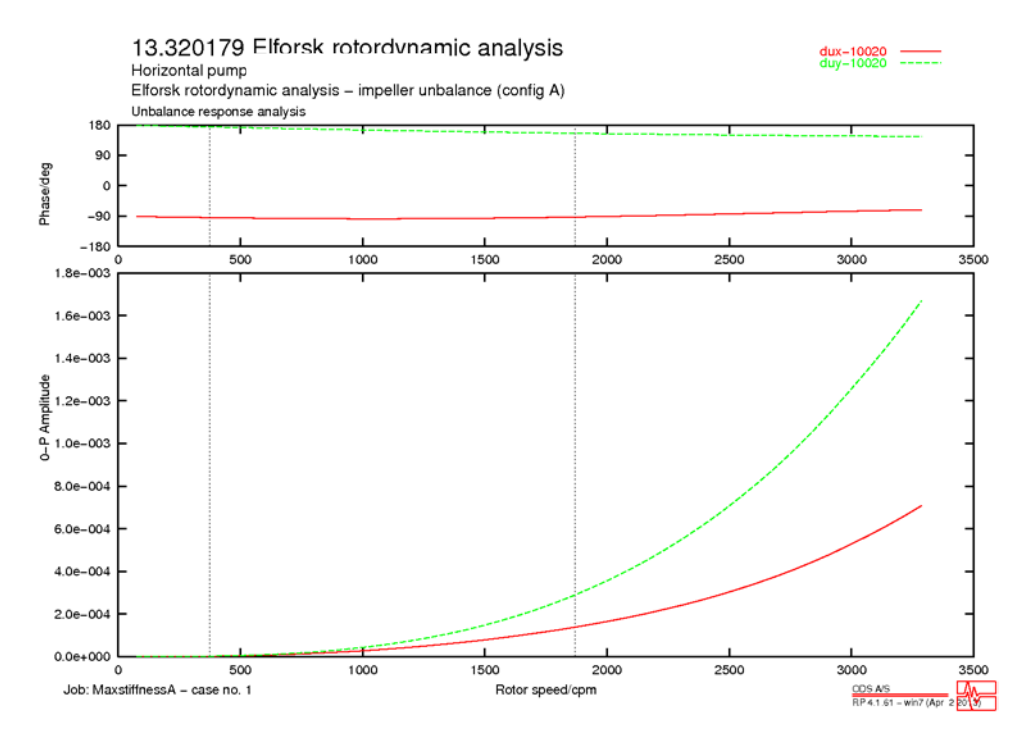


Figure A 13. Bode plot showing the velocity at the pump DE bearing for unbalance Case A. Maximum bearing stiffness is used.

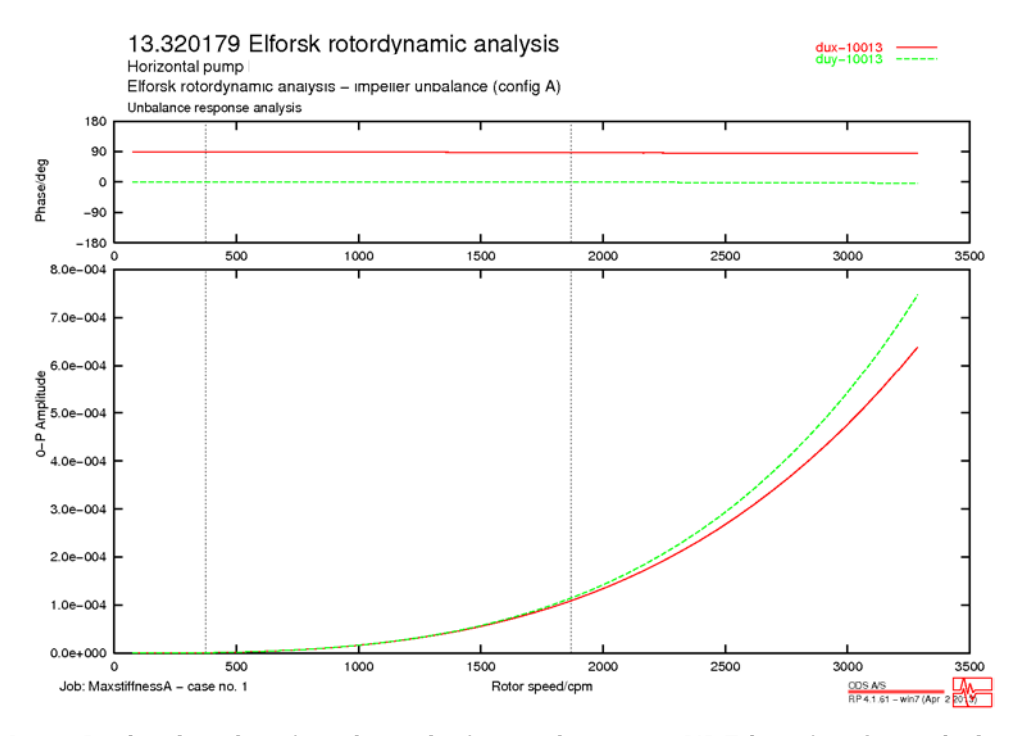


Figure A 14. Bode plot showing the velocity at the pump NDE bearing for unbalance Case A. Maximum bearing stiffness is used.

Unbalance response analysis Deflected Shape @ 1494 rpm Subcase no.20

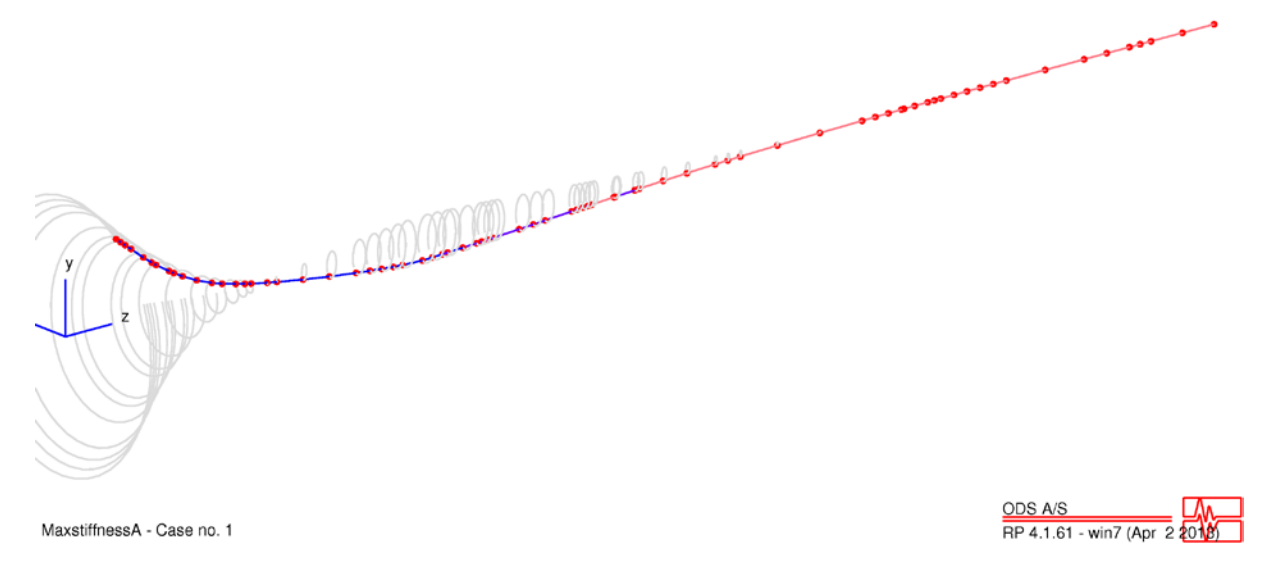


Figure A 15. Shape of the first mode at rated speed (1494 rpm). Unbalance case A and maximum bearing stiffness is used.

# Motor unbalance (Configuration B) – Minimum bearing stiffness

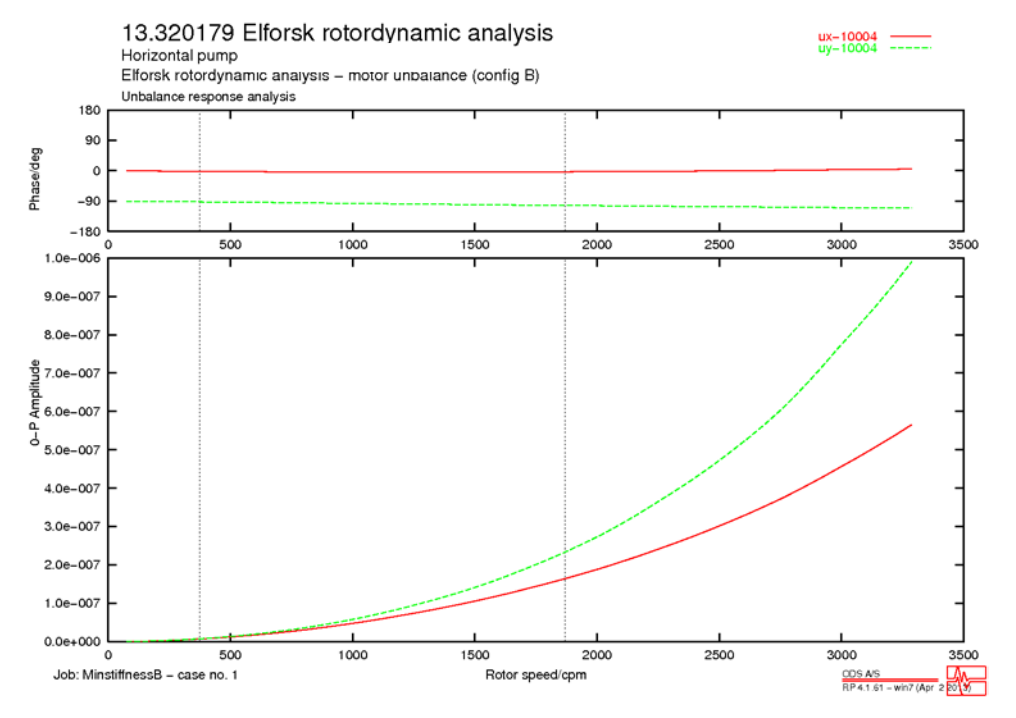


Figure A 16. Bode plot showing the displacement at the impeller for unbalance Case B. Minimum bearing stiffness is used.

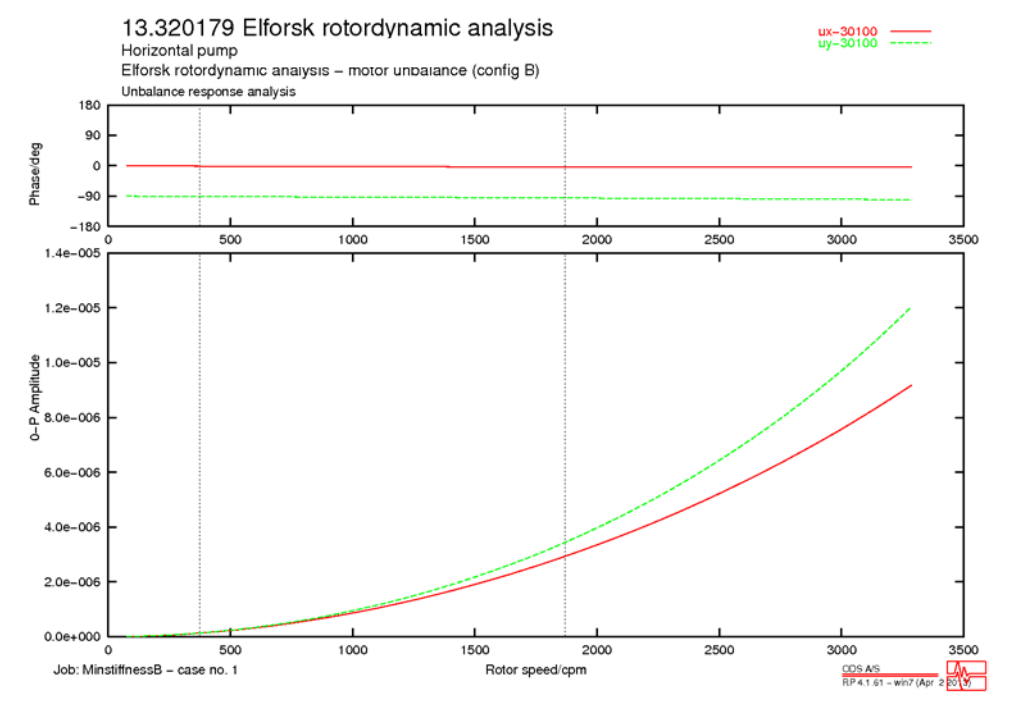


Figure A 17. Bode plot showing the displacement at the motor bearing mid-span for unbalance Case B. Minimum bearing stiffness is used.

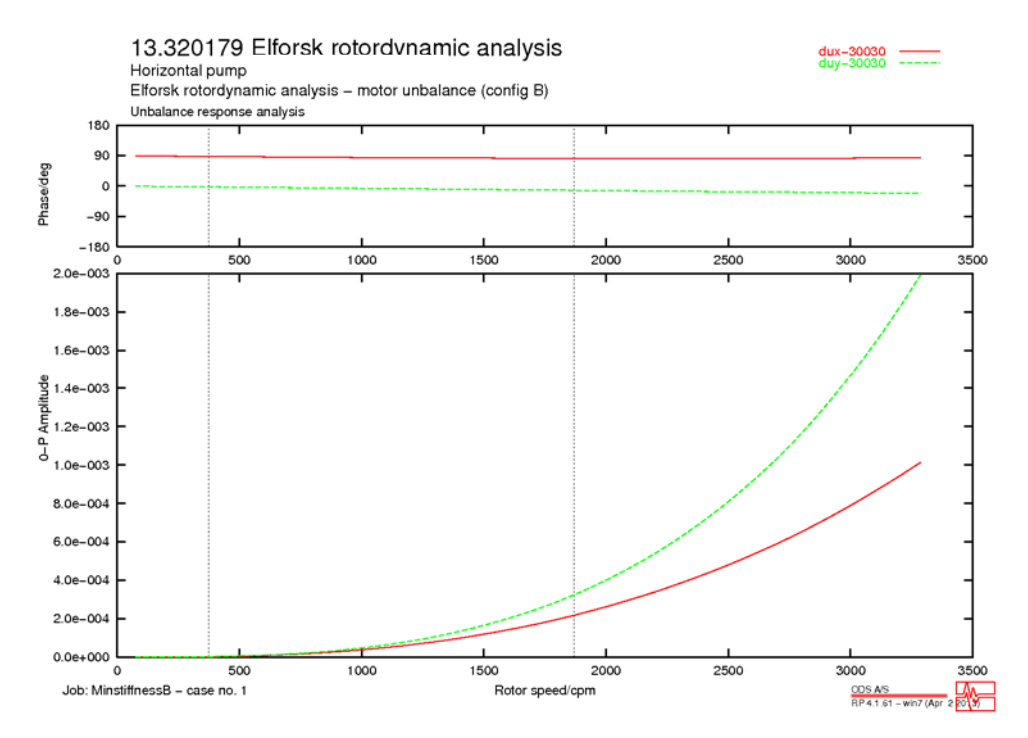


Figure A 18. Bode plot showing the velocity at the motor NDE bearing for unbalance Case B. Minimum bearing stiffness is used.

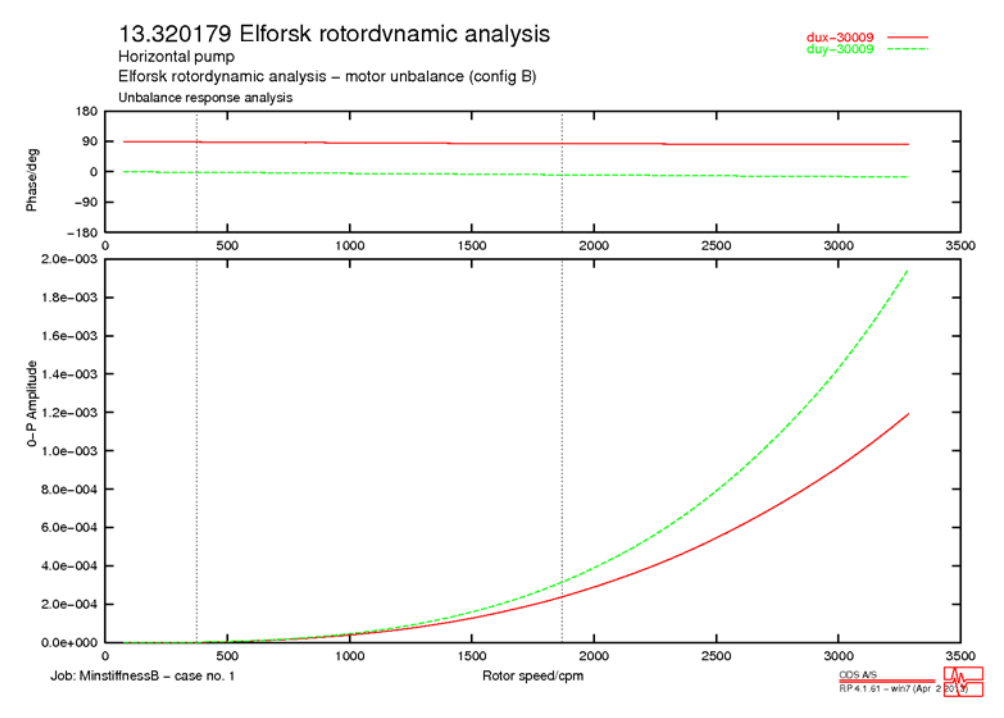


Figure A 19. Bode plot showing the velocity at the motor DE bearing for unbalance Case B. Minimum bearing stiffness is used.

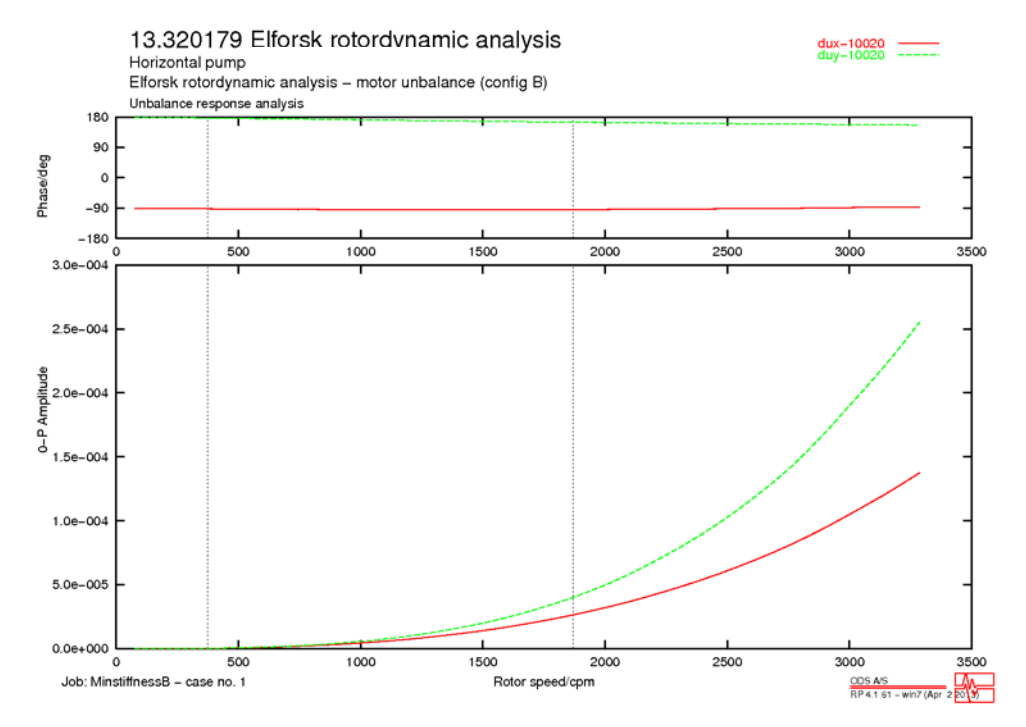


Figure A 20. Bode plot showing the velocity at the pump DE bearing for unbalance Case B. Minimum bearing stiffness is used.

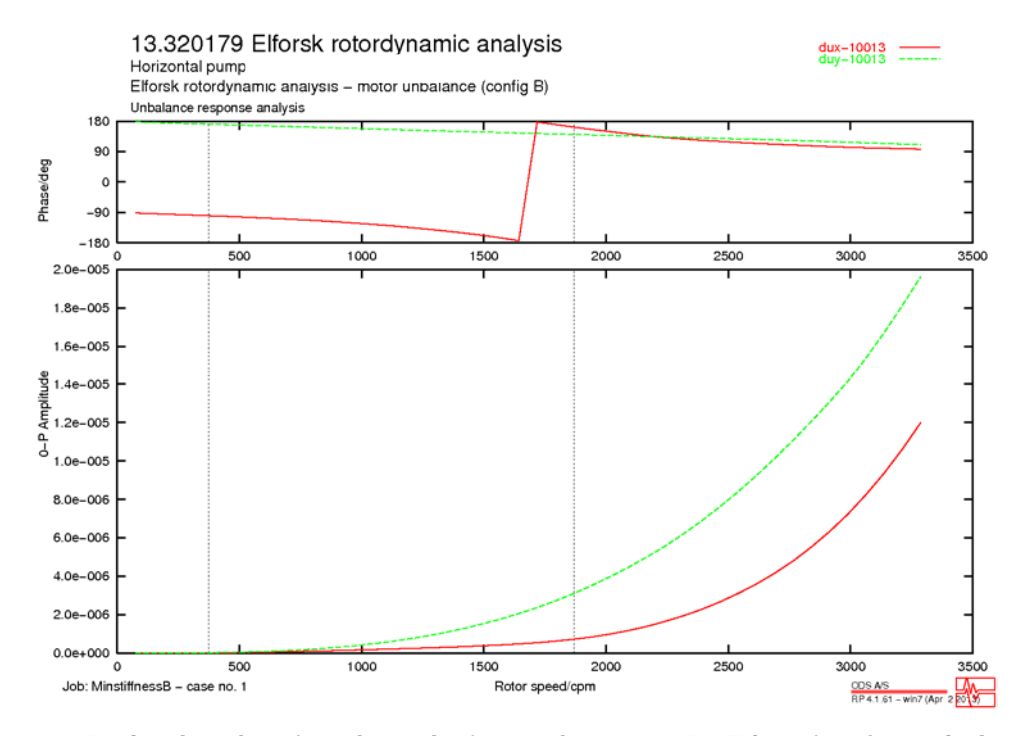


Figure A 21. Bode plot showing the velocity at the pump NDE bearing for unbalance Case B. Minimum bearing stiffness is used.

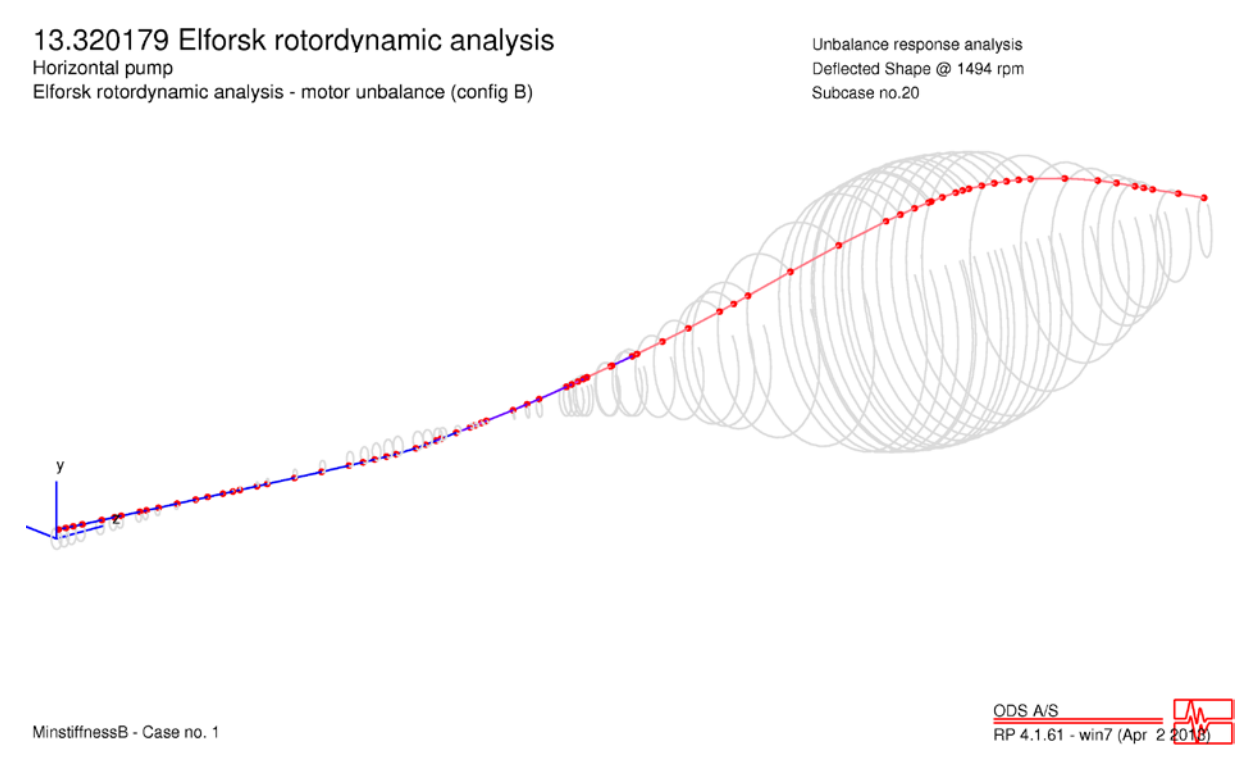


Figure A 22. Shape of the first mode at rated speed (1494 rpm). Unbalance case B and minimum bearing stiffness is used.

# Motor unbalance (Configuration B) – Maximum bearing stiffness

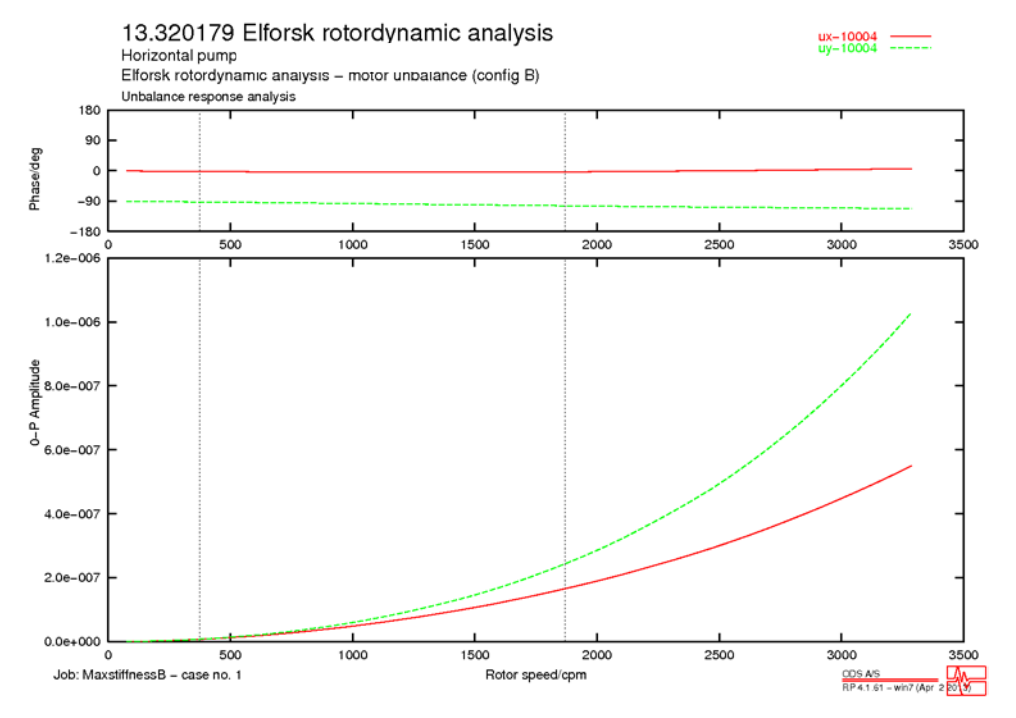


Figure A 23. Bode plot showing the displacement at the impeller for unbalance Case B. Maximum bearing stiffness is used.

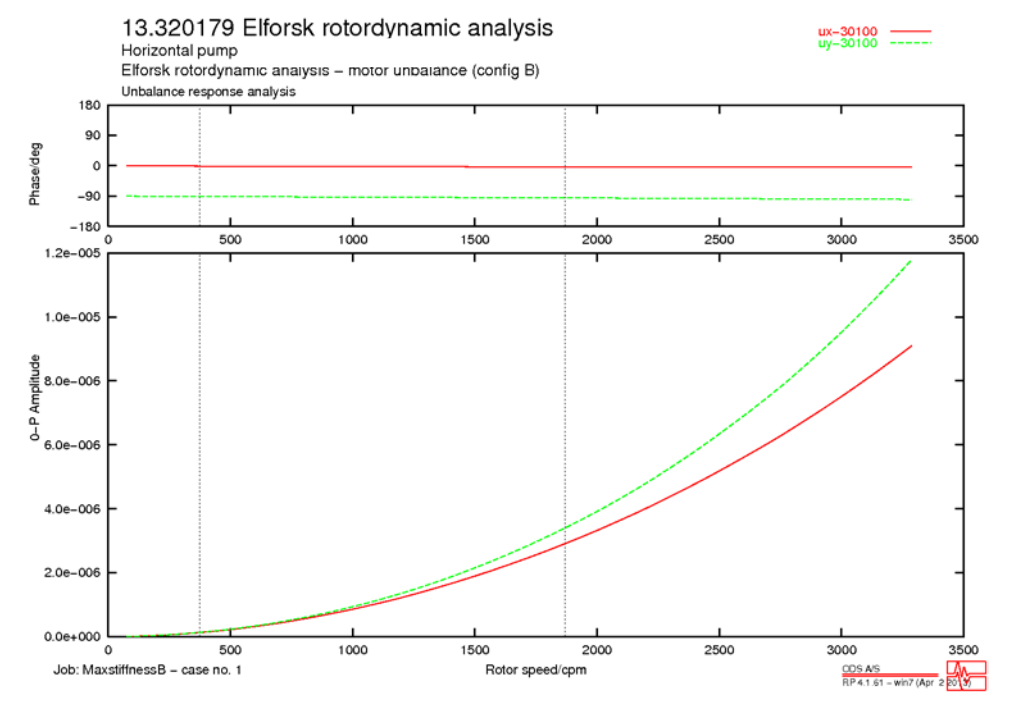


Figure A 24. Bode plot showing the displacement at the motor bearing mid-span for unbalance Case B. Maximum bearing stiffness is used.

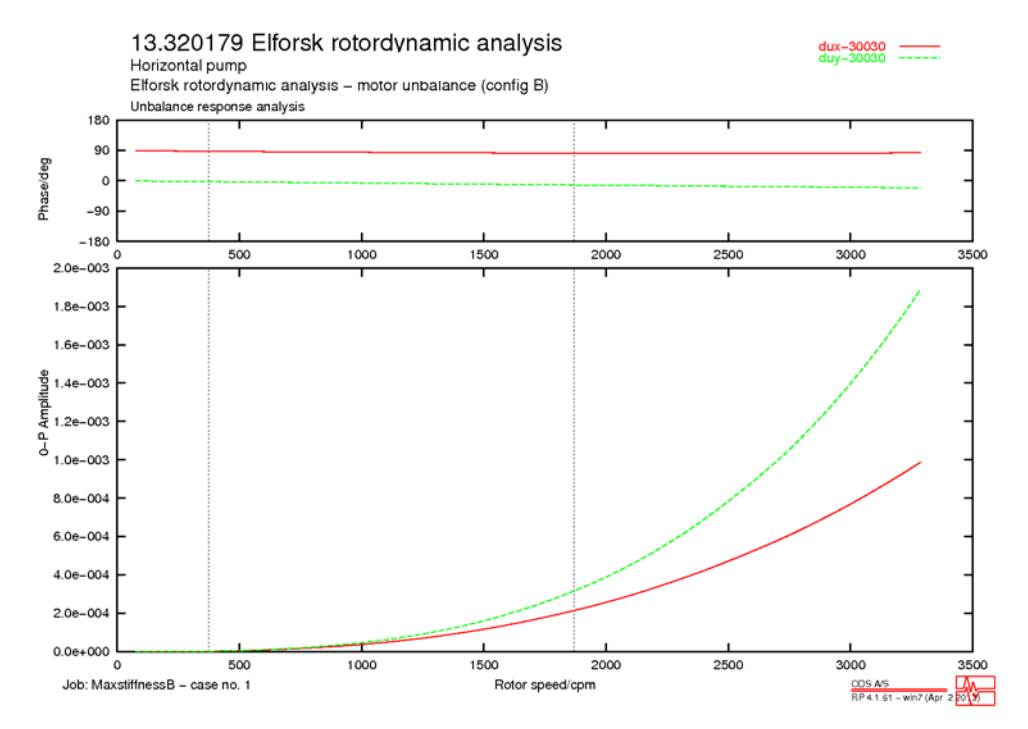


Figure A 25. Bode plot showing the velocity at the motor NDE bearing for unbalance Case B. Maximum bearing stiffness is used.

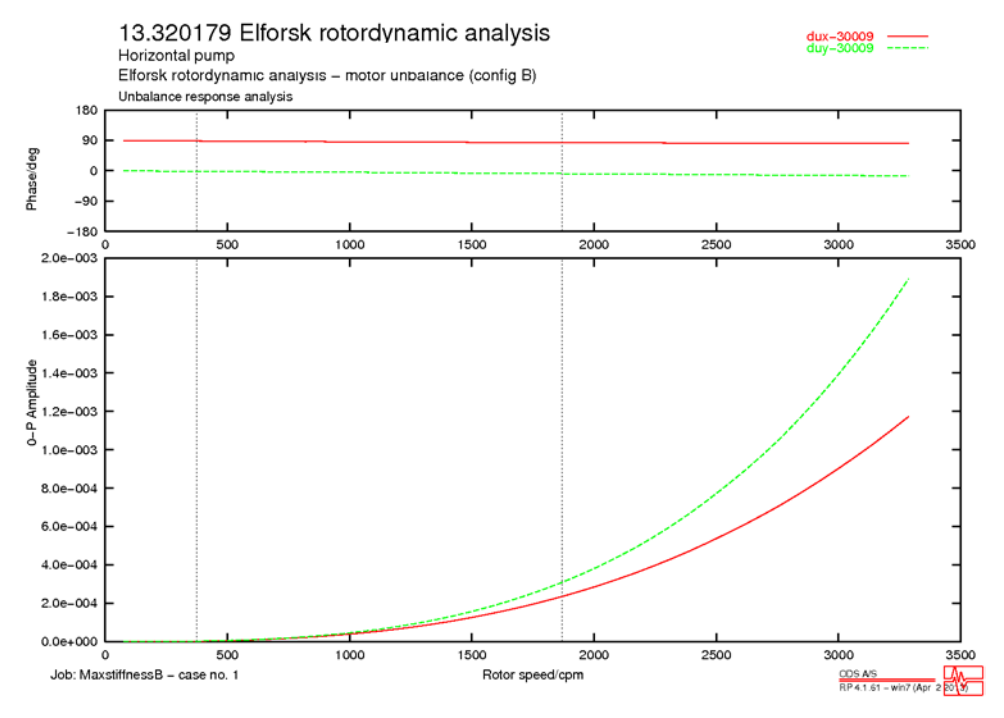


Figure A 26. Bode plot showing the velocity at the motor DE bearing for unbalance Case B. Maximum bearing stiffness is used.

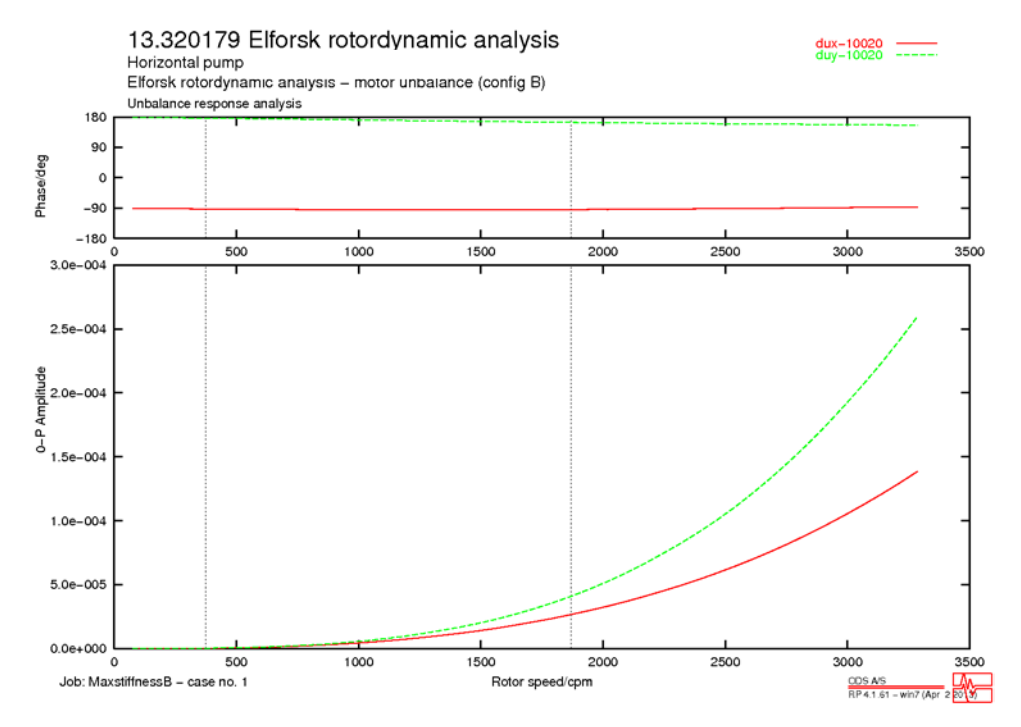


Figure A 27. Bode plot showing the velocity at the pump DE bearing for unbalance Case B. Maximum bearing stiffness is used.

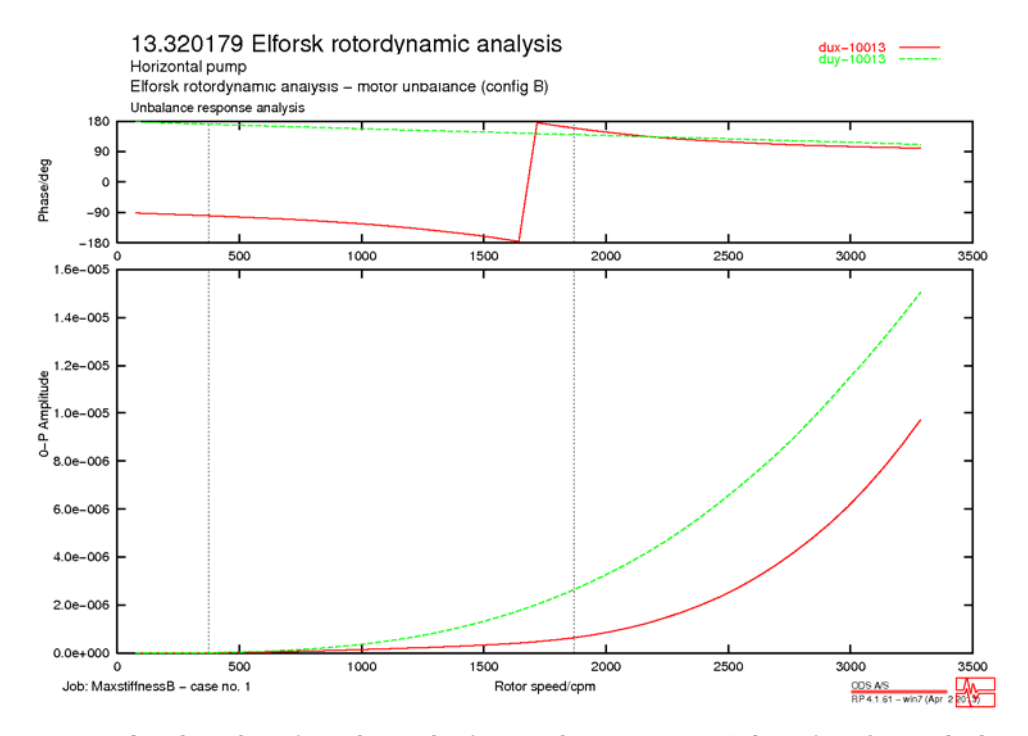


Figure A 28. Bode plot showing the velocity at the pump NDE bearing for unbalance Case B. Maximum bearing stiffness is used.

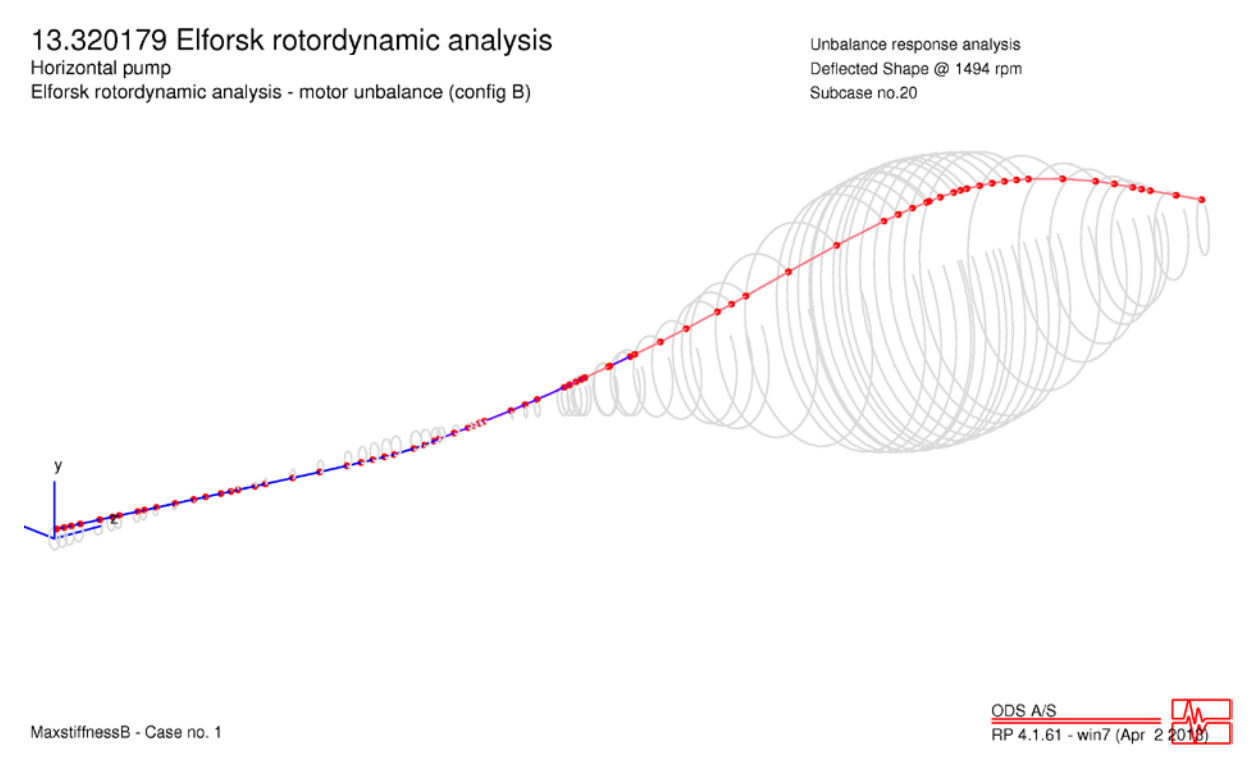


Figure A 29. Shape of the first mode at rated speed (1494 rpm). Unbalance case B and maximum bearing stiffness is used.

# Coupling unbalance (Configuration C) – Minimum bearing stiffness

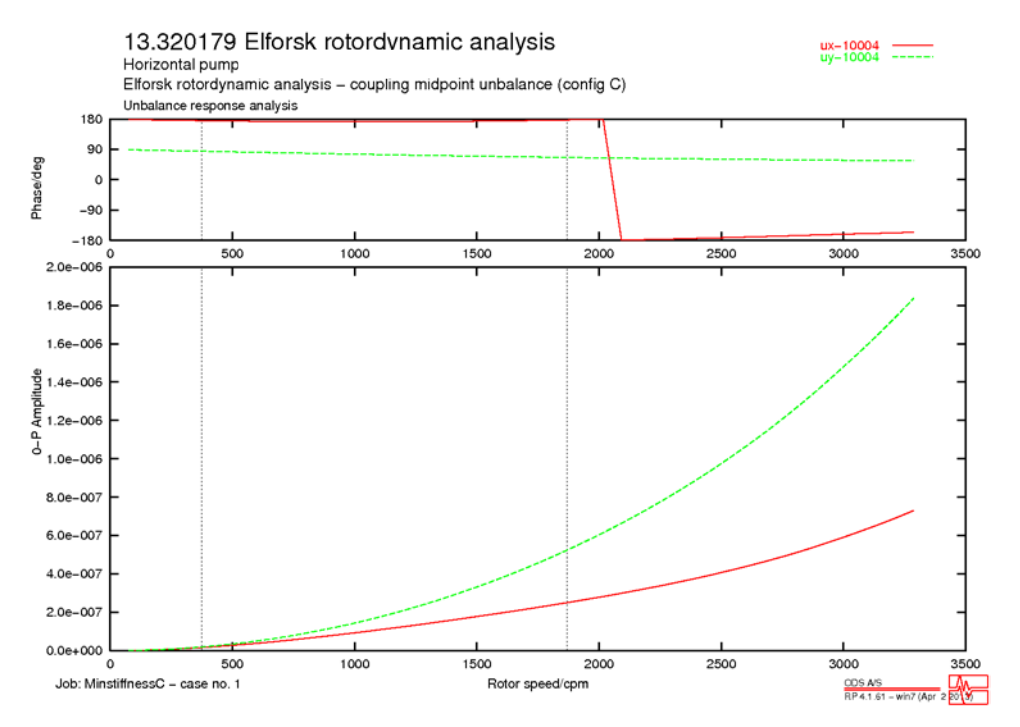


Figure A 30. Bode plot showing the displacement at the impeller for unbalance Case C. Minimum bearing stiffness is used.

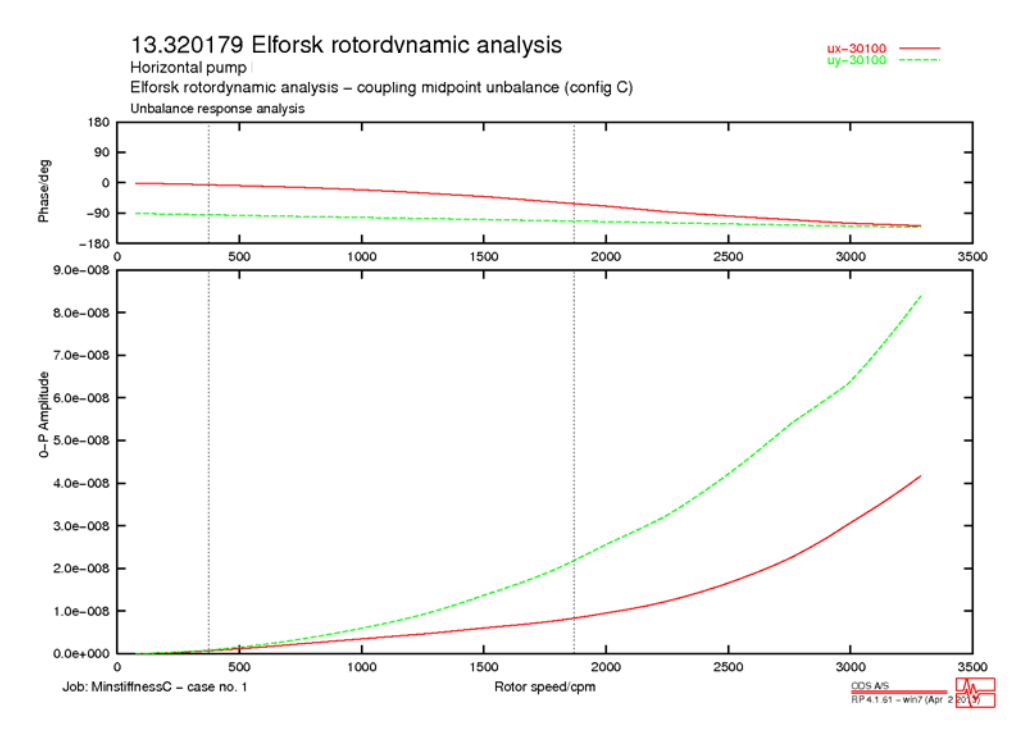


Figure A 31. Bode plot showing the displacement at the motor bearing mid-span for unbalance Case C. Minimum bearing stiffness is used.

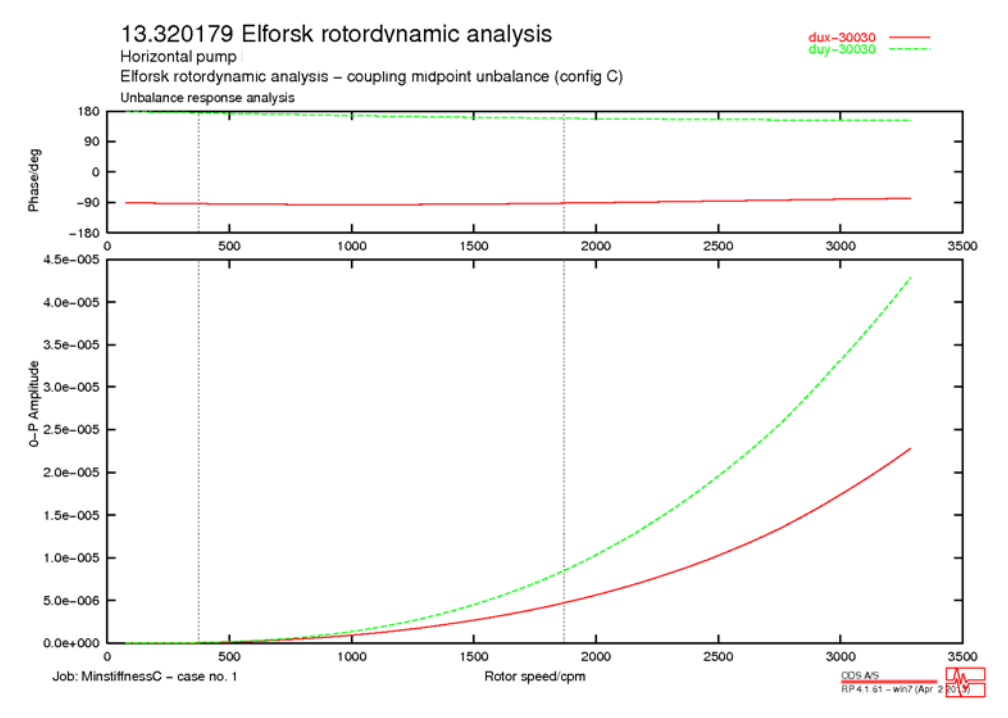


Figure A 32. Bode plot showing the velocity at the motor NDE bearing for unbalance Case C. Minimum bearing stiffness is used.

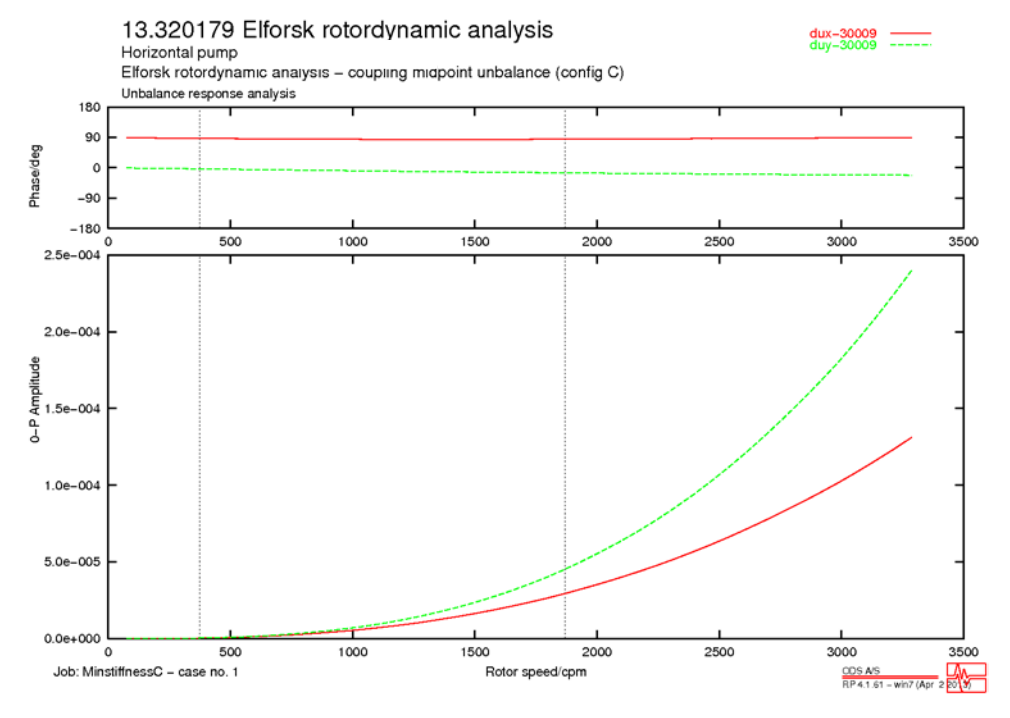


Figure A 33. Bode plot showing the velocity at the motor DE bearing for unbalance Case C. Minimum bearing stiffness is used.

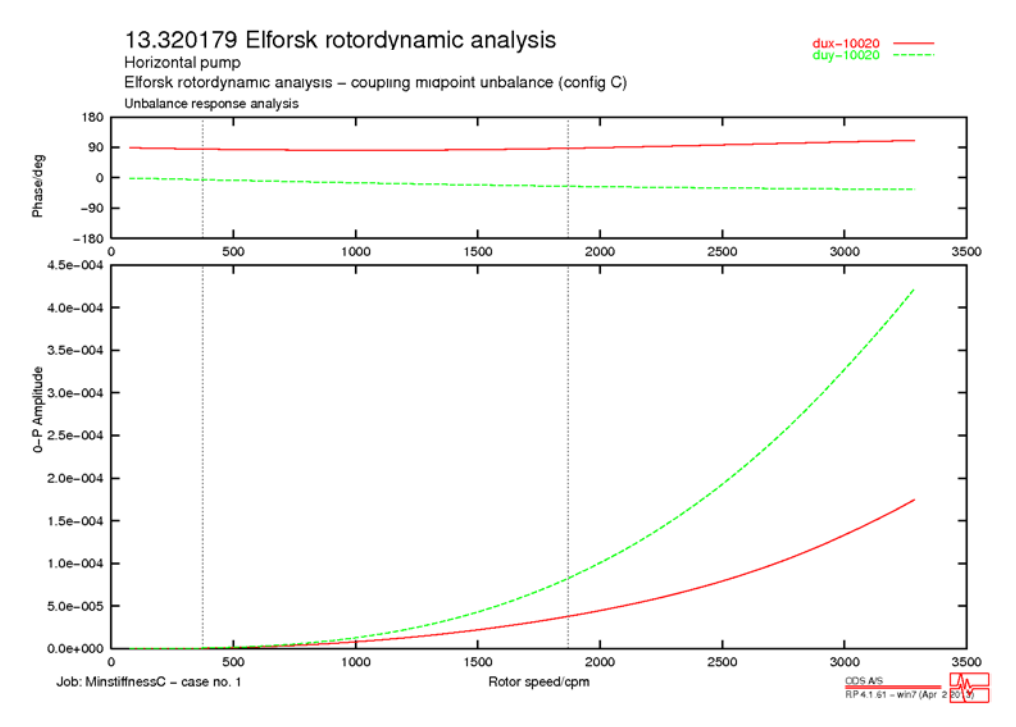


Figure A 34. Bode plot showing the velocity at the pump DE bearing for unbalance Case C. Minimum bearing stiffness is used.

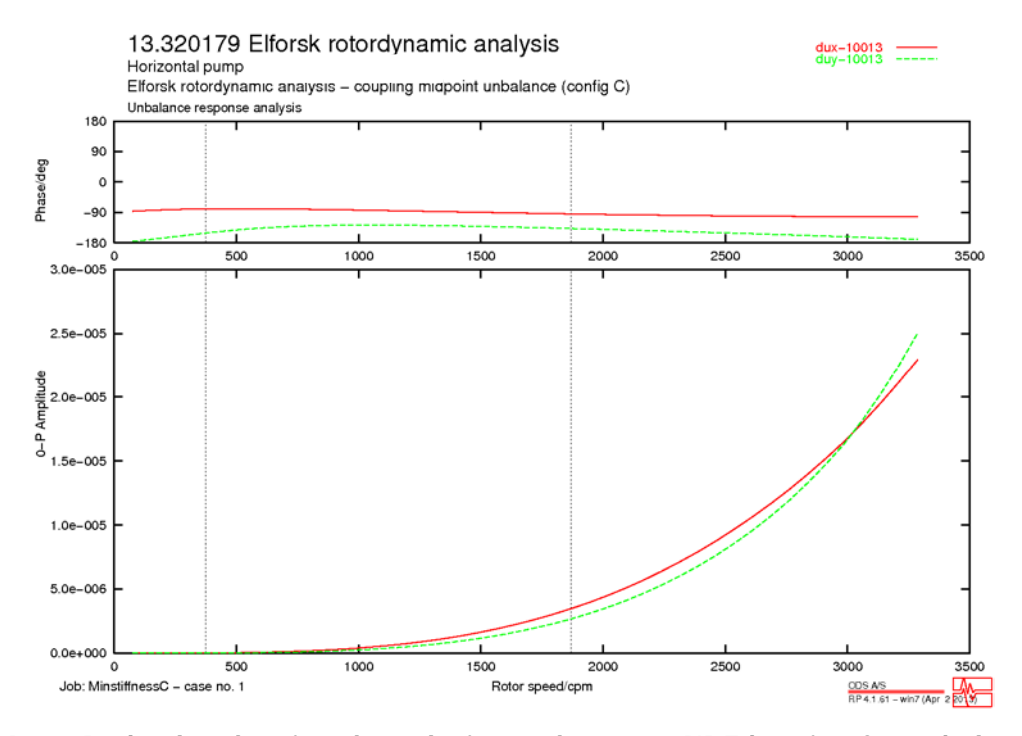


Figure A 35. Bode plot showing the velocity at the pump NDE bearing for unbalance Case C. Minimum bearing stiffness is used.

13.320179 Elforsk rotordynamic analysis Horizontal pump Elforsk rotordynamic analysis - coupling midpoint unbalance (config C)

Unbalance response analysis Deflected Shape @ 1494 rpm Subcase no.20

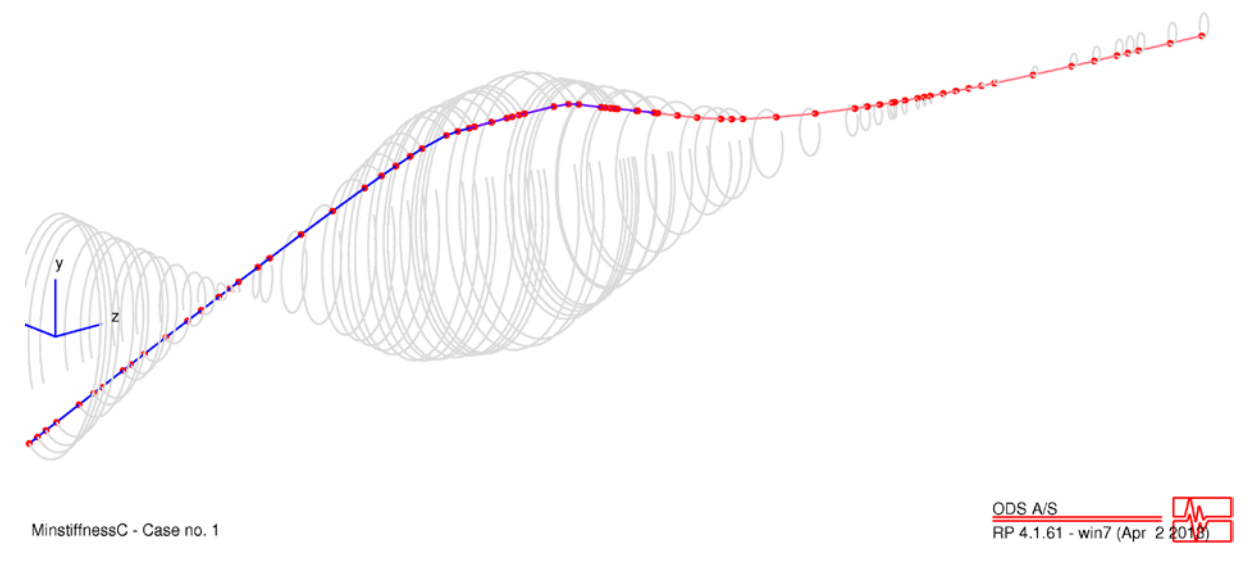


Figure A 36. Shape of the first mode at rated speed (1494 rpm). Unbalance case C and minimum bearing stiffness is used.

# Coupling unbalance (Configuration C) – Maximum bearing stiffness

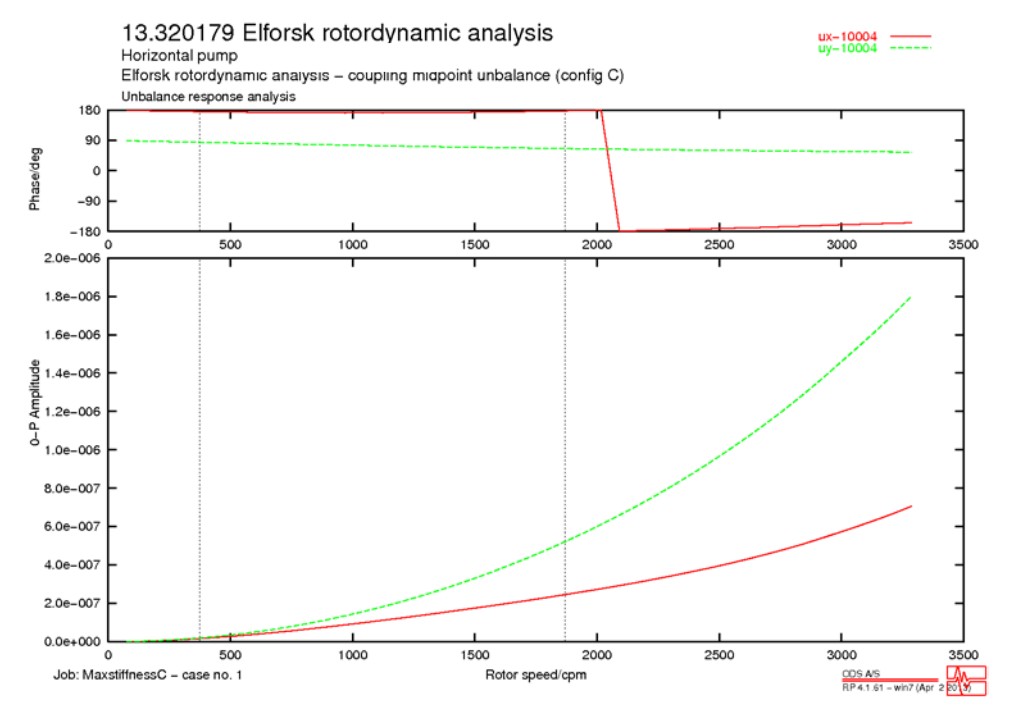


Figure A 37. Bode plot showing the displacement at the impeller for unbalance Case C. Maximum bearing stiffness is used.

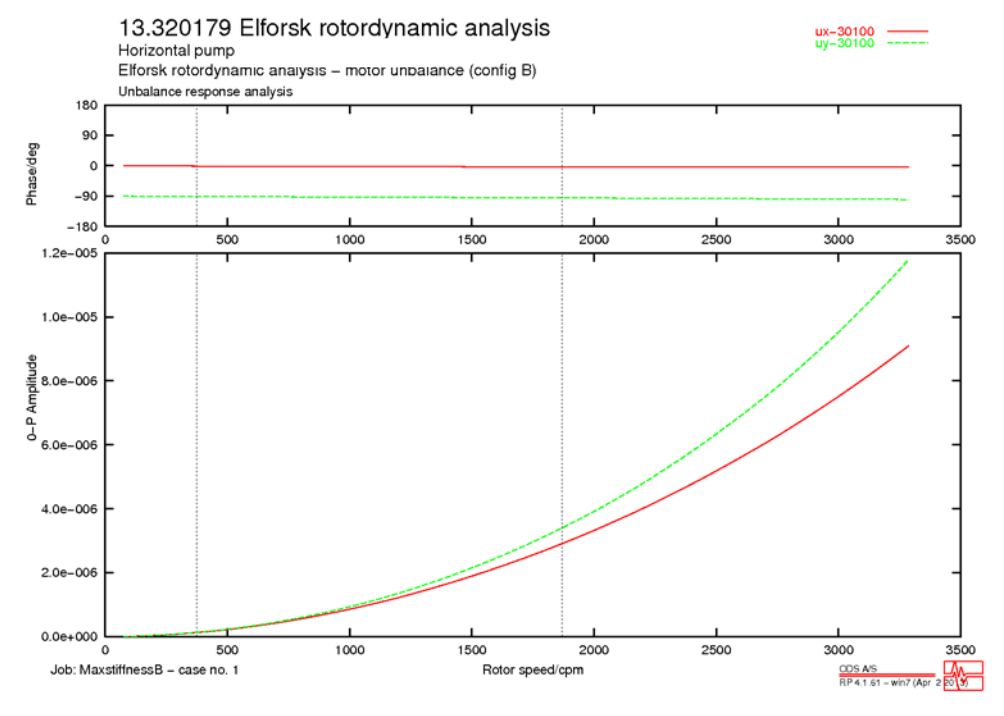


Figure A 38. Bode plot showing the displacement at the motor bearing mid-span for unbalance Case C. Maximum bearing stiffness is used.

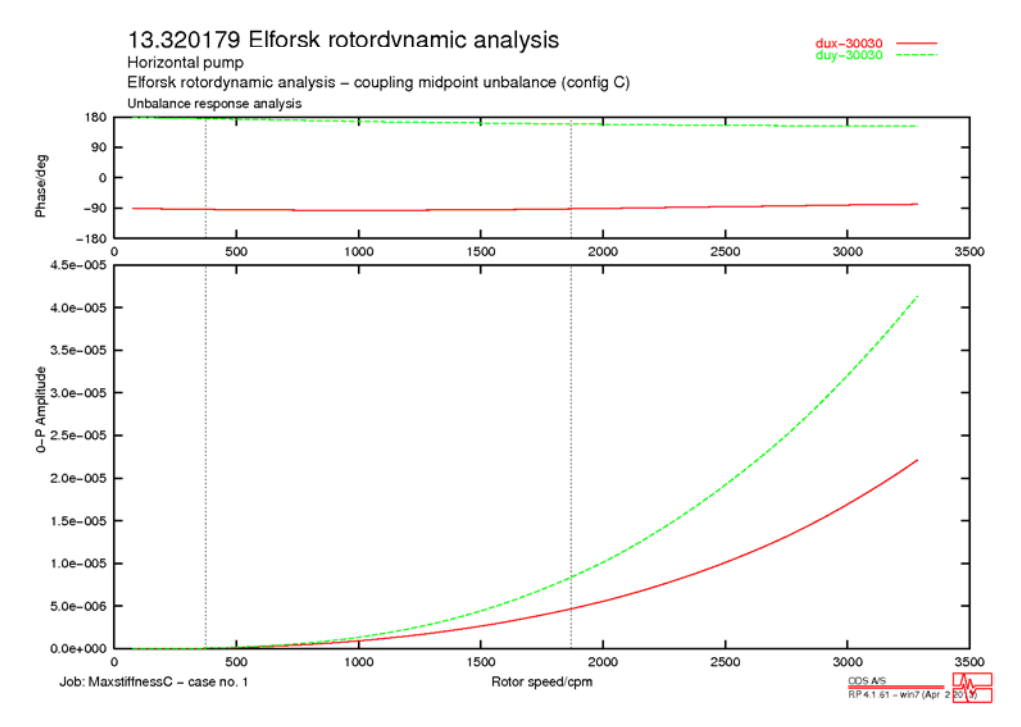


Figure A 39. Bode plot showing the velocity at the motor NDE bearing for unbalance Case C. Maximum bearing stiffness is used.

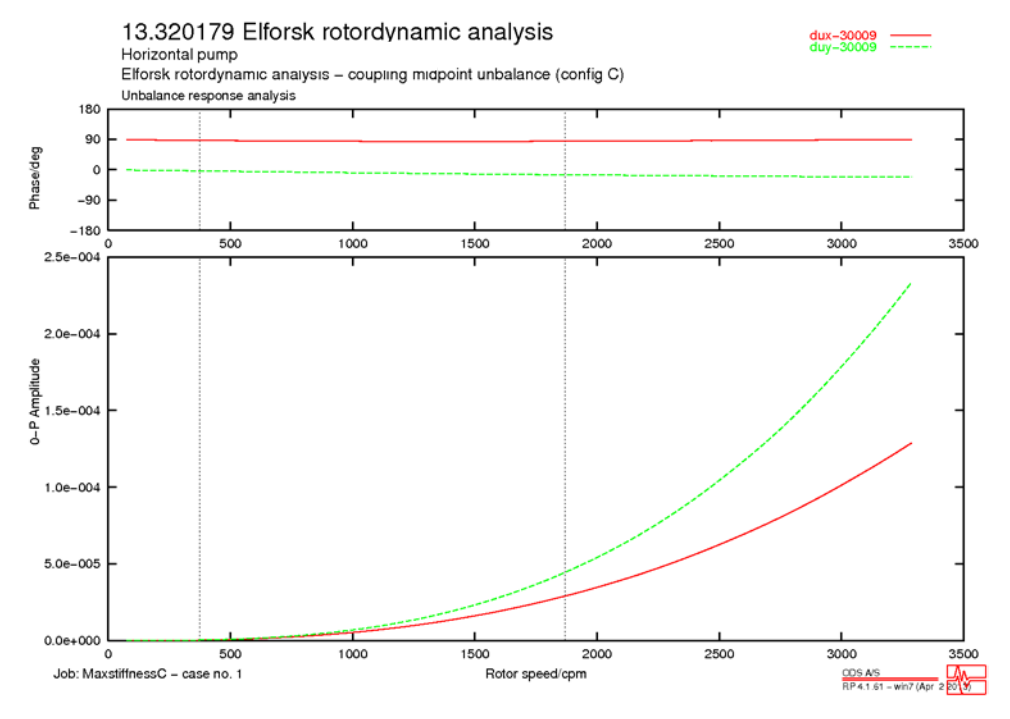


Figure A 40. Bode plot showing the velocity at the motor DE bearing for unbalance Case C. Maximum bearing stiffness is used.

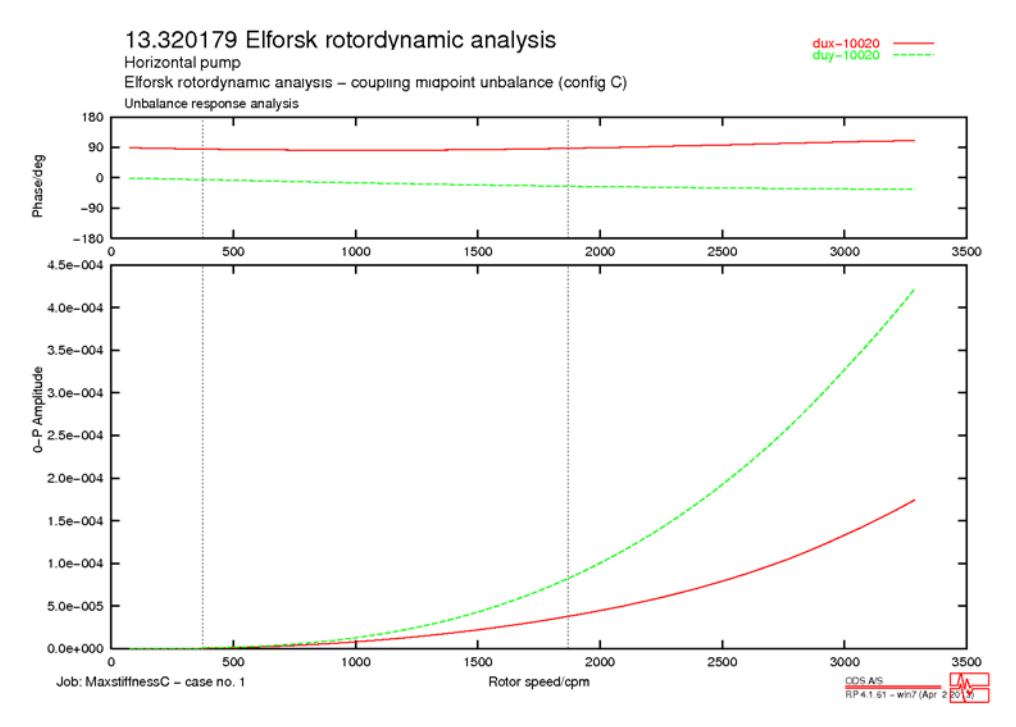


Figure A 41. Bode plot showing the velocity at the pump DE bearing for unbalance Case C. Maximum bearing stiffness is used.

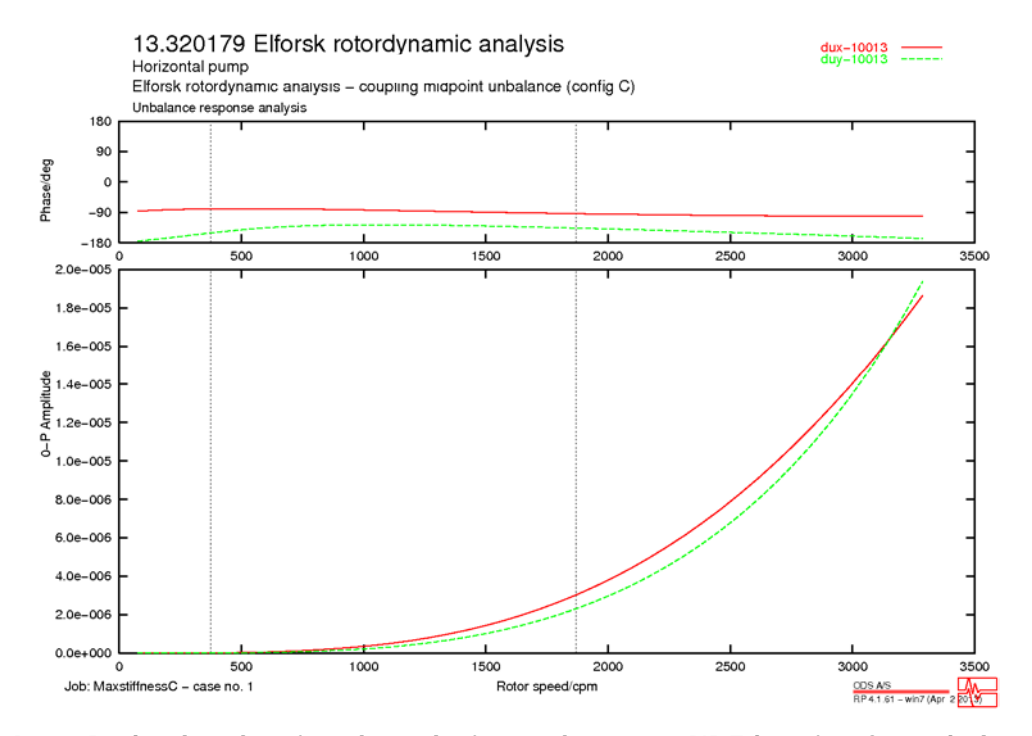


Figure A 42. Bode plot showing the velocity at the pump NDE bearing for unbalance Case C. Maximum bearing stiffness is used.

13.320179 Elforsk rotordynamic analysis Elforsk rotordynamic analysis - coupling midpoint unbalance (config C)

Unbalance response analysis Deflected Shape @ 1494 rpm Subcase no.20

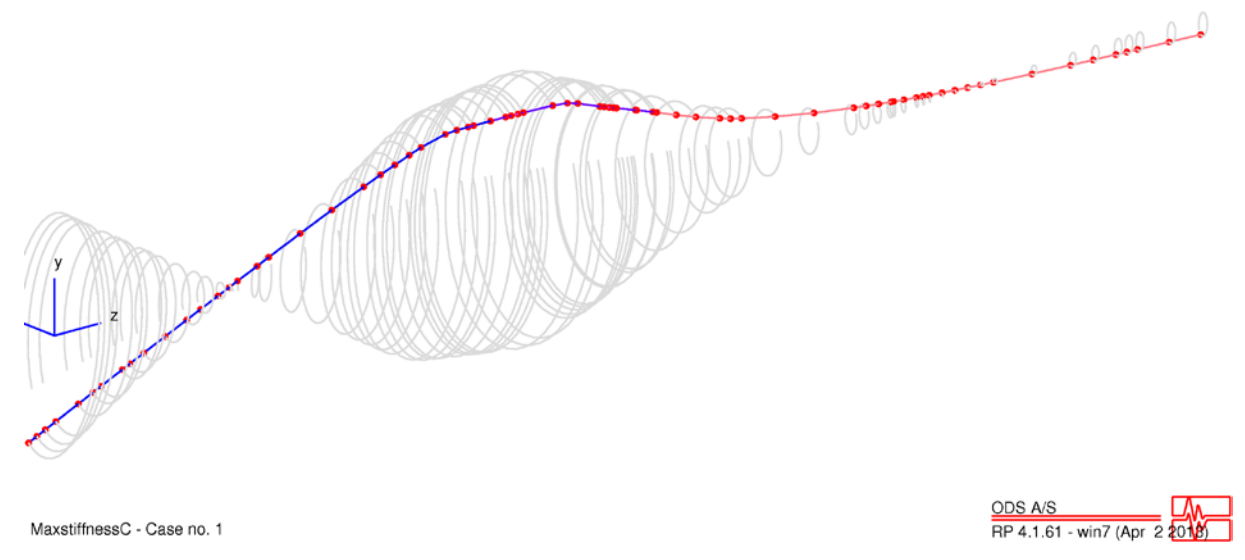


Figure A 43. Shape of the first mode at rated speed (1494 rpm). Unbalance case C and maximum bearing stiffness is used.

# Lateral rotordynamic analysis

Vertical pump

Appendix C

Mattias Lindblad

#### Summary

At the request of Elforsk AB, a lateral analysis of a vertical pump has been performed.

The undamped critical speed map showed that the critical speeds of the pump are well separated from the running speed with the lowest critical speed on rigid bearings located at 1541 rpm compared to the nominal operating speed of 371 rpm.

The stability analysis showed that the critical speeds were well separated from the first and second order of the running speed; the first critical speed is located at 1520 rpm and the second critical speed at 3700 rpm. The separation margin to the running speed suggests that the pump will operate well below the critical speed.

In the unbalance response analysis four times the allowable unbalance weight (G2.5) was analysed at different shaft locations. The worst cases for the unbalance response for the running speed are seen in the table below. The different unbalance cases resulted in 0.78 - 0.80 mm/s RMS vibration at the bearings depending on the place of the unbalance. On the DE coupling end the highest shaft displacement was 65  $\mu m$  peak to peak. For the impeller response the maximum displacement was 64  $\mu m$  peak to peak. For low speed rotors such as the main cooling water pumps, the maximum allowable vibration level is 1 mm/s rms [7]. This is not directly comparable since the values stated in this report is 1X filtered, however the 1X component on site is often dominating the vibration spectra. Further, the applied unbalance can be considered very conservative.

Case	Radial displacement in µm peak-peak (1X filtered)	Bearing radial velocity in mm/s rms (1X filtered)
Min stiffness midspan unbalance	DE coupling: 12.1	Mid bearing: 0.78
Min stiffness DE coupling unbalance	DE coupling 65.4	Upper bearing: 0.78
Min stiffness impeller unbalance	Impeller: 64	Mid bearing: 0.81

The pump is equipped with two water lubricated bearings and one oil film bearing. The information on these bearings was limited, i.e. running clearances, bearing types and dimensions were unknown. This leaves some uncertainties in the modeling which have been investigated via parameter variation methodology. The parameter study showed that the bearing stiffness has a significant influence of the natural frequencies of the shaft.

## Table of contents

1	Introdu	iction	1
2	Machin	ery data	3
		Jmp	3
		1.1 Impeller and impeller hub	
		1.2 Bearings	
	2.	1.3 Motor Coupling	
	2.	1.4 Pump middle Coupling	
	2.	1.5 Mechanical seal	
3	Calcula	tion model	6
	3.1 SI	haft	6
		Ifluence of water forces	
		npeller	
	3.4 Be	earings	8
4	Results		9
	4.1 U	CSM – Undamped Critical Speed Map	9
		tability analysis	
		2.1 Campbell diagram	
	4.	2.2 Frequency ratio vs damping	17
	4.3 Ui	nbalance response	18
5	Discuss	sion	20
6	Conclus	sion	21
7	Referer	nces	22

## 1 Introduction

At the request of Elforsk AB, Lloyd's Register Consulting (LRC) has performed a lateral rotordynamic analysis of a vertical cooling water pump. An overview of the pump is given in Figure 1. The analysis is conformed to the specifications described in API 610 (11th Edition 2010) [1].

The present report describes the rotordynamic calculations performed and covers:

- Description of the calculation model including pump and intermediate shafts to the coupling at the motor,
- Calculation of the first four undamped bending natural frequencies of the pump,
- · Undamped critical speed analysis of the pump,
- Unbalance response analysis
- Separation margin between the critical speeds and running speed.

Both the pump and motor are mounted vertically. The string has a flexible coupling between the motor and the pump rotor, a mechanical seal to prevent the pump from leakage, two shafts in line connected with a stiff coupling, impeller and an impeller hub. Bearings to support the shaft are located above the seal, in the middle of the rotor and one close to the impeller, see Figure 1.

The flexible coupling suggests that the pump can be analysed with respect to the lateral dynamics without influence from the dynamics of the motor. For the rotordynamic calculations the LR Consulting in-house FE software RP has been used. It is assumed throughout the entire analysis that the pumped fluid is seawater as in the operational state.

The pump is equipped with two water lubricated bearings and one oil film bearing. The analysis is carried out for minimum and maximum bearing stiffness. But this data is unknown to LR Consulting, hence assumed values are used in order to allow for a variable sensitivity check. The performed analyses are:

- Undamped critical speed map (UCSM). Where the undamped critical running speeds are determined against the bearing stiffness.
- Stability analysis, *i.e.* a damped eigenvalue analysis. In this analysis the systems tendency towards unstable vibrations is investigated. A Campbell diagram is produced and the separation margin is investigated.
- Unbalance response analysis. Where the system response due to an assumed unbalance is determined. The most severe unbalance cases are investigated.

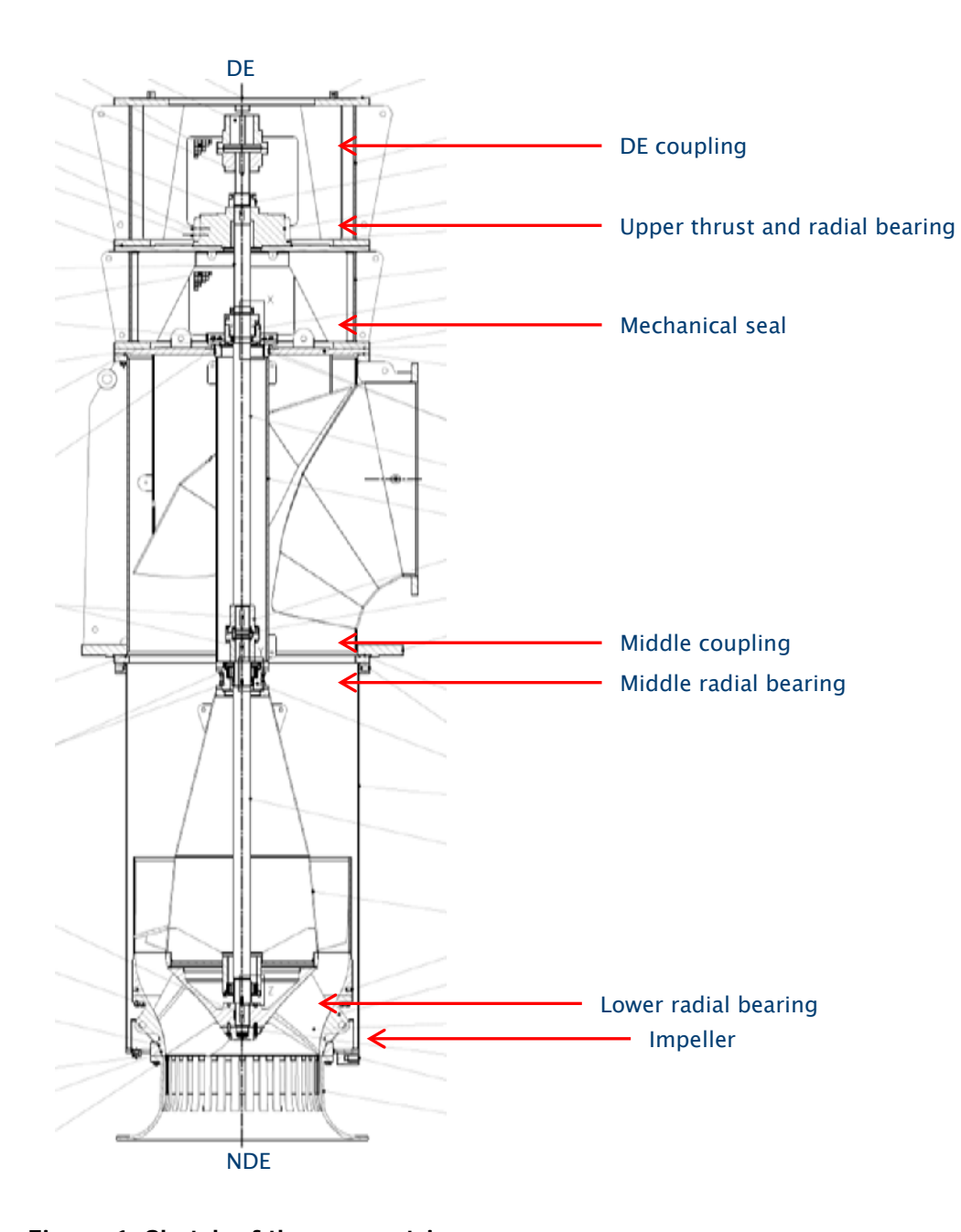


Figure 1. Sketch of the pump string.

# 2 Machinery data

### 2.1 Pump

The pump is a vertical VS3 classed pump according to API 610 [1]. The machinery specifics are presented in Table 1. The rotor mass and moments of inertia are extracted from the ProE-model provided by The operator. The pump rated nominal speed and the temperature of the water is listed in [2]. The density of the water is an approximation and the Mol and mass of the rotor are calculated with data from the ProE-model provided.

Table 1. The machinery specifics of the investigated pump.

Property	Value	Unit
Rated speed	371	rpm
Density of pumped liquid	1000	kg/m³
Temperature of pumped liquid	7	°C
Rotating mass	1180.8	Kg
Total rotor polar Mol	67.8	kgm²
Total rotor transverse Mol	5096	kgm²

#### 2.1.1 Impeller and impeller hub

The impeller and the impeller hub masses and moments of inertia are extracted from the ProE-model provided by the operator. The impeller and the impeller hub data can be seen in Table 2 and Table 3.

Table 2. Properties of the impeller.

Property	Value	Unit
Impeller diameter	1160	mm
Impeller mass	516	kg
Impeller polar Mol	65.2	kgm²
Impeller transverse MoI	42.7	kgm²

Table 3. Properties of the impeller hub.

Property	Value	Unit
Inner diameter	100	mm
Mass	26.4	kg
polar Mol	0.22	kgm²
transverse Mol	0.12	kgm²

#### 2.1.2 Bearings

The pump unit is supported by three bearings. The data for the bearings was not provided to LRC. The properties of the bearings used in the calculations are extracted from the ProE-model seen in Table 4.

Table 4. Properties of the top bearing, mid bearing and lower bearing.

Property	Top bearing	Mid bearing	Lower bearing	Unit
Inner diameter	110	105	105	mm
Rotating mass	45.3	5.4	4.3	kg
Polar Mol	0.54	0.0019	0.014	kgm²
Transverse Mol	0.46	0.0018	0.015	kgm²

#### 2.1.3 Motor Coupling

The coupling is a flexible coupling of the model ZAPEX CPLG ZINV 4.5 B. The coupling half is modelled according to the drawing in [3] and the inertias of the coupling are calculated by RP. The mass and the MoIs are seen in Table 5.

Table 5. Calculated properties of the coupling.

Property	Value	Unit
Mass	60.2	kg
Polar Mol	0.79	kgm²
Transverse Mol	0.47	kgm²

#### 2.1.4 Pump middle Coupling

The middle coupling is rigid and connects the upper and lower shaft. The coupling is modelled according to the ProE-model provided by the operator and the MoI of the coupling is calculated by RP. The mass and the MoIs are seen in Table 6.

Table 6. Properties of the coupling taken from provided drawings.

Property	Value	Unit
Mass	69.7	kg
Polar Mol	0.48	kgm2
Transverse Mol	0.85	kgm2

#### 2.1.5 Mechanical seal

A mechanical seal made of steel is placed in below the thrust bearing to prevent the pump from leaking seawater. The mass, the MoI and the CoG of the seal are extracted from the ProE-model. It is then modelled in RP as a disk element with discrete mass and MoIs, placed at the CoG of the seal. The properties of the seal can be seen in Table 7.

Table 7. Properties of the mechanical seal.

Property	Value	Unit
Mass	9.8	kg
Polar Mol	0.048	kgm2
Transverse Mol	0.068	kgm2

## 3 Calculation model

#### 3.1 Shaft

The rotor shaft is modelled in RP with Timoshenko theory beam elements, and disk elements representing discrete masses and MoIs. Nodes are placed with approximately 0.15 m intervals and where there are changes in the cross-section, in the axial CoG of rotor elements such as the impeller, and where possible forces or unbalances might be applied.

The pump rotor shaft is modelled in RP based on the dimensions provided by the ProE-model. It is modelled with 80 beam elements. The mass and inertias of the impeller, the coupling, the bearings and the mechanical seals are modelled with discrete disks without stiffness contribution. The pump rotor shaft can be seen in Figure 2.

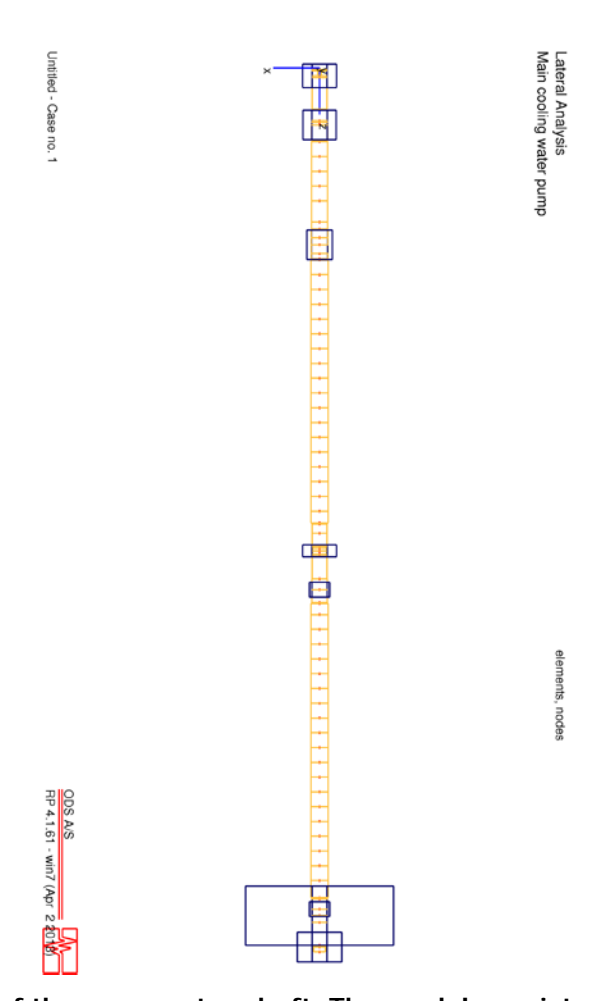


Figure 2. RP model of the pump rotor shaft. The model consists of 80 beam elements (yellow) and 8 disk elements (blue).

#### 3.2 Influence of water forces

The part of the pump shaft below the mechanical seal will be surrounded by water. This has to be accounted for by adding the mass of the water that is set in movement during the lateral vibrations. Because of the symmetry of the cross-section, no cross-coupled masses or Mols has to be accounted for. According to [4], the added mass per unit length for a cylindrical cross-section in water is calculated as

$$m_{\alpha} = \pi \rho_{W} R^{2}. \tag{1}$$

where the added mass per unit length is denoted  $m_{\alpha}$ , the density of the water is denoted R.

### 3.3 Impeller

The dynamic stiffness and damping coefficients arising from the interaction between the impeller and the pumped water are modelled in RP as a bearing element. Mainly two phenomenons from the impeller/water interaction are causing the dynamic radial effects on the rotor. These are:

- Forces between the impeller shroud and the fluid.
- Interaction effects between the impeller and the diffuser.

The coefficients for the forces are calculated from a theory further described in [5]. The equations used in this theory, seen in Equations (2) to (5), are based on experimental data. The dynamic coefficients are seen in the matrices below. The entity  $\mathbf{K}$  is the stiffness matrix,  $\mathbf{B}$  is the damping matrix and  $\mathbf{M}$  is the added mass matrix.

$$\mathbf{K} = \begin{pmatrix} K_{xx} & K_{xy} \\ -K_{yx} & K_{yy} \end{pmatrix}, \quad \mathbf{B} = \begin{pmatrix} B_{xx} & B_{xy} \\ -B_{yx} & B_{yy} \end{pmatrix}, \quad \mathbf{M} = \begin{pmatrix} M_{xx} & M_{xy} \\ -M_{yx} & M_{yy} \end{pmatrix}$$

The stiffness coefficients are calculated according to Equation (2), the damping coefficients are calculated according to Equation (3) and the added mass coefficients are calculated according to Equation (4).

$$\mathbf{K} = \begin{pmatrix} -4.2C\omega^2 & 5.1C\omega^2 \\ -5.1C\omega^2 & -4.2C\omega^2 \end{pmatrix}. \tag{2}$$

$$\mathbf{B} = \begin{pmatrix} 4.6C\omega & 13.5C\omega \\ -13.5C\omega & 4.6C\omega \end{pmatrix}. \tag{3}$$

$$\mathbf{M} = \begin{pmatrix} 11C & 4C \\ -4C & 11C \end{pmatrix}. \tag{4}$$

In Equations (2) to (4) ,  $\omega$  is the shaft angular frequency and  $\mathcal C$  is the mass coefficient of the fluid, calculated as

$$C = \pi \rho b_2 r^2. \tag{5}$$

In Equation (5) the entities p,  $b_2$  and r represents the mean density of the fluid, the impeller discharge width and the impeller tip radius.

The stiffness, damping and mass terms are determined for a number of shaft running speeds. Based on these values, RP then interpolates the corresponding coefficients for the speed to be analysed.

## 3.4 Bearings

The bearings are modelled in RP by assumed values for the dynamic stiffness, inertias and the damping. All tree bearings have been assumed to have the same properties, see Table 8.

**Table 8 Bearing properties** 

Property	Min value	Max value	Unit
Direct stiffness	0.8.108	1.2·108	N/m
Cross coupled stiffness	0	0	N/m
Damping	105	105	Ns/m

## 4 Results

The results presented in this chapter are divided into three subchapters. The UCSM, that presents the undamped critical speeds vs bearing stiffness, followed by a stability analysis that introduces damping in the model. Finally the results from the unbalance analysis are presented, which assumes rotor unbalance at certain, critical points, and calculates the response due to these unbalances.

### 4.1 UCSM – Undamped Critical Speed Map

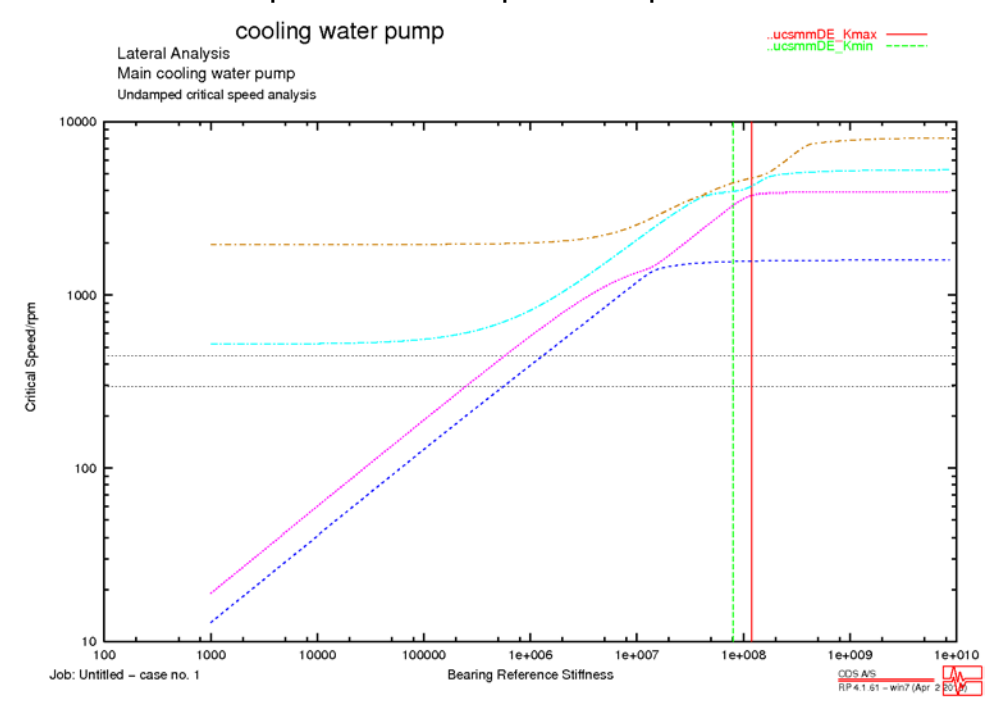


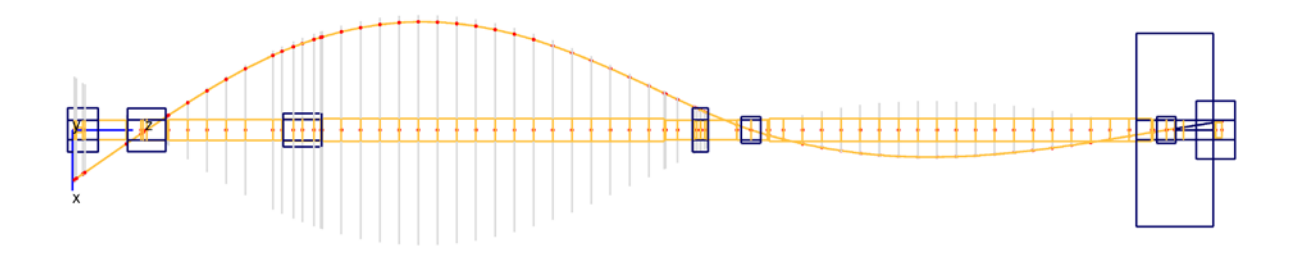
Figure 3. Unbalanced critical speed map for the pump. The vertical lines represents the minimum and maximum bearing stiffness, the coloured lines (horizontal/diagonal) represents the critical speeds of the system and. The grey horizontal lines are 75% and 125% of the operating speed (371 rpm).

The UCSM in Figure 3 shows the four first forward modes against bearing stiffness for an undamped system. No damping or stiffness from the bearings or the impeller is taken into account. The critical speeds and natural frequencies of the first four undamped modes with infinite bearing stiffness are presented in Table 9 and can be seen in Figure 4 to Figure 7. The table suggests that the modes are well separated from the running speed.

Table 9. The three first undamped critical speeds at infinite bearing stiffness.

Mode	Critical speed [rpm]
1	1541
2	3767
3	5125
4	7889

Undamped critical speed analysis elements, nodes, critical speed no. 1: 1541.24 rpm K: 8.65964e+009 (112)

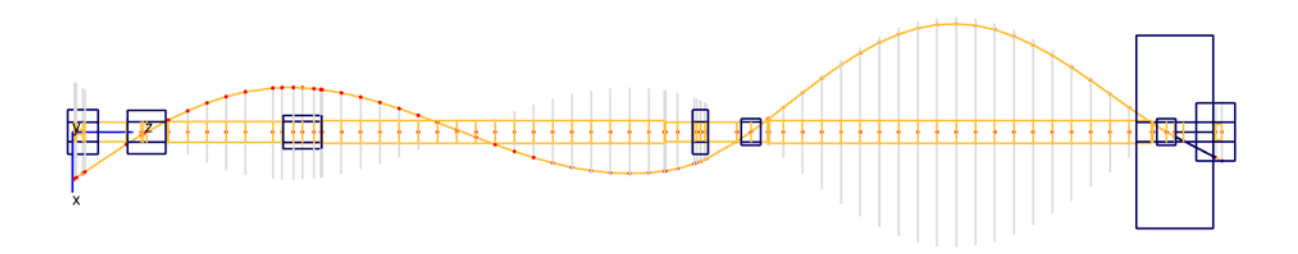


Untitled - Case no. 1



Figure 4 Deflection shape of the first undamped mode at 1541 rpm with infinite bearing stiffness.

Undamped critical speed analysis elements, nodes , critical speed no. 2: 3767.89 rpm K: 8.65964e+009 (112)

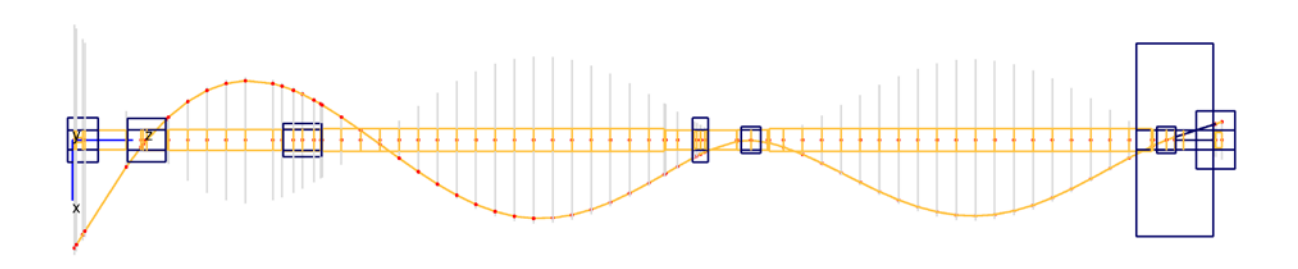


Untitled - Case no. 1



Figure 5 Deflection shape of the second undamped mode at 3767 rpm with infinite bearing stiffness.

Undamped critical speed analysis elements, nodes , critical speed no. 3: 5125.07 rpm K: 8.65964e+009 (112)

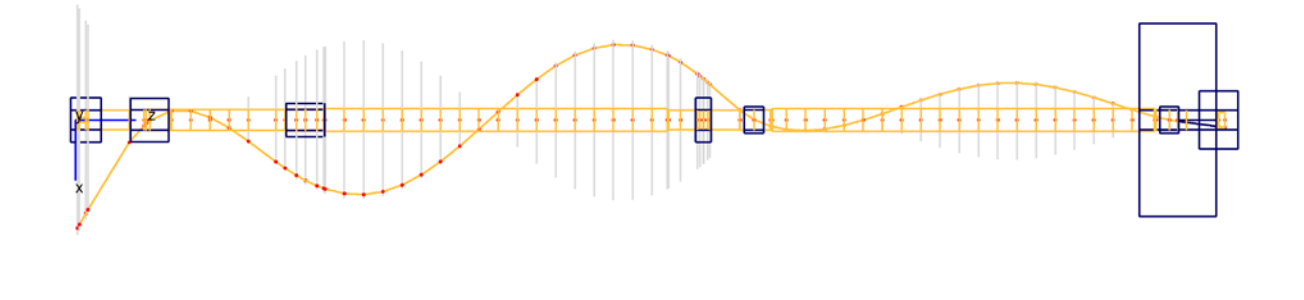


Untitled - Case no. 1



Figure 6 Deflection shape of the third undamped mode at 5125 rpm with infinite bearing stiffness.

Undamped critical speed analysis elements, nodes, critical speed no. 4: 7889.18 rpm K: 8.65964e+009 (112)



Untitled - Case no. 1

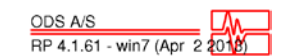


Figure 7 Deflection shape of the fourth undamped mode at 7889 rpm with infinite bearing stiffness.

## 4.2 Stability analysis

The stability analysis is a damped eigenvalue analysis of the system. From this analysis a Campbell diagram is produced in order to investigate whether any possible resonance might occur. Also, the damping is investigated against the separation margin between the natural frequencies and the running frequency.

Both these investigations are carried out for minimum and maximum bearing stiffness (values to be found in Table 8).

#### 4.2.1 Campbell diagram

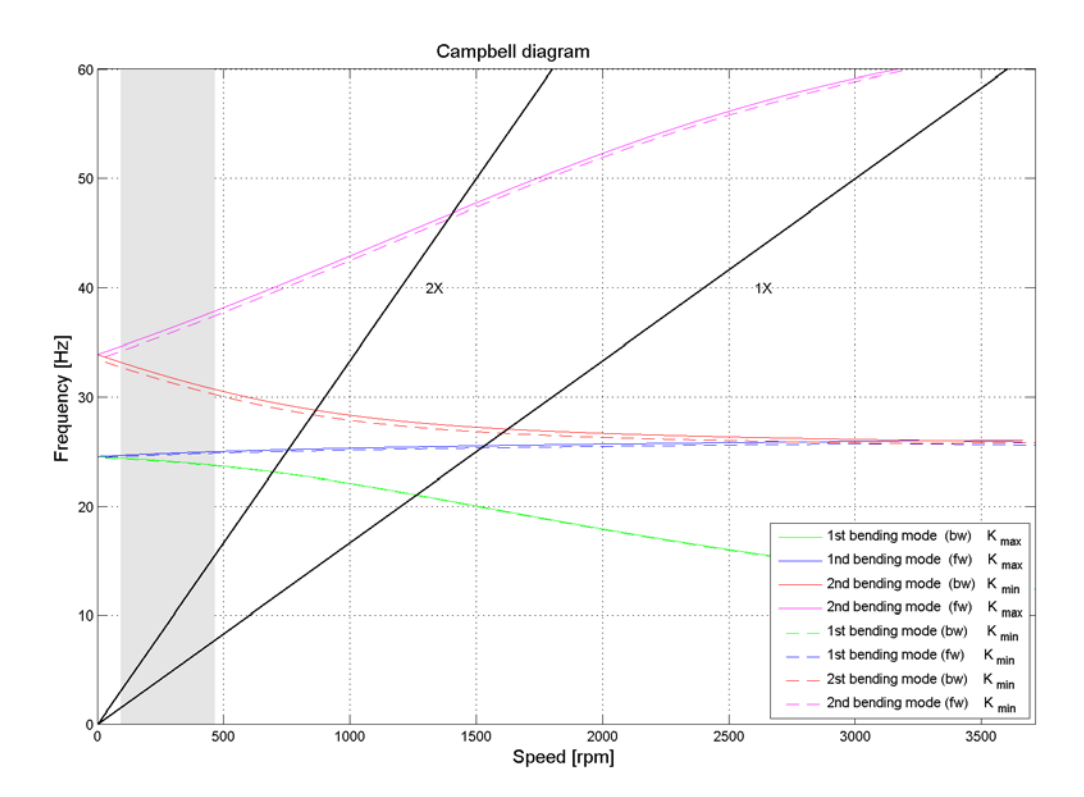
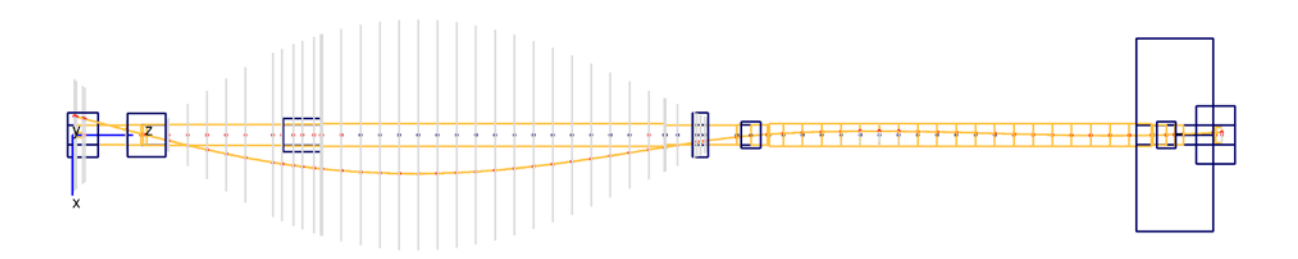


Figure 8. Campbell diagram showing the pumps first two natural frequencies for minimum and maximum bearing stiffness respectively. The black lines are the 1X and 2X frequencies, the solid coloured lines represent the modes calculated with maximum bearing stiffness, and the dashed coloured lines represent the modes calculated with the minimum bearing stiffness. Finally, the grey area is the operating area according to API [1], 25%-125% of the running speed (371 rpm).

In Figure 8 the Campbell diagram for the pump is seen. No modes are crossing the 1X or 2X frequency lines in the operating range. The system is governed by the flexibility of the rotor. This is in line with what to be expected for a system with bearing stiffness of the magnitude present in the analysed system. The critical speeds (1X interaction with 1st and 2nd forward bending mode) are found at 1520 rpm and 3700 rpm, respectively. These modes can be recognized from modes #1 and #2 in the undamped critical speed map. Hence the added damping has little influence on the location of the natural frequencies for this pump.

Damped eigenvalue analysis elements, nodes , mode no. 2: 25.8563 Hz, log. dec = 0.00! Speed: 3710 (1)

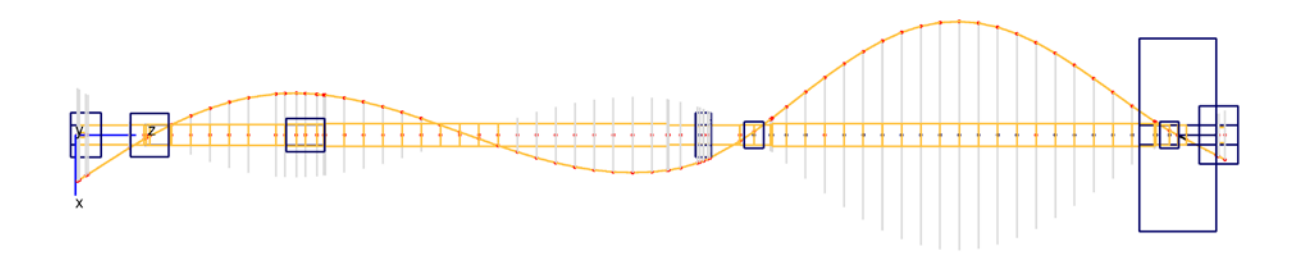


Campbell\_maxstiff - Case no. 1



Figure 9 Mode shape of the first forward mode that interacts with the running speed line (1X) at 1521 rpm.

Damped eigenvalue analysis elements, nodes , mode no. 4: 62.0455 Hz, log. dec = 0.018 Speed: 3710 (1)



Campbell\_maxstiff - Case no. 1



Figure 10 Mode shape of the second forward mode that interacts with the running speed line (1X) at 3700 rpm.

In order to investigate the effects of variations in bearing stiffness, the stiffness of the middle bearing and the lower bearing has been decreased to the point where it would be a risk of the critical frequencies of the shaft to coincide with the running speed. Figure 11 shows the Campbell diagram for the critical speeds at the maximum stiffness (1.2 · 10 N/m) and also for the stiffness where the natural frequencies have decreased to interfere with the running speed area (grey area in the figure). The corresponding stiffness of the middle and the lower bearing was 5 · 10 while the top bearing still had a stiffness of 1.2 · 10 N/m. In Table 10 the critical speeds are listed for the case when the rotor is at nominal speed 371 rpm, corresponding to the frequencies seen in Figure 11 at 371 rpm. The decreased support stiffness has the effect of triggering modes other than the pure bending modes. As seen in Figure 12, the supports are highly deformed and cause an almost conical whirling of the bottom part of the pump. This shows the natural frequencies dependency on the support stiffness.

Table 10 Critical speeds at 371 rpm for the bearing stiffness 5-10<sup>6</sup> N/m and for the maximum analysed bearing stiffness, 1.2-10<sup>8</sup> N/m.

Modes	Critical modes in Hz at 371 rpm for 5.0E+6 [N/m]		Critical modes at 371 rpm for max stiffness: 1.2E+8 [N/m]	
	Freq. [Hz] Shape		Freq. [Hz]	Shape
1 <sup>st</sup> forward	7.6	Conical	25.0	1 <sup>st</sup> bending
2 <sup>nd</sup> forward	25.3	1 <sup>st</sup> bending	37.4	2 <sup>nd</sup> bending
3 <sup>rd</sup> forward	25.2	2 <sup>nd</sup> bending	Out of range	

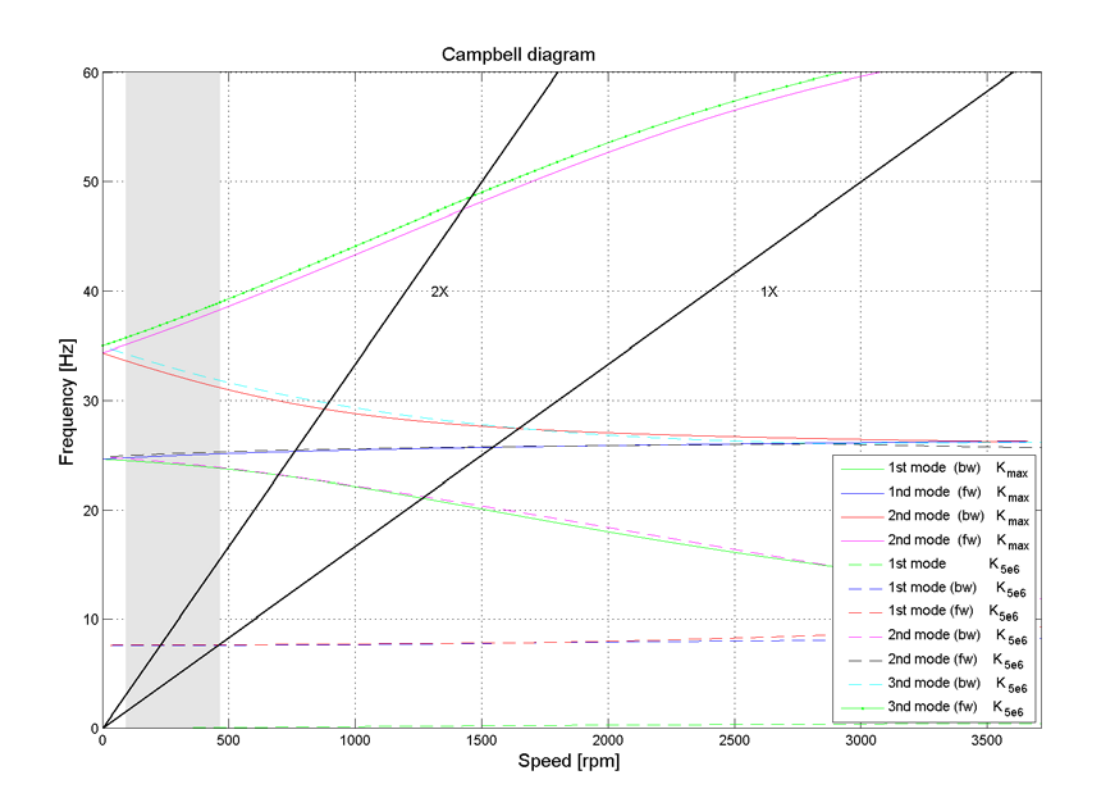


Figure 11. Campbell diagram showing the pumps first two forward and backward natural frequencies for maximum (1.2-10<sup>8</sup>) and the three first natural frequencies for 5-10<sup>6</sup> N/m bearing stiffness. The black lines are the 1X and 2X frequencies, the solid coloured lines represent the modes calculated with maximum bearing stiffness, and the dashed coloured lines represent the modes calculated with the minimum bearing stiffness. Finally, the grey area is the operating area according to API [1], 25%-125% of the running speed (371 rpm).

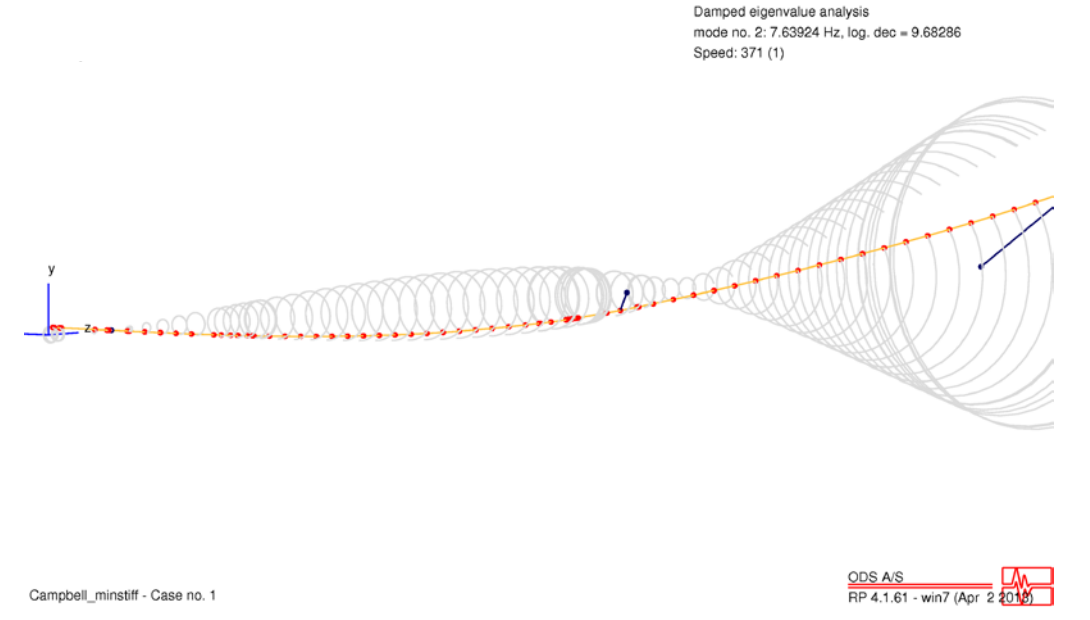


Figure 12 Mode shape of the first natural frequency at 371 rpm with decreased stiffness on the two lower bearings..

#### 4.2.2 Frequency ratio vs damping

Below the damping ratio vs the frequency ratio is presented for the nominal operational speed 1xMCOS. The frequency ratio, *Fr*, for centrifugal pumps is defined as (API 610):

$$Fr = \frac{f_{\text{nat,i}}}{f_{\text{run}}},\tag{6}$$

where  $f_{\text{nat,i}}$  is natural frequency number i and  $f_{\text{run}}$  is the running frequency. This is compared against the damping factor,  $\xi$ , which is defined through the logarithmic decrement  $\delta$  as

$$\delta = \frac{(2\pi\xi)}{(1-\xi^2)^{0.5}},\tag{7}$$

Equation (7) can, for damping factors lower than 0.4, be approximated as

$$\delta = 2\pi\xi \Rightarrow \xi = \frac{\delta}{2\pi}.$$
 (8)

The approximation of the damping factor in Equation (8) is used in the comparisons of the damping factor vs the separation margin in the calculations in this report.

In Figure 13 the damping ratios as a function of the frequency ratio are plotted for the nominal speed (371 rpm). The area below the black lines, marked "UA", in the plot represents unacceptable damping ratios, while the area outside of the lines, marked "A", represents acceptable damping ratios. The circles represent the minimum stiffness case while the stars represent the maximum stiffness case.

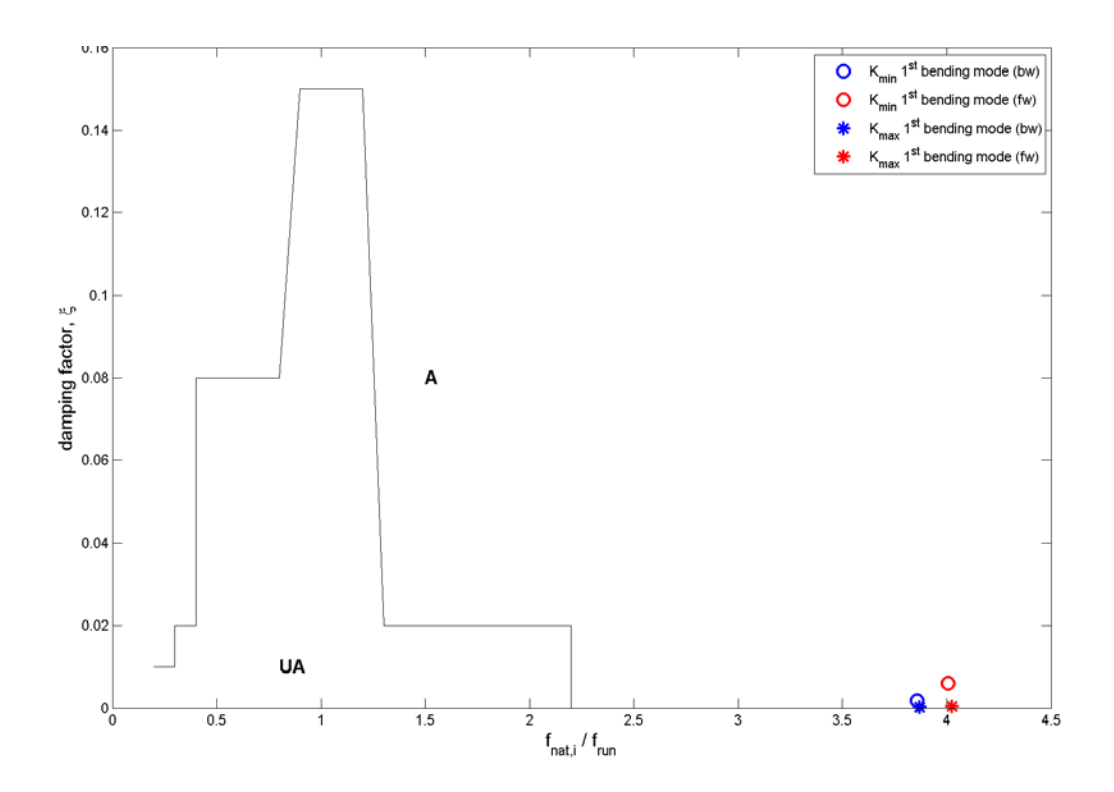


Figure 13. Damping vs frequency ratio plot for 1xMCOS. The circles represent the minimum bearing stiffness case and the stars the maximum stiffness case. The region marked "A" is the acceptable region and the region marked "UA" is the unacceptable region.

In Figure 13 it is clear that the first two modes have an acceptable damping since they are well separated from the unacceptable area, i.e. they are well separated from the running speed.

## 4.3 Unbalance response

The unbalance response analysis is carried out for five different unbalance cases chosen to excite the 1<sup>st</sup> and 2<sup>nd</sup> bending modes according to the Campbell diagram in Figure 8. The unbalance is calculated according to [6] as

$$U = 4 \cdot e_{per} \cdot W, \tag{9}$$

where  $\boldsymbol{U}$  is the unbalance in g·mm,  $\boldsymbol{W}$  is the rotating mass and  $\boldsymbol{e}_{per}$  is the allowable residual unbalance per unit mass in g·mm/kg. In order to be conservative, four times the balancing grade G2.5 in [6] has been used when calculating the unbalance response. In Table 11 the unbalance cases and their corresponding unbalance can be seen.

Table 11. List over the five unbalance cases to be tested and their corresponding application points.

Case	Unbalance position	Total residual unbalance [g·mm]
Α	Impeller	3.77 · 10 <sup>5</sup>
В	DE Coupling	3.77 · 10 <sup>5</sup>
С	Midspan	3.77 · 10 <sup>5</sup>
D	DE+NDE of the shaft out of phase (half the weight on each side)	3.77 · 10 <sup>5</sup>
Е	DE+NDE of the shaft in phase (half the weight on each side)	3.77 · 10 <sup>5</sup>

In Appendix A bode plots and the two first mode shapes are presented for each unbalance case with minimum and maximum bearing stiffness, and the response at the running speed. The upper plots display the phase of the displacements or the velocities. Typical resonance behaviour is a phase shift of 90 degrees.

API recommends a comparison of the maximum displacement against the diametric clearance of the rotor [1]. These data are unavailable at the time of writing this report for LRC. However the results are presented in the following tables. In Table 12 the radial displacement of the impeller and the DE coupling together with the corresponding velocities are shown for the bearings. The highest displacement for the impeller was 64 µm peak to peak at minimum stiffness of the bearing with the unbalance applied in the middle of the rotor. The highest response at the DE coupling, 65 µm peak to peak, was obtained with minimum stiffness of the bearings and with the unbalance applied in the DE coupling. The highest vibration velocity for the DE bearing, 0.8 mm/s RMS, was obtained for minimum stiffness of the bearings with the unbalance applied in DE coupling. The NDE bearing had the highest response, 0.8 mm/s RMS, with the unbalance applied in the midspan of the rotor. Finally the mid bearing responded with 0.8 mm/s RMS with the unbalance applied in the impeller with minimum stiffness. For low speed rotors such as the main cooling water pumps, the maximum allowable vibration level is 1 mm/s RMS according to TBM [7]. This is not directly comparable since the values stated in this report are 1X filtered.

Table 12 Displacement and velocity (1X filtered) at the bearings and at the impeller of the rotor at 371 rpm

Unbalance case	Imp. rad. disp. [µm] P-P	DE coup. rad. disp. [µm] P-P	DE bear. rad. vel. [mm/s] RMS	NDE bear. rad.vel. [mm/s] RMS	Mid bear. rad. vel. [mm/s] RMS
Min stiffness A	1.2	12.1	0.00	0.00	0.78
Max stiffness A	0.6	4.9	0.00	0.00	0.31
Min stiffness B	0.0	65.4	0.78	0.00	0.00
Max stiffness B	0.0	26.1	0.31	0.00	0.00
Min stiffness C	64.0	1.0	0.00	0.81	0.02
Max stiffness C	27.8	3.0	0.00	0.32	0.01
Min stiffness D	32.0	33.2	0.39	0.40	0.01
Max stiffness D	13.9	14.5	0.16	0.16	0.00
Min stiffness E	32.0	32.2	0.39	0.40	0.01
Max stiffness E	13.9	11.6	0.16	0.16	0.00

## 5 Discussion

Due to the limited data provided for the bearings, assumptions have been made of all of the bearing properties. With the correct data of the bearings and the clearances the results are likely to differ somewhat to the results presented in this report. The data from the impeller manufacturer was not confirmed and can have introduced uncertainties if the impeller data in the ProE-model were not confirmed.

Since the pump is hanging in the thrust bearing without any preload on the bearings it is a challenge to model and estimate the bearing properties. When the shaft is rotating in the centre of the bearing the stiffness of the bearing has a small influence of the dynamics of the rotor. However this is unlikely since the residual unbalance, alignment and the water forces will force the rotor to have a precession within the bearings. Due to the precession of the rotor the lateral dynamics will be influenced by the stiffness and the damping of the bearings.

During operation of the pump the shaft is pushed down by the water forces and this has a straightening effect on the shaft which has not been taken into account in this analysis.

## 6 Conclusion

At the request of Elforsk AB, a lateral analysis of a vertical pump has been performed.

#### **UCSM**

The undamped critical speed map showed that the critical speeds of the pump were well separated from the running speed with the lowest critical speed on rigid bearings located at 1541 rpm compared to the nominal operating speed of 371 rpm.

#### Stability analysis

The stability analysis showed that the critical speeds were well separated from the first and second order of the running speed, first critical speed were approximately 1520 rpm and the second critical speed was approximately 3700 rpm. The separation margin to the running speed suggests that the pump will operate well below the critical speed.

#### Unbalance response

In the unbalance response analysis four times the allowable unbalance weight was analysed at different shaft locations. The worst cases for the unbalance response for the running speed are seen in the table below. The different unbalance cases caused 0.78 - 0.81 mm/s RMS vibration at the nodes at the bearings depending on the place of the unbalance. On the DE coupling end the highest displacement was 65  $\mu$ m peak to peak. For the impeller response the maximum displacement was 64  $\mu$ m peak to peak. For low speed rotors such as the main cooling water pumps, the maximum allowable vibration level according to TBM is 1 mm/s RMS [7]. This is not directly comparable since the values stated in this report is 1X filtered, however the 1X component on site is often dominating the vibration spectra.

Case	Radial displacement [µm] P-P (1X filtered)	Bearing radial velocity [mm/s] RMS (1X filtered)	
Min stiffness midspan unbalance	DE coupling: 12.1	Mid bearing: 0.78	
Min stiffness DE coupling unbalance	DE coupling 65.4	Upper bearing: 0.78	
Min stiffness impeller unbalance	Impeller: 64	Mid bearing: 0.81	

The pump is equipped with two water lubricated bearings and one oil film bearing. The information on these bearings was limited, i.e. running clearances, bearing types and dimensions were unknown. This leaves some uncertainties in the modeling which have been investigated via parameter variation methodology. The parameter study showed that the bearing stiffness has a significant influence of the natural frequencies of the shaft.

## 7 References

- [1] American Petroleum Institute, "Standard 610; Centrifugal Pumps for Petroleum, Petrochemical and Natural Gas Industries, 11th edition," 2010.
- [2] Manufacturer starting characteristics rev 00, 2012
- [3] Manufacturer Drawing.
- [4] R. D. Blevins, Formulas for Natural Frequencies and Mode Shapes, Florida: Krieger Publishing Company, 1995.
- [5] D. W. Childs, Turbomachinery Rotordynamics, Phenomena, Modelling, and Analysis, John Wiley & Sons, 1993.
- [6] ISO 1040-1, Mechanical vibration Balance quality requirements of rigid rotors Part 1: Determination of permissible residual unbalance, First edition, 1987
- [7] *"TBM Tekniska Bestämmelser för Mekaniska Anordningar"* Utgåva 6, 2013-06-32, Svenska Kärnkraftsföretagen

# Appendix A.1 Bode and mode plots for the unbalance response analysis

In Appendix A.1 to A.10 all Bode plots and mode shapes determined from the unbalance analysis are presented. The response in the Bode plots is presented at the pump DE side and NDE side. The two first mode shapes are presented together with the response at the running speed. The types of shapes are the same for all unbalance cases. Mode 1 is the 1<sup>st</sup> bending mode and mode 2 is the 2<sup>nd</sup> bending mode.

# Midspan unbalance (Configuration A) – Maximum bearing stiffness

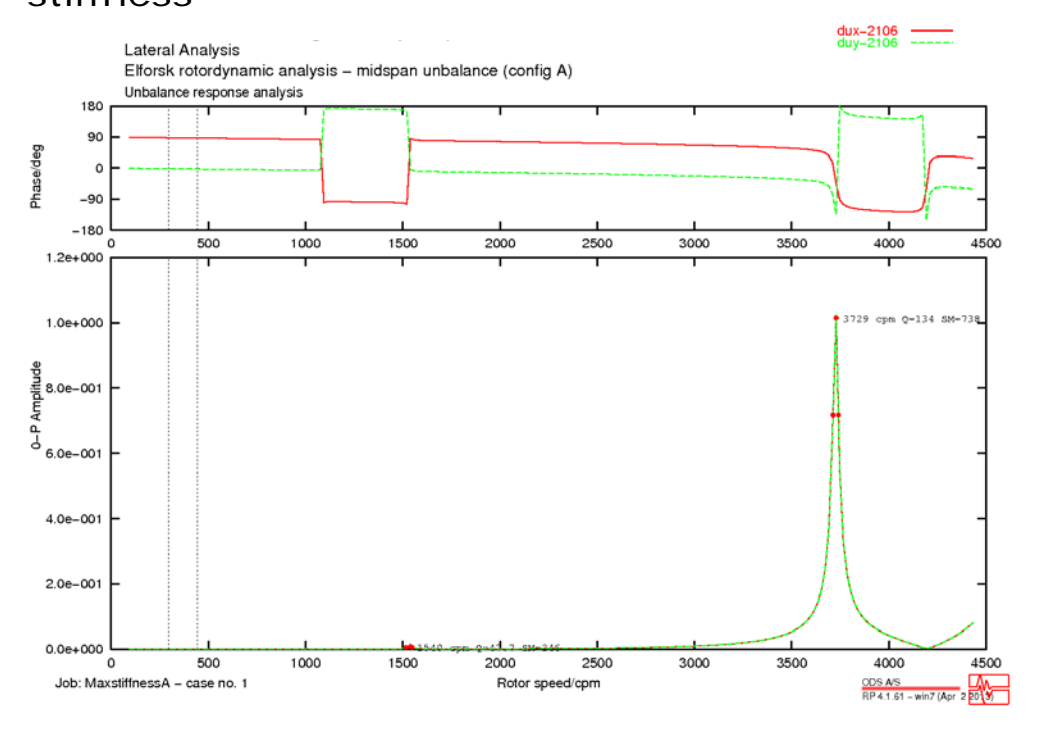


Figure XIV. Bode plot showing the response at the lower pump bearing in m/s zero to peak for unbalance Case A, with the unbalance in the middle coupling.

Maximum bearing stiffness is used.

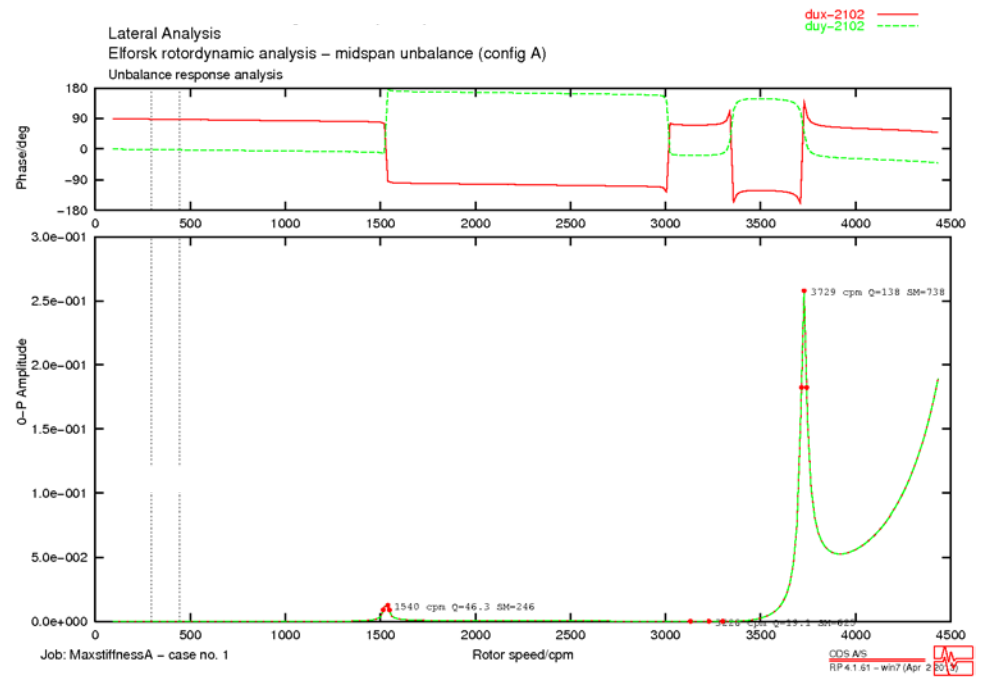


Figure XV. Bode plot showing the response at the upper pump bearing in m/s zero to peak for unbalance Case A, with the unbalance in the middle coupling.

Maximum bearing stiffness is used.

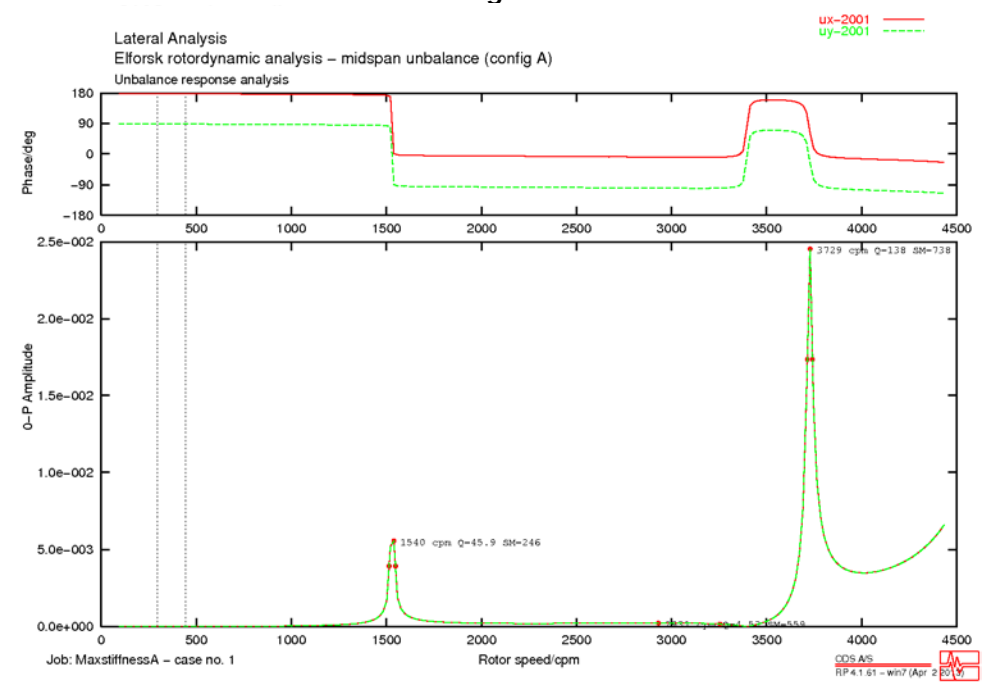


Figure XVI. Bode plot showing the response at the DE coupling in m zero to peak for unbalance Case A, with the unbalance in the middle coupling. Maximum bearing stiffness is used.

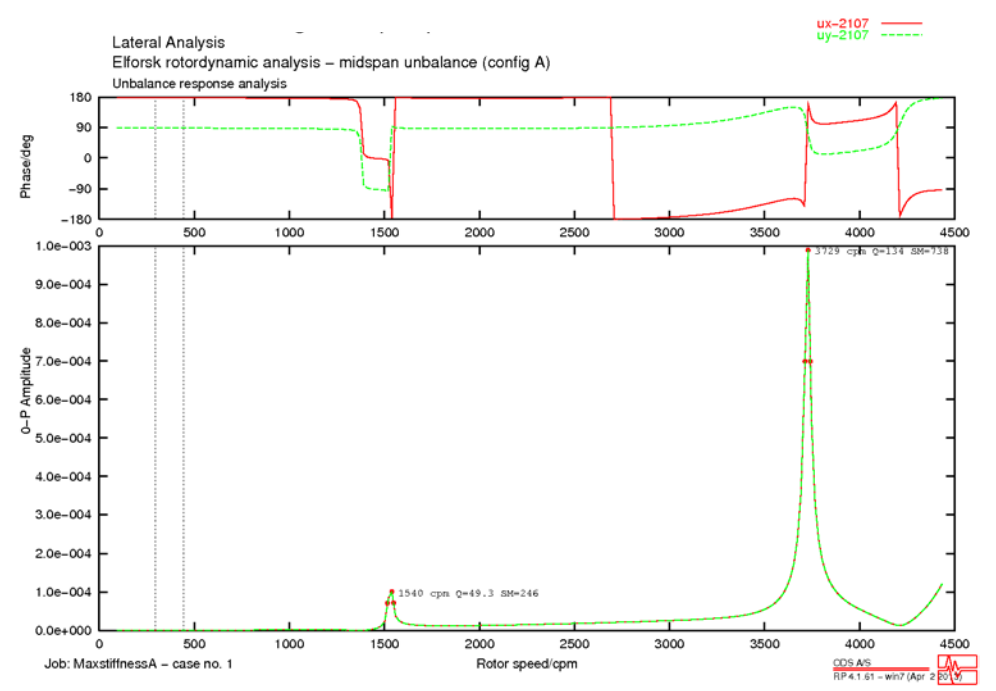


Figure XVII. Bode plot showing the response at the impeller in m zero to peak for unbalance Case A, with the unbalance in the middle coupling. Maximum bearing stiffness is used.

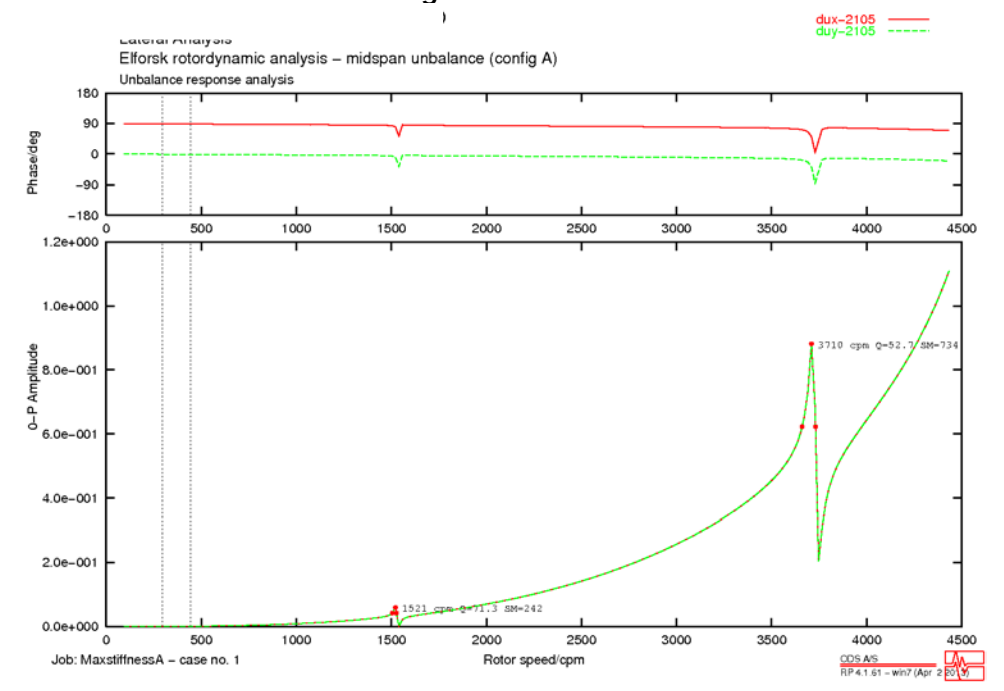
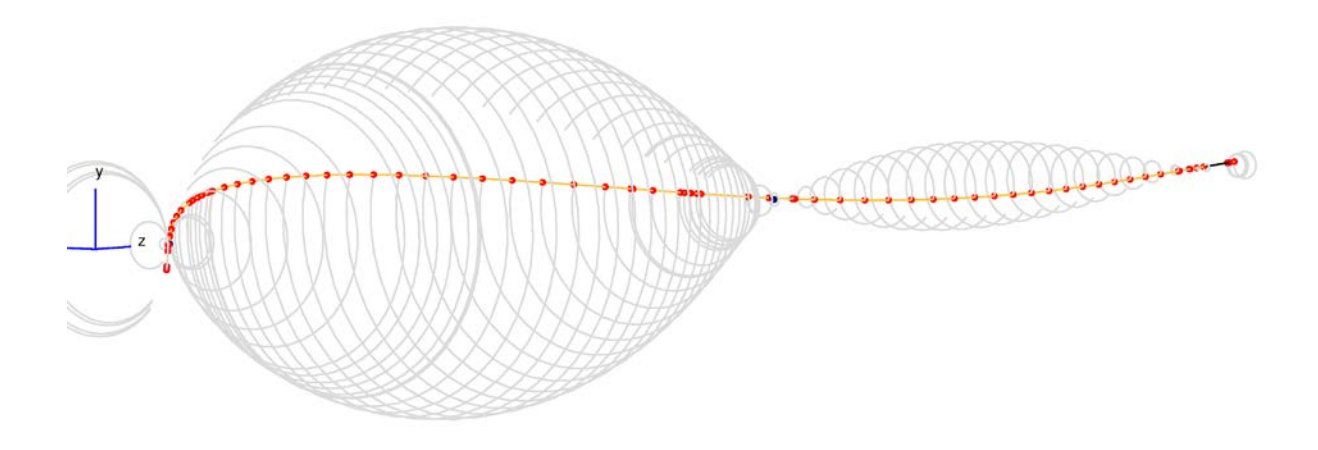


Figure XVIII. Bode plot showing the response at the middle pump bearing in m/s zero to peak for unbalance Case A, with the unbalance in the middle coupling. Maximum bearing stiffness is used.

Lateral Analysis Elforsk rotordynamic analysis - midspan unbalance (config A) Unbalance response analysis Deflected Shape @ 1521.1 rpm Subcase no.78



MaxstiffnessA - Case no. 1

ODS A/S RP 4.1.61 - win7 (Apr 2 2018)

Figure XIX. First bending mode shape for unbalance Case A with maximum bearing stiffness.

Lateral Analysis
Elforsk rotordynamic analysis - midspan unbalance (config A)

Unbalance response analysis
Deflected Shape @ 3728.55 rpm
Subcase no.197

MaxstiffnessA - Case no. 1



Figure XX. Second bending mode shape for unbalance Case A with maximum bearing stiffness.

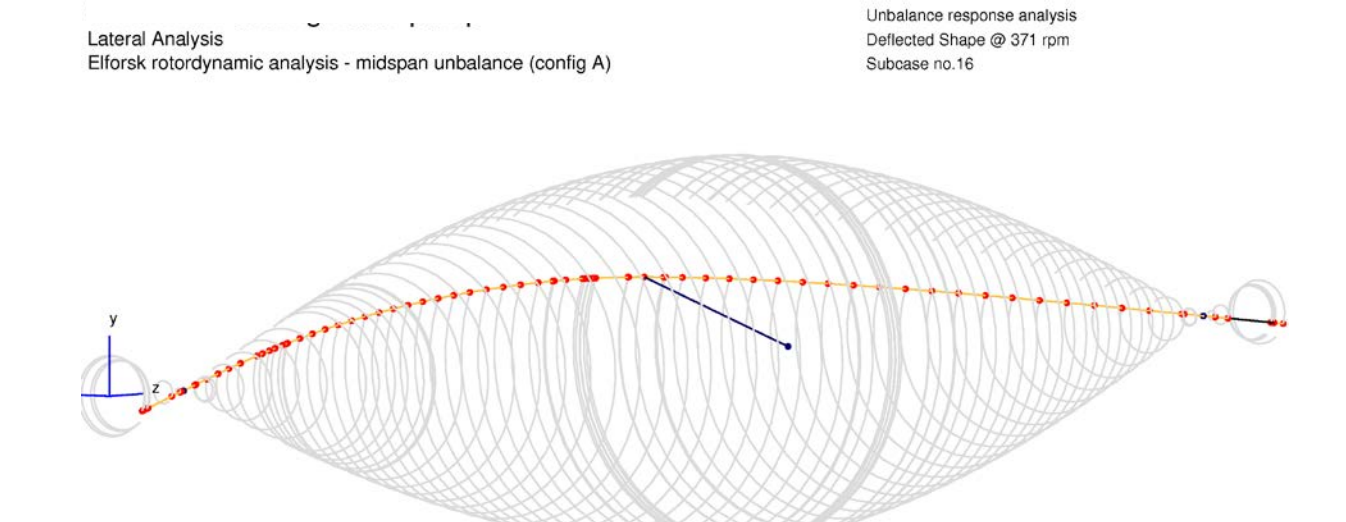


Figure XXI. Response for the unbalance Case A at the running speed with maximum bearing stiffness.

MaxstiffnessA - Case no. 1

ODS A/S RP 4.1.61 - win7 (Apr 2 201

## Appendix A.2

# Impeller unbalance (Configuration A) – Minimum bearing stiffness

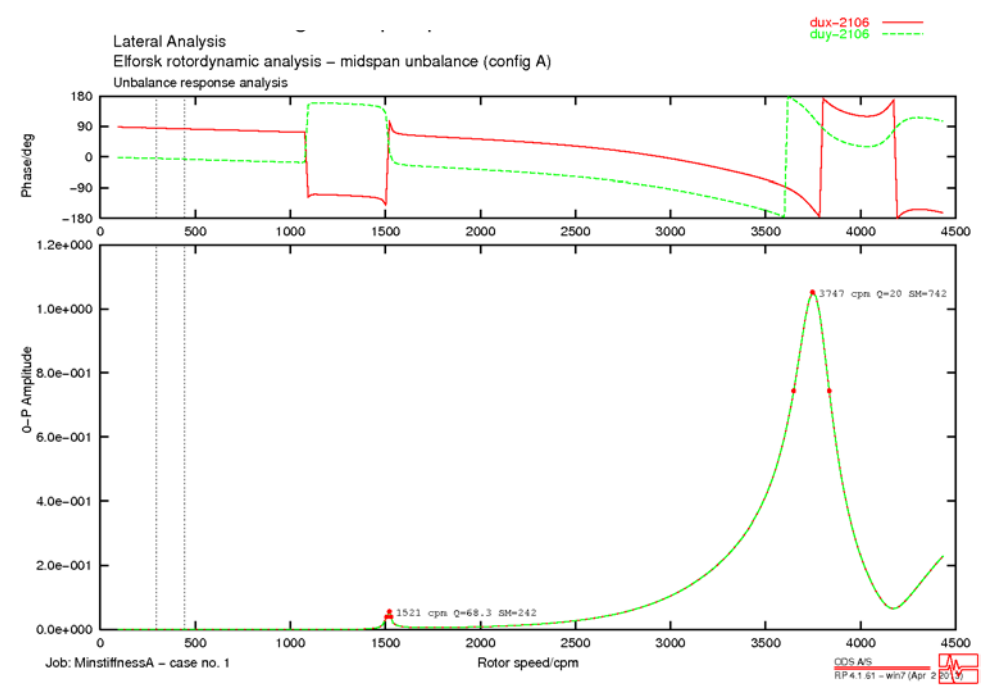


Figure XXII. Bode plot showing the response in m/s zero to peak at the bottom pump bearing for unbalance Case A, with the unbalance in the middle coupling. Minimum bearing stiffness is used.

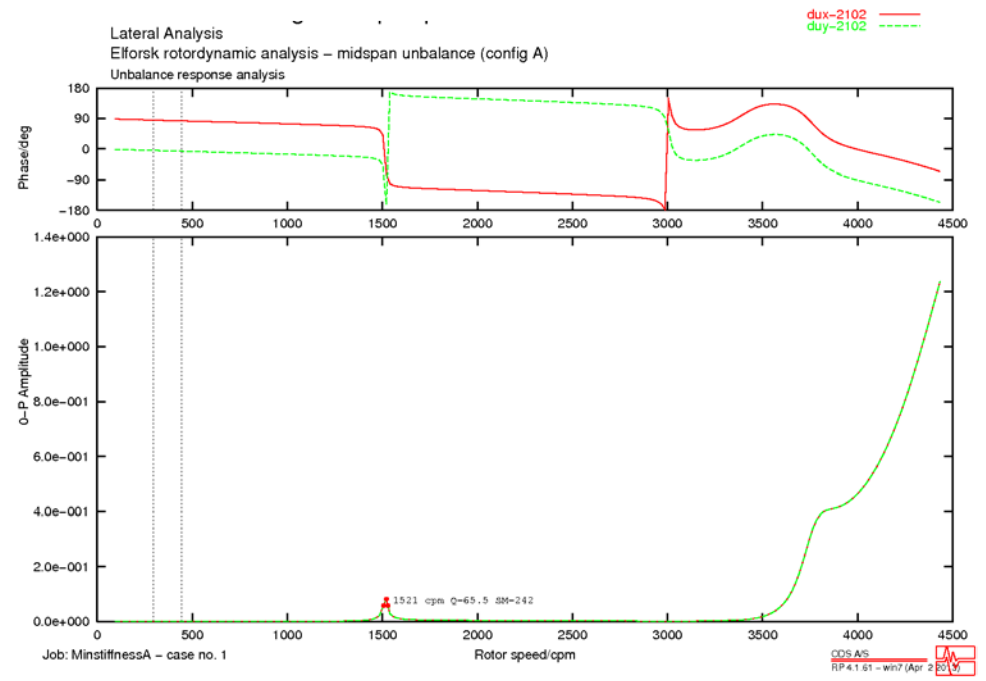


Figure XXIII. Bode plot showing the response at the upper pump bearing in m/s zero to peak for unbalance Case A, with the unbalance in the middle coupling. Minimum bearing stiffness is used.

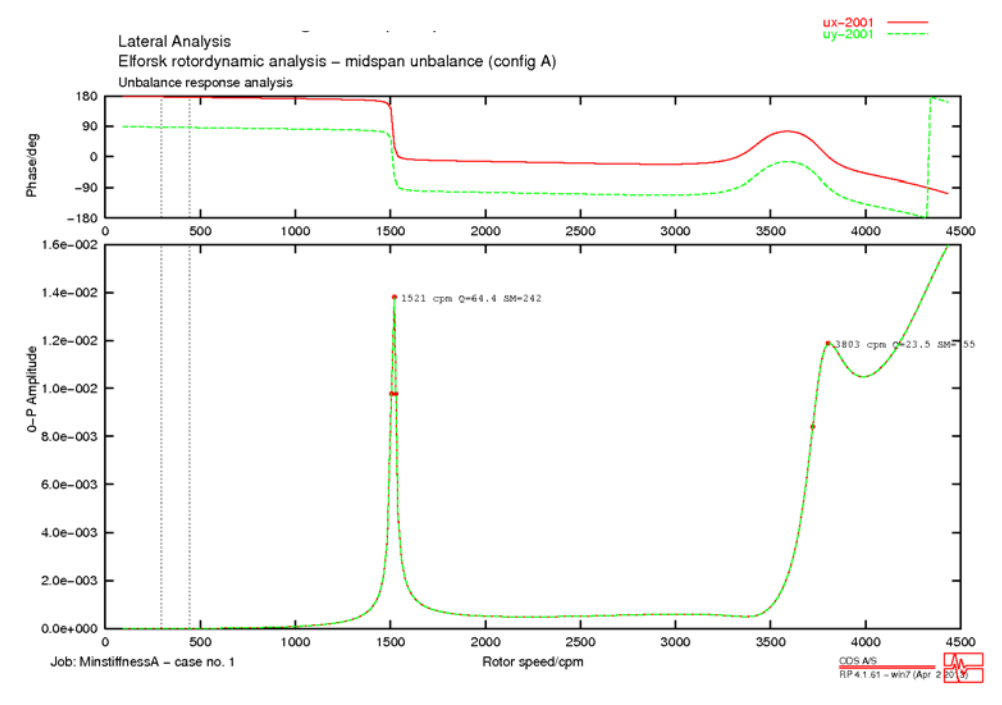


Figure XXIV. Bode plot showing the response at the DE coupling in m zero to peak for unbalance Case A, with the unbalance in the middle coupling.

Minimum bearing stiffness is used.

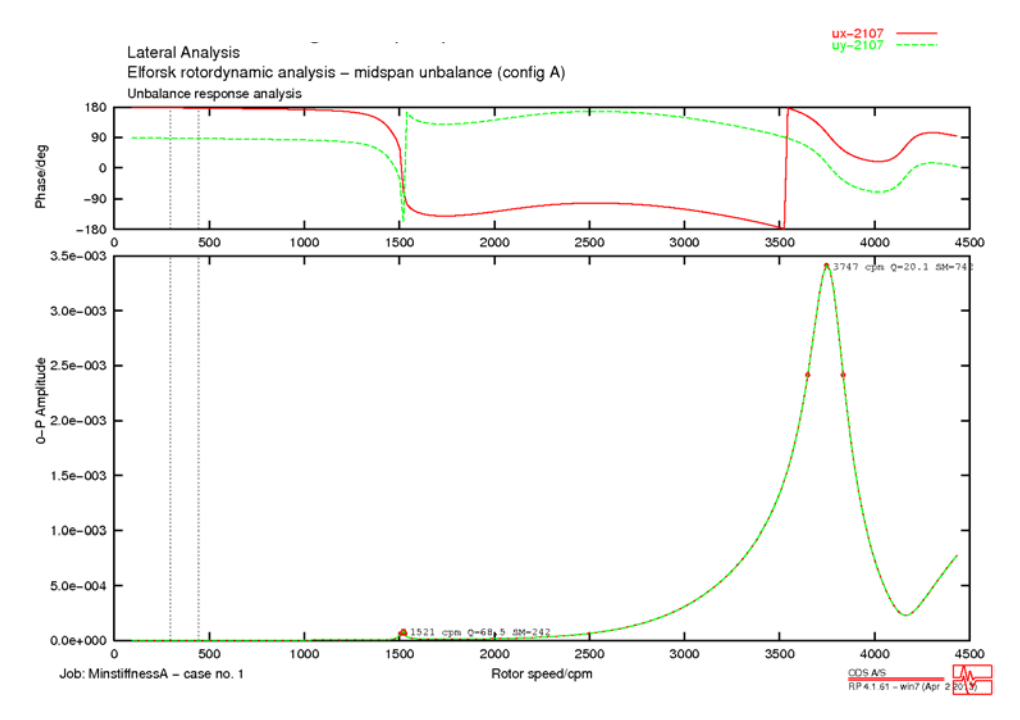


Figure XXV. Bode plot showing the response at the impeller in m zero to peak for unbalance Case A, with the unbalance in the middle coupling. Minimum bearing stiffness is used.

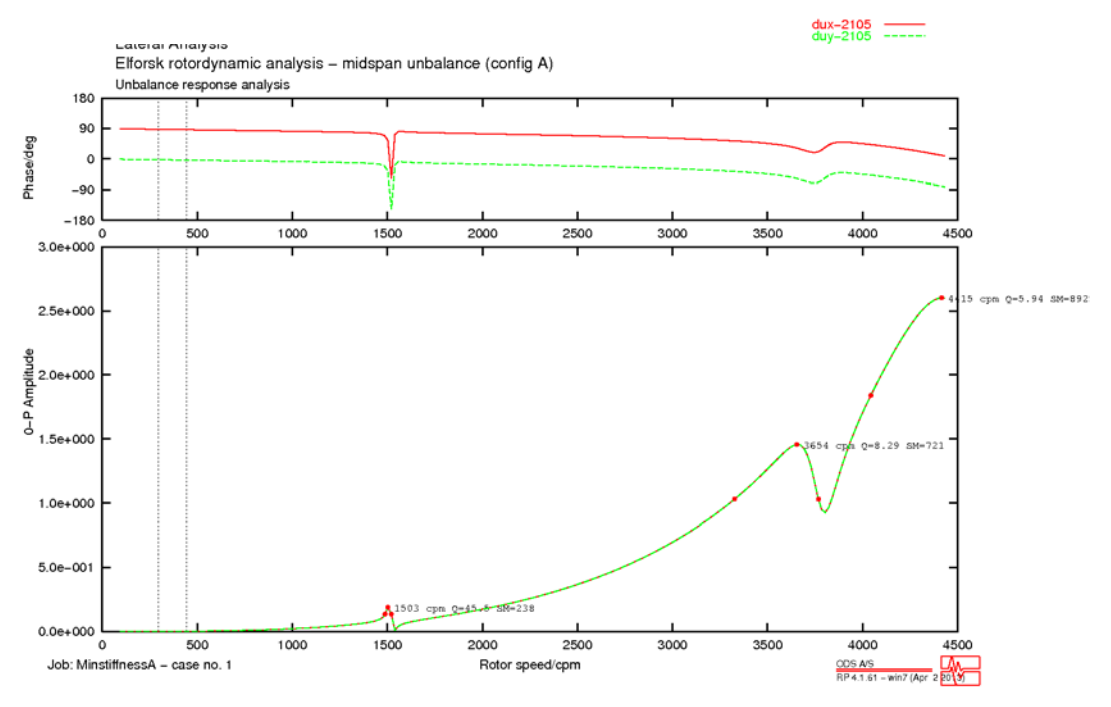


Figure XXVI. Bode plot showing the response at the middle pump bearing in m/s zero to peak for unbalance Case A, with the unbalance in the middle coupling. Minimum bearing stiffness is used.

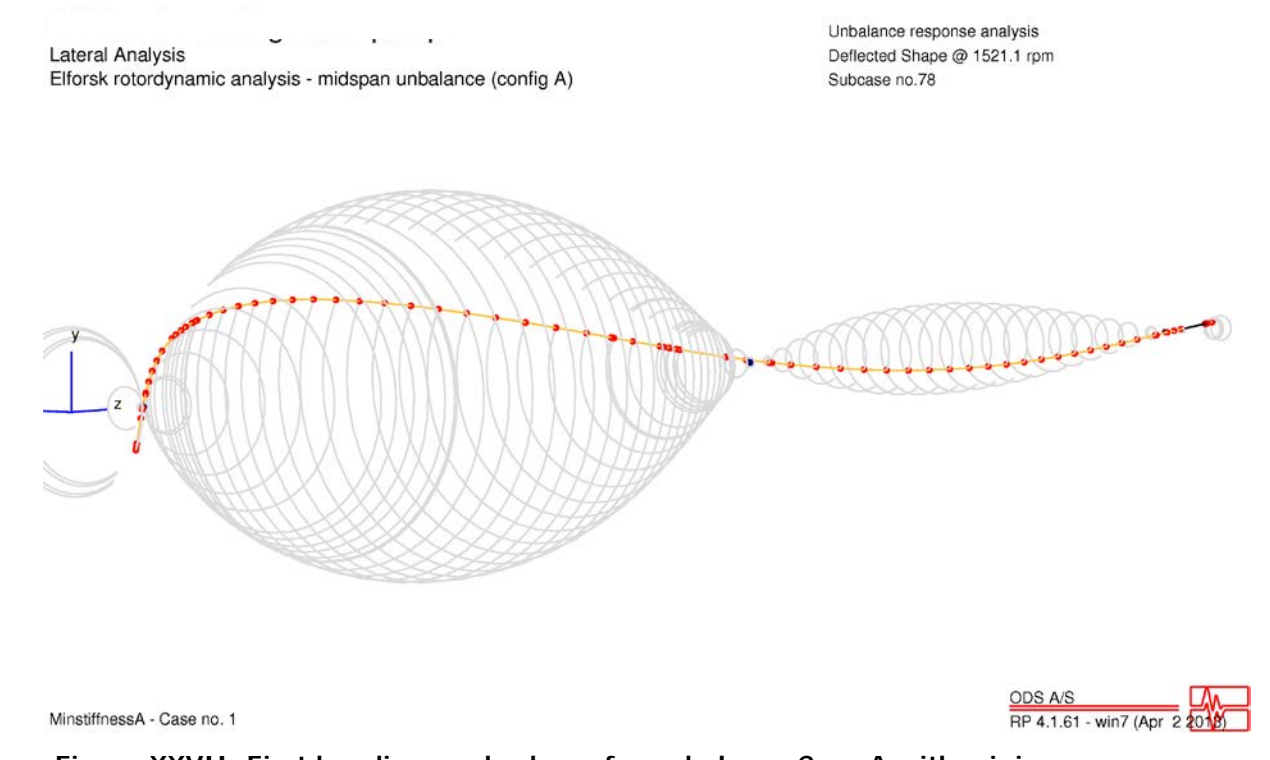


Figure XXVII. First bending mode shape for unbalance Case A with minimum bearing stiffness.

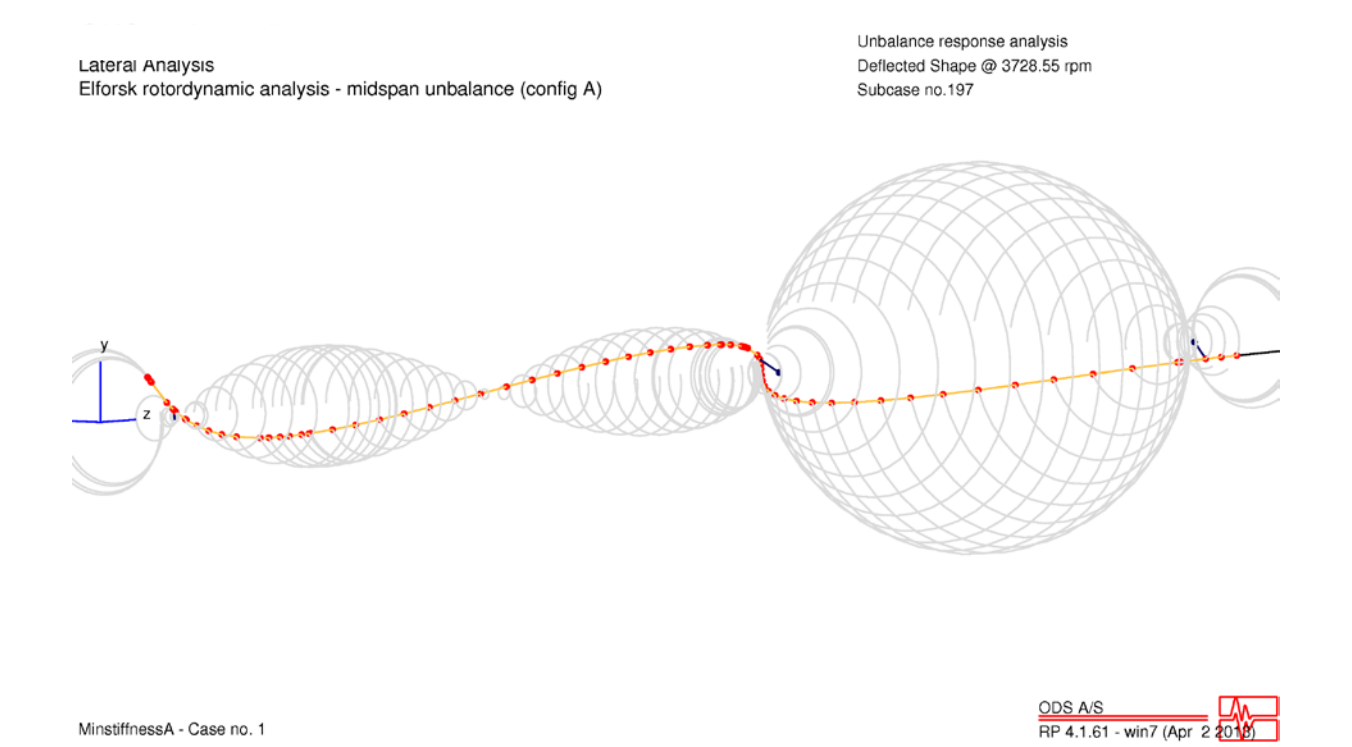
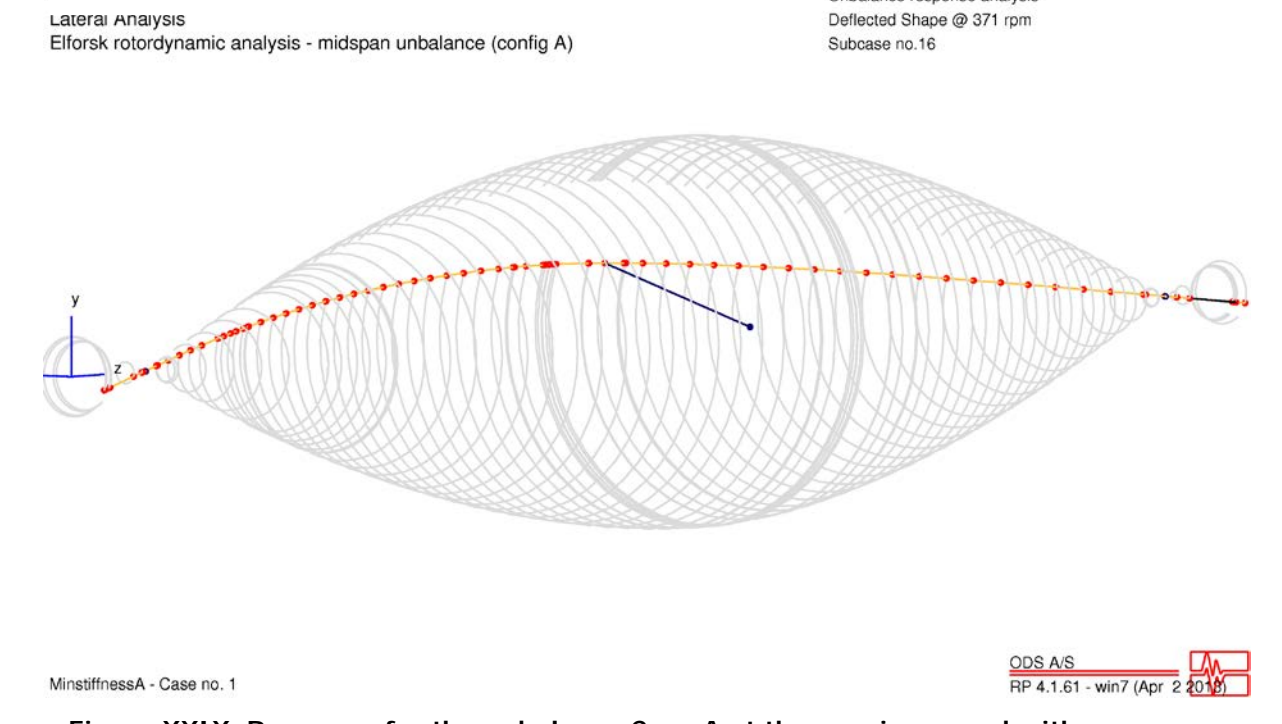


Figure XXVIII. Second bending mode shape for unbalance Case A with minimum bearing stiffness.

MinstiffnessA - Case no. 1



Unbalance response analysis

Figure XXIX. Response for the unbalance Case A at the running speed with minimum bearing stiffness.

# Appendix A.3

Coupling unbalance (Configuration B) – Minimum bearing stiffness

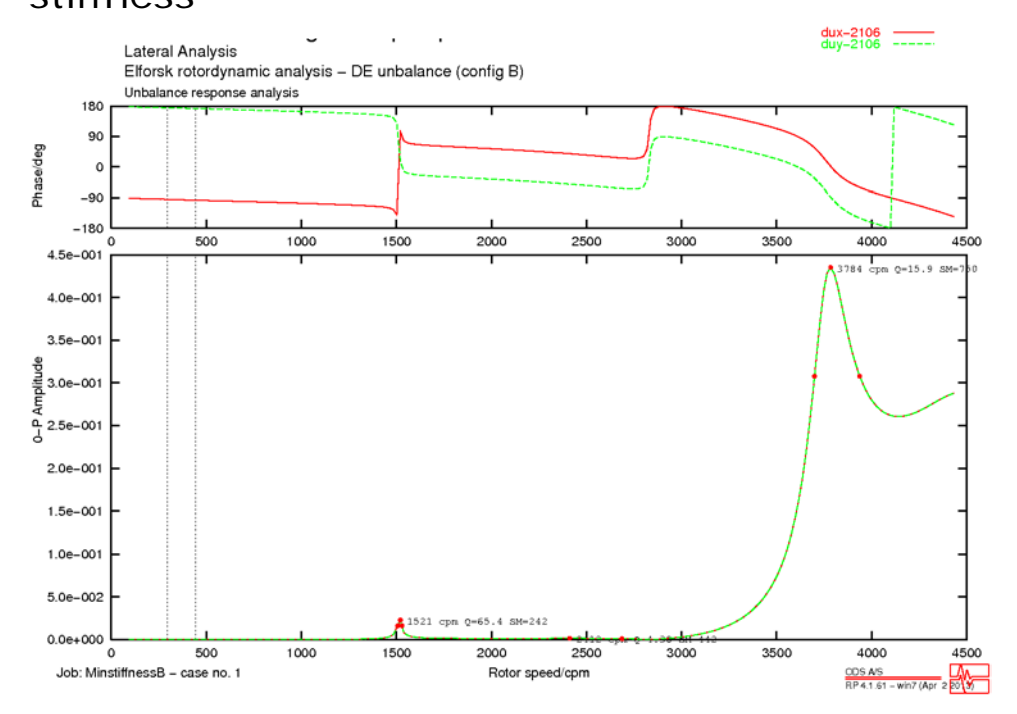


Figure XXX. Bode plot showing the response at the bottom pump bearing in m/s zero to peak for unbalance Case B, with the unbalance in the DE coupling. Minimum bearing stiffness is used.

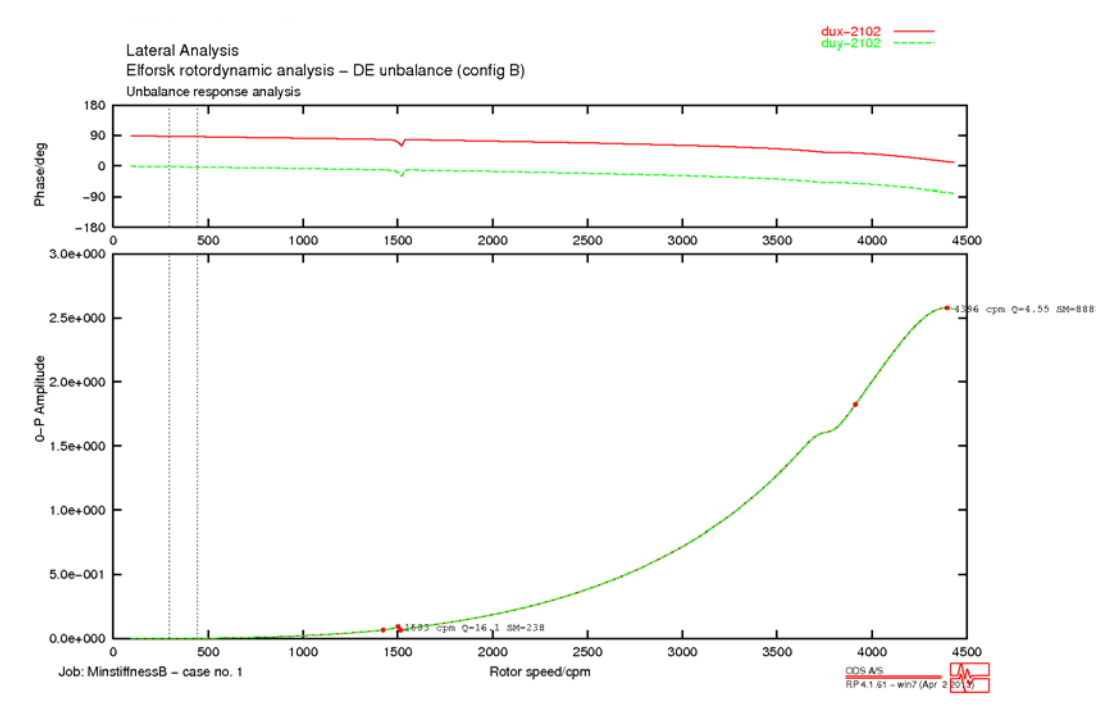


Figure XXXI. Bode plot showing the response at the upper pump bearing in m/s zero to peak for unbalance Case B, with the unbalance in the DE coupling. Minimum bearing stiffness is used.

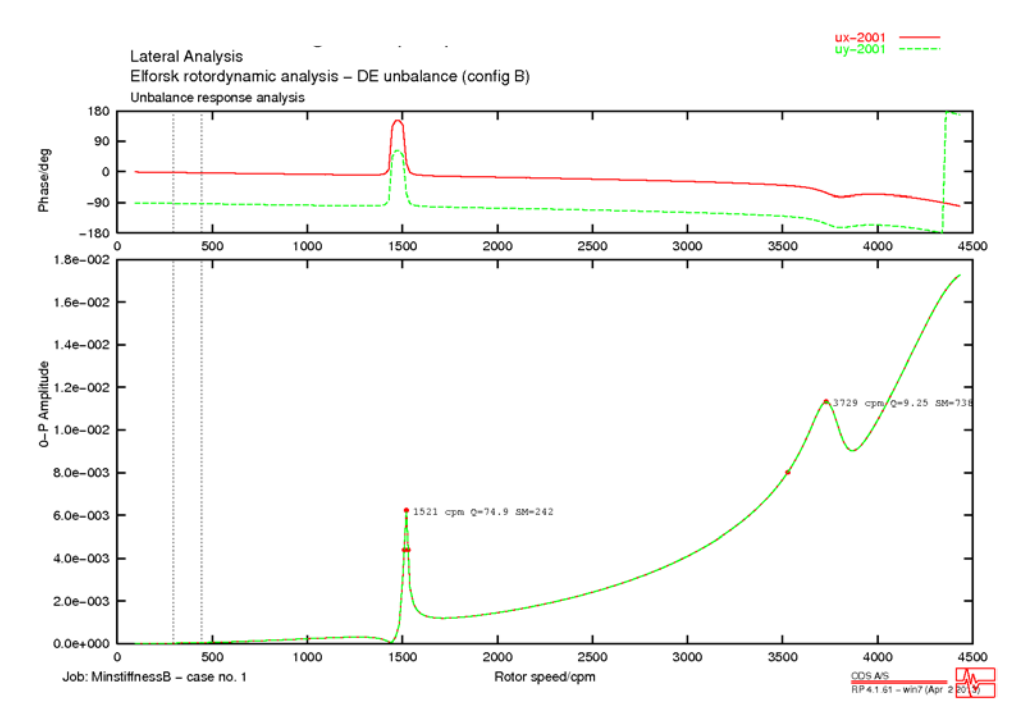


Figure XXXII. Bode plot showing the response at the DE coupling in m zero to peak for unbalance Case B, with the unbalance in the DE coupling. Minimum bearing stiffness is used.

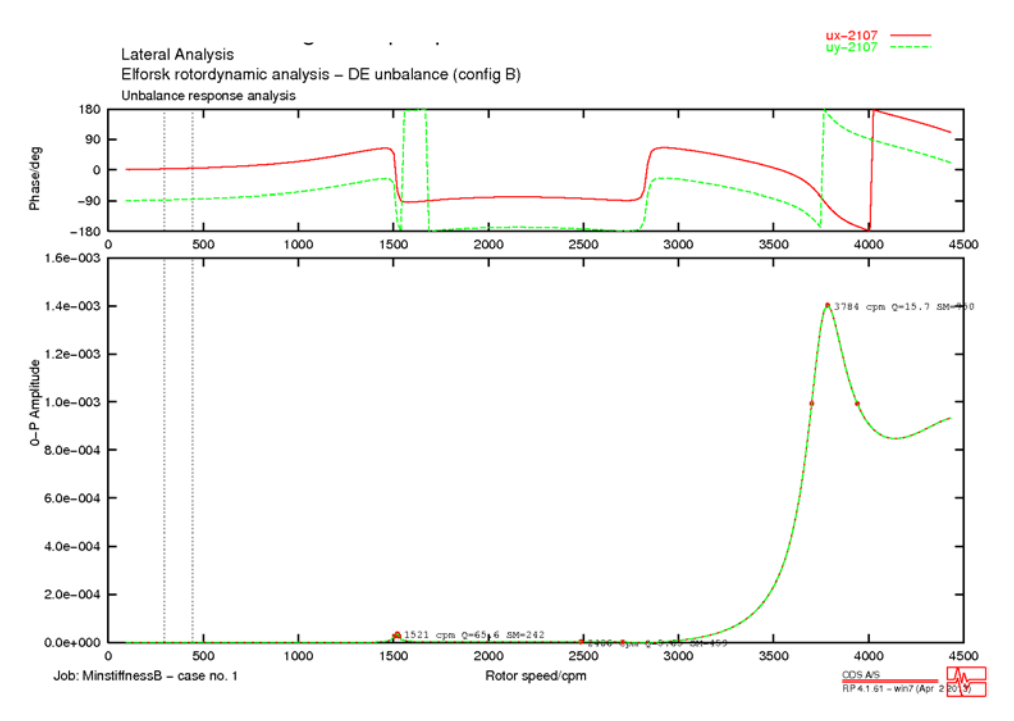


Figure XXXIII. Bode plot showing the response at the impeller in m zero to peak for unbalance Case B, with the unbalance in the DE coupling. Minimum bearing stiffness is used.

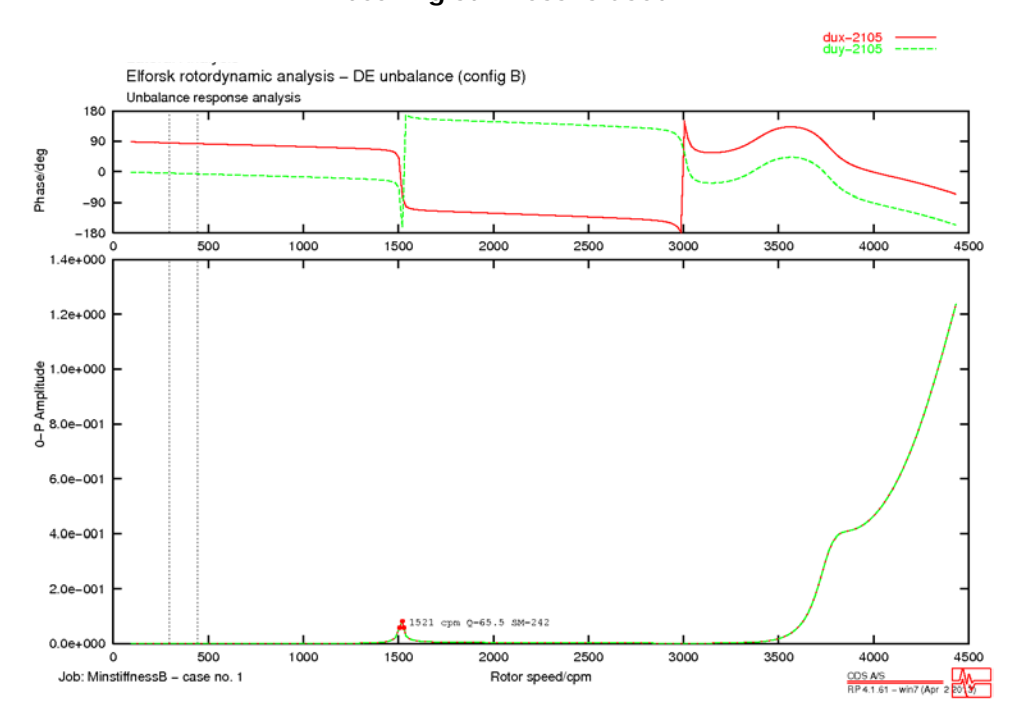


Figure XXXIV. Bode plot showing the response at the middle pump bearing in m/s zero to peak for unbalance Case B, with the unbalance in the DE coupling. Minimum bearing stiffness is used.

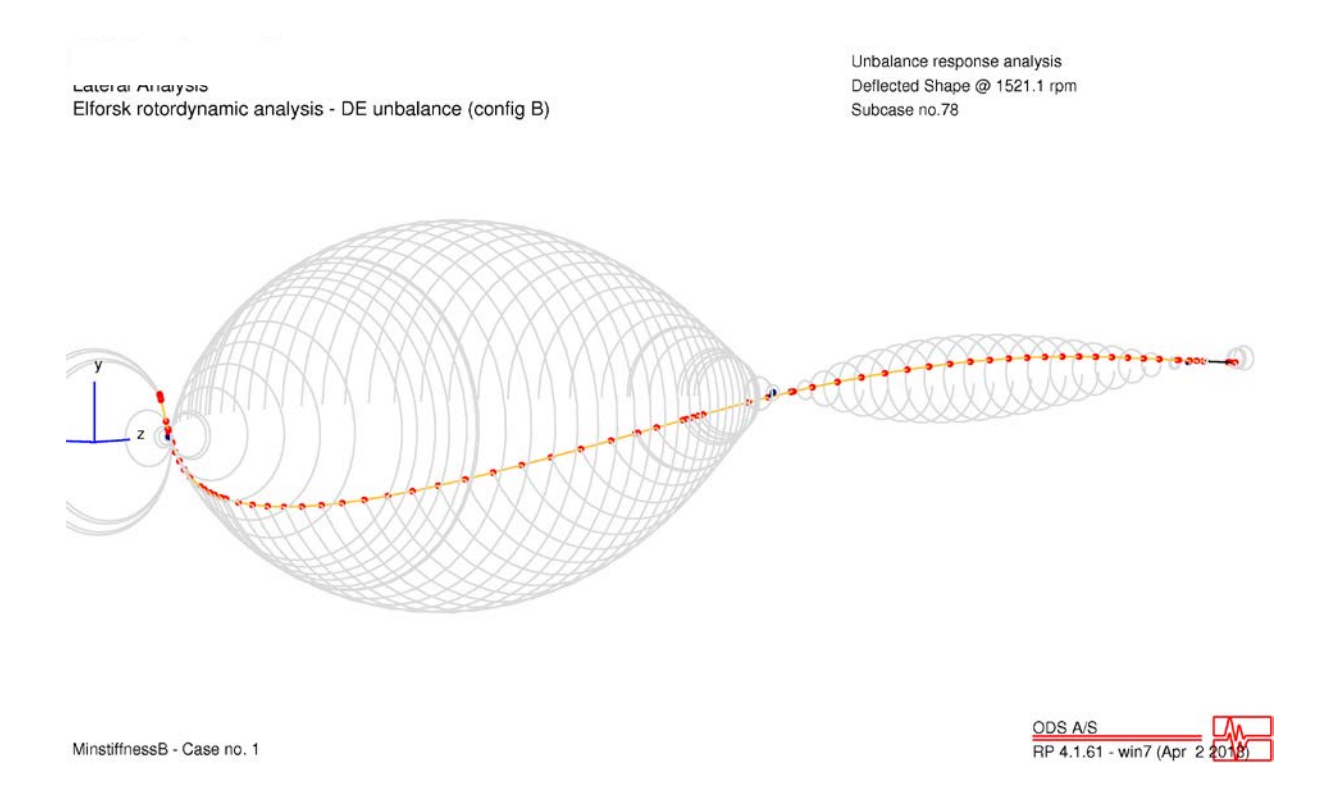


Figure XXXV. First bending mode shape for unbalance Case B with minimum bearing stiffness.

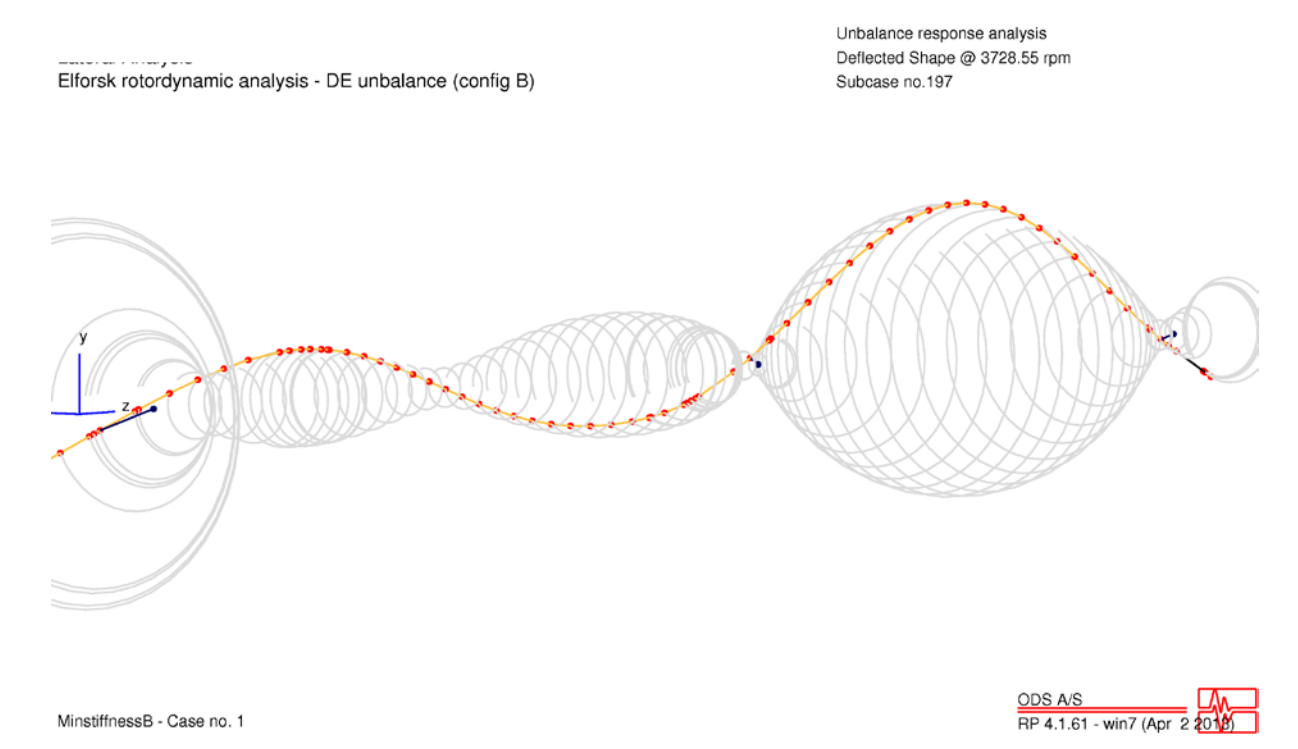
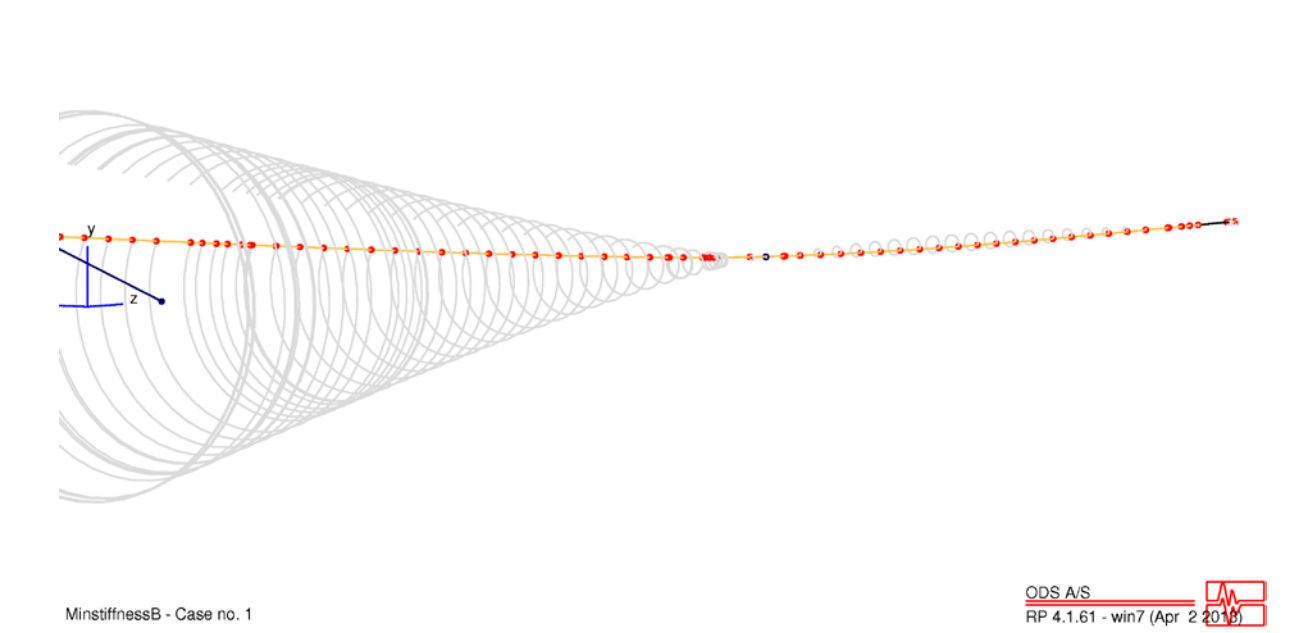


Figure XXXVI. Second bending mode shape for unbalance Case B with minimum bearing stiffness.



Lateral Analysis Elforsk rotordynamic analysis - DE unbalance (config B) Unbalance response analysis

Deflected Shape @ 371 rpm

Subcase no.16

Figure XXXVII. Response for the unbalance Case B at the running speed with minimum bearing stiffness.

# Coupling unbalance (Configuration B) – Maximum bearing stiffness

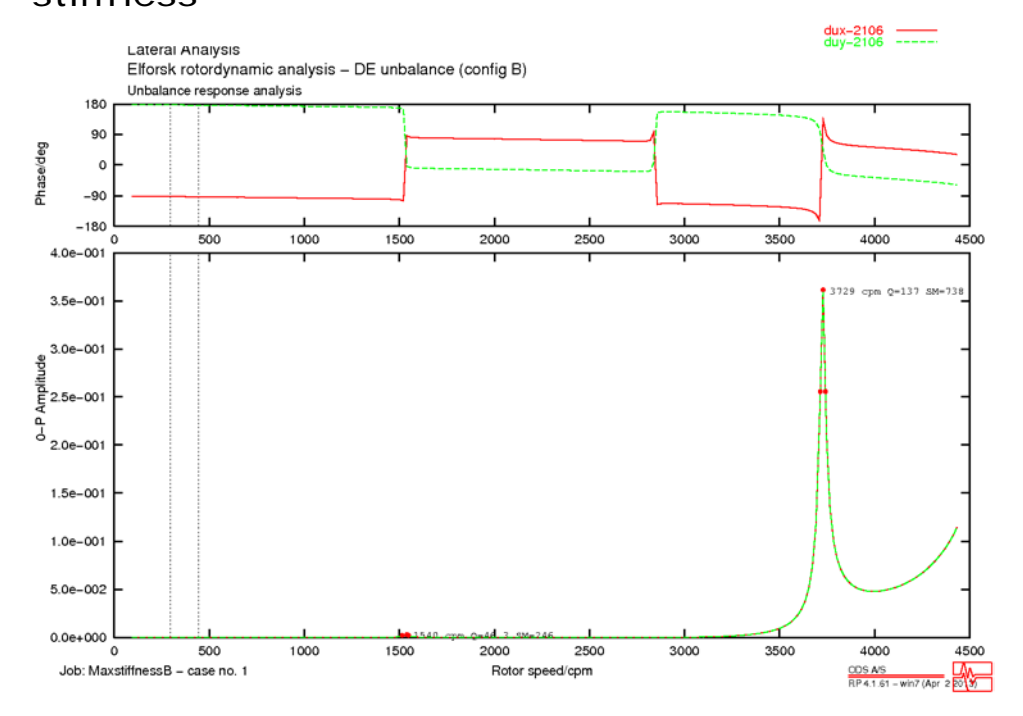


Figure XXXVIII. Bode plot showing the response at the bottom pump bearing in m/s zero to peak for unbalance Case B, with the unbalance in the DE coupling. Maximum bearing stiffness is used.

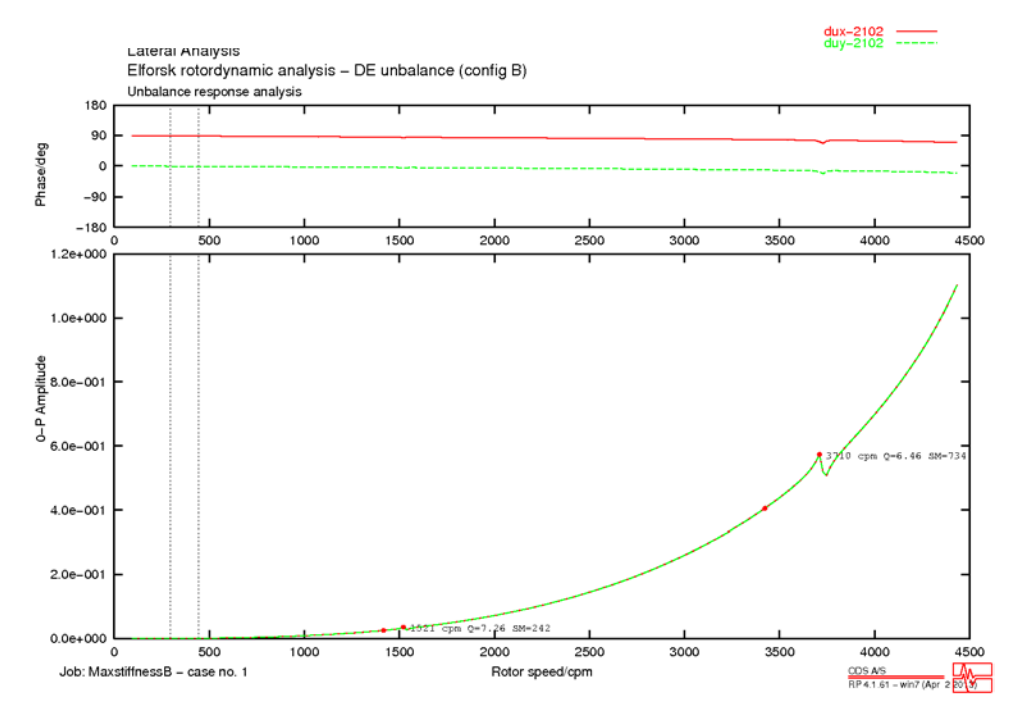


Figure XXXIX. Bode plot showing the response at the upper pump bearing in m/s zero to peak for unbalance Case B, with the unbalance in the DE coupling. Maximum bearing stiffness is used.

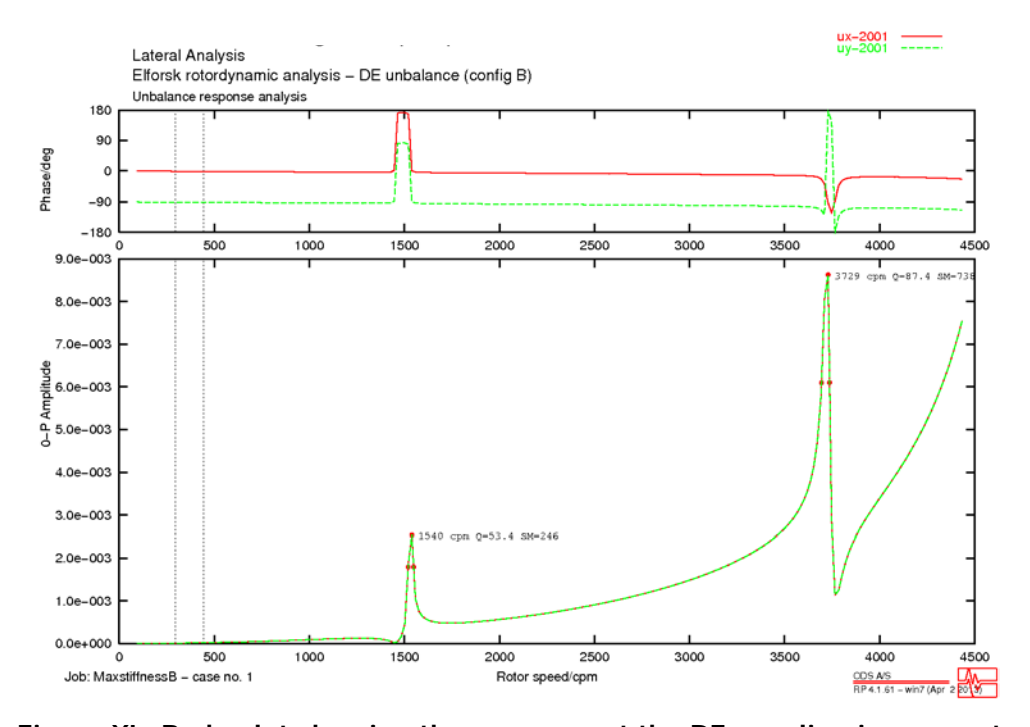


Figure XL. Bode plot showing the response at the DE coupling in m zero to peak for unbalance Case B, with the unbalance in the DE coupling. Maximum bearing stiffness is used.

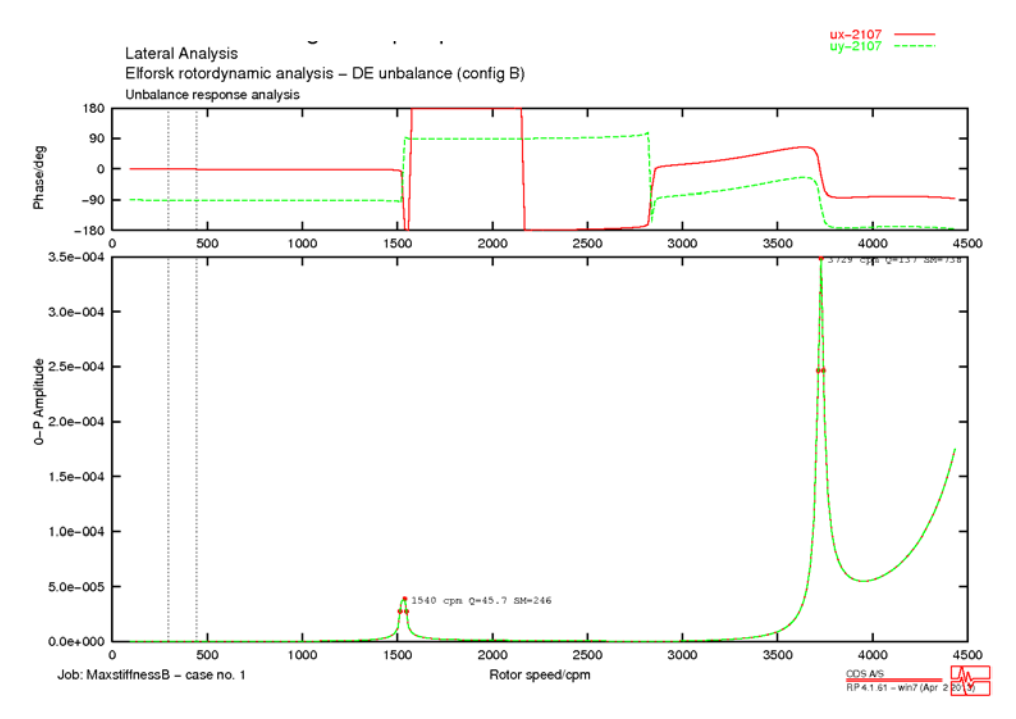


Figure XLI. Bode plot showing the response at the impeller in m zero to peak for unbalance Case B, with the unbalance in the DE coupling. Maximum bearing stiffness is used.

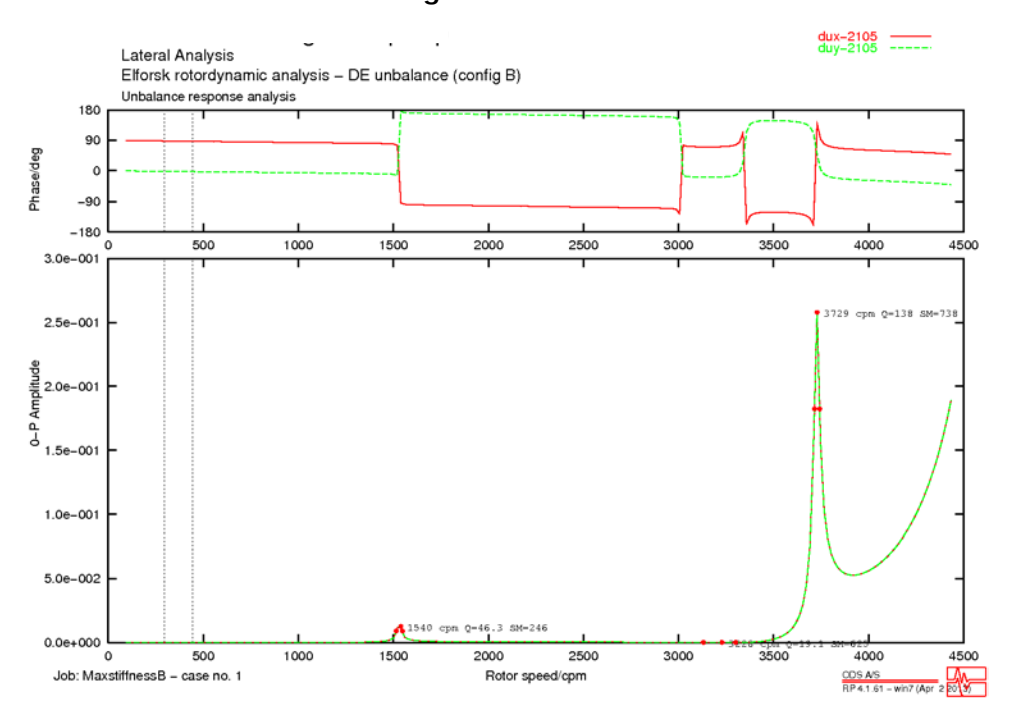


Figure XLII. Bode plot showing the response at the middle pump bearing in m/s zero to peak for unbalance Case B, with the unbalance in the DE coupling. Maximum bearing stiffness is used.

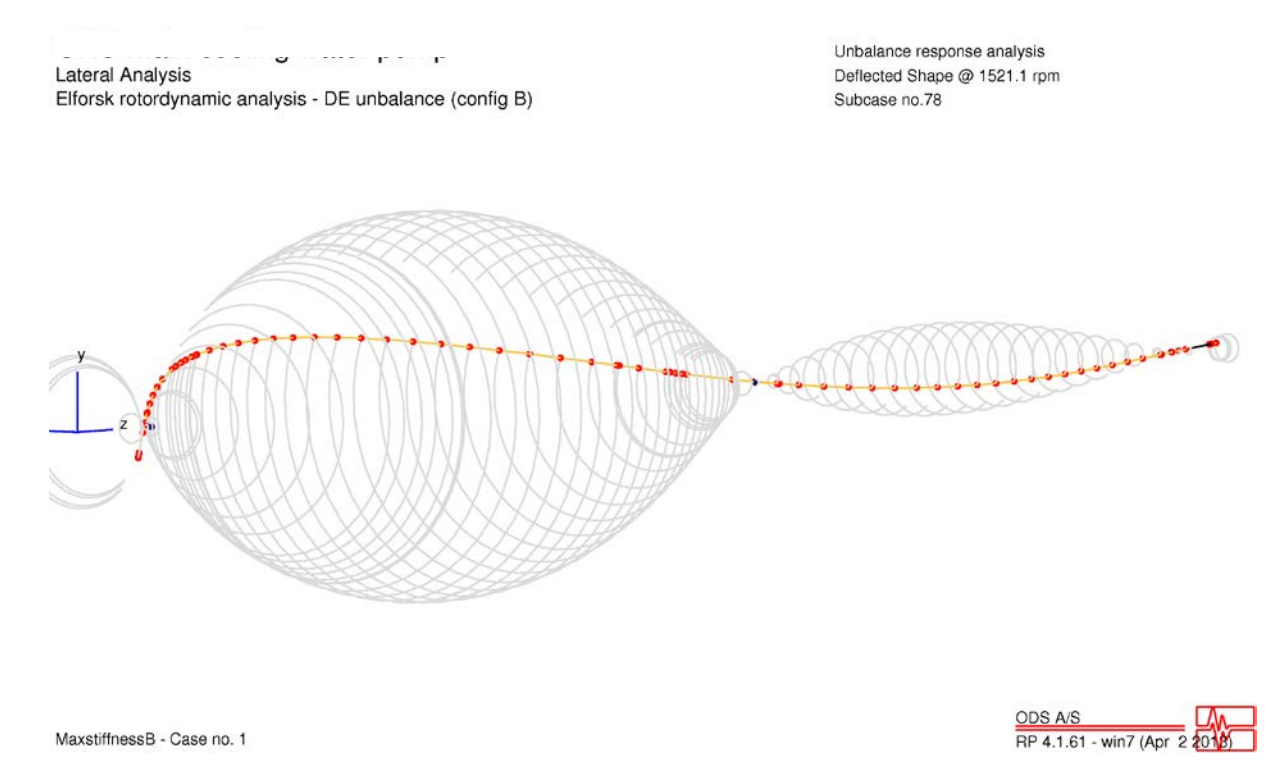


Figure XLIII. First bending mode shape for unbalance Case B with maximum bearing stiffness.

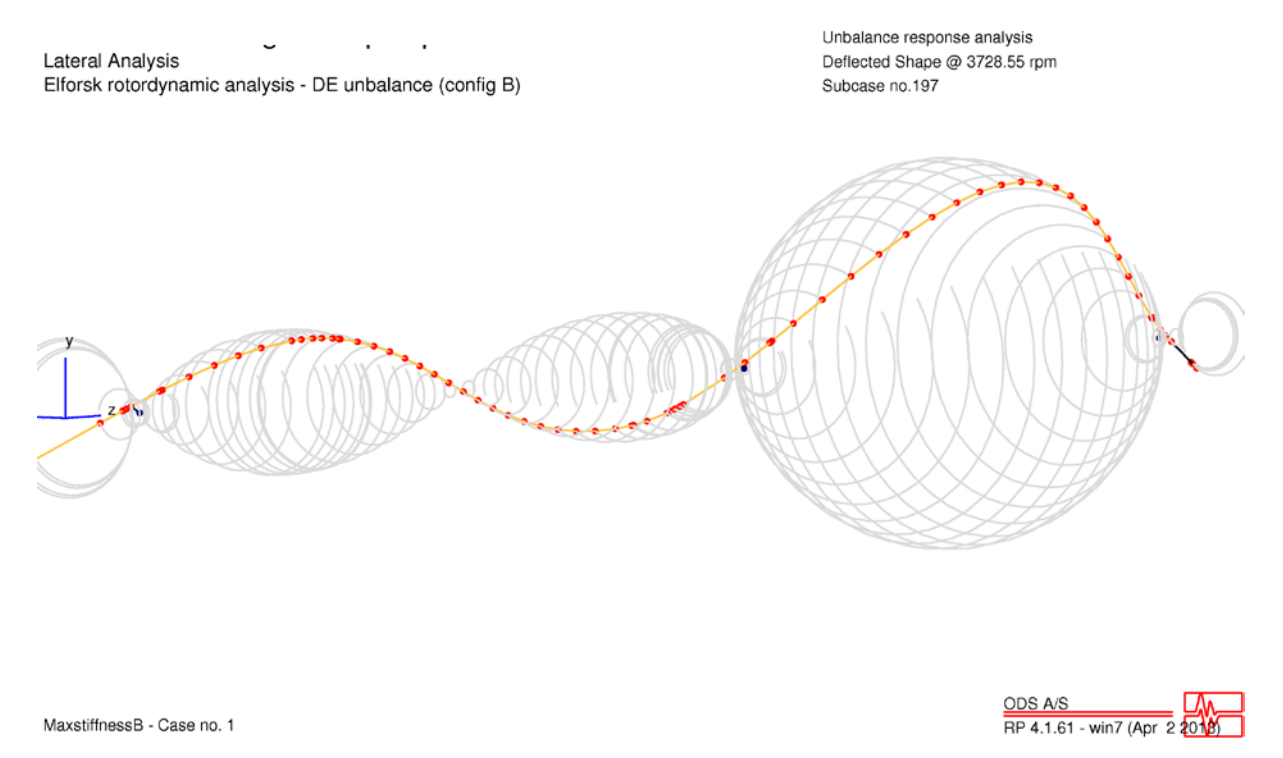
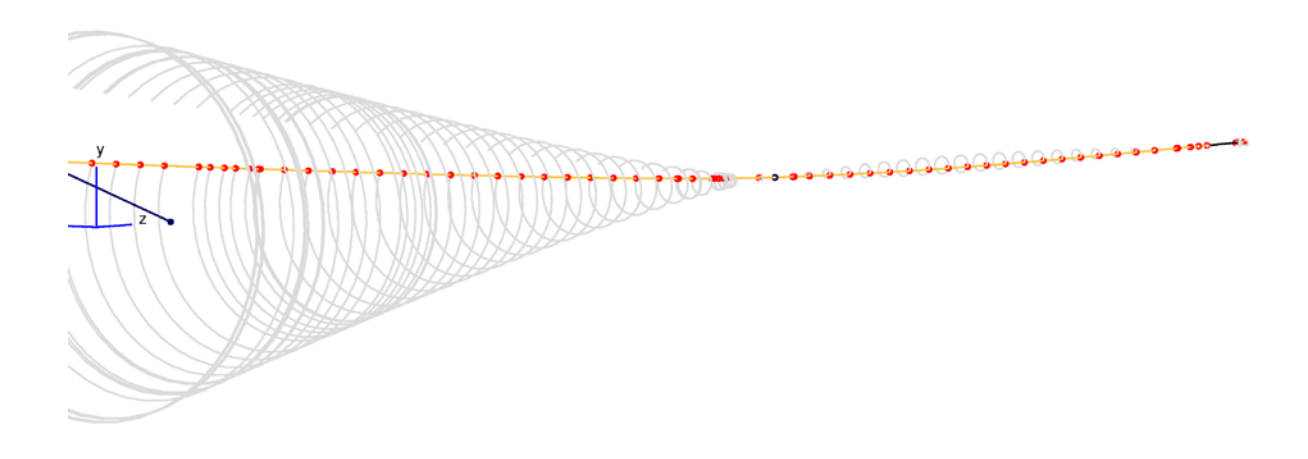


Figure XLIV. Second bending mode shape for unbalance Case B with maximum bearing stiffness.

Lateral Analysis Elforsk rotordynamic analysis - DE unbalance (config B) Unbalance response analysis Deflected Shape @ 371 rpm Subcase no.16



MaxstiffnessB - Case no. 1



Figure XLV. Response for the unbalance Case B at the running speed with maximum bearing stiffness.

Midspan unbalance (Configuration C) – Minimum bearing stiffness

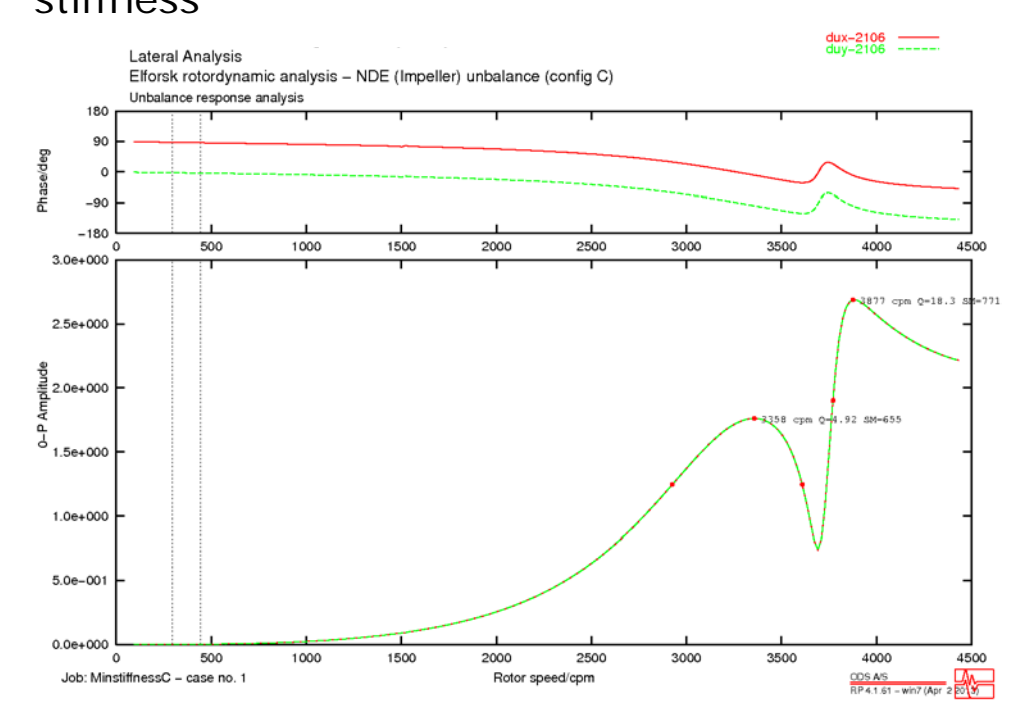


Figure XLVI. Bode plot showing the response at the bottom pump bearing in m/s zero to peak for unbalance Case C, with the unbalance in the NDE impeller. Minimum bearing stiffness is used.

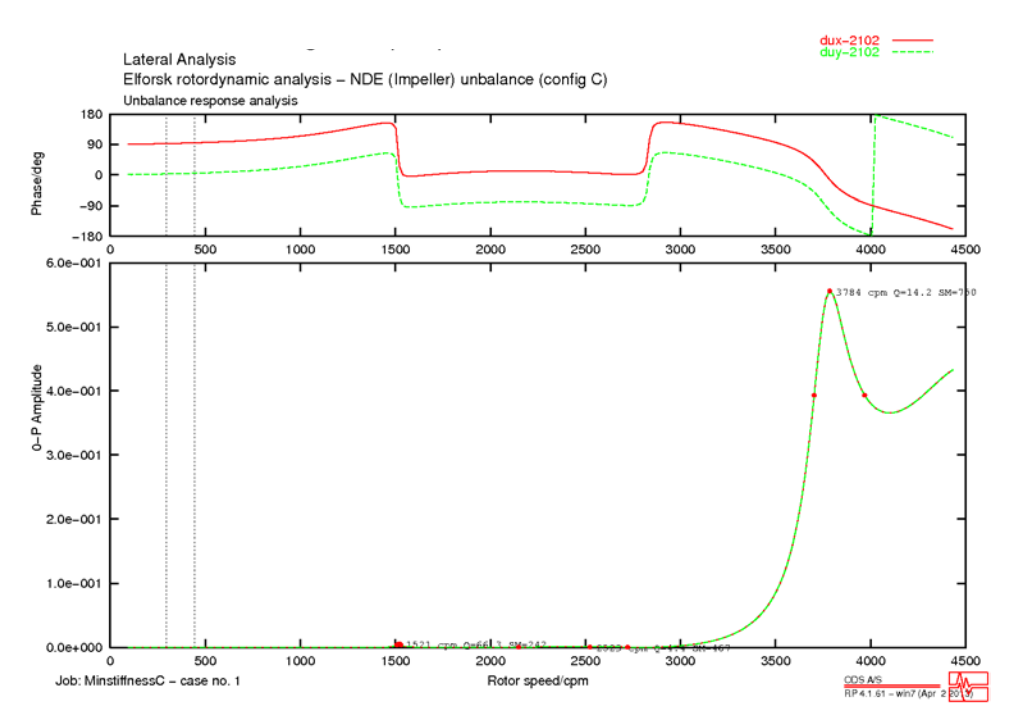


Figure XLVII. Bode plot showing the response at the upper pump bearing in m/s zero to peak for unbalance Case C, with the unbalance in the NDE impeller. Minimum bearing stiffness is used.

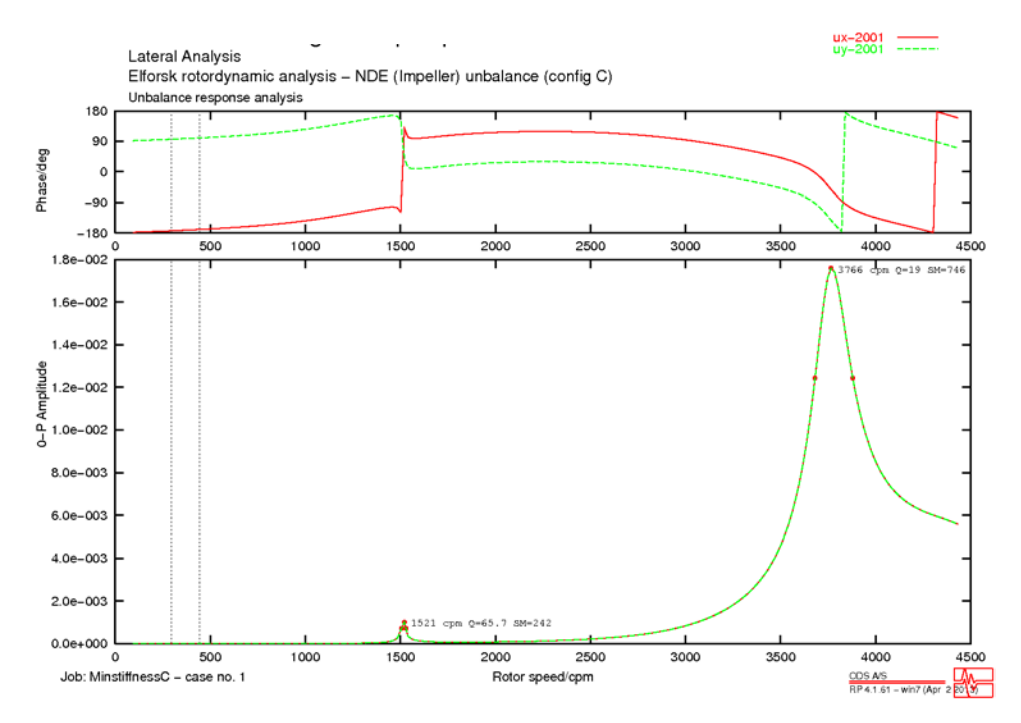


Figure XLVIII. Bode plot showing the response at the DE coupling in m zero to peak for unbalance Case C, with the unbalance in the NDE impeller.

Minimum bearing stiffness is used.

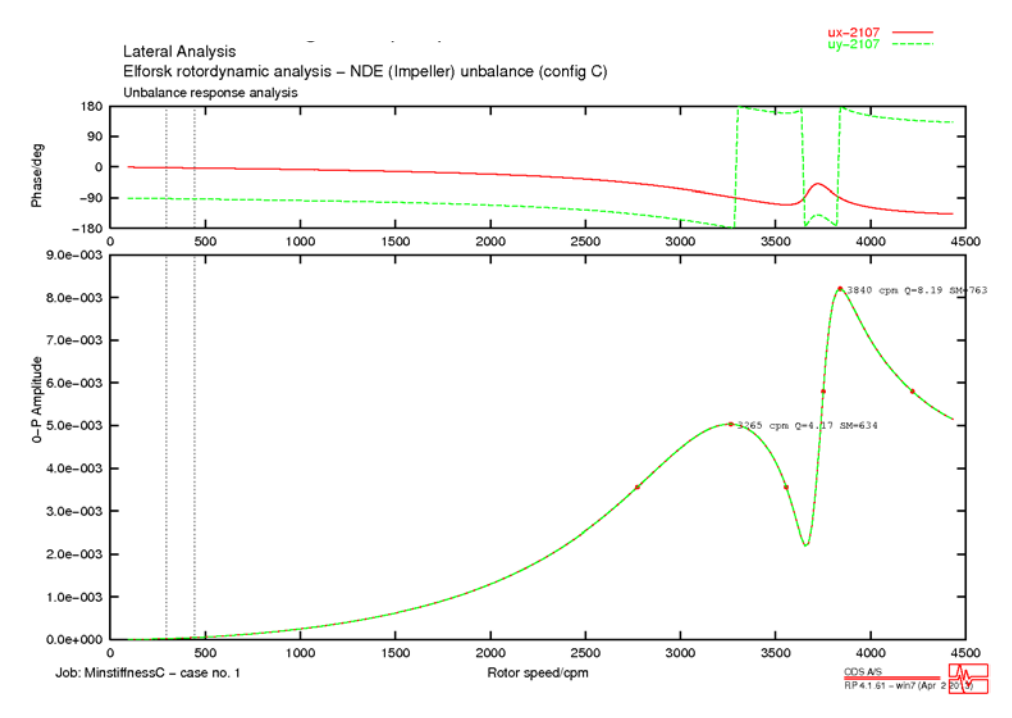


Figure XLIX. Bode plot showing the response at the impeller in m zero to peak for unbalance Case C, with the unbalance in the NDE impeller. Minimum bearing stiffness is used.

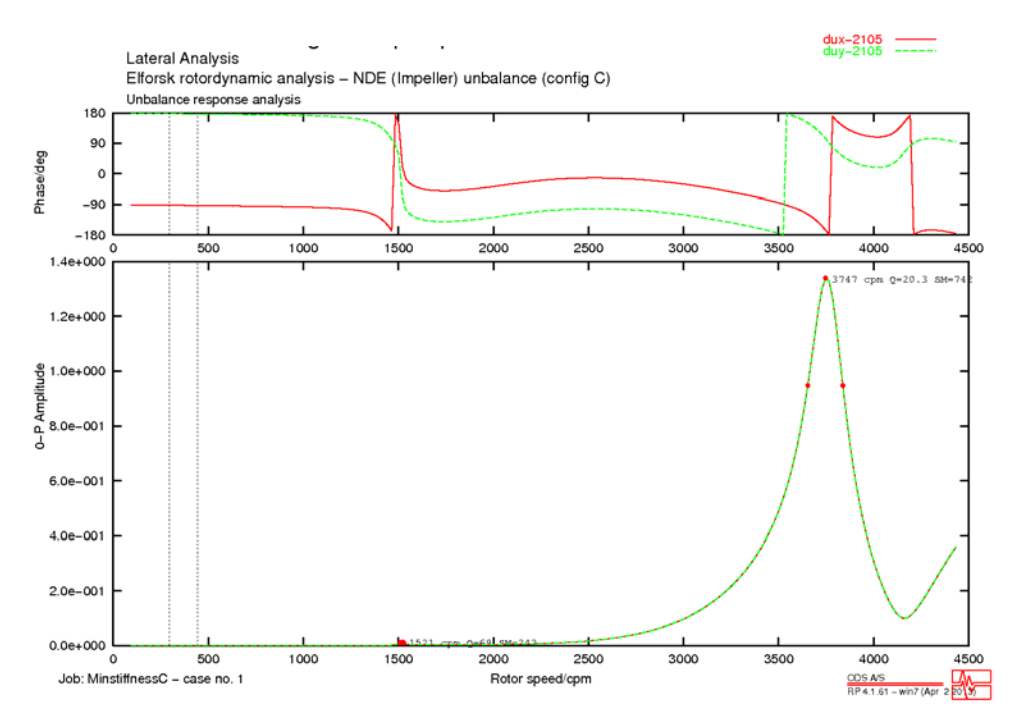
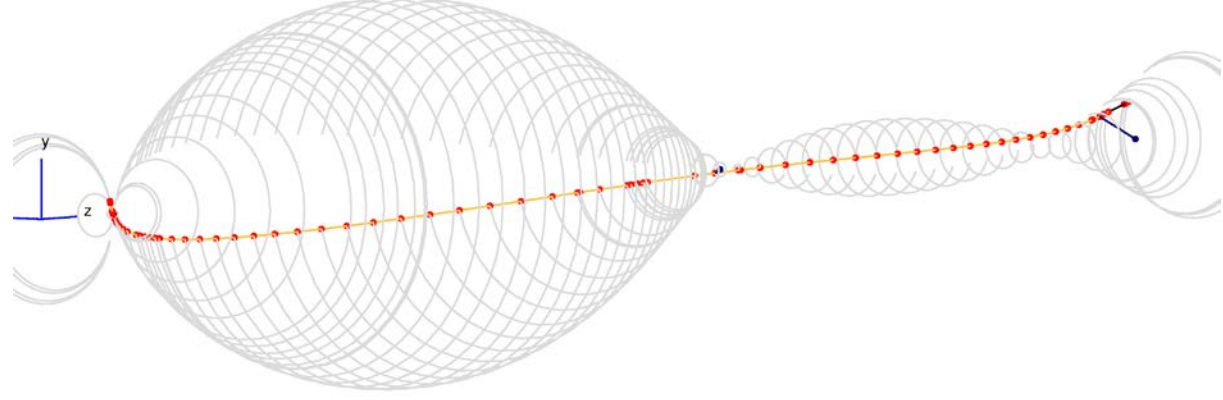


Figure L. Bode plot showing the response at the middle pump bearing in m/s zero to peak for unbalance Case C, with the unbalance in the NDE impeller.

Minimum bearing stiffness is used.

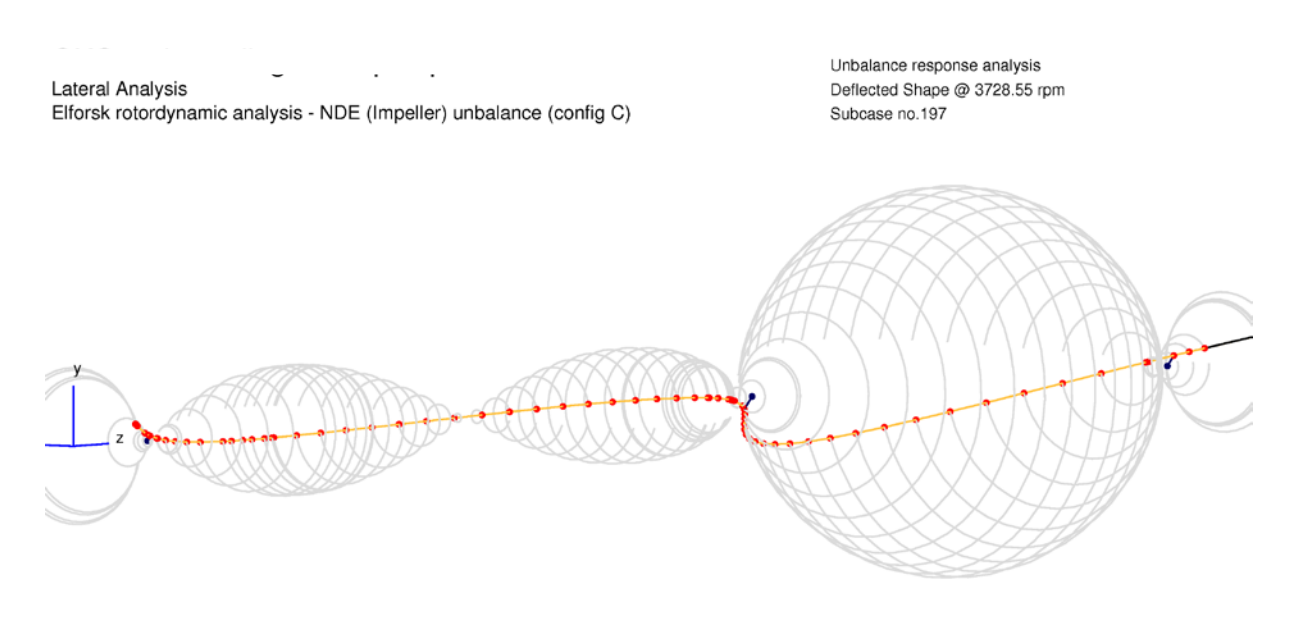




MinstiffnessC - Case no. 1

ODS A/S RP 4.1.61 - win7 (Apr 2 2018)

Figure LI. First bending mode shape for unbalance Case C with minimum bearing stiffness.



MinstiffnessC - Case no. 1

ODS A/S
RP 4.1.61 - win7 (Apr 2 2018)

Figure LII. Second bending mode shape for unbalance Case C with minimum bearing stiffness.

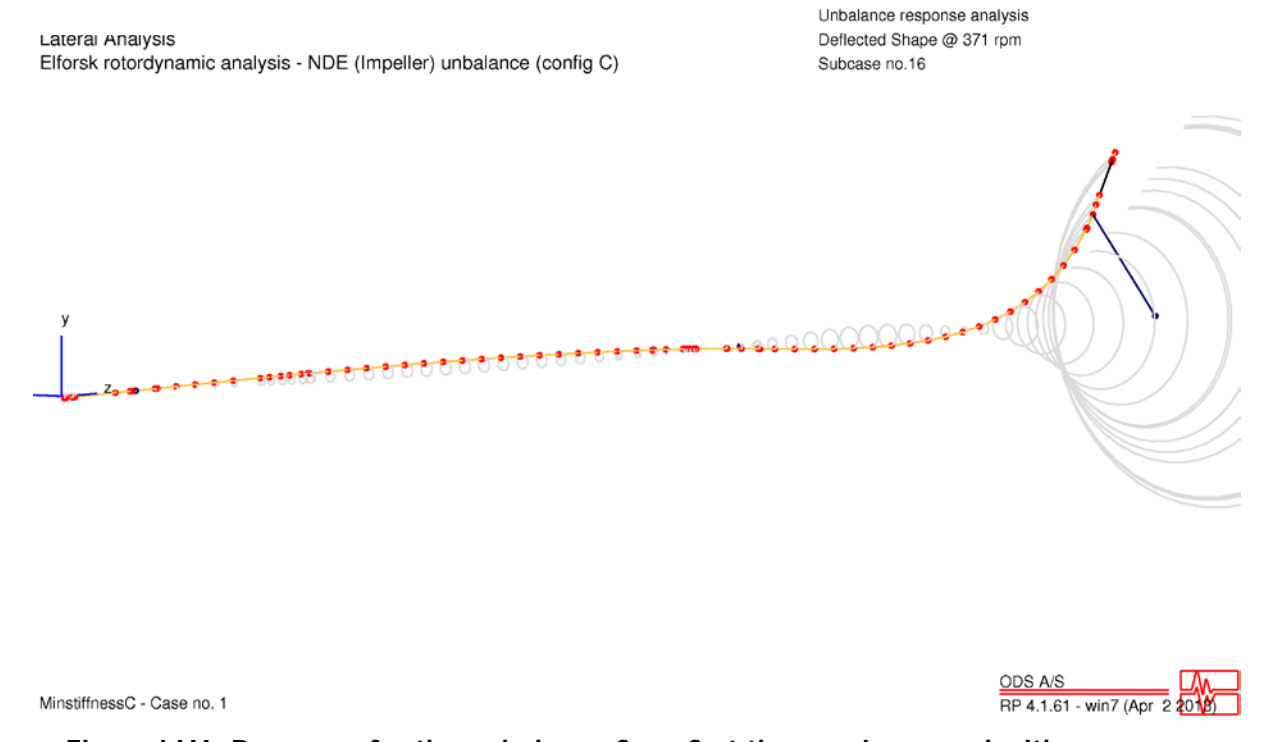


Figure LIII. Response for the unbalance Case C at the running speed with minimum bearing stiffness.

Midspan unbalance (Configuration C) – Maximum bearing stiffness

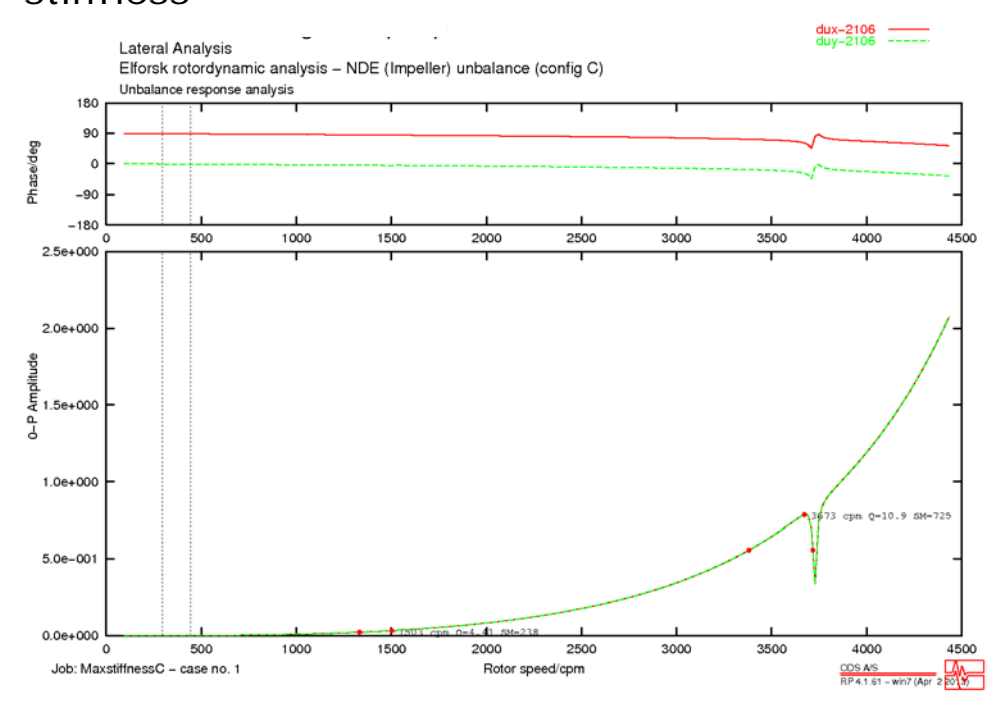


Figure LIV. Bode plot showing the response at the bottom pump bearing in m/s zero to peak for unbalance Case C, with the unbalance in the NDE impeller. Maximum bearing stiffness is used.

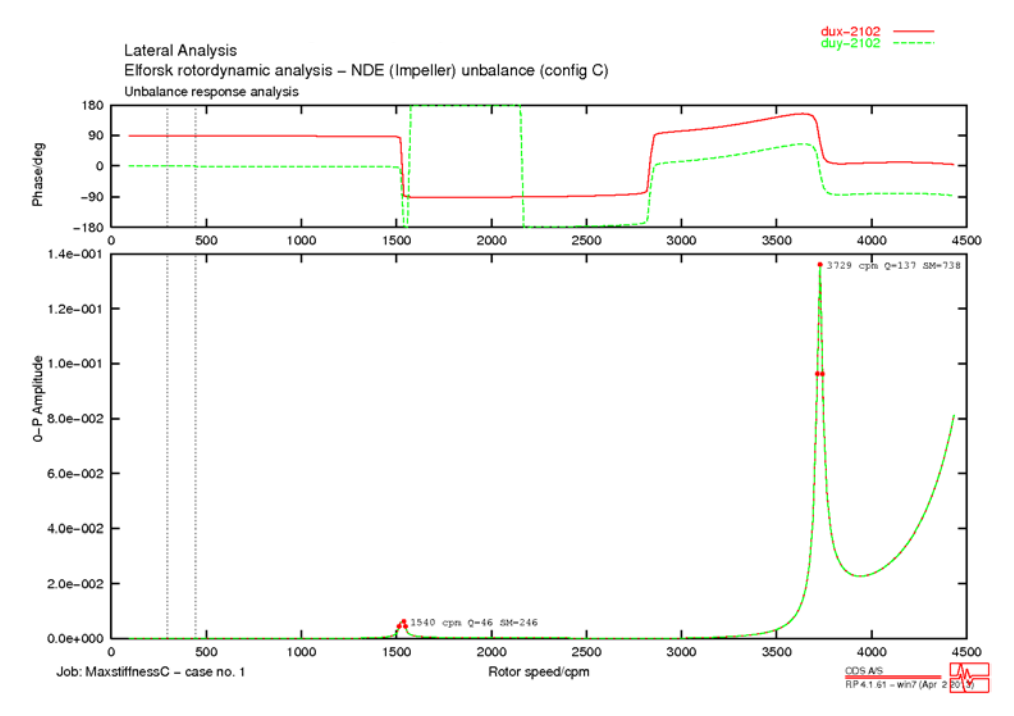


Figure LV. Bode plot showing the response at the upper pump bearing in m/s zero to peak for unbalance Case C, with the unbalance in the NDE impeller.

Maximum bearing stiffness is used.

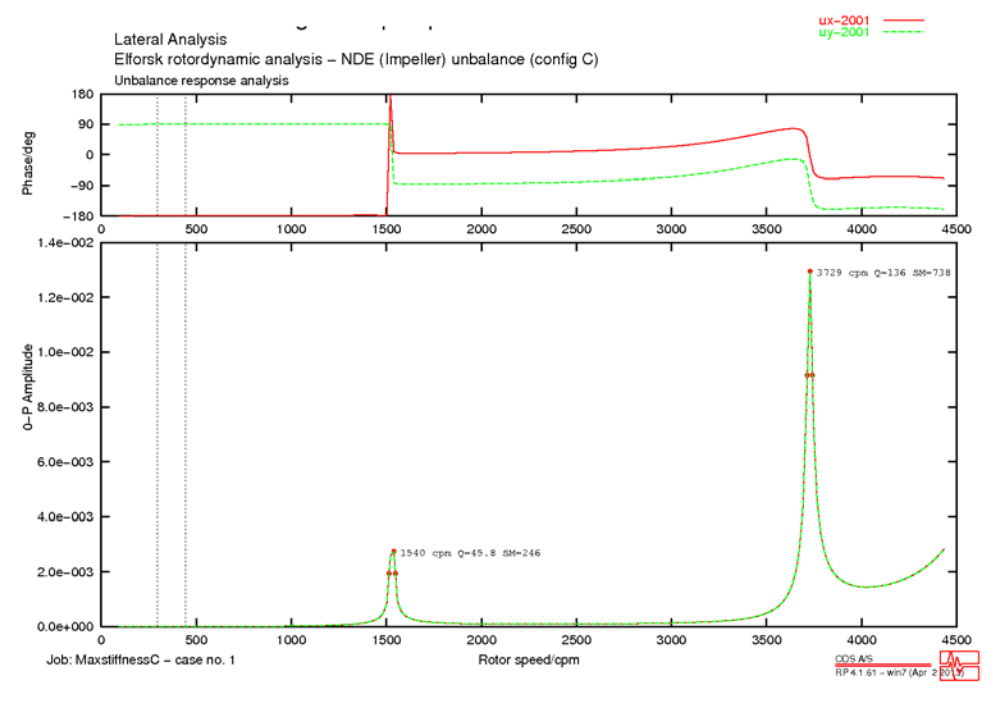


Figure LVI. Bode plot showing the response at the DE coupling in m zero to peak for unbalance Case C, with the unbalance in the NDE impeller. Maximum bearing stiffness is used.

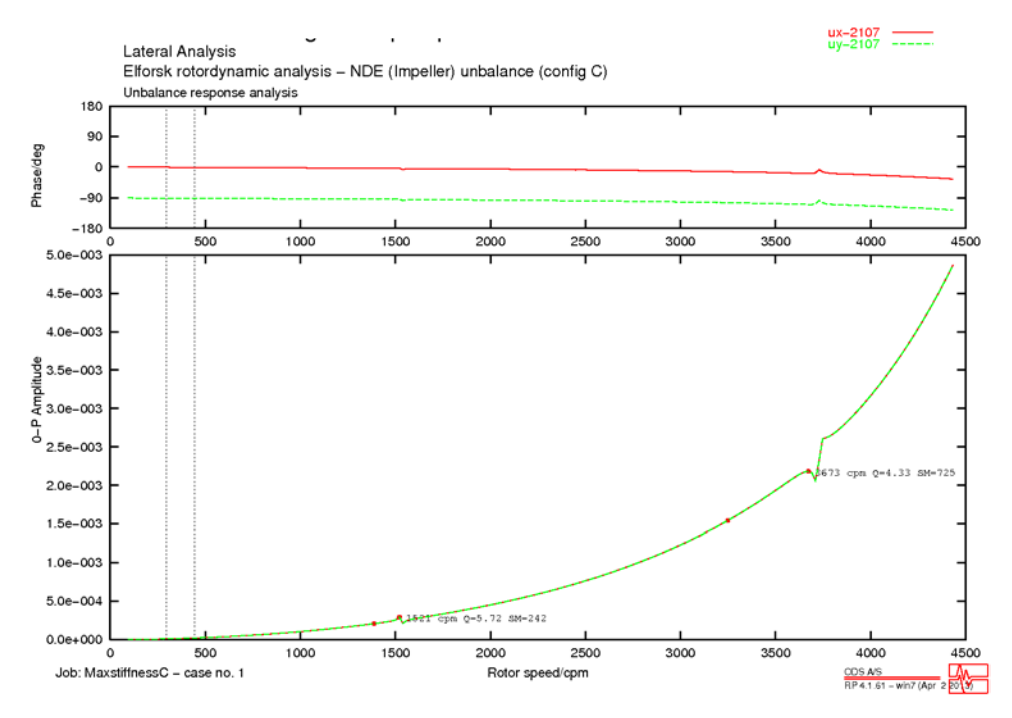


Figure LVII. Bode plot showing the response at the impeller in m zero to peak for unbalance Case C, with the unbalance in the NDE impeller. Maximum bearing stiffness is used.

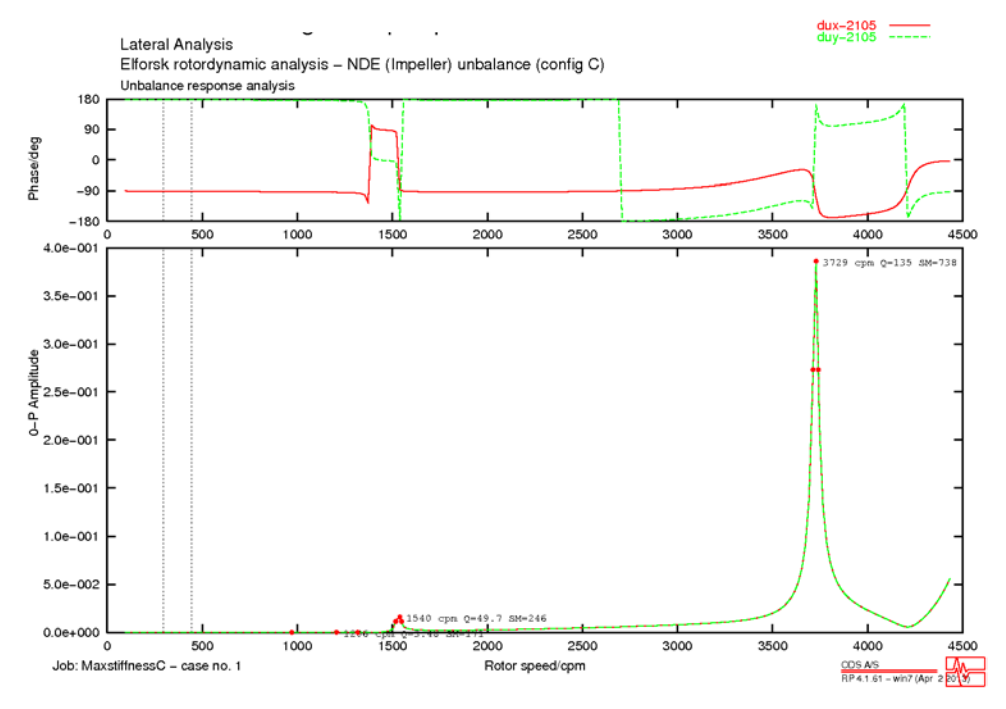
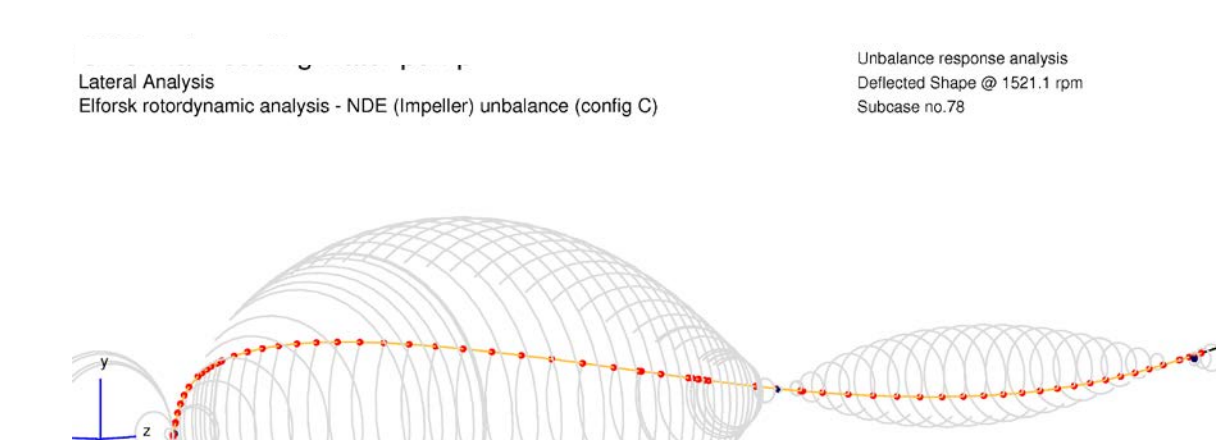


Figure LVIII. Bode plot showing the response at the middle pump bearing in m/s zero to peak for unbalance Case C, with the unbalance in the NDE impeller. Maximum bearing stiffness is used.



MaxstiffnessC - Case no. 1

ODS A/S

RP 4.1.61 - win7 (Apr 2 2018)

Figure LIX. First bending mode shape for unbalance Case C with maximum bearing stiffness.

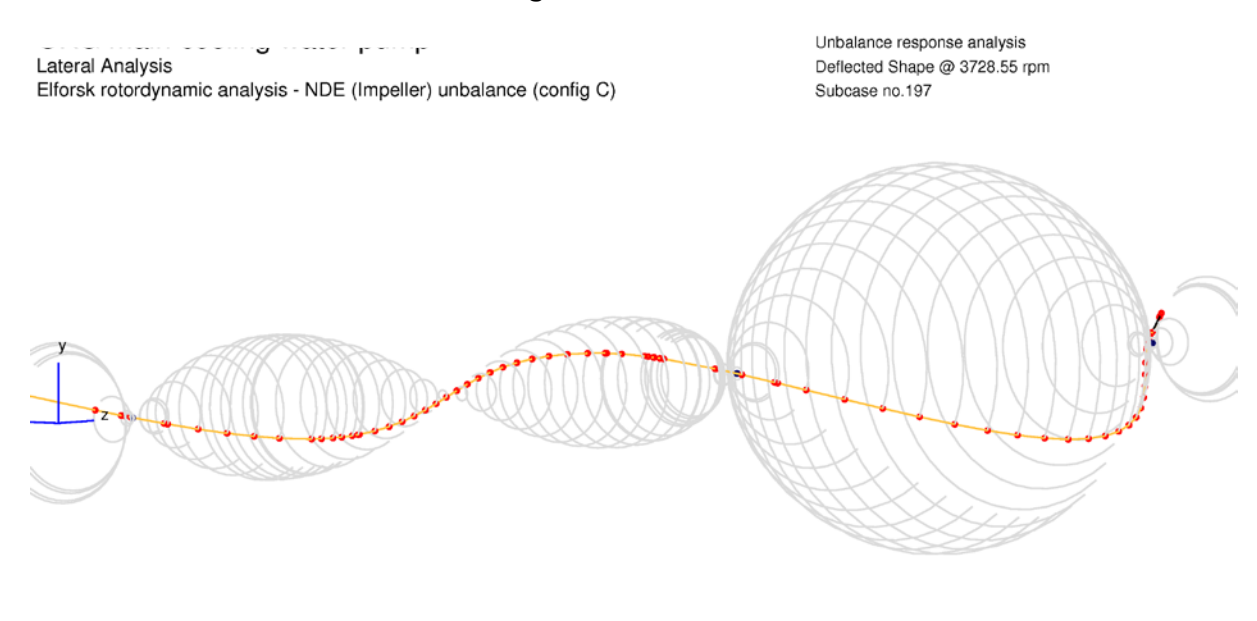


Figure LX. Second bending mode shape for unbalance Case C with maximum bearing stiffness.

MaxstiffnessC - Case no. 1

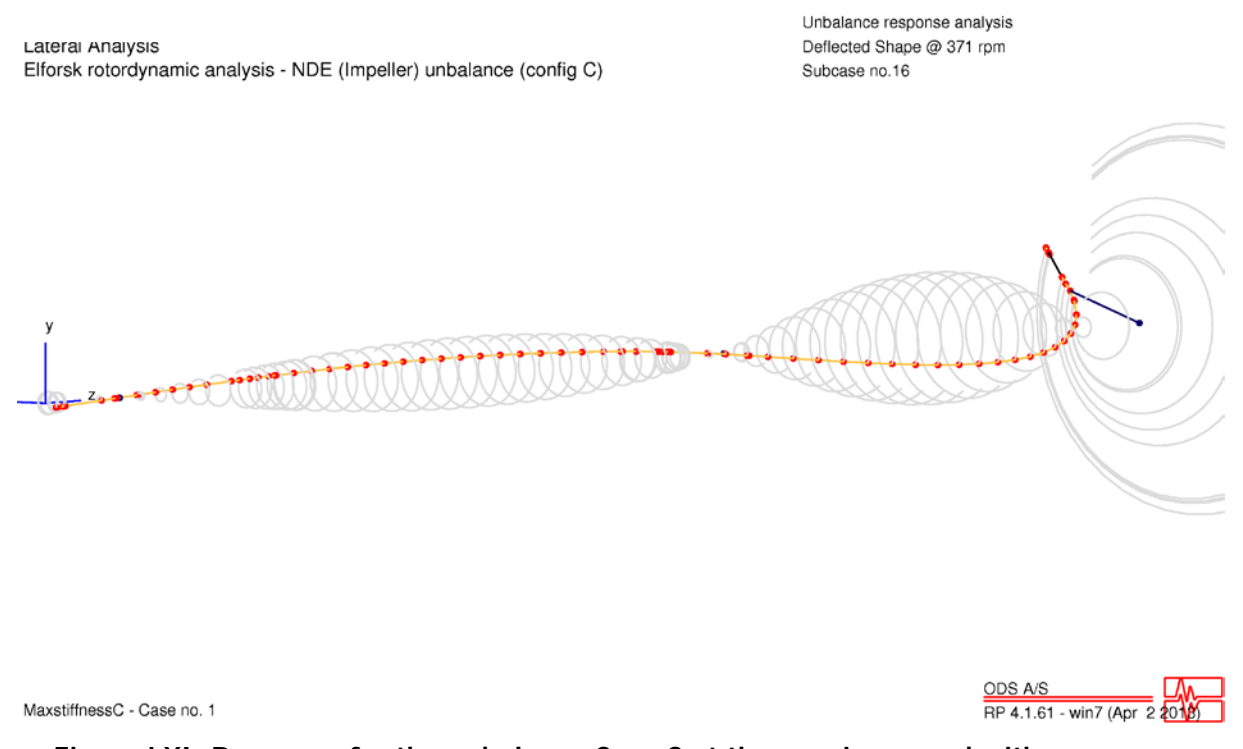


Figure LXI. Response for the unbalance Case C at the running speed with maximum bearing stiffness.

DE+NDE out of phase unbalance (Configuration D) – Minimum bearing stiffness

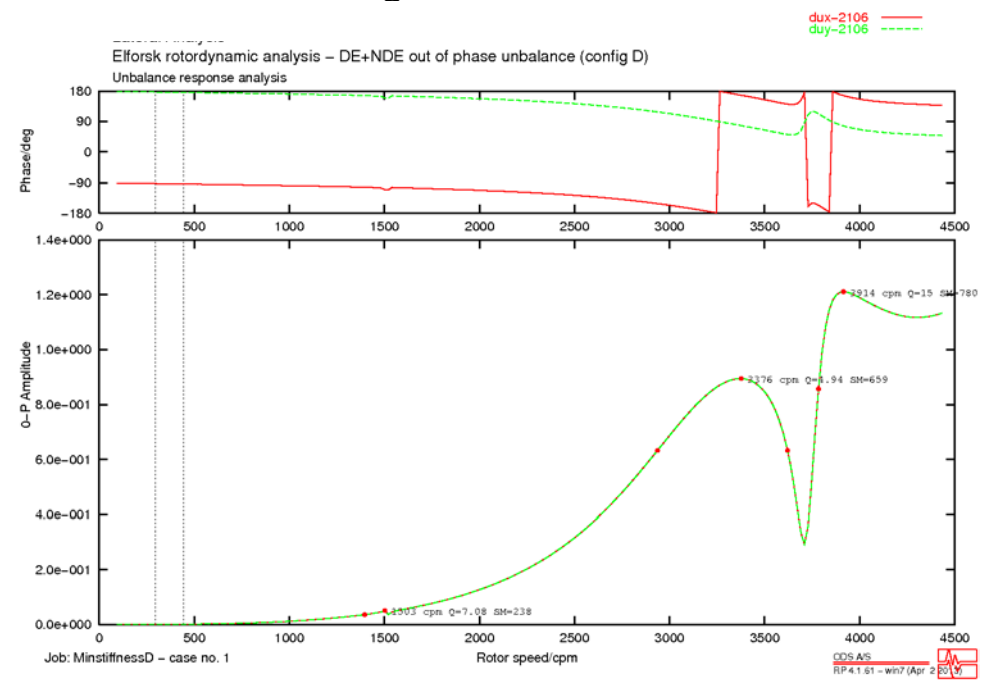


Figure LXII. Bode plot showing the response at the bottom pump bearing in m/s zero to peak for unbalance Case D, with half the unbalance in the NDE impeller and the other half in DE coupling with opposite phase. Minimum bearing stiffness is used.

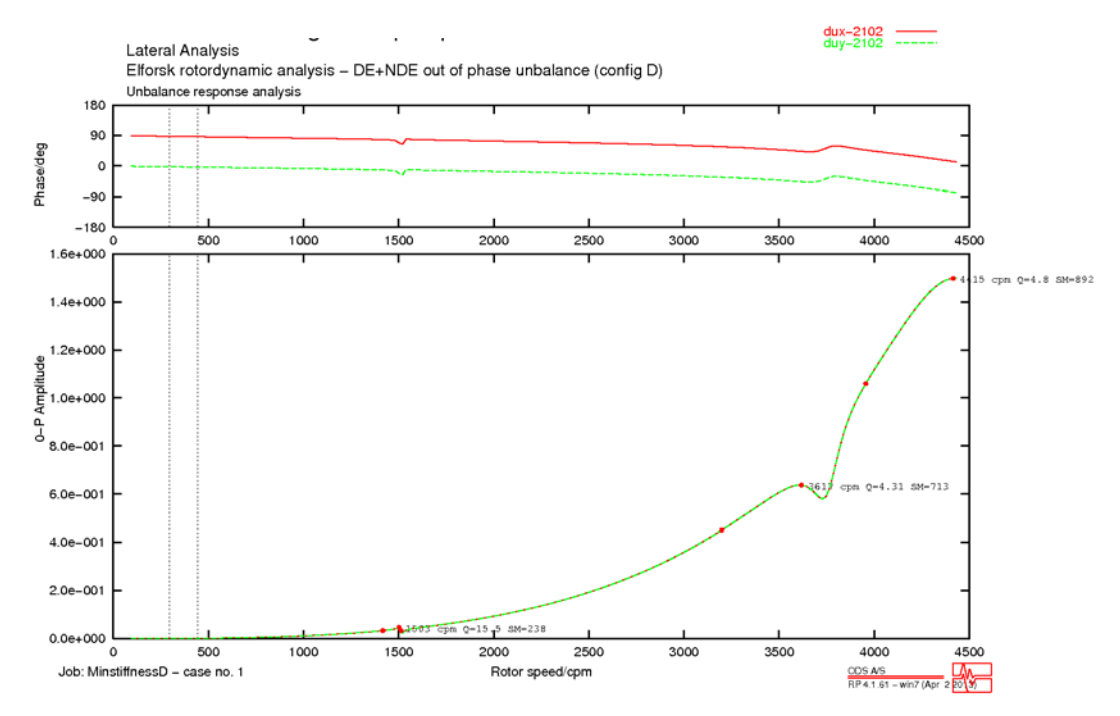


Figure LXIII. Bode plot showing the response at the upper pump bearing in m/s zero to peak for unbalance Case D, with half the unbalance in the NDE impeller and the other half in DE coupling with opposite phase. Minimum bearing stiffness is used.

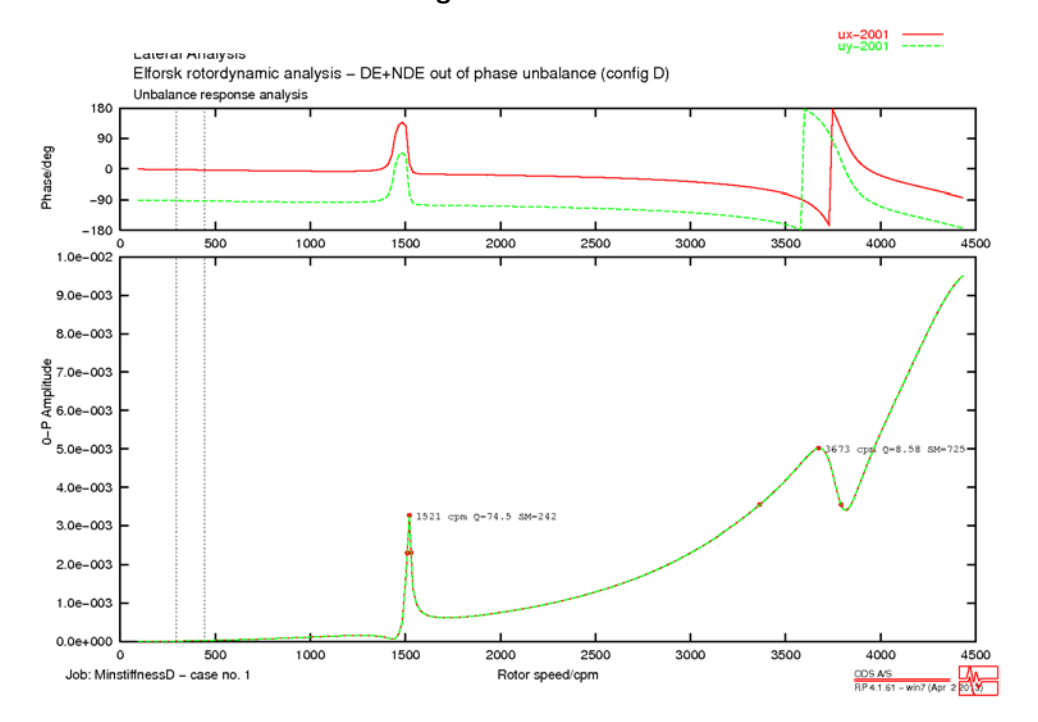


Figure LXIV. Bode plot showing the response at the DE coupling in m zero to peak for unbalance Case D, with half the unbalance in the NDE impeller and the other half in DE coupling with opposite phase. Minimum bearing stiffness is used.

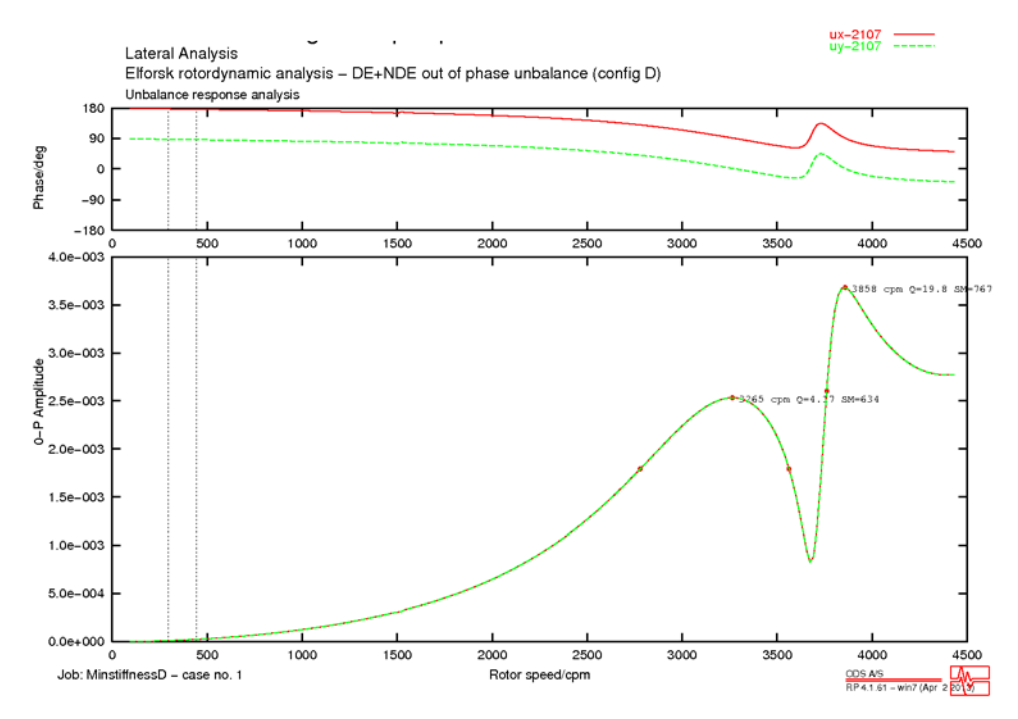


Figure LXV. Bode plot showing the response at the impeller in m zero to peak for unbalance Case D, with half the unbalance in the NDE impeller and the other half in DE coupling with opposite phase. Minimum bearing stiffness is used.

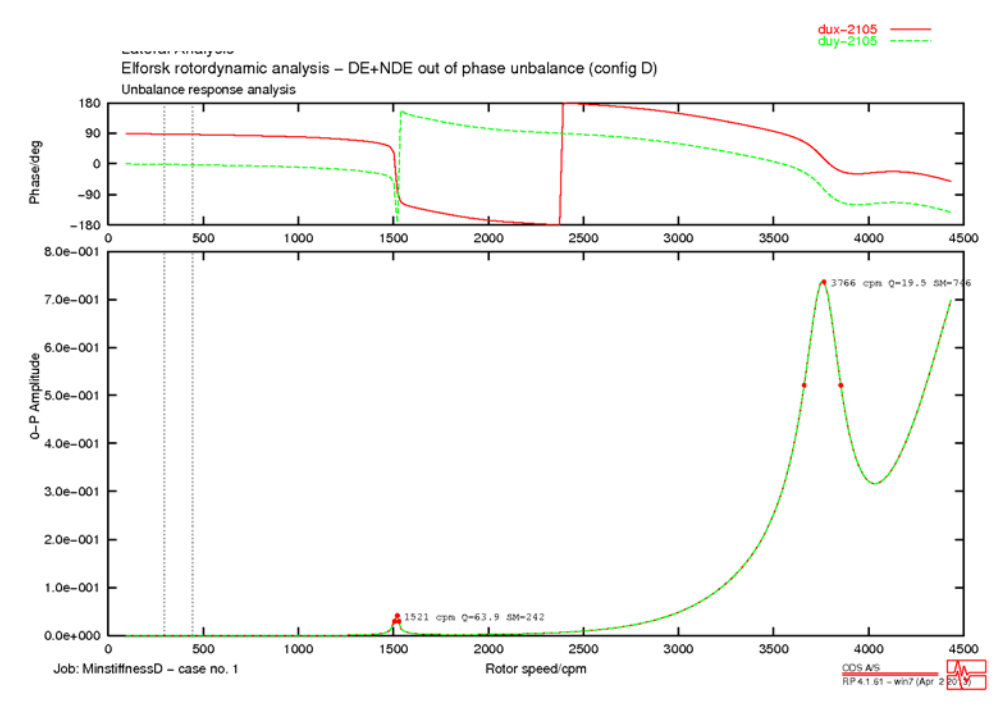
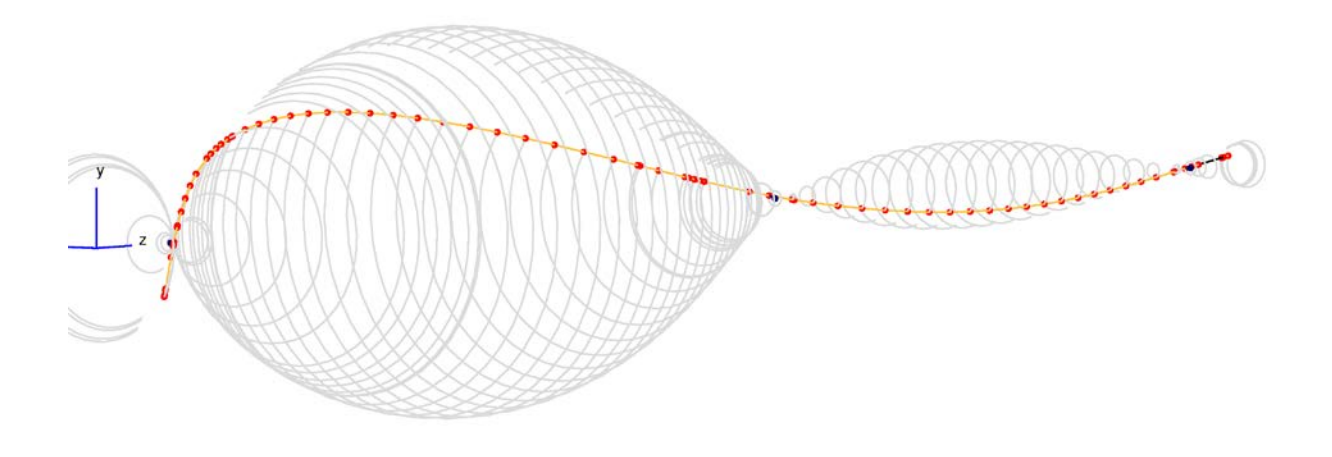


Figure LXVI. Bode plot showing the response at the middle pump bearing in m/s zero to peak for unbalance Case D, with half the unbalance in the NDE impeller and the other half in DE coupling with opposite phase. Minimum bearing stiffness is used.

Lateral Analysis
Elforsk rotordynamic analysis - DE+NDE out of phase unbalance (config D)

Unbalance response analysis Deflected Shape @ 1521.1 rpm Subcase no.78



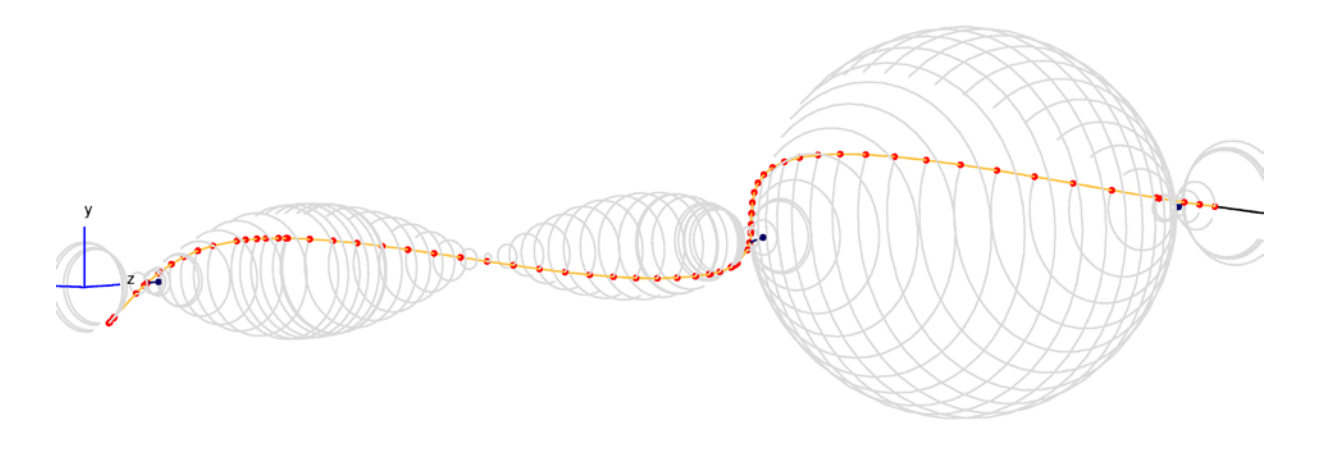
MinstiffnessD - Case no. 1

ODS A/S RP 4.1.61 - win7 (Apr 2 2018)

Figure LXVII. First bending mode shape for unbalance Case D with minimum bearing stiffness.

Lateral Analysis
Elforsk rotordynamic analysis - DE+NDE out of phase unbalance (config D)

Unbalance response analysis Deflected Shape @ 3728.55 rpm Subcase no.197



MinstiffnessD - Case no. 1



Figure LXVIII. Second bending mode shape for unbalance Case D with minimum bearing stiffness.

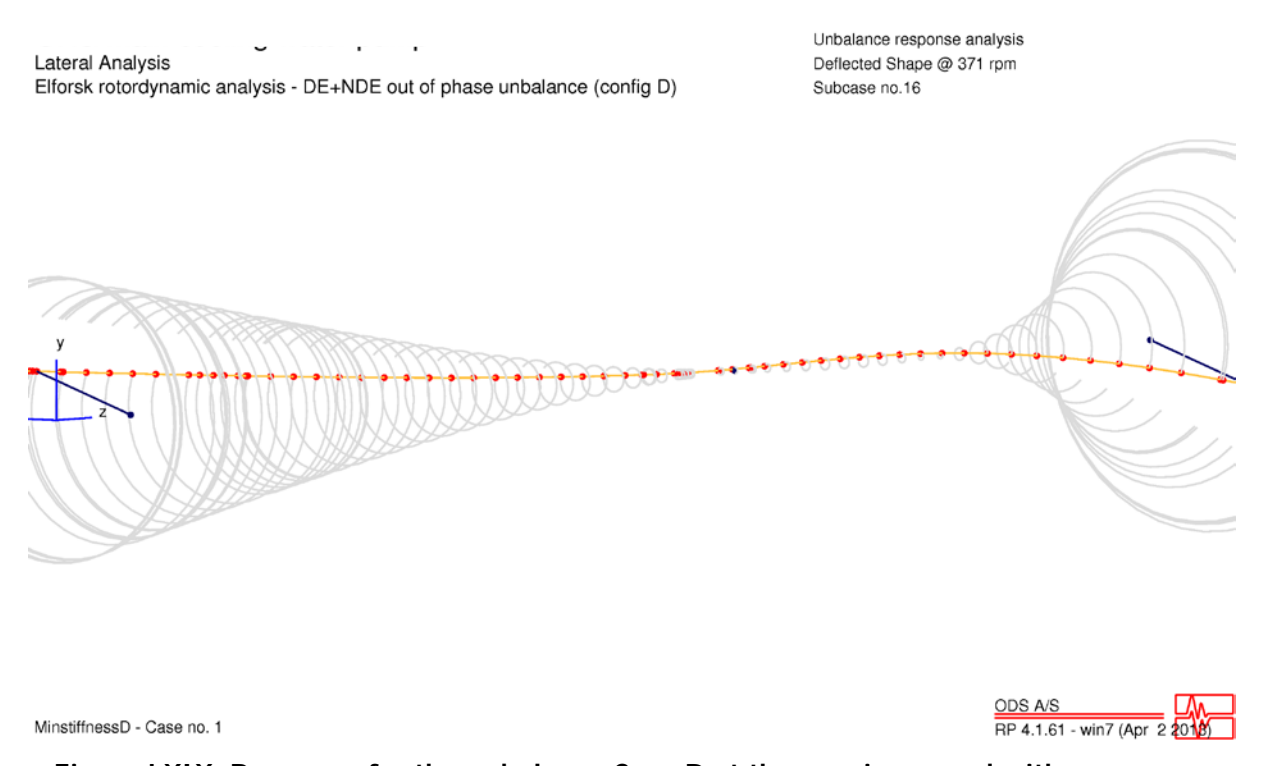


Figure LXIX. Response for the unbalance Case D at the running speed with minimum bearing stiffness.

DE+NDE out of phase unbalance (Configuration D)

– Maximum bearing
stiffness

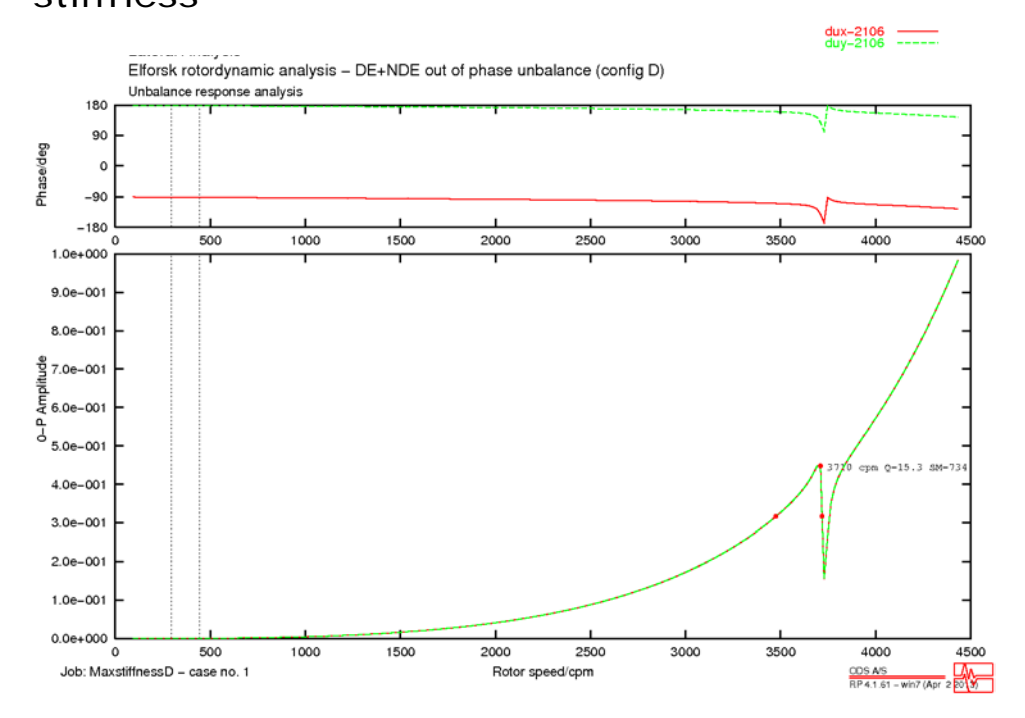


Figure LXX. Bode plot showing the response at the bottom pump bearing in m/s zero to peak for unbalance Case D, with half the unbalance in the NDE impeller and the other half in DE coupling with opposite phase. Maximum bearing stiffness is used.

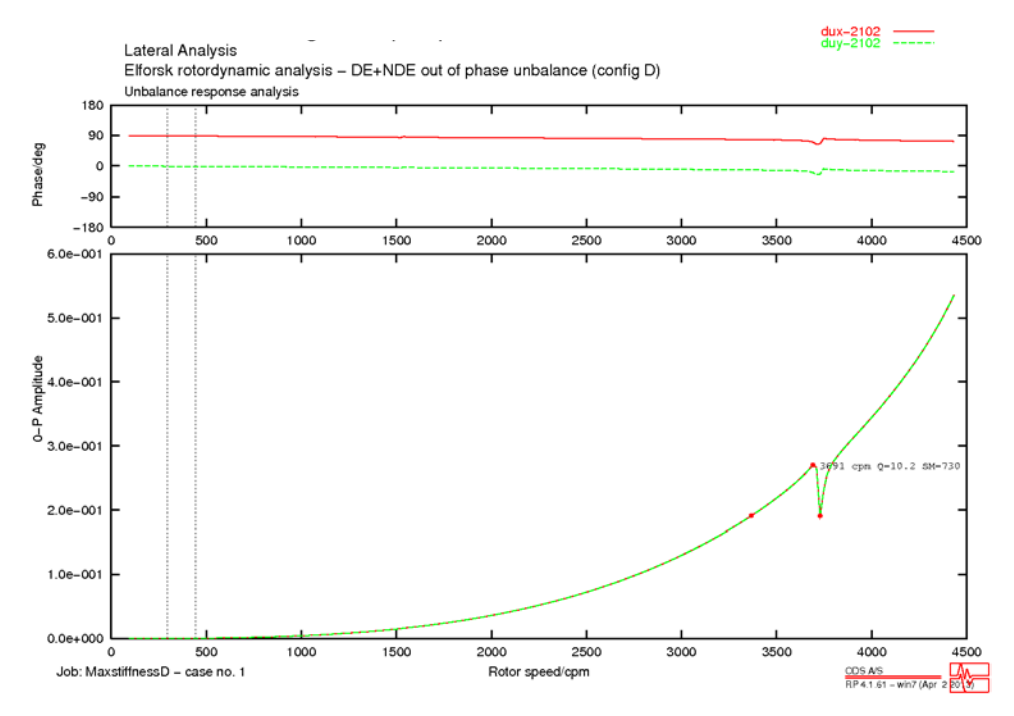


Figure LXXI. Bode plot showing the response at the upper pump bearing in m/s zero to peak for unbalance Case D, with half the unbalance in the NDE impeller and the other half in DE coupling with opposite phase. Maximum bearing stiffness is used.

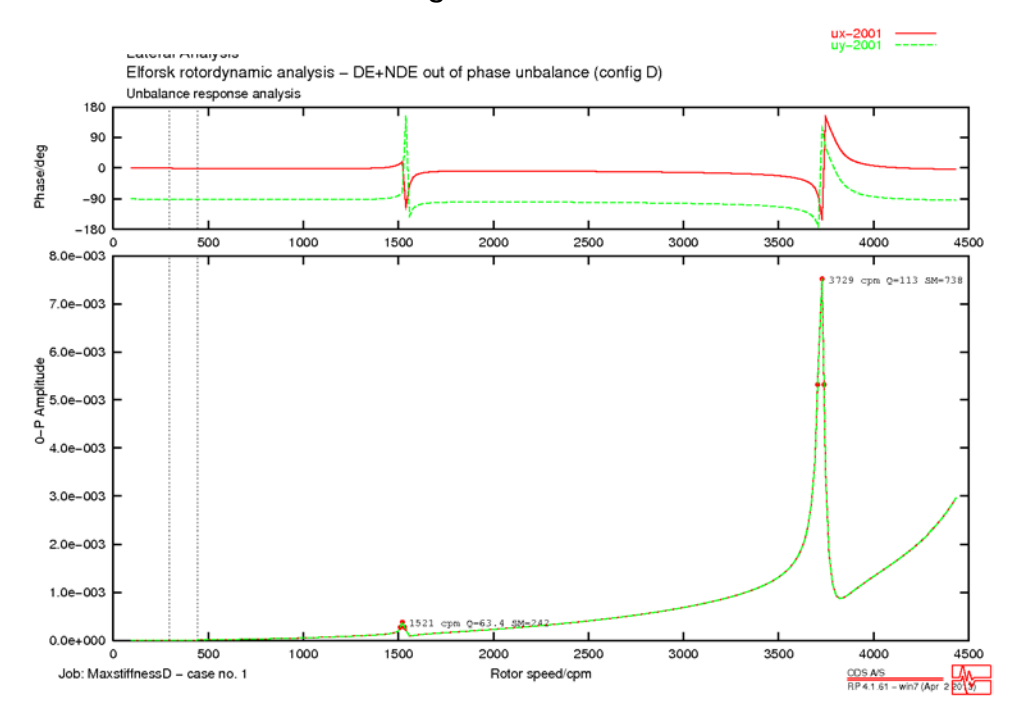


Figure LXXII. Bode plot showing the response at the DE coupling in m zero to peak for unbalance Case D, with half the unbalance in the NDE impeller and the other half in DE coupling with opposite phase. Maximum bearing stiffness is used.

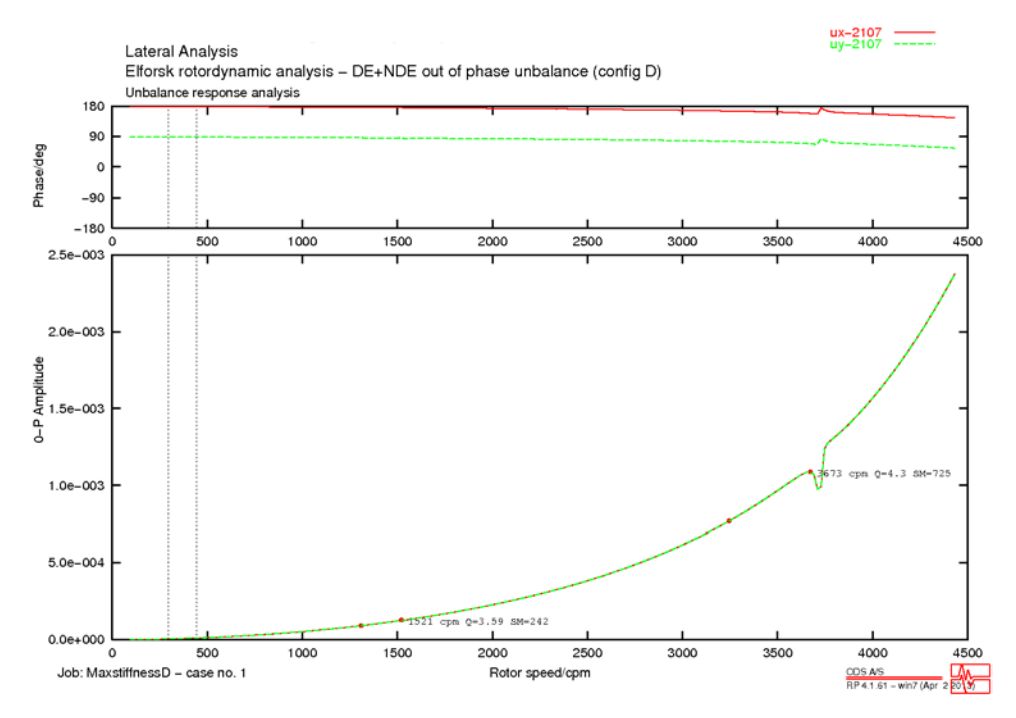


Figure LXXIII. Bode plot showing the response at the impeller in m zero to peak for unbalance Case D, with half the unbalance in the NDE impeller and the other half in DE coupling with opposite phase. Maximum bearing stiffness is used.

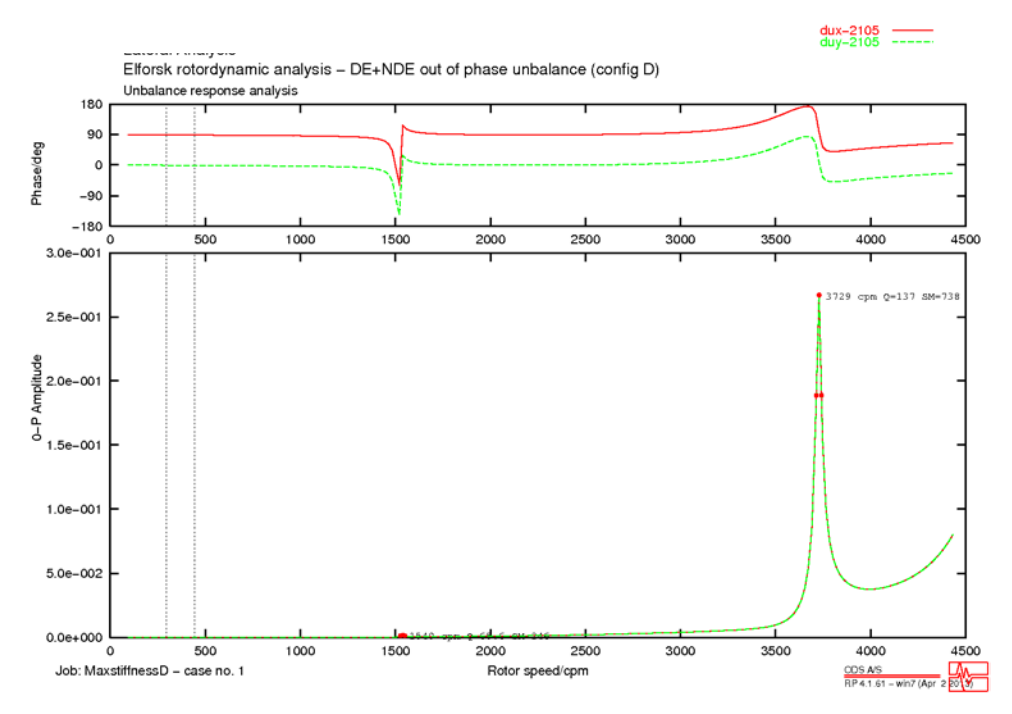
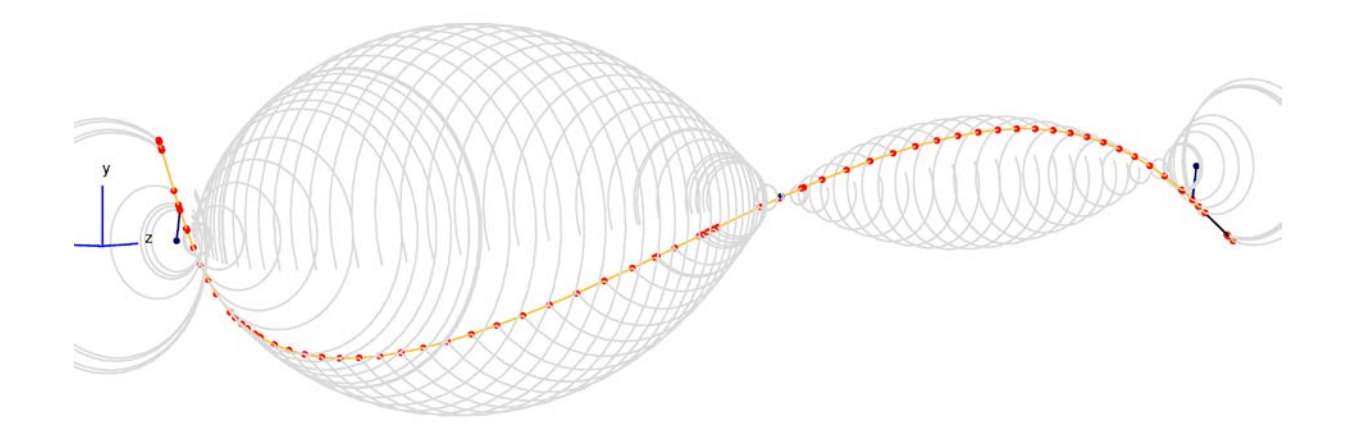


Figure LXXIV. Bode plot showing the response at the middle pump bearing in m/s zero to peak for unbalance Case D, with half the unbalance in the NDE impeller and the other half in DE coupling with opposite phase. Maximum bearing stiffness is used.

Lateral Analysis

Elforsk rotordynamic analysis - DE+NDE out of phase unbalance (config D)

Unbalance response analysis Deflected Shape @ 1521.1 rpm Subcase no.78



MaxstiffnessD - Case no. 1

ODS A/S

RP 4.1.61 - win7 (Apr 2 2018)

Figure LXXV. First bending mode shape for unbalance Case D with maximum bearing stiffness.

Lateral Analysis
Elforsk rotordynamic analysis - DE+NDE out of phase unbalance (config D)

Unbalance response analysis
Deflected Shape @ 3728.55 rpm
Subcase no.197

MaxstiffnessD - Case no. 1

ODS A/S

RP 4.1.61 - win7 (Apr 2 2018)

Figure LXXVI. Second bending mode shape for unbalance Case D with maximum bearing stiffness.

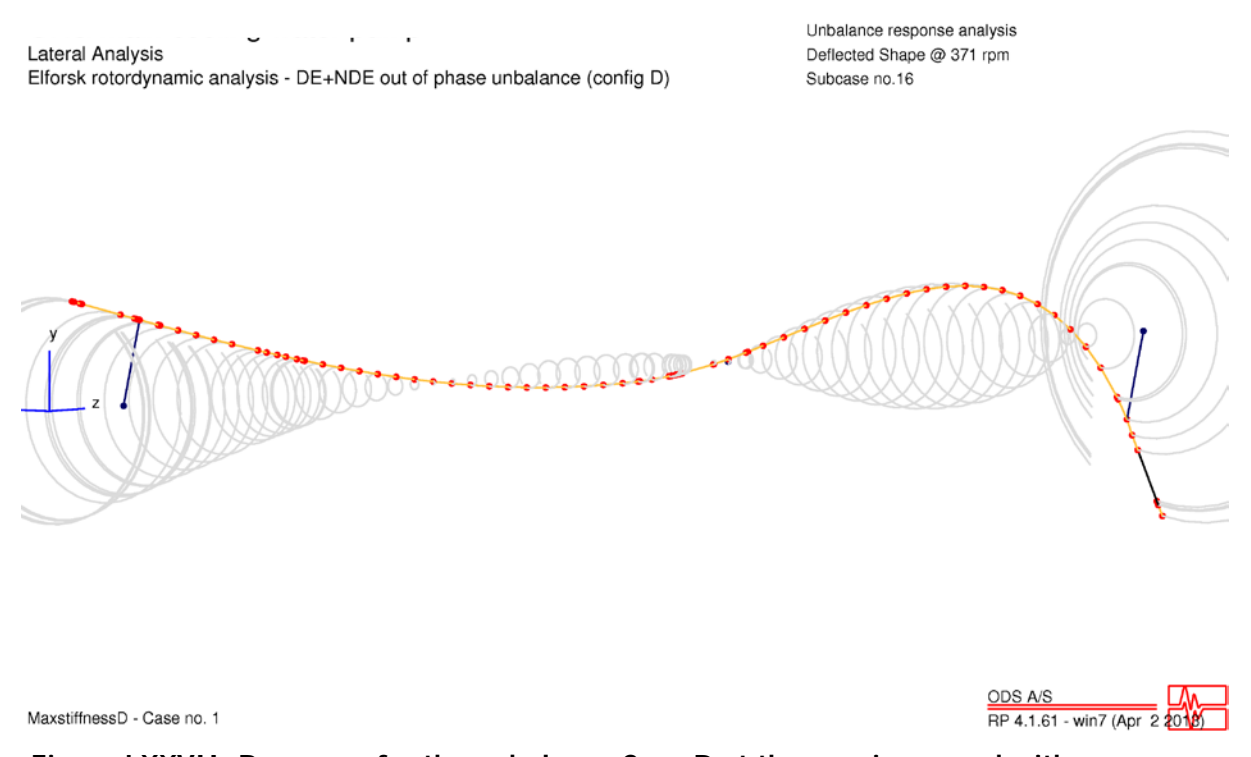


Figure LXXVII. Response for the unbalance Case D at the running speed with maximum bearing stiffness.

DE+NDE in phase unbalance (Configuration E) – Minimum bearing stiffness

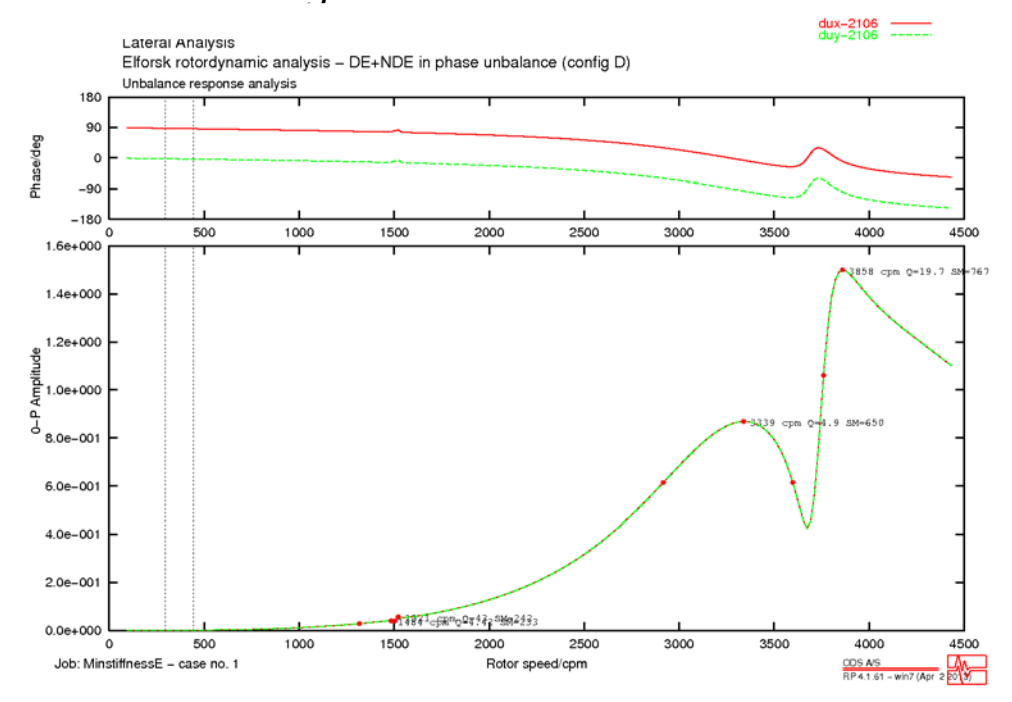


Figure LXXVIII. Bode plot showing the response at the bottom pump bearing in m/s zero to peak for unbalance Case D, with half the unbalance in the NDE impeller and the other half in DE coupling with opposite phase. Minimum bearing stiffness is used.

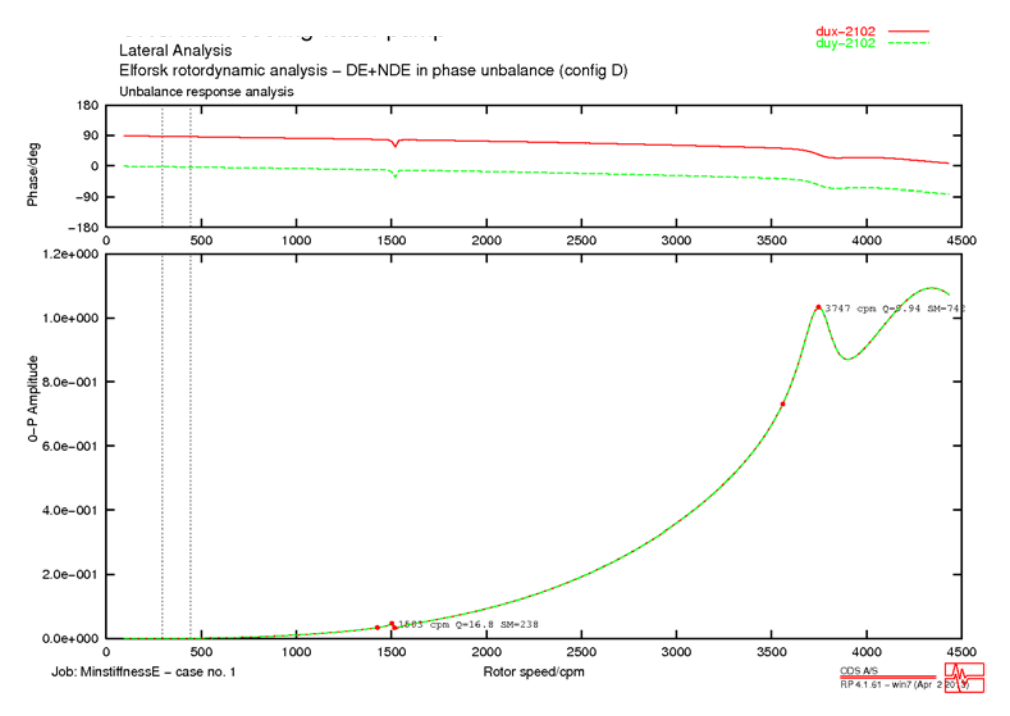


Figure LXXIX. Bode plot showing the response at the upper pump bearing in m/s zero to peak for unbalance Case D, with half the unbalance in the NDE impeller and the other half in DE coupling with opposite phase. Minimum bearing stiffness is used.

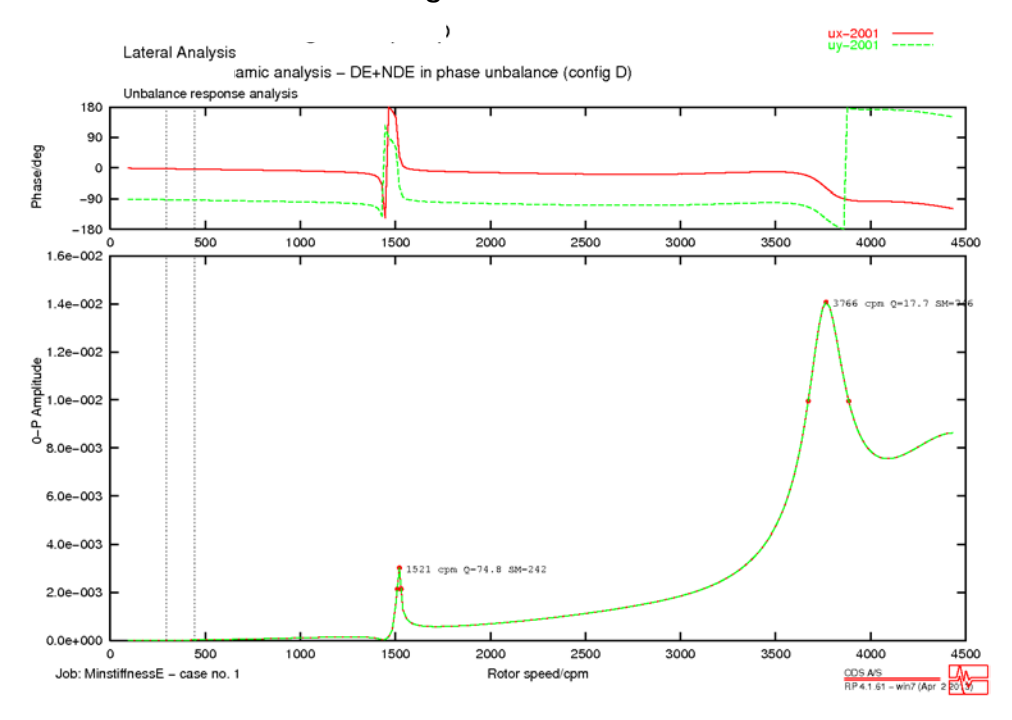


Figure LXXX. Bode plot showing the response at the DE coupling in m zero to peak for unbalance Case D, with half the unbalance in the NDE impeller and the other half in DE coupling with opposite phase. Minimum bearing stiffness is used.

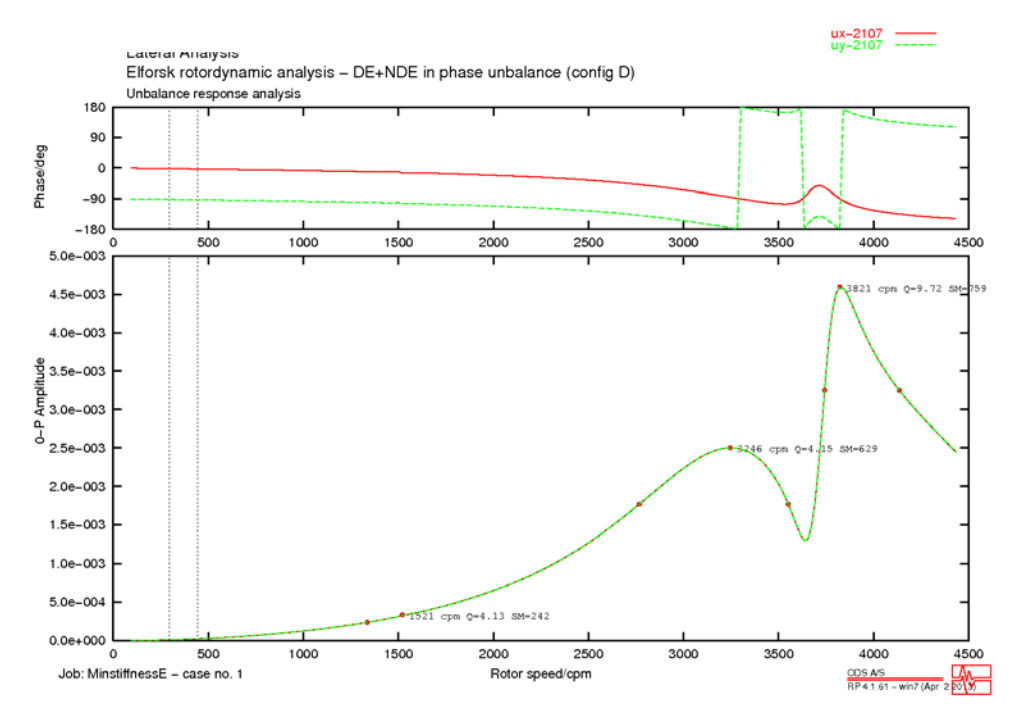


Figure LXXXI. Bode plot showing the response at the impeller in m zero to peak for unbalance Case D, with half the unbalance in the NDE impeller and the other half in DE coupling with opposite phase. Minimum bearing stiffness is used.

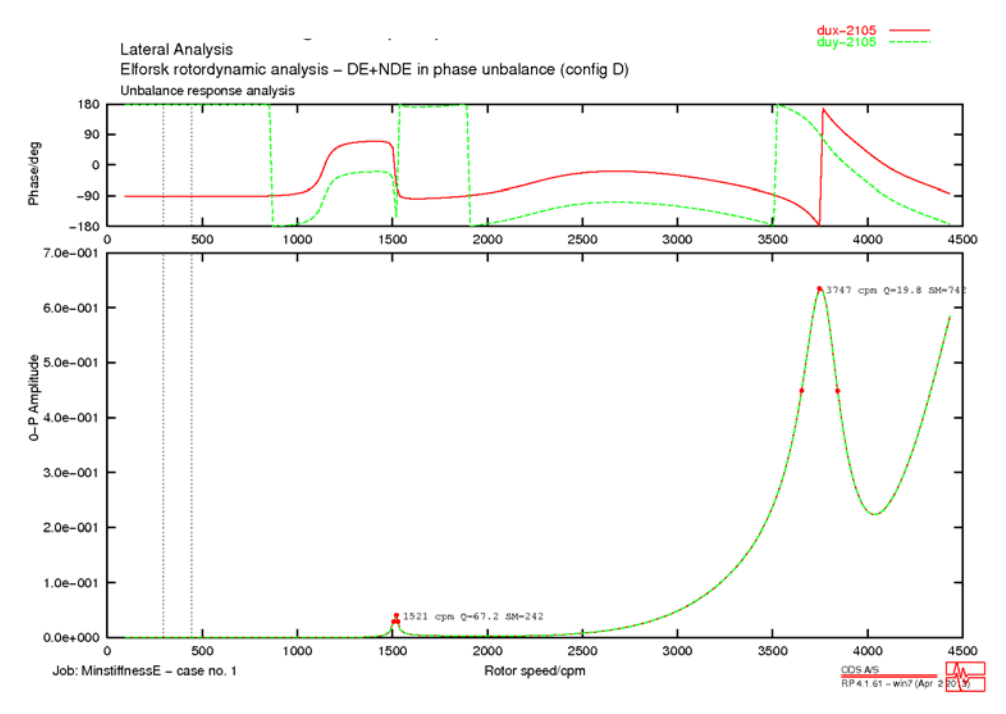
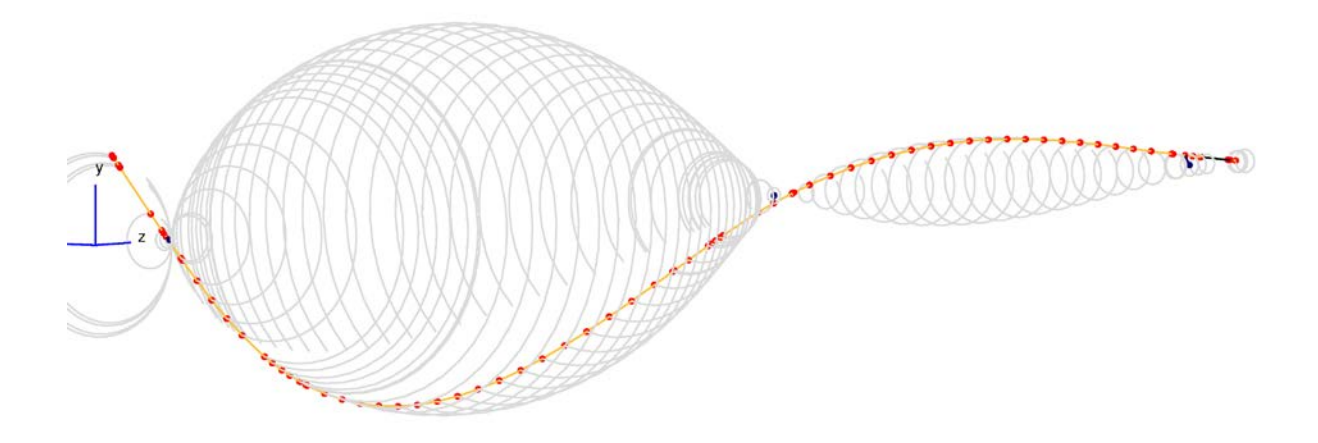


Figure LXXXII. Bode plot showing the response at the middle pump bearing in m/s zero to peak for unbalance Case D, with half the unbalance in the NDE impeller and the other half in DE coupling with opposite phase. Minimum bearing stiffness is used.





MinstiffnessE - Case no. 1

ODS A/S RP 4.1.61 - win7 (Apr 2 2018)

Figure LXXXIII. First bending mode shape for unbalance Case D with minimum bearing stiffness.

Lateral Analysis
Elforsk rotordynamic analysis - DE+NDE in phase unbalance (config D)

Unbalance response analysis
Deflected Shape @ 3728.55 rpm
Subcase no.197

MinstiffnessE - Case no. 1



Figure LXXXIV. Second bending mode shape for unbalance Case D with minimum bearing stiffness.

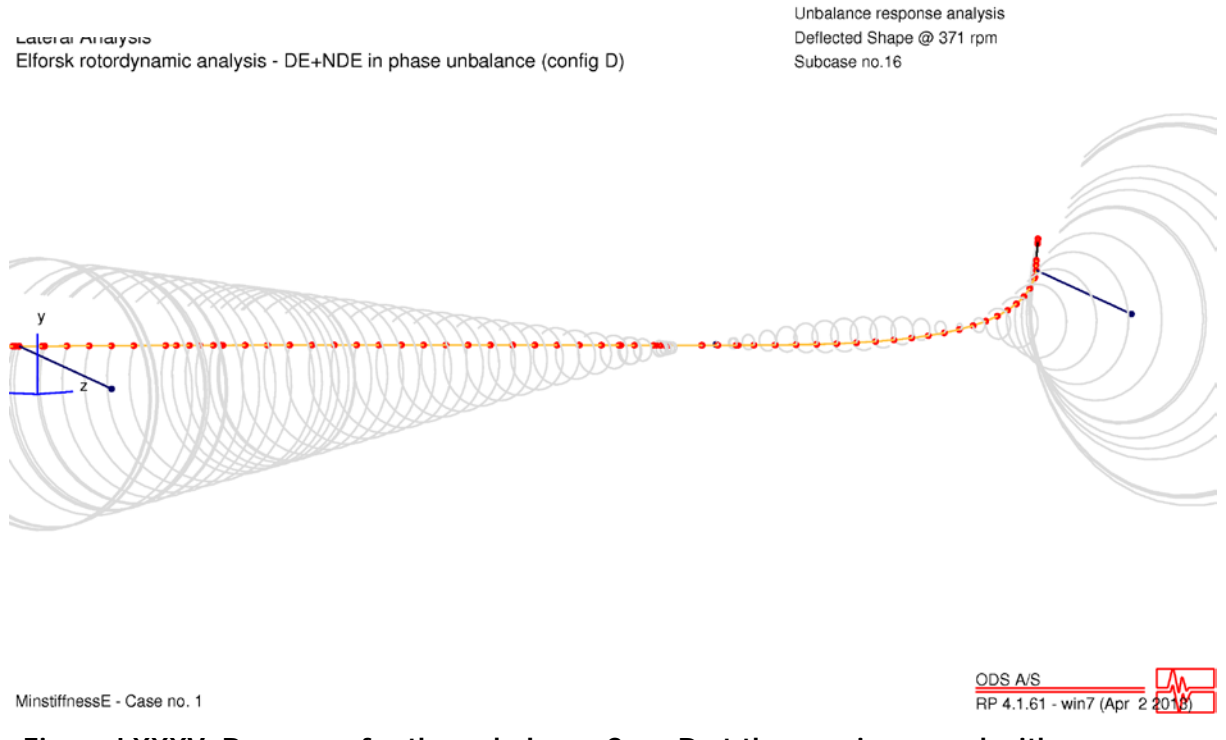


Figure LXXXV. Response for the unbalance Case D at the running speed with minimum bearing stiffness.

### DE+NDE in phase unbalance (Configuration E) – Maximum bearing stiffness

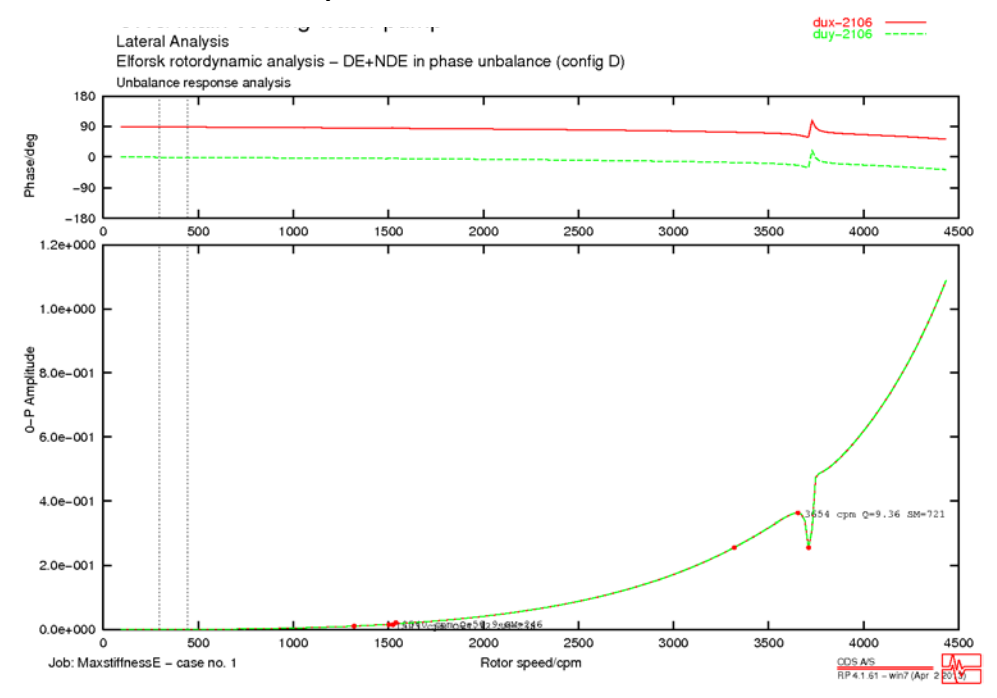


Figure LXXXVI. Bode plot showing the response at the bottom pump bearing in m/s zero to peak for unbalance Case E, with half the unbalance in the NDE impeller and the other half in DE coupling with the same phase. Maximum bearing stiffness is used.

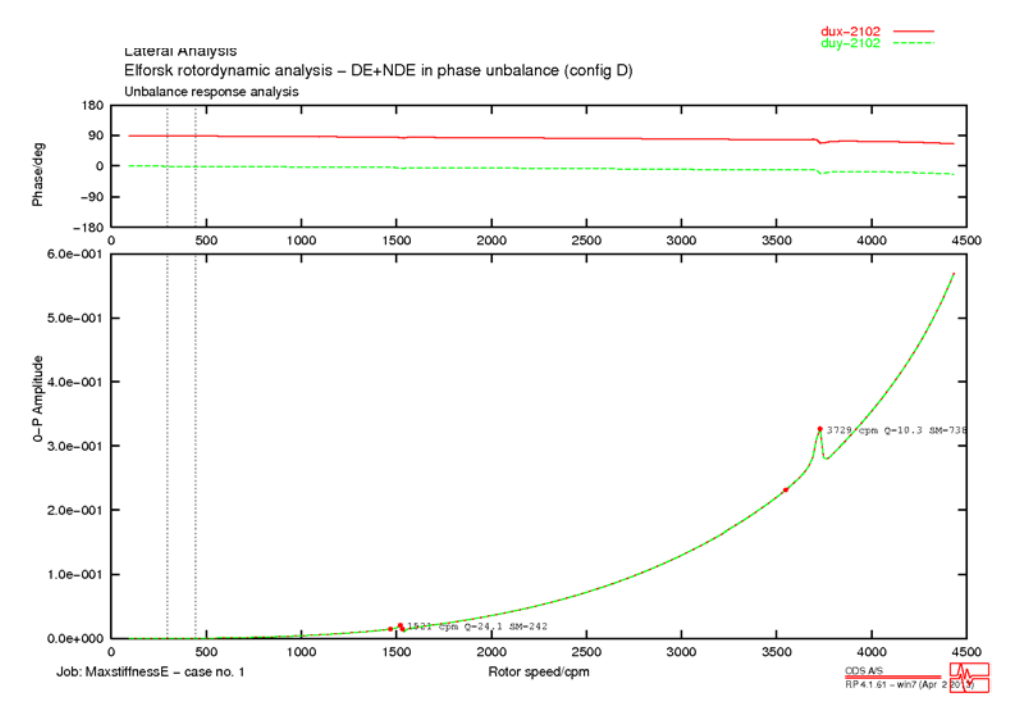


Figure LXXXVII. Bode plot showing the response at the upper pump bearing in m/s zero to peak for unbalance Case E, with half the unbalance in the NDE impeller and the other half in DE coupling with the same phase. Maximum bearing stiffness is used.

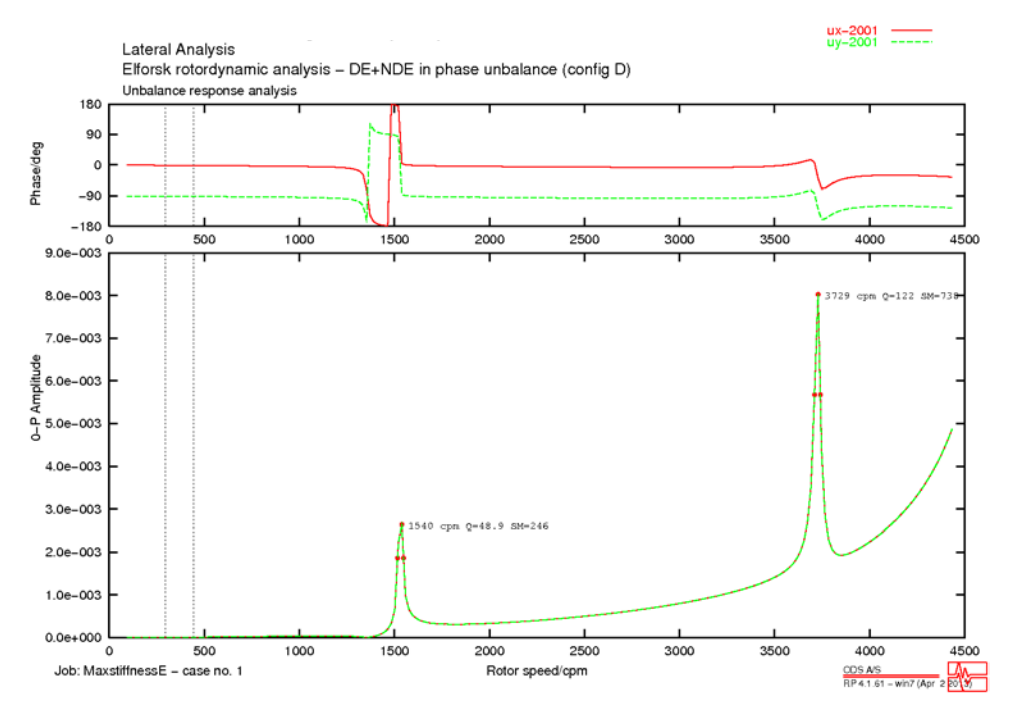


Figure LXXXVIII. Bode plot showing the response at the DE coupling in m zero to peak for unbalance Case E, with half the unbalance in the NDE impeller and the other half in DE coupling with the same phase. Maximum bearing stiffness is used.

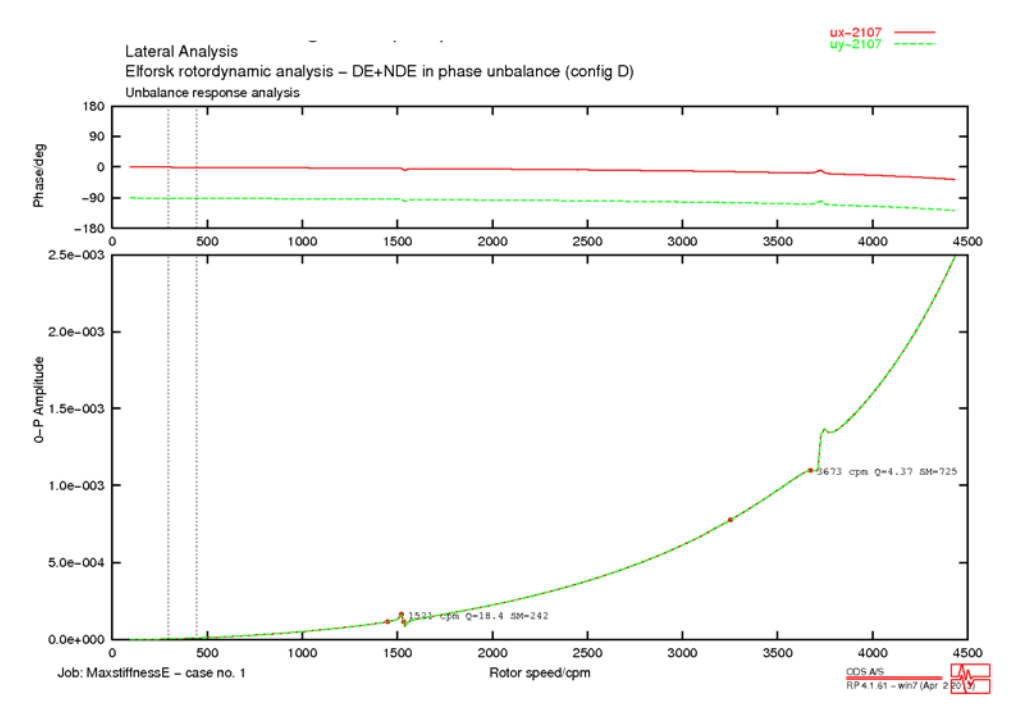


Figure LXXXIX. Bode plot showing the response at the impeller in m zero to peak for unbalance Case E, with half the unbalance in the NDE impeller and the other half in DE coupling with the same phase. Maximum bearing stiffness is used.

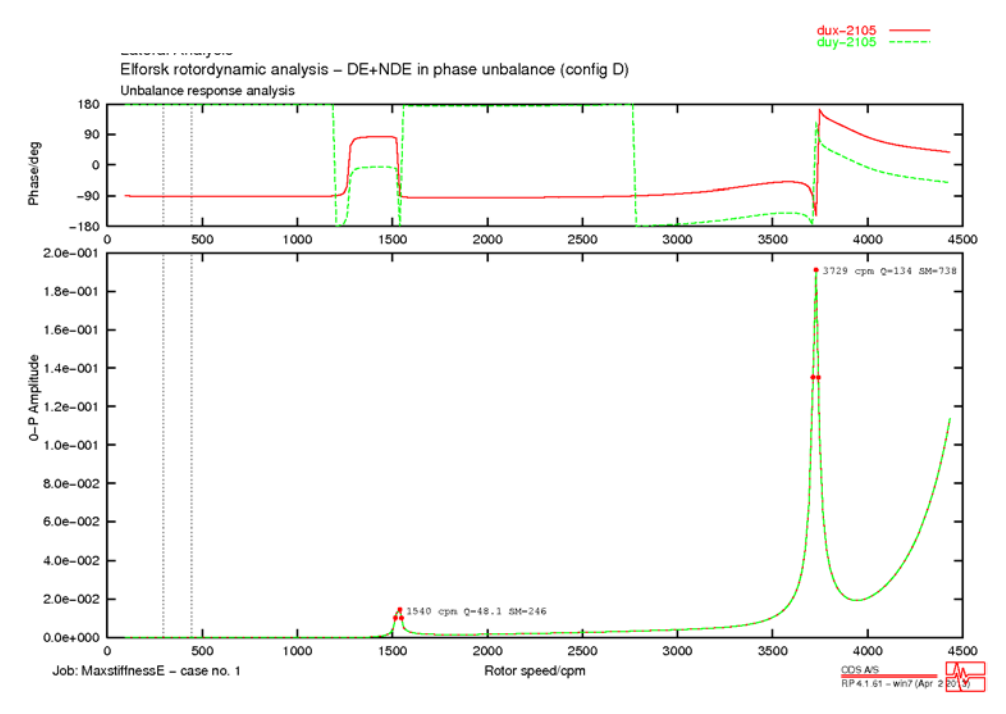


Figure XC. Bode plot showing the response at the middle pump bearing in m/s zero to peak for unbalance Case E, with half the unbalance in the NDE impeller and the other half in DE coupling with the same phase. Maximum bearing stiffness is used.

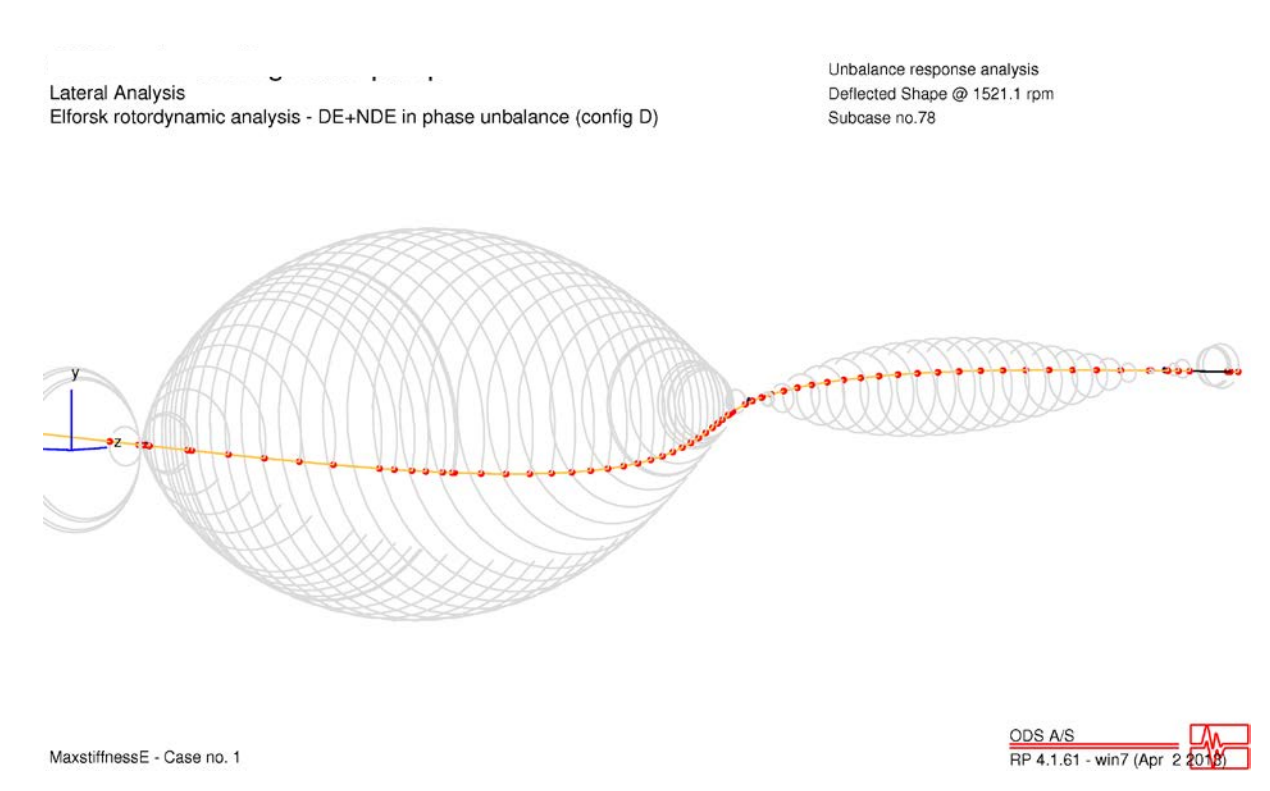


Figure XCI. First bending mode shape for unbalance Case E with maximum bearing stiffness.

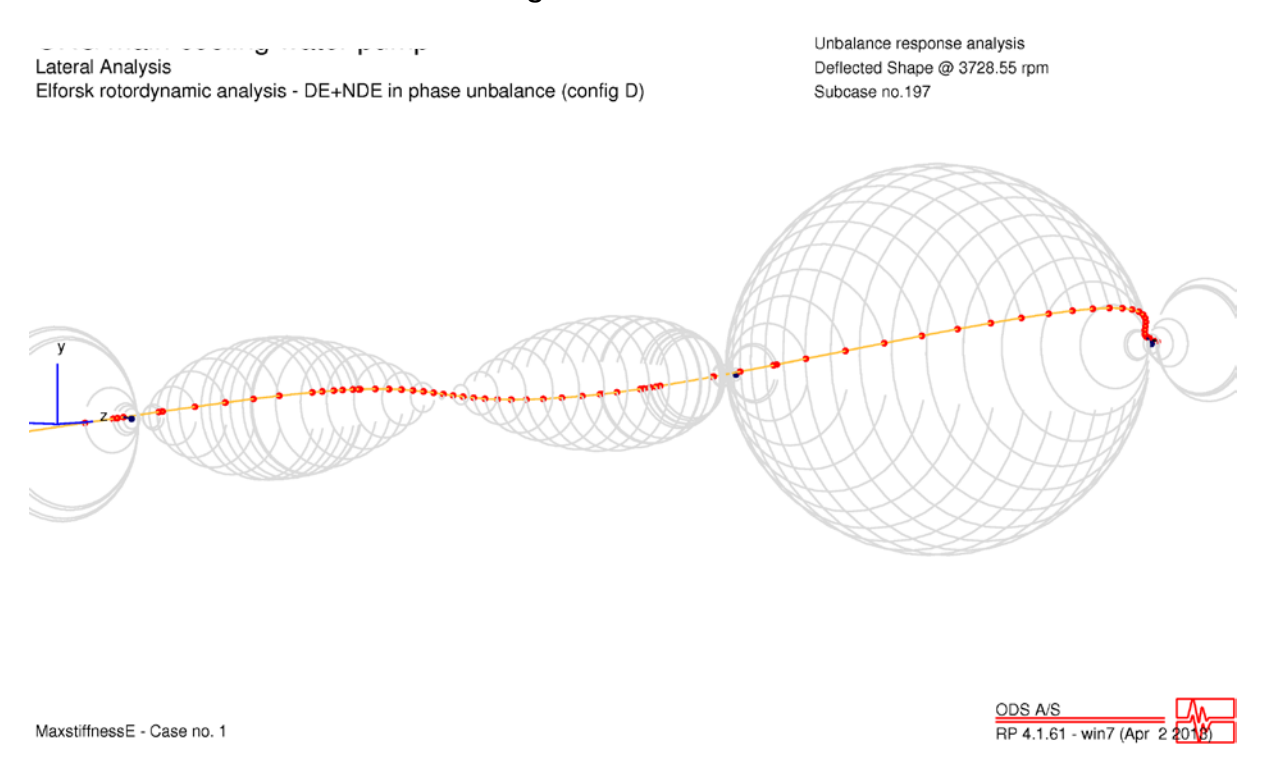
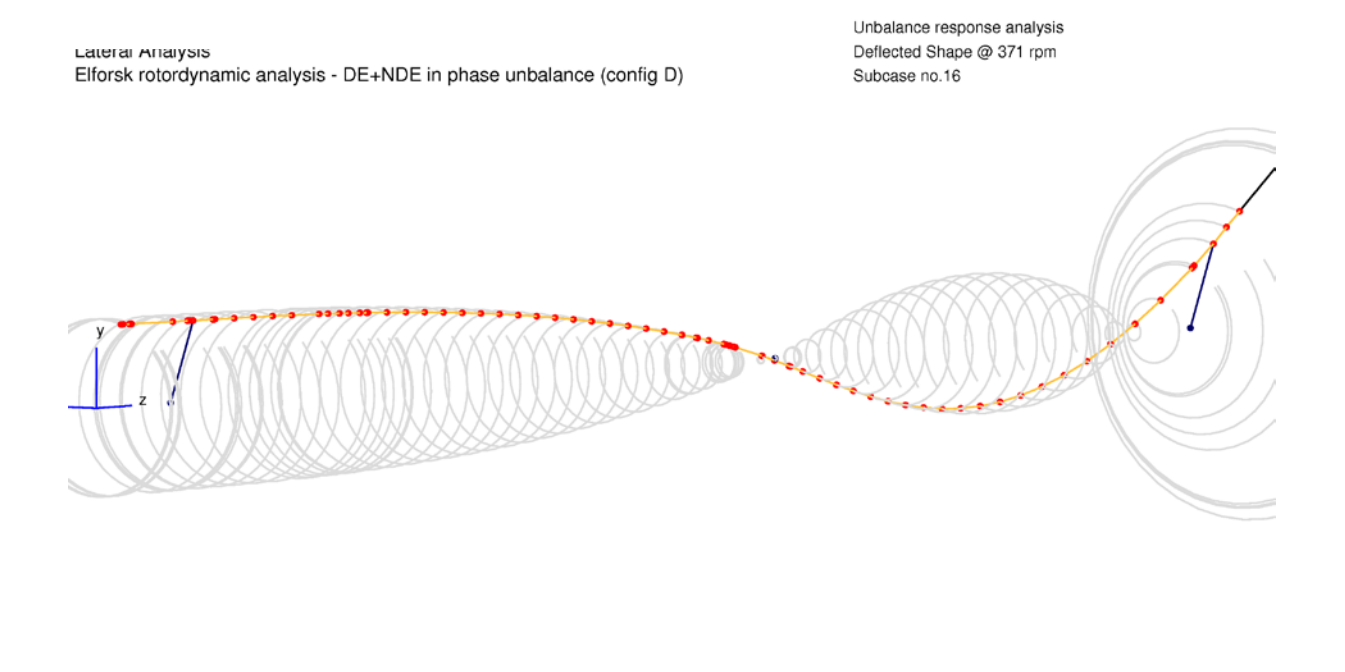


Figure XCII. Second bending mode shape for unbalance Case E with maximum bearing stiffness.



ODS A/S RP 4.1.61 - win7 (Apr 2 201

Figure XCIII. Response for the unbalance Case E at the running speed with maximum bearing stiffness.

MaxstiffnessE - Case no. 1

## ROTORDYNAMIC STUDY OF PUMPS IN THE NUCLEAR INDUSRTY

The outcome of a study on the rotor dynamics of pumps in the nuclear industry are described here. The Swedish nuclear power plants' technical rules for mechanical equipment has been examined and compared with other available international standards for pumps. The results show that technical provisions contain limited information on the rotor dynamic problems and the lack of classification of pumps, the characteristics and potential problems can differ alot.

The study suggests a number of changes that would improve the requirements and procedures within the rotor dynamic analysis of nuclear power plants. An increased frequency of rotor dynamic third-party analysis means for example avoiding problems during commissioning and during normal operation.

#### Ett nytt steg i energiforskningen

Energiforsk är en forsknings- och kunskapsorganisation som samlar stora delar av svensk forskning och utveckling om energi. Målet är att öka effektivitet och nyttiggörande av resultat inför framtida utmaningar inom energiområdet. Vi verkar inom ett antal forskningsområden, och tar fram kunskap om resurseffektiv energi i ett helhetsperspektiv – från källan, via omvandling och överföring till användning av energin. www.energiforsk.se

